

**Studies in Dendritic Scaffolds and Surface Functionalisation for
Applications in Nanoscience**

Author

Atkinson, Sarah Jane

Published

2007

Thesis Type

Thesis (PhD Doctorate)

School

School of Biomolecular and Physical Sciences

DOI

[10.25904/1912/1771](https://doi.org/10.25904/1912/1771)

Rights statement

The author owns the copyright in this thesis, unless stated otherwise.

Downloaded from

<http://hdl.handle.net/10072/366865>

Griffith Research Online

<https://research-repository.griffith.edu.au>

**STUDIES IN DENDRITIC SCAFFOLDS AND
SURFACE FUNCTIONALISATION FOR
APPLICATIONS IN NANOSCIENCE**

Sarah Jane Atkinson

(née Head)

B.Sc.(Hons), B.Com.

Submitted in fulfilment of the requirements of the degree of Doctor of Philosophy

School of Biomolecular and Physical Sciences

Faculty of Science, Environment, Engineering and Technology

Griffith University

February 2007

Statement of Originality

This work has not previously been submitted for a degree or diploma in any university. To the best of my knowledge and belief, the thesis contains no material previously published or written by another person except where due reference is made in the thesis itself.

Sarah Atkinson (née Head)

BSc(Hons) BCom

Preface

Unless otherwise stated, the results in this thesis are those of the author. Parts of this work have appeared elsewhere.

Refereed Journal Publications

'Synthesis and characterisation of peripherally functionalised dendritic molecules'

Sarah J. Atkinson, Vicky-June Ellis, Sue E. Boyd and Christopher L. Brown, *New J. Chem.*, **2007**, *31*, 155-162 .

'Succinimido 4-(N-maleimidomethyl)cyclohexanecarboxylate'

Christopher L. Brown, Sarah J. Atkinson and Peter C. Healy, *Acta. Cryst. E.*, **2005** *E61*, o1203-1204.

'N,N'-Ethylenedisuccinimide'

Christopher L. Brown, Sarah J. Atkinson and Peter C. Healy, *Acta. Cryst. E.*, **2005** *E61*, o1072-1073.

Conference Posters

'Click Chemistry Reactions in the Modular Assembly of Dendritic Macromolecules - a Model Study'

Sarah J. Atkinson, Vicky-June Ellis, Sue E. Boyd, Christopher L. Brown, presented at the International Symposium of Supramolecular Chemistry XIII, Notre Dame, USA, July 2004.

'Click Chemistry on Surfaces for the Immobilisation of Macromolecules'

Sarah J. Atkinson, Christopher L. Brown, presented at the International Symposium of Supramolecular Chemistry XIII, Notre Dame, USA, July 2004.

Conference Lectures

'Modular Synthesis of Dendritic Macromolecules'

Sarah J. Atkinson, presented at the Brisbane Biological and Organic Chemistry Symposium, November, 2004.

Table of Contents

<i>Section</i>	<i>Page</i>
Statement of Originality	i
Preface	ii
Table of Contents	iii
List of Figures	vii
List of Schemes	x
List of Tables	xii
List of Supplementary Material	xii
List of Abbreviations	xiii
Acknowledgements	xvii
Preamble	xviii
Abstract	xix
1 Modular Synthesis of Dendritic Molecules	1
1.1 Introduction	2
1.1.1 Structure and Properties	2
1.1.2 Construction – Synthetic Strategies	3
1.1.2.1 Divergent Synthesis	4
1.1.2.2 Convergent Synthesis	5
1.1.2.3 Other Synthetic Approaches	5
1.1.3 Characterisation	6
1.1.4 Applications	6
1.1.5 Click Chemistry	8
1.1.6 Urea-Linked Dendrimers	10

1.1.7	Background to present work	15
1.2	Results and Discussion	16
1.2.1	Synthesis of the core	16
1.2.2	Synthesis of the dendrons	19
1.2.2.1	Protection of the branch point synthon	20
1.2.2.2	Attachment of peripheral units to branch point synthon	21
1.2.2.3	Deprotection of dendrons	25
1.2.3	Coupling of the dendrons to the trifunctional core	28
1.2.4	Coupling of the dendrons to the bifunctional core	32
1.2.5	Functional Group Interconversions on Dendritic Molecules	34
1.2.5.1	Hydrogenation – Nitro to Amino	34
1.2.5.2	Ether Cleavage	37
1.2.6	Summary	39
1.3	References	40
2	Self-Assembled Monolayers on Gold	47
2.1	Introduction	48
2.1.1	Functioning Devices	48
2.1.2	Substrate Choice – Why Gold?	49
2.1.3	Self-Assembled Monolayers	50
2.1.3.1	SAMs of Thiols on Gold	51
2.1.3.1	Application of SAMs	52
2.1.4	Patterning Techniques for SAMs	52
2.1.4.1	UV Lithography	52
2.1.4.2	Microcontact printing	54
2.1.4.3	Other Patterning Techniques	54

2.1.5	Chemical Reactions and Transformations on Surface of SAMs	55
2.1.6	Attachment of Proteins to Surfaces	56
2.1.7	Techniques for the Characterisation and Analysis of Surfaces	57
2.1.7.1	Contact Angle Measurements	57
2.1.7.2	IR Spectroscopy of Surfaces	58
2.1.7.3	X-ray Photoelectron Spectroscopy	59
2.1.7.4	Atomic Force Microscopy	60
2.1.7.5	Fluorescence Microscopy	61
2.1.8	Fluorescent Markers	62
2.1.8.1	Fluorescein	62
2.1.8.2	Green Fluorescent Protein	63
2.1.9	Background to Present Work	64
2.2	Results and Discussion	67
2.2.1	Preparation of Gold Surfaces	68
2.2.2	Chemical Synthesis of SAM Monomers (Adsorbates)	69
2.2.2.1	N-hydroxysuccinimide Monomer	69
2.2.2.2	Tri(ethyleneglycol) Monomer	70
2.2.2.3	Acyl Azide Monomer	71
2.2.3	Formation and Characterisation of Monolayers on Gold	
–	GFP Studies	77
2.2.4	SAM Patterning Trials	80
2.2.5	Attachment of GFP to SAM	85
2.2.6	Heat Activated SAM	89
2.2.7	Summary	93
2.3	References	94

3	Synthesis of Heterobifunctional Linkers	101
3.1	Introduction	102
3.1.1	Amine Reactive Functionalities	103
3.1.2	Irreversible Thiol Reactive Functionalities	104
3.1.3	Examples of Heterobifunctional Thiol/Amine Cross-Linkers	106
3.1.4	Background to Present Work	110
3.2	Results and Discussion	112
3.2.1	Synthesis of Known Maleimide/NHS linkers	112
3.2.2	Attempted Synthesis of Novel Maleimide/NHS Linker	118
3.2.3	Synthesis of Crown-Ether for Protein Modification	126
3.2.4	Further Applications	128
3.2.5	Summary	129
3.3	References	131
4	Concluding Comments	134
5	Experimental	140
5.1	General Procedures	141
5.2	Chapter One	144
5.3	Chapter Two	168
5.4	Chapter Three	176
5.5	References	190
	Appendix A Crystal Structure Data	192
	Appendix B XPS Data	200

List of Figures

<i>Section</i>	<i>Page</i>
Chapter 1	
Figure 1-1. Diagram of dendritic structure highlighting the three architectural regions	3
Figure 1-2. Schematic representation of divergent and convergent synthetic strategies	4
Figure 1-3. Schematic representation of the host-guest systems	11
Figure 1-4. Urea-linked dendritic wedges on amine terminated beads	14
Figure 1-5. Comparison of ^1H NMR spectra (400 MHz, toluene- d_8) of a) acyl azide core 14 and b) after conversion to the isocyanate 15 via the Curtius rearrangement	17
Figure 1-6. ^1H NMR spectrum (400 MHz, DMSO- d_6) with expanded excerpt of $^1\text{H}/^{13}\text{C}$ gHMBC spectra of 17 showing the cross-peaks correlating to the NH protons and the carbonyl carbon of the urea linkage	19
Figure 1-7. ^1H NMR spectrum (400 MHz, DMSO- d_6) of 25	22
Figure 1-8. ORTEP diagram for the molecular structure of 26	23
Figure 1-9. ORTEP diagram for the molecular structure of 35	27
Figure 1-10. ^1H NMR spectrum (400 MHz, DMSO- d_6) of 39	28
Figure 1-11. Expansion of the $^1\text{H}/^{13}\text{C}$ gHMBC spectrum of the nitro 9-mer, 41 (400 MHz, acetone- d_6). Basic ^1H and $^{13}\text{C}\{^1\text{H}\}$ spectra are provided as axial references with the cross-peaks correlating to the NH protons and the carbon of the central carbonyl of the urea linkage highlighted in blue	30
Figure 1-12. ESMS spectra of 43 in a) the positive mode, and b) lithium doped	31
Figure 1-13. ^1H NMR spectrum (400 MHz, DMSO- d_6) of 47	33
Figure 1-14. ^1H NMR spectra (400 MHz, acetone- d_6) comparing a) the hydrogenation product 50 [<i>p</i> -aminobenzoyl 9-mer] and b) the parent compound 41 [<i>p</i> -nitrobenzoyl 9-mer]	35
Figure 1-15. ^1H NMR spectra (400 MHz, DMSO- d_6) comparing a) the parent compound 42 [<i>p</i> -anisoyl 9-mer] and b) 52 after the ether cleavage reaction [<i>p</i> -phenoxy 9-mer]	38
Chapter 2	
Figure 2-1. Formation of a Self-Assembled monolayer	51

Figure 2-2. Schematic illustration of UV lithography as a patterning technique for thiol-SAMs on gold	53
Figure 2-3. Attachment of ferrocene to a SAM surface on gold via ‘Click-type’ chemistry	55
Figure 2-4. Diagram of a contact angle measurement	58
Figure 2-5. Schematic illustration of the principle of ATR spectroscopy	59
Figure 2-6. Diagram of AFM	60
Figure 2-7. Cartoon representation of Green Fluorescent Protein illustrating the β -barrel structure and the location of the chromophore within	63
Figure 2-8. Potential for preparation of functionalised surfaces using heat activated monolayer	66
Figure 2-9. Schematic illustration of the sputtering process with photograph	67
Figure 2-10. Schematic illustration of metal evaporation and photograph	68
Figure 2-11. AFM image of gold surface sputtered at 200°C	69
Figure 2-12. ESMS spectrum of 61	73
Figure 2-13. FTIR Spectrum of 62	75
Figure 2-14. ^1H NMR spectrum (400MHz, 298K, CDCl_3) of the purified SAM monomer, 59	76
Figure 2-15. Survey scans of a) 53 and b) 59 monolayer surfaces	79
Figure 2-16. a) silicon wafer square; b) metal mask with holes the size of TEM grids; c) the mask is placed on top of the silicon wafer square and placed in the sputterer; d) on removal from the sputterer the silicon square has four gold circles sputtered onto the surface	81
Figure 2-17. Topographical image (400 line resolution) of NHS/dodecanethiol SAM	82
Figure 2-18. Fluorescence microscope images of (a) a 30 minute UV patterned [through a 20 μm TEM grid] Dodecane/ <i>N</i> -hydroxysuccinimide surface after reaction with aminofluorescein, and (b) magnified image of the same type of surface patterned through a 100 μm TEM grid	83
Figure 2-19. AFM images obtained from the NHS+aminofluorescein/ dodecanethiol surfaces imaged under 2-butanol. a) Topographical image, b) lateral force	84
Figure 2-20. Higher resolution AFM image obtained from the dodecanethiol/NHS+ aminofluorescein surfaces imaged under 2-butanol (300 line resolution)	85
Figure 2-21. Diagram of the covalent attachment of GFP to the SAM	86
Figure 2-22. Fluorescence microscope images focussing in on the regions of GFP attached to the patterned surface	88

Figure 2-23. Schematic representation of heat activated SAM	89
Figure 2-24. Survey scans of a) acyl azide 59 monolayer surface and b) after heating for one hour in a solution of toluene	92
Chapter 3	
Figure 3-1. Cartoon representation of the bioconjugation process	103
Figure 3-2. Expansion of ¹ H NMR spectra (400MHz, DMSO- <i>d</i> ₆) showing the NH and alkene proton resonances of a) the <i>trans</i> isomer 82 and b) the <i>cis</i> isomer 79 of <i>trans</i> -4-([3-carboxyprop-2-enoyl]-amino)-methyl)-cyclohexane-carboxylic acid	114
Figure 3-3. ¹ H NMR (400 MHz, DMSO- <i>d</i> ₆) of 74	115
Figure 3-4. ORTEP diagram for the molecular structure of a) 79 and b) 74	116
Figure 3-5. ORTEP diagram for the molecular structure of 84	117
Figure 3-6. ORTEP diagram of the molecular structure of 89	119
Figure 3-7. Expansion of the aliphatic region of the gCOSY spectrum of 93	122
Figure 3-8. ESMS spectra of 98 in a) the positive mode and b) lithium doped	127
Figure 3-9. Representation of EYFP – DNA bioconjugate	129

List of Schemes

<i>Section</i>	<i>Page</i>
Chapter 1	
Scheme 1-1. Copper(I) catalysed synthesis of 1,4-disubstituted 1,2,3-triazoles	9
Scheme 1-2. Urea formation via reaction of isocyanate and amine	9
Scheme 1-3. Mechanism of the Curtius rearrangement	9
Scheme 1-4. Poly(propylene imine) urea functionalised dendrimers	10
Scheme 1-5. One-pot synthesis by Okinawa <i>et al.</i>	14
Scheme 1-6. Synthesis of core	16
Scheme 1-7. Test functionalisation of core	18
Scheme 1-8. <i>N</i> -Boc protection of TRIS	21
Scheme 1-9. Formation of <i>N</i> -BOC protected 3mers	21
Scheme 1-10. Formation of isonicotinoyl 3mer	23
Scheme 1-11. Formation of maleimidobenzoyl end group	24
Scheme 1-12. Formation of maleimidobenzoyl 3mer	25
Scheme 1-13. Deprotection strategies of 3mers	26
Scheme 1-14. Formation of functionalised dendritic molecules (9mers)	29
Scheme 1-15. Formation of functionalised dendritic molecules (6mers)	33
Scheme 1-16. Hydrogenation of the <i>p</i> -nitrobenzoyl 9mer to the <i>p</i> -aminobenzoyl 9mer	35
Scheme 1-17. Hydrogenation of the <i>p</i> -nitrobenzoyl 6mer to the <i>p</i> -aminobenzoyl 6mer	36
Scheme 1-18. Ether cleavage of the <i>p</i> -anisoyl 9mer to the <i>p</i> -phenoxy 9mer	38
Chapter 2	
Scheme 2-1. Synthesis of the <i>N</i> -hydroxysuccinimide SAM monomer	70
Scheme 2-2. Synthesis of the tri(ethyleneglycol) SAM monomer	71
Scheme 2-3. Attempted synthesis of acyl azide terminated SAM monomer – 1	72
Scheme 2-4. Synthesis of acyl azide end group	74
Scheme 2-5. Attempted synthesis of acyl azide terminated SAM monomer – 2	75
Scheme 2-6. Synthesis of acyl azide terminated SAM monomer	76

Chapter 3

Scheme 3-1. Traditional method for synthesis of SMCC	112
Scheme 3-2. Formation of cis and trans isomers 79 and 82	113
Scheme 3-3. Two step synthesis of 74	115
Scheme 3-4. Two step synthesis of 71	117
Scheme 3-5. Synthesis of extended linker 75	118
Scheme 3-6. Synthesis of amide spacer unit 88	118
Scheme 3-7. Attempted synthetic strategy for preparation of 85 – 1	119
Scheme 3-8. Byproduct from synthesis of amide spacer unit	120
Scheme 3-9. Synthesis of isolated byproduct from attempted synthesis of 85	121
Scheme 3-10. Synthesis of mono-BOC-ethylenediamine extended linker 93	122
Scheme 3-11. BOC deprotection of 93	123
Scheme 3-12. Attempted synthetic strategy for preparation of 85 – 2	124
Scheme 3-13. Synthesis of disuccinimidyl ester of succinic acid 92	125
Scheme 3-14. Attempted synthetic strategy for preparation of 85 – 3	126
Scheme 3-15. Synthesis of maleimide functionalised crown-ether 98	127

List of Tables

<i>Section</i>	<i>Page</i>
Chapter 2	
Table 2-1. Water contact angles for self assembled monolayer surfaces on Au	78
Table 2-2. Water contact angles for self assembled monolayer surfaces on Au	90
Chapter 3	
Table 3-1. Summary of Amine Reactive groups	104
Table 3-2. Summary of Thiol Reactive Functionalities	106

List of Supplementary Material

The CD included in the back cover pocket contains the crystallographic information files (CIFs) for the X-ray crystal structures reported in this thesis. The crystal data for the individual compounds is given in Appendix A.

List of Abbreviations

(-ve)	negative
(+ve)	positive
θ	angle
δ	chemical shift
$^{\circ}\text{C}$	degrees Celsius
Δ	heat
%	percentage
λ	wavelength
\AA	angstroms
AcOH	acetic acid
AFM	atomic force microscopy
Ag	silver
aq	aqueous
Au	gold
atm	atmospheres
bp	boiling point
BOC	tert-butoxycarbonyl
^{13}C NMR	Carbon-13 Nuclear Magnetic Resonance Spectroscopy
CHCl_3	chloroform
CDCl_3	<i>d</i> -chloroform
cm^{-1}	wavenumbers
conc.	concentrated
Cys	cysteine
d	doublet

D ₂ O	deuterium oxide
dec	decomposition
DCC	dicyclohexylcarbodiimide
DCM	dichloromethane
DCU	dicyclohexylurea
DMF	<i>N,N</i> -dimethylformamide
DMSO- <i>d</i> ₆	dimethyl- <i>d</i> ₆ sulfoxide
ESMS-	Electrospray Mass Spectrometry (negative ionisation mode)
ESMS+	Electrospray Mass Spectrometry (positive ionisation mode)
FTIR	fourier transform infra-red spectroscopy
g	gram
gCOSY	gradient correlation spectroscopy
GFP	green fluorescent protein
gHMBC	gradient heteronuclear multiple bond coherence
gHSQC	gradient heteronuclear single-quantum correlation
¹ H NMR	Proton nuclear magnetic resonance spectroscopy
H ₂ O	water
H ₂ O ₂	hydrogen peroxide
H ₂ SO ₄	sulphuric acid
HCl	hydrochloric acid
HPLC	high performance liquid chromatography
hrs	hours
Hz	hertz
IUPAC	International Union of Pure and Applied Chemistry
KBr	potassium bromide

KOH	potassium hydroxide
LiBr	lithium bromide
Lit.	literature
m	multiplet
M	moles per litre
MeOH	methanol
mg	milligram
MgSO ₄	magnesium sulphate
MHz	megahertz
ml	millilitre
mm	millimetre
mmol	millimole
mol	mole
mp	melting point
MS	mass spectrum
N ₂	nitrogen gas
Na ₂ CO ₃	sodium carbonate
NaHCO ₃	sodium hydrogen carbonate
NaOH	sodium hydroxide
NaN ₃	sodium azide
NHS	n-hydroxysuccinimide
nm	nanometer
NMR	nuclear magnetic resonance spectroscopy
<i>p</i> -	para
PAMAM	polyamidoamine

pH	$-\log[\text{H}^+]$
PNA	peptide nucleic acid
ppm	parts per million
RFE	rotary film evaporation
rt	room temperature
s	singlet
SAM	self assembling monolayer
Si	silicon
SMCC	succinimidyl 4-(N-maleimidomethyl)-cyclohexane-1-carboxylate
SMP	β -maleimidopropionic acid N-hydroxysuccinimide ester
t	triplet
TFA	trifluoroacetic acid
THF	tetrahydrofuran
TLC	thin layer chromatography
w/v	weight per volume

Acknowledgements

I could not have done this without the ongoing support and encouragement of my family and friends. A huge thank you to my husband Christopher for his continual positive outlook and encouragement. My fabulous sisters, Rachel and Amy, (I promised I'd put your names in!) and Harls my brother-in-law, I salute you all for your understanding and encouragement. Thanks also to my parents, Collin and Lorraine, for their unwavering faith in me. Last, but not least, I would like to thank in particular Dr Kathryn Fairfull-Smith, Dr Michelle McCleary and Ms Vicky Ellis for their invaluable support throughout.

I would like to thank my principal supervisor Dr Chris Brown, for his vision and guidance throughout my project. Additionally I also thank Dr Sue Boyd for her valuable help in editing this thesis and for her advice, both personal and professional. Thank you to Professor Peter Healy for his work towards my crystal X-ray data collection and structure determination. Thank you to Mr Mark Baker for initial guidance in the preparation of gold surfaces, and to Miss Bianca Heagney for technical assistance. A very big thank you goes out to Dr Jola Watson and Dr Greg Watson for their help with learning to drive the AFM and for helping with the collection of data and presentation of the images obtained. I would also like to thank Mr Ian Gentle from the Brisbane Surface Science Centre for his help with collecting XPS data on my surfaces. Throughout my candidature technical support was always available from Mr Alan White, Mr Ross Stevens and Mrs Dianne Carmody.

My candidature was funded by an Australian Postgraduate Award and a scholarship top-up funded by the CRC for microTechnology, for both I am truly thankful.

Preamble

Funding for this work was provided by the CRC for MicroTechnology. For the development of platform technologies, that would have applications in the construction of functional molecular devices. As such, the work presented in this thesis may initially seem diverse as it outlines foundation studies in three areas of chemical nanoscience. However, these areas are closely interrelated and all three, macromolecular assembly, surface modification and functional linker design are required for the assembly of any molecular device. Chapter one describes the synthesis and characterisation of a number of peripherally functionalized dendritic molecules with the potential to be functionalized as biosensor substrates, chemotherapeutic agents or drug transport vehicles. The range of functional groups used, and the functional group conversions achieved in the preparation of the dendritic molecules illustrates the potential scope for the use of the isocyanate-amine coupling reaction in the synthesis of highly ordered macromolecular dendritic systems. Chapter two describes preliminary studies in substrate design. It describes the methodology behind the covalent attachment of fluorescent proteins to self-assembled monolayers on gold surfaces. Once located on the surface these molecules may act as potential signalling agents in array based fluorescent biosensor devices, or high density molecular information storage arrays. Additionally chapter two describes preliminary studies towards the development of a new compound that could act as a novel heat activated SAM surface for the preparation of high density biomolecule arrays. Finally, chapter three investigated the synthesis of a number of heterobifunctional linking reagents and protein modification reagents to support both the work in the previous two chapters of this thesis as well as other projects occurring within the CRC for MicroTechnology.

Abstract

Chapter 1 includes a review on dendrimers, their synthesis and applications, with a particular focus on urea-linked dendritic species. The synthetic strategy utilised in this body of work was based on the preparation of a number of branched synthetic building blocks possessing differing terminal functionality. These branched dendrons, bearing three terminal residues and based on the cheap starting material tris(hydroxymethyl)aminomethane (TRIS) **23**, involved the coupling of 3.3 equivalents of an appropriately para-substituted benzoic acid chloride with BOC protected TRIS **24** in DCM in the presence of triethylamine. The *p*-nitro, *p*-methoxy and *p*-methyl benzoyl chloride starting materials were obtained commercially, whilst *N*-(4-carboxyphenyl)maleimide was synthesised according to literature procedures. The BOC protected dendrons (**25–27**, **34**) were synthesized in yields ranging from 50–92%. Deprotection of the BOC protected dendrons **25** and **26** in DCM with TFA, followed by the addition of 1M Na₂CO₃ afforded the TFA salts **35** and **36**, respectively. The corresponding free base amines **37** and **38** were obtained on further treatment of the TFA salts with sodium carbonate. Deprotection of the BOC protected dendrons **27** and **34** afforded the free amines **39** and **48** directly after treatment with sodium carbonate. Synthesis of functionalised branched molecules containing 6- and 9-peripheral functionalities was achieved by refluxing 2 or 3 equivalents of the free amine dendrons with the bi- or tri- functional isocyanate cores, **15** and **45**, in refluxing DCM, in most cases the products precipitated from the reaction mixture after 18 h and were isolated simply by filtration, otherwise the removal of the solvent from the reaction mixture afforded the spectroscopically pure product. Conversion of the peripheral nitro functionalised species **14** and **21** to the corresponding amines occurred smoothly via hydrogenation using 5% Pd/C under

elevated temperature and pressure (DMF, 55 °C, 600 psi) and afforded the polyamine 6-mer **51** in 92% yield and the 9-mer **50** in 90% yield, respectively. Similarly, conversion of the methoxy coated 9-mer **42**, to the corresponding phenolic compound (AlBr₃, dodecane thiol, DCM) afforded the 9-mer polyphenol **52** in an 87% yield. All compounds prepared were fully characterised and crystal structures were obtained for **26** and **35**.

Chapter 2 includes a review on self-assembled monolayers of organosulfur compounds on gold, applications, patterning techniques and techniques for the characterisation of these surfaces. A number of surface monomers were successfully synthesized, to be used for various surface functionalisations, including the formation of an amine reactive *N*-hydroxysuccinimide (NHS) disulfide **53**, *via* the DCC coupling of 11,11'-dithiobisundecanoic acid **54** with *N*-hydroxysuccinimide with an isolated yield of 30%. A novel protein-resistant monomer **58** was also synthesized from 11-undecanoic acid **55** *via* an acid chloride coupling with triethylene glycol monomethyl ether **58**, and isolated in a 72% yield. A number of attempts were made to produce an acyl azide SAM monomer **59**, with success finally achieved *via* the acid chloride coupling of 11,11'-dithiobisundecanoic acid **54** with 5-amino-1,3-benzenedicarbonyl diazide **62** to produce **59** with an isolated yield of ~30%. Gold surfaces were prepared on atomically flat silicon wafers using an argon sputterer. SAM films were formed on the gold surfaces *via* traditional solution based self-assembly methodology. A UV patterning protocol was developed, and a successful patterning trial using the NHS terminated monomer to backfill the UV exposed areas of a dodecane thiol monolayer was achieved and visualized using AFM and fluorescence microscopy after treating the surface with aminofluorescein. The covalent attachment of green fluorescent protein to the monolayer surface *via*

reaction with the NHS terminated monolayer was demonstrated. The fluorescence of the biomolecule was preserved. The formation of a monolayer using the acyl azide monomer **59**, was characterised by contact angle and XPS analysis. However, preliminary studies into the activation of the acyl azide surface into the reactive isocyanate were unsuccessful. There is however, significant scope for further investigations into this interesting surface technology.

Chapter 3 includes a review on heterobifunctional linker technology with a particular focus on amine and thiol reactive moieties and literature examples of heterobifunctional linkers of this type. Synthesis of heterobifunctional reagents such as **71** and **74** *via* a two step synthetic methodology involving the coupling of maleic anhydride with the parent amino-acids in acetic acid, followed by a one pot cyclisation and NHS esterification using DCC in DMF were successful, with overall yields of 9% and 32% respectively for the two reaction steps. The one pot extension of **74** with 6-aminohexanoic acid, followed by DCC, facilitated NHS esterification was achieved successfully in a yield of 30%. Attempts to extend **74** with the synthesised amino acid **88** were unsuccessful due to the insolubility of **88** in organic solvents. A different synthetic strategy was devised towards the synthesis of **85** with the coupling of **74** and mono BOC protected ethylene diamine **91** in DCM to give **93** in an isolated yield of 60%. Deprotection of the terminal amine was achieved *via* reaction with TFA in DCM however all attempts to prepare the free amine were unsuccessful. Subsequent attempts to couple **94** with both succinic anhydride and **92** were unsuccessful. A maleimide functionalized crown ether was synthesised as a molecule for protein modification via the reaction of **74** with 4'-aminobenzo-15-crown-5 **97** to produce **98** in an 80% yield. All compounds were fully characterised with crystal structures obtained for **74**, **79** and **89**.

CHAPTER ONE

MODULAR SYNTHESIS OF DENDRITIC MOLECULES

1.1 Introduction

Dendrimers^{1,2} and dendritic molecules are a unique class of macromolecules that differ greatly from more traditional linear and branched polymeric systems in both structure and observed properties. The term dendrimers (Gk *dendron* tree; *meros* part) graphically describes the characteristic branching architecture observed in this class of molecule.³ Since the initial report by Vögtle *et al.*⁴ in 1978, many different structural classes (families) and surface modifications of dendritic macromolecules have been reported. A large variety of building blocks sourced from organic, organometallic or inorganic chemistry have been employed for the construction of these systems, including biologically important molecules such as peptides,⁵ sugars⁶ and nucleic acids.⁷ An exponential growth of published material relating to dendrimer synthesis, characterisation, properties and applications has been observed over the past two decades, placing dendritic molecules at the forefront of research in many fields including organic and inorganic chemistry, materials science, nanotechnology and the biological sciences. A review article authored by Fréchet and Tomalia,⁸ provides a thorough historical account of the discovery and development of dendrimers and dendritic systems.

1.1.1 Structure and Properties

Dendrimers have characteristic features and unique properties that differentiate them from other polymers. They are highly ordered, regularly branched, globular ‘nanoparticles’ possessing diameters in the range ~1-10 nm⁹ and have a compact, precisely defined structure with a multipodent exterior.¹⁰ Their structure is divided into three distinct architectural components (Figure 1-1):

- 1) a central core or focal unit,
- 2) a regularly branched interior region emerging radially from the core and
- 3) terminal functional groups on the outer peripheral layer forming the surface of the dendrimer.

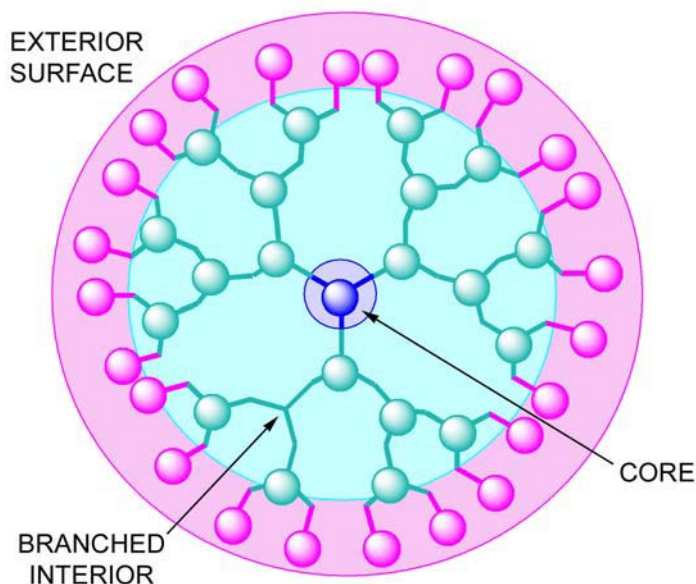


Figure 1-1. Schematic diagram of dendritic structure highlighting the three architectural regions.

1.1.2 Construction - Synthetic Strategies

Most methods of dendrimer synthesis iterate growth reaction and activation reaction cycles. This often makes for a difficult and tedious synthesis, however it can allow for elegant tailoring of architectural features.¹¹ Often these reactions have to be performed at many sites on the same molecule simultaneously, thus these reactions must be very ‘clean’ and high yielding if the construction of large ‘nano-molecules’ is to be a feasible goal. The choice of the growth reaction is also of fundamental importance since it dictates the way in which branching is introduced into a dendrimer. Synthetic strategies have been developed to vary the terminal groups, the

internal subunits and the core.⁵ There are two basic strategies that may be employed, either exclusively or in combination, in dendrimer synthesis: convergent and divergent growth.

1.1.2.1 Divergent Synthesis

The divergent approach is possibly the most widely used method and involves the reaction of a central core molecule with a branching molecule to produce G_0 (Generation 0), which is then reacted with other branching molecules to create further generations of growth (Figure 1-2). One major problem associated with this method is polydispersity, which arises from incomplete reaction and purification of components, leading to inseparable mixtures of macromolecules that become almost impossible to modify chemically in a controlled manner.¹² While polydispersity does not constitute a significant setback when used in ‘classical’ polymer-type applications, in more exacting applications, such as drug development it poses a severe limitation.

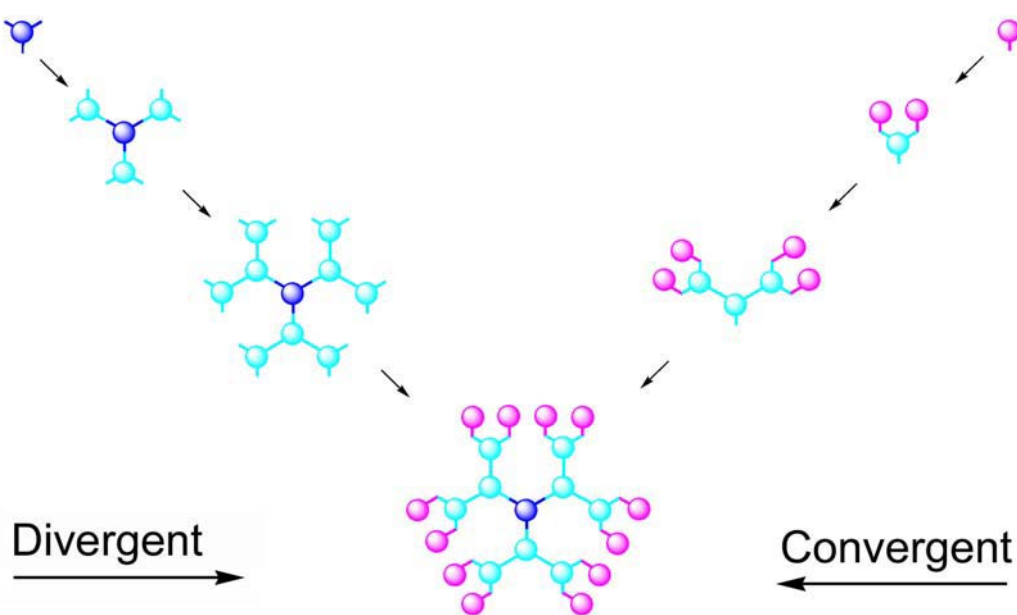


Figure 1-2. Schematic representation of divergent and convergent synthetic strategies.

1.1.2.2 Convergent Synthesis

The convergent method, pioneered by Fréchet,^{13, 14} was inspired by the classical organic disconnection approach. Growth begins with the exterior surface of the dendrimer, coupling of a terminal subunit to branching units pre-forms dendritic ‘wedges’, also termed dendrons, that are subsequently attached to a central poly-functional core subunit (Figure 1-2). Unlike the divergent method, the number of coupling reactions is constant per generation.⁵ There is more control over the focal point and the surface or terminal functional groups with the convergent approach compared to the divergent approach. The surface groups do not have to be of the same functionality using this method which can allow for the synthesis of non-uniform functionalised surfaces. In addition, the need for large excesses of reagents required for the divergent method is avoided which simplifies purification and lowers the cost.⁵ Convergent syntheses can, however, suffer from low yields that are often attributed to steric hindrance as the functional group at the focal points of the large wedges are masked by the growing macromolecule.¹⁵ This problem can be somewhat lessened by utilising monomers possessing more flexible geometries.

1.1.2.3 Other Synthetic Approaches

Research into the acceleration of long and tedious growth methodologies has resulted in the demonstration of hypercores,¹⁶ branched monomers,¹⁷ the two-step approach,¹⁸ self-assembling synthetic approaches⁶ and double exponential growth.¹⁹ These methods involve the pre-assembly of oligomeric species which can then be linked together to give dendrimers in fewer steps or higher yields, taking advantage of the best points of both the convergent and the divergent techniques.²⁰ The non-specific solid-phase synthesis of dendrimers has also been investigated allowing for peptides

and small molecules to be “grown” directly onto the periphery of the dendrimer while it was still attached to the resin bead.⁵

1.1.3 Characterisation

The elucidation of dendritic structures and properties can be approached either from the perspective of a synthetic or a polymer chemist. The size of the molecules involved means that methods familiar to synthetic chemists are stretched to their limits, while the methods used by polymer chemists are insufficiently precise.²⁰ Concurrent with developments in the synthesis of dendrimers are novel analytical techniques for their characterisation. The various analytical techniques that have been used to characterise dendrimers have been reviewed.²¹ These techniques include multinuclear NMR spectroscopy, various mass spectrometry methods, chromatographic methods especially gel permeation chromatography, electrophoresis, X-ray scattering, neutron scattering, small-angle neutron scattering, electron microscopy, ESR spectrometry and computational molecular dynamics. However, the direct observation and assessment of dendritic topology is difficult. To date, computer modelling studies have possibly provided the best insight into the three-dimensionality of dendritic systems.¹²

1.1.4 Applications

Previously, the focus of dendrimer research was to gain control over synthetic and structural aspects of dendrimers. Recently the focus has changed towards a more application-based approach. Flexibility in tailoring dendrimer structure and functionality has led to a diversity of applications. Consequently, dendrimers have become an important focus of interdisciplinary research. Their potential applications

rely, to a large extent, on their unique topologies and on properties attributable to their highly branched structures.

The structural precision and multimeric nature of dendrimers has motivated numerous studies aimed at biomedical applications^{7, 10} for example, as nucleic acid²² and drug delivery agents,^{23, 24} drug carriers (by small molecule encapsulation),²⁵⁻²⁷ molecular labels or signal amplification systems for microarrays or other assays,²⁸ probe moieties and cell surface targets,²² medical diagnostic reagents including magnetic resonance imaging agents,^{10, 22, 25} protein mimetics²² and for anti-cancer and anti-viral therapeutic applications.¹⁰

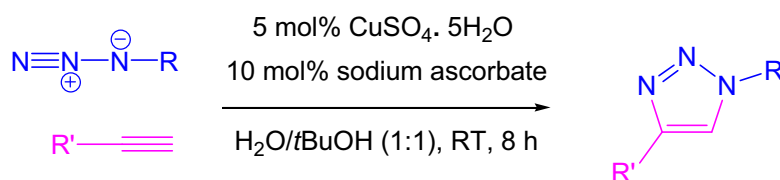
The highly compact and globular shape, as well as the uniform size, multifunctionality and the modularity of their assembly make dendrimers ideal molecular building blocks for materials science including self-assembled monolayers,^{11, 29} Langmuir films³⁰ and multilayers³¹ and other surface confined assemblies^{32, 33} with applications in microelectronic materials research³⁴ including components of photochemical switches³⁵ or in chemical and biological sensing.³⁶⁻³⁸ Monolayers of dendrimers have been prepared on surfaces for various applications,^{39, 40} such as resists for scanning probe lithography,⁴¹ as a biomolecular interface for the binding of proteins to surfaces⁴² and for creating patterns on surfaces using dip-pen nanolithography.⁴³

Other uses for these well defined, unique macromolecules include nanoscale reaction vessels, molecular-scale catalysis,⁴⁴ micelle mimics possessing cavities capable of

accommodating guest molecules ('dendritic box'),¹¹ adhesives,⁴⁵ separation media,⁴⁶ and as a support in organic synthesis.¹⁰

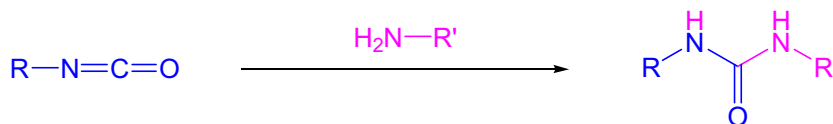
1.1.5 Click Chemistry

Click chemistry as defined by Sharpless,⁴⁷ encompasses a set of powerful, highly reliable and selective chemical reactions. A high thermodynamic driving force gives these reactions highly desirable characteristics including, rapid completion of a reaction that is highly selective for a single product; generating high yields and few, if any by-products. Ideally reaction conditions are mild, insensitive to oxygen and water and use simple product isolation and non-chromatographic purification methods. Carbon-heteroatom bond forming reactions comprise the most common examples, specifically cycloaddition reactions and carbonyl chemistry of the "non-aldol" type, such as the formation of ureas, *vide infra*. This is more a revival of classical chemistry than an emerging area of chemistry, however there are numerous potential applications in modern organic chemistry,⁴⁷⁻⁴⁹ supramolecular chemistry,⁵⁰ drug discovery,⁵¹ bioconjugation chemistry⁵² and materials science.⁵³ To date, the literature describing click chemistry in relation to dendrimer synthesis is limited to only a few papers that mainly focus on the Cu(I) catalysed coupling reaction of azides with terminal acetylenes (Scheme 1-1).^{50,54,55} Libraries of structurally diverse dendritic components have been prepared in almost quantitative yields under very mild conditions.⁵⁶ Lee *et al.* have also utilised this reaction in dendrimer synthesis,⁵⁷ initially reacting a tripodal acetylene core with Fréchet-type azido-dendrons to form 1,4-disubstituted triazole dendrimers.⁵⁸ Further work by the same group also reversed the functionality and a tripodal azide core was coupled to Fréchet-type acetylenic-dendrons.⁵⁹ Both strategies reported high yields and purity of dendrimers.



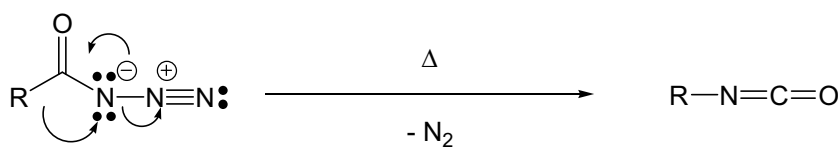
Scheme 1-1. Copper(I)-catalysed synthesis of 1,4-disubstituted 1,2,3-triazoles.

Isocyanates are highly reactive molecules that when added to primary or secondary amines produce ureas (Scheme 1-2) in a pure fusion process; that is, the combined formulae of the reactants equals the formula of the product. Isocyanates also react with alcohols to form carbamates.



Scheme 1-2. Urea formation via reaction of isocyanate and amine.

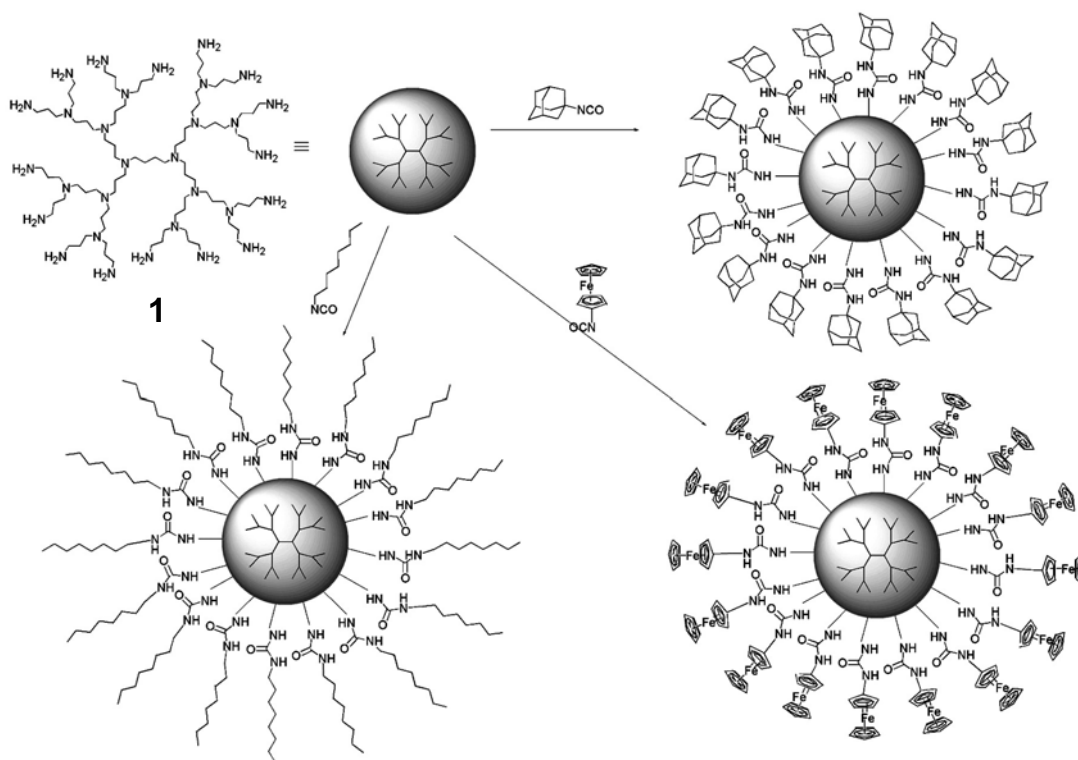
The isocyanate group is easily masked as a carbonyl azide (acyl azide) group. The advantage of this lies in the stability of the compounds at room temperature, ease of purification and that only the application of heat is required for quantitative conversion to the reactive isocyanate group *via* the Curtius Rearrangement (Scheme 1-3). This rearrangement releases gaseous N_2 as a side product, so there is no contamination of the isocyanate product. Quantitative conversion is achieved when no water is present to competitively hydrolyse the isocyanate to the amine.⁶⁰



Scheme 1-3. Mechanism of the Curtius Rearrangement.

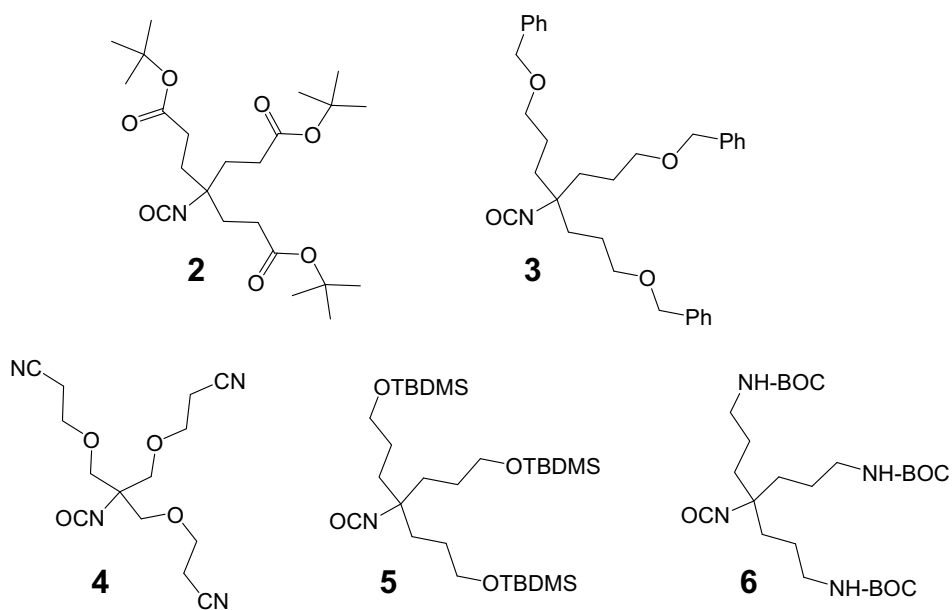
1.1.6 Urea-Linked Dendrimers

The first reported synthesis of a hyperbranched or dendritic polymer based on urea linkages was published by Kumar and Meijer in 1998.⁶¹ Since then, much of the literature on urea-containing dendrimers is attributed to the functionalisation of amino terminated dendrimers with molecules displaying an isocyanate moiety. Typically, this involves the functionalisation of commercially available poly(propyleneimine) dendrimers **1**, (Scheme 1-4) to form ferrocenyl-urea dendrimers,⁶² lipophilic dendrimers *via* hexyl, octyl and dodecyl⁶³ and phenyl urea^{64, 65} adamantane-urea⁶⁶ and adamantane-thiourea⁶⁷ functionalised dendrimers and liquid crystalline forming oligo(*p*-phenylene vinylene)-urea dendrimers.⁶⁸



Scheme 1-4. Poly(propylene imine) urea functionalised dendrimers.

Similarly, Newkome *et. al.*^{69, 70} functionalised the periphery of fourth generation poly(propylene imine) dendrimers with branched isocyanate building blocks **2-6**.



These urea terminated poly(propylene imine) dendrimers have been demonstrated to be suitable motifs for host-guest interactions (Figure 1-3).⁷¹ Complexation on the dendrimer periphery of either a carboxylic, phosphonic or methane sulfonic acid guest is enabled by a combination of multivalent hydrogen bonding between the urea parts of the guest and host and electrostatic interactions between the tertiary amines of the host and the acidic part of the guest.⁷²

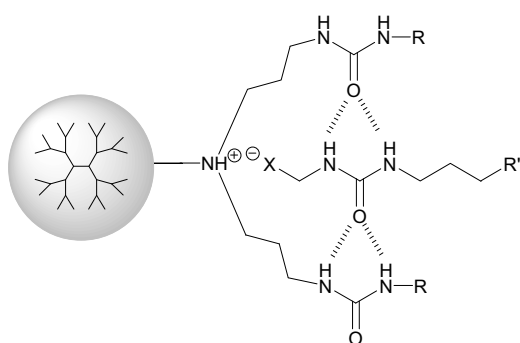


Figure 1-3. Schematic representation of the host-guest systems, where $X = \text{COO}^-$, $\text{PO}(\text{OH})\text{O}^-$ or SO_3^- .

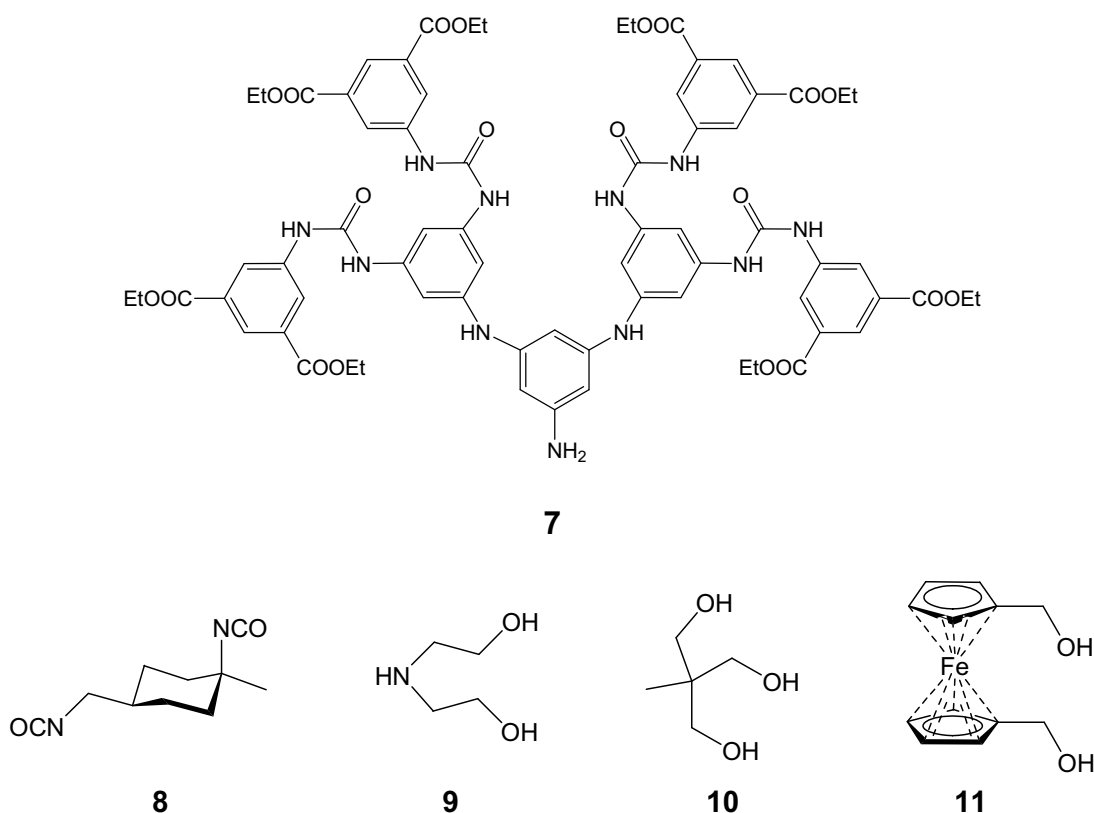
Reported guest molecule functionalities include:

- 1) phosphine ligands that act as a multi-ligand system for palladium-catalysed allylic amination reactions,⁷³
- 2) oligo(*p*-phenylene vinylene)s as an improved system in the formation of light emitting diodes,⁷⁴
- 3) poly(ethyleneglycol) terminated guest molecules⁷⁵ that allows for the noncovalent formation of supramolecular dendritic architectures in water,⁷⁶
- 4) *N*-BOC protected peptide sequences to form chloroform-soluble complexes where the complete peptide sequences are released under mildly acidic conditions,⁷⁷
- 5) an *N*-BOC protected L-phenylalanine spacer moiety to investigate chirality in supramolecular dendrimer complexes.⁷⁸

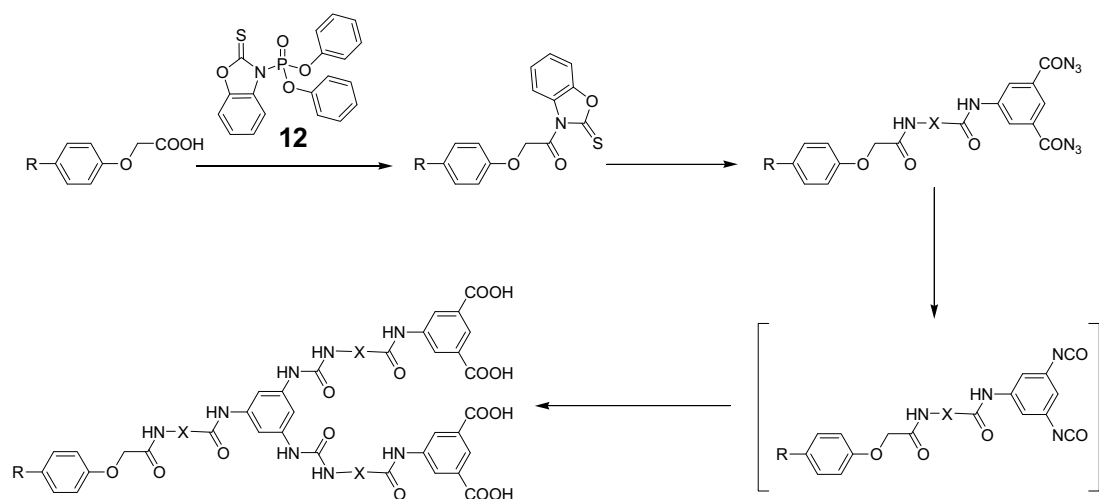
Significantly less literature is available on the actual linking of dendritic units *via* a urea linkage. Ambade and Kumar⁷⁹ reported a convergent synthesis of dendritic wedges and hyperbranched polymers using this methodology. Their stepwise synthesis, involved the coupling of the terminal amine group, with a BOC protected amino diisocyanate. Deprotection of the amine by removal of the BOC group and reaction with another BOC protected amino diisocyanate afforded the wedge **7**. Other syntheses of urea-linked 'classical' hyperbranched polymeric systems have also been reported.^{61, 80}

Peerlings *et al.*⁸¹ report a fast and simple synthetic procedure for the synthesis of polycarbamate/urea linked dendrimers. The divergent synthetic method is based on a diisocyanate building block, *cis*-4-isocyanatomethyl-1-methylcyclohexylisocyanate **8**, with diethanolamine **9** as the branching unit, and either an organic (1,1,1-

tris(hydroxymethyl)ethane **10**), or organometallic (1,1'-ferrocenedimethanol **11**), based core reagent.



Okaniwa *et al.*^{82, 83} have reported a divergent synthesis of poly(amide-urea) linked dendrimers of up to four generations. Their cyclic one-pot synthetic procedure proceeds in several steps (Scheme 1-5). Treatment of a terminal carboxylic acid with diphenyl(2,3-dihydro-2-thioxo-3-benzoxazolyl)phosphonate (DBOP) **12**, provides an activated amide equivalent. Treatment of the activated species with an amine terminated aminodicarbonyl azide provides a branch point precursor which is readily rearranged to the active diisocyanate on warming. Further treatment with an amine terminated dicarboxylic acid furnishes an extended, branched system with terminal carboxylic acids that may be extended in turn.



Scheme 1-5. One-pot synthesis by Okaniwa *et al.* where $X = -C_6H_6CH_2CH_2-$.

Lebreton *et al.*⁸⁴ report the solid phase divergent synthesis of dendritic wedges on amino terminated polystyrene beads (Figure 1-4). This procedure allows for cleavable and non-cleavable products that have the potential for increasing single-bead loading capacities. The synthetic procedure alternates between a growth step and a deprotection step of the terminal amines.

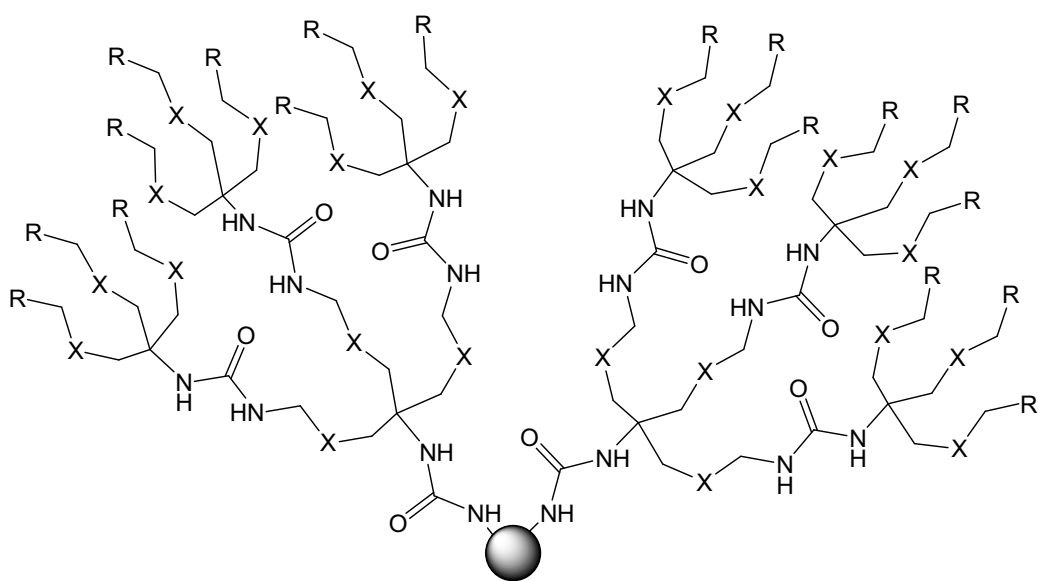


Figure 1-4. Urea-linked dendritic wedges on amine terminated beads.

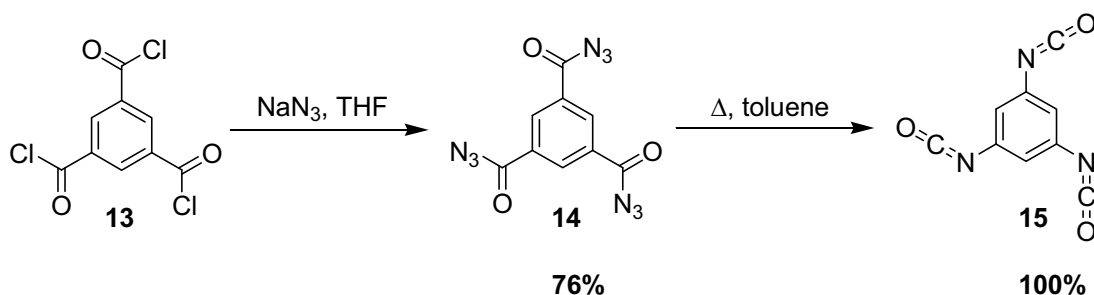
1.1.7 Background to Present Work

A rising demand for well-defined, functional materials for nano-scale applications has stimulated the development of synthetic procedures for the efficient assembly of dendritic and polymeric species. This work investigates the design, synthesis and characterisation of components for the construction of dendritic molecules with differing peripheral functionality. The designed systems are highly symmetrical dendritic molecules, that are based on an AB₃ branched wedge. The methodology reported here could however, be extended for the synthesis of larger, dendritic structures or dendrimers. The coupling strategy for linking the dendrons to the central core is based on 'click chemistry' principles, utilising the quantitative coupling of isocyanates with amines. The synthetic scheme is based on convergent growth and the use of a coupling reaction that is both quantitative and eliminates the need for chromatographic purification. An added advantage is the thermal activation of the coupling reaction that releases only gaseous side products. This precludes the use of any extra reagents or catalysts, consequently there is little contamination of the final product. These novel dendritic molecules were synthesised as prototype molecular scaffolds, possessing a range of chemically attractive peripheral functionalities, for subsequent applications in materials science and biological chemistry.

1.2 Results and Discussion

1.2.1 Synthesis of the Core

Synthesis of 1,3,5-benzenetricarbonyl triazide **14**, was carried out by the reaction of 1,3,5-benzenetricarbonyl trichloride **13** with sodium azide in THF according to a literature procedure⁷⁹ (Scheme 1-6). Extraction of the reaction mixture with diethyl ether and subsequent removal of the solvent *in vacuo* at room temperature (<30°C) afforded **14** as a white solid in a 76% yield (Lit.⁷⁹ 71%). Characterisation of this material by NMR (¹H and ¹³C) and IR spectroscopy gave results consistent with those published for **14**.^{79, 85} Given the volatility and potentially explosive nature of **14** in the solid state under heat or pressure,⁸⁵ the compound was stored in the freezer (at ~ -20°C) and due care was taken when in use. Only small quantities of this compound were used at any one time and the compound was always dissolved in solvent under an atmosphere of nitrogen before any heat was applied.



Scheme 1-6

Heating **14** in refluxing, dry toluene under an atmosphere of nitrogen resulted in the quantitative formation of 1,3,5-benzene triisocyanate **15** (Scheme 1-6) *via* the Curtius rearrangement (refer to Scheme 1-3 for mechanism). Characterisation of compound **15** by ¹H and ¹³C NMR spectroscopy were consistent with published data.⁸⁵ The diagnostic upfield change in the chemical shift of the aromatic proton resonance, attributable to the conversion of **14** (8.6ppm) to **15** (5.7ppm), are

highlighted in the ^1H NMR spectrum (Figure 1-5). This drastic change in chemical shift, due to the electron donating nature of the isocyanate group, was used routinely as a diagnostic tool to verify that the reaction had proceeded to completion.

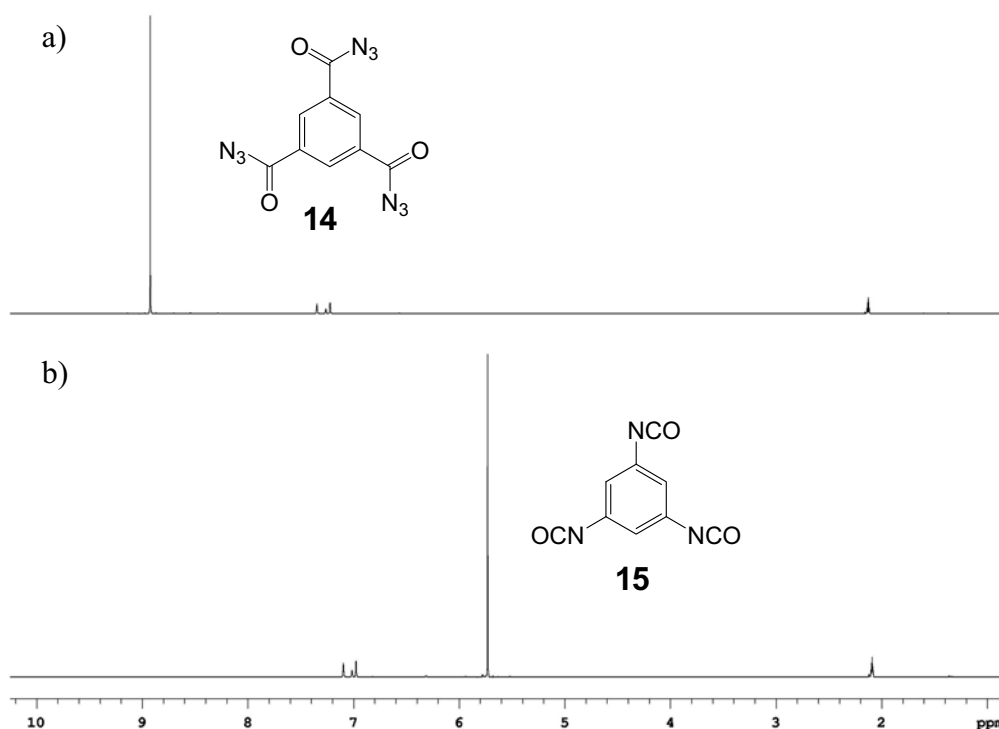
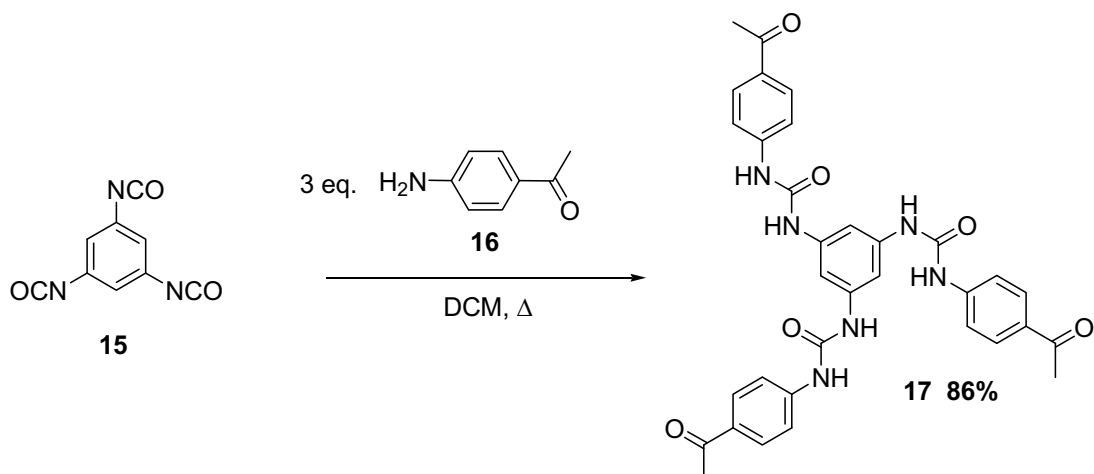


Figure 1-5. Comparison of ^1H NMR spectra (400 MHz, $\text{toluene-}d_8$) of a) acyl azide core **14** and b) after conversion to the isocyanate **15** via the Curtius Rearrangement.

The viability of the formation of dendritic molecules using this core was tested using *p*-aminoacetophenone **16**. Accordingly, 3 equivalents of **16** were added to a toluene solution of the triisocyanate **15** (formed *in situ*). Initial attempts at the coupling were hampered by the poor solubility of **16** in toluene at room temperature. However, under gentle reflux a precipitate began to form within 12 minutes of the addition of **16** to the toluene solution of **15** and the reaction was left to stir for a further 18 hours before collecting the precipitated material by filtration. NMR analysis of this precipitate showed a mixture of the starting materials, however some product formation was evident due to the appearance of the NH signals attributable to the

urea bond. Incomplete conversion to the product in this instance was attributed to the insolubility of **16** in toluene. The reaction was therefore repeated with the removal of toluene *in vacuo* after initial formation of the triisocyanate core **15**. Three equivalents of *p*-aminoacetophenone **16** dissolved in DCM were added to the isolated triisocyanate core **15** and the mixture gently refluxed for 18 hours (Scheme 1-7) whereupon a white precipitate was evident. The product was collected by filtration, washed with ethyl acetate (to remove any unreacted starting materials) and dried affording the stoichiometric product **17** in an 86% yield and very high purity, as assessed by ^1H NMR.



Scheme 1-7

Spectral analysis of this compound by NMR gave results consistent with those expected for 1,3,5-tris-((4-methoxyaniline)carbonylamino)benzene **17** and the ESMS in the negative mode showed peaks consistent with the desired product, $[\text{M}^-]$ (605 amu). Signals corresponding to the lithium (613 amu) and sodium (629 amu) adducts respectively in the positive mode were also evident. Microanalysis results however attested to the hygroscopic nature of this material as, despite rigorous drying of the product, the elemental analysis was consistent with the incorporation of one water

molecule *i.e.* C₃₃H₃₀N₆O₆·H₂O. Further confirmation of the formation of the urea linkages was evidenced by 2D NMR spectroscopy. Figure 1-6 shows an excerpt of the gHMBC spectrum highlighting the correlation between the NH resonances of the urea-linkage in the proton NMR with the C=O peak of the urea in the carbon NMR, confirming the structural analysis.

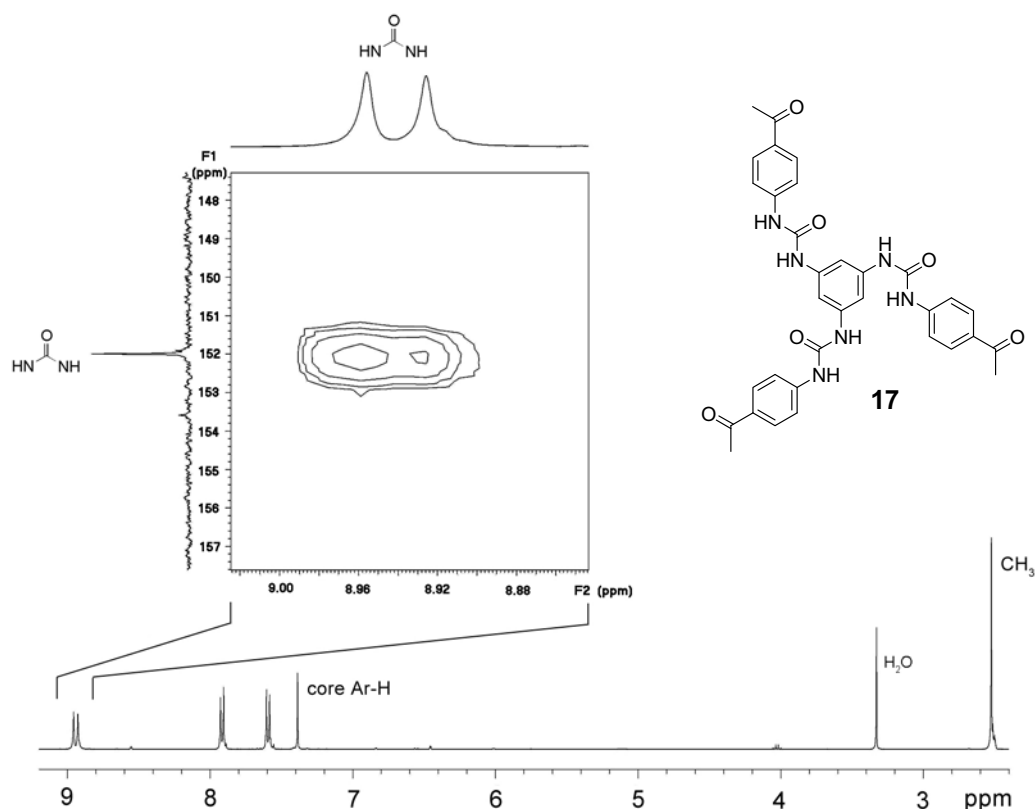
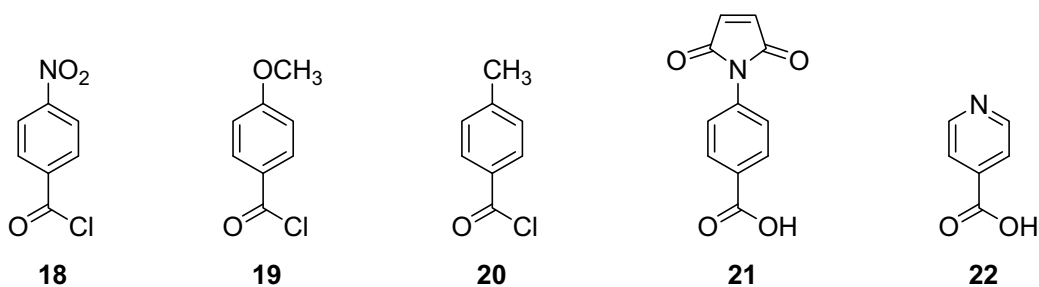


Figure 1-6. ¹H NMR spectrum (400 MHz, DMSO-*d*₆) with expanded excerpt of ¹H/¹³C gHMBC spectra of **17** showing the cross-peaks correlating to the NH protons and the carbonyl carbon of the urea linkage.

1.2.2 Synthesis of the dendrons

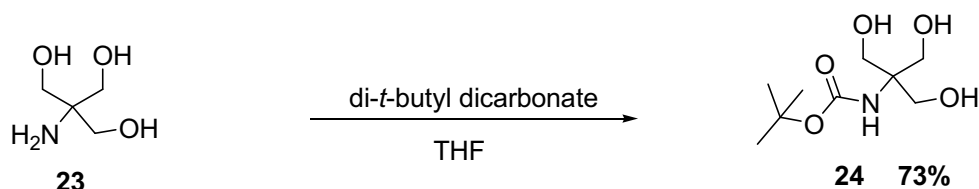
The dendritic wedges are based on tris(hydroxymethyl)methylamine (TRIS) **23** as this has been successfully used as a branch point in other dendrimer syntheses.⁶ The molecule is inherently suited to dendritic syntheses due to its symmetrical nature, the three primary hydroxyl groups are available for further functionalisation and its

single amine can act as the focal point of the branching unit. The functional groups that were selected for attachment to TRIS **23**, and consequently form the periphery of the dendritic wedges, were *para*-substituted benzoic acids or benzoyl chlorides **18-22**. All these materials were commercially available or readily synthesised, each possessing functionality enabling them to be useful in the construction of more elaborate macromolecular systems. These included a maleimide group (**21**) to enable the attachment of thiol-substituted bio- or bioactive- molecules; a nitro group (**18**) that can be used as hydrogen bond acceptor and can also be reduced to amines, which are particularly interesting as they can act as targets for the attachment of bioactive molecules via heterobifunctional linking reagents. In addition, the methyl ether group (**19**) can be cleaved to give a phenol and the isonicotinoyl group (**22**) can act as an hydrogen bond acceptor species.



1.2.2.1 Protection of the branch point synthon

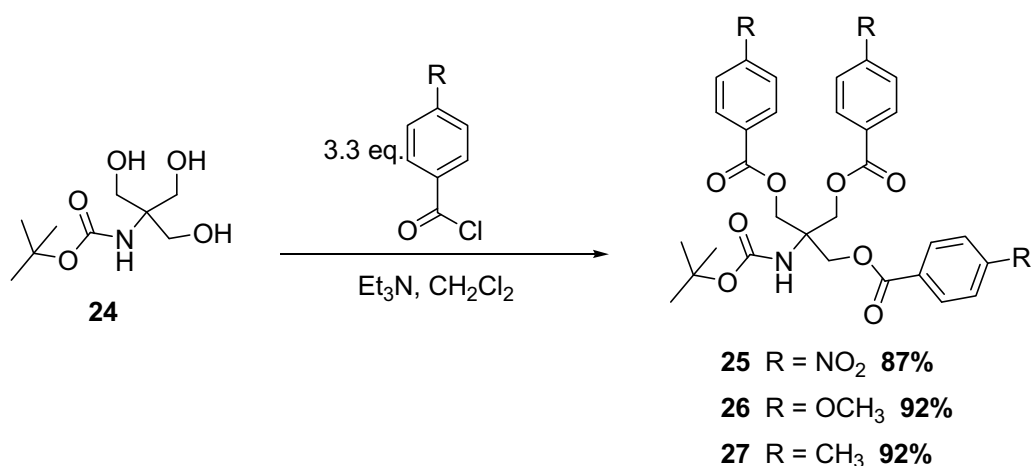
Synthesis of the dendritic wedges begins simply with the protection of the primary amine of TRIS **23**, by stirring in a THF solution of di-*tert*-butyl dicarbonate at room temperature (Scheme 1-8). The pure product precipitated from solution and was collected by filtration and analysed using standard techniques (mp, MS, ¹H and ¹³C NMR) providing results consistent with reported literature values,⁸⁶ confirming the formation of *t*-BOC-TRIS **24** in a 73% yield.



Scheme 1-8

1.2.2.2 Attachment of peripheral units to branch point synthon

Attachment of the functionalised benzoyl groups to the three primary hydroxyl groups of *t*-BOC-TRIS **24**, via an acid chloride coupling reaction, to form AB₃ branched ester-linked monomers, referred to from this point on as ‘3-mers’, was straightforward in most cases.



Scheme 1-9

Typical reaction conditions are illustrated in the synthesis of the *t*-BOC protected *p*-nitrobenzoyl 3-mer **25** (Scheme 1-9). A DCM solution of 3.3 equivalents of *p*-nitrobenzoyl chloride **18** was added dropwise to a dry DCM solution of *t*-BOC-TRIS **24** with triethylamine present as a base. The mixture was gently refluxed for 20 hours, subjected to work up and the resultant crude product purified by column chromatography, affording **25** in an 87% yield. Evidence for the formation of **25** was

obtained in the mass spectrum with peaks observed at 675 amu (M+Li) and 691 amu (M+Na). The IR spectrum also displayed bands consistent with ester linkages (1725 cm^{-1} , C=O; 1276 cm^{-1} , C-O-C). Microanalysis results for **25** and all following novel compounds, unless otherwise specified, were consistent with calculated values. NMR spectra attest to the symmetrical nature of the compound (Figure 1-7).

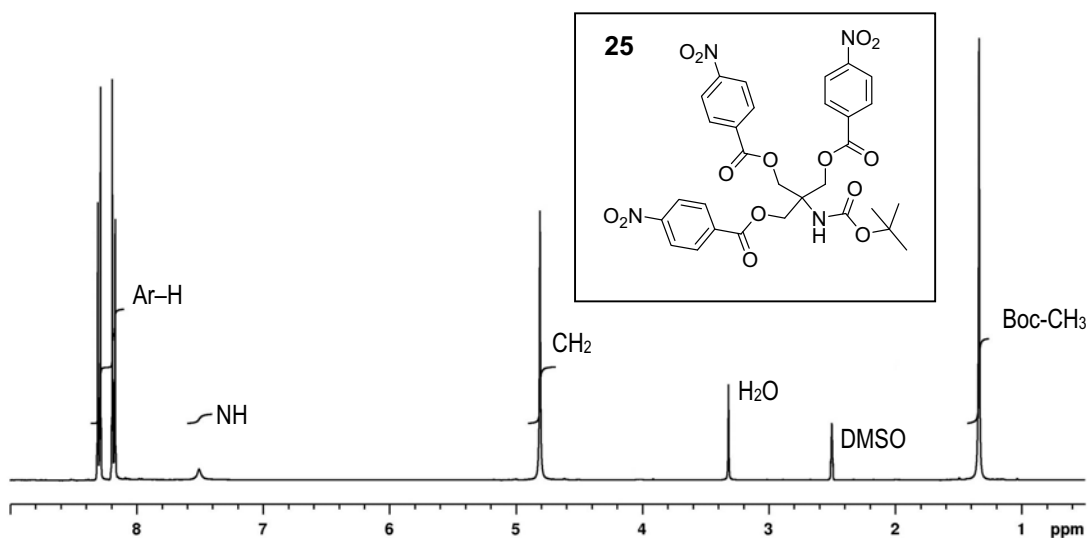


Figure 1-7. ^1H NMR spectrum (400 MHz, $\text{DMSO-}d_6$) of **25**.

Synthesis of the *p*-anisoyl and *p*-toluoyl 3-mers followed a similar procedure (Scheme 1-9) and afforded the pure *t*-BOC protected 3-mers **26** and **27** in a high yield (92% for both compounds) after purification by column chromatography. In both cases, IR spectra confirmed the formation of the ester bonds and peaks corresponding to the sodium and lithium adducts of **26** (647 and 630 amu) and **27** (598 and 582 amu) were present in their mass spectra. The ^1H NMR of these compounds were similar to that acquired for **25** with additional resonances attributable to the terminal CH_3 resonance of the anisoyl (3.82ppm) and toluoyl (2.36ppm). Crystals of the *p*-anisoyl 3-mer **26**, suitable for X-ray diffraction were grown by the diffusion method from DCM/ether (Figure 1-8).

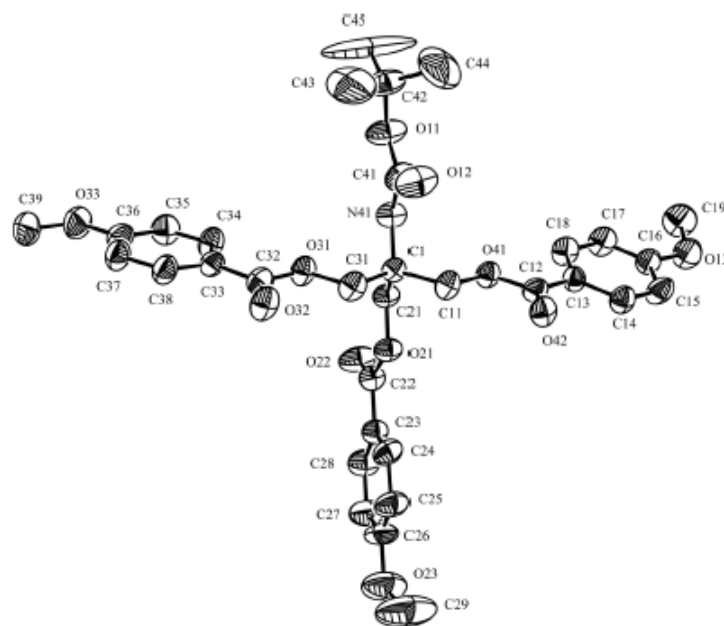
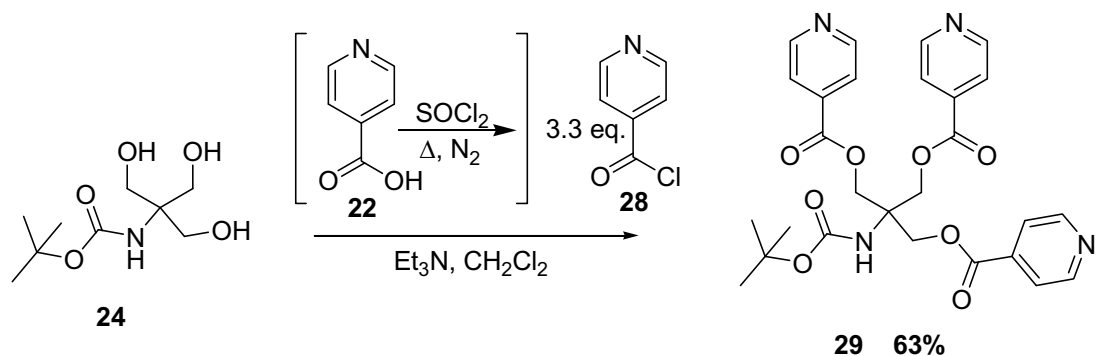


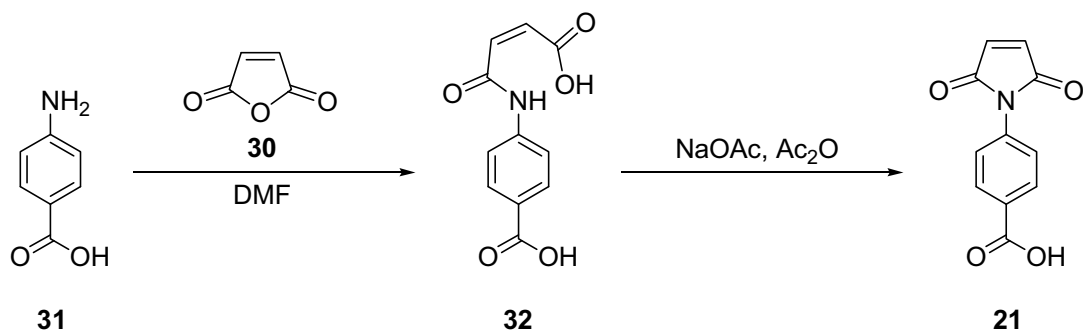
Figure 1-8. ORTEP diagram for the molecular structure of **26**.

Synthesis of the isonicotinoyl 3-mer (Scheme 1-10) began with the preparation of isonicotinoyl chloride **28**. Refluxing isonicotinic acid **22** in thionyl chloride for two hours under an atmosphere of nitrogen, followed by removal of the excess thionyl chloride provided the required synthon **28**. 3.3 equivalents of this material was added gradually, as a solid, to **24** in DCM/ Et_3N . After filtration to remove the precipitated triethylamine hydrochloride and work up, the residue was recrystallised (DCM, Et_2O and petroleum spirits 40-60°C) and the pure product, **29** isolated as a low melting, glassy, yellow solid in a 63% yield. Evidence for the formation of **29** was observed in the ESMS in positive mode [537 amu (M^+) and 543 amu (M^+Li)]. The NMR data was again consistent with previous examples.



Scheme 1-10

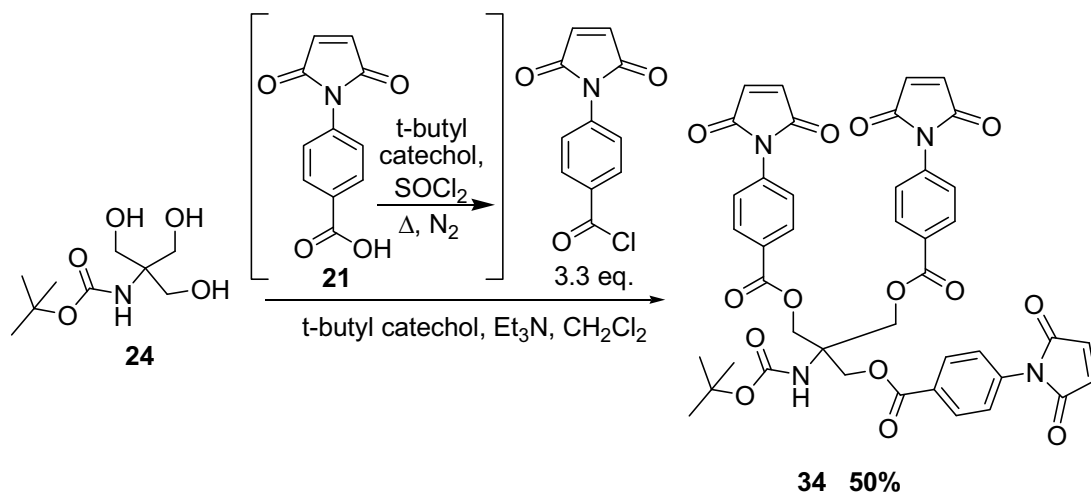
The peripheral maleimide group **21**, was synthesised following a literature procedure⁸⁷ (Scheme 1-11). The maleamic acid **32**, was obtained from maleic anhydride **30**, and *p*-aminobenzoic acid **31**, with subsequent intramolecular ring closure to form the maleimide **21**. Both compounds were characterised by standard techniques providing results consistent with those published.⁸⁷



Scheme 1-11

The initial attempt to synthesise the *p*-maleimidobenzoyl 3-mer **34** (Scheme 1-12) followed a similar procedure to that used for the isonicotinoyl 3-mer. **21** was heated in refluxing thionyl chloride to form the corresponding acid chloride. The excess thionyl chloride was removed *in vacuo*, and the resultant solid was added in portions to the branch point synthon **24**. During the work up of the reaction however, a

gelatinous red substance was seen to separate from the reaction mixture during the sodium bicarbonate and sodium chloride washes. Consequently, only a 13% yield of **34** was isolated after purification by column chromatography (10% EtOAc/DCM). Maleimides are renowned as self-initiating monomers of free radical polymerisation⁸⁸ and this was presumably occurring during the course of these reactions causing the formation the red, polymeric gel. Therefore, in order to suppress the polymerisation of the maleimide, a radical polymerization inhibitor, *t*-butyl catechol, was added prior to the commencement of each reaction.⁸⁷ On work up, significantly less gelatinous by-product was observed in the mixture and a yield of 50% of **34** was obtained after purification. Electrospray mass spectrometry in the positive mode revealed the lithium and sodium adducts of **34** at 825 amu and 841 amu respectively.

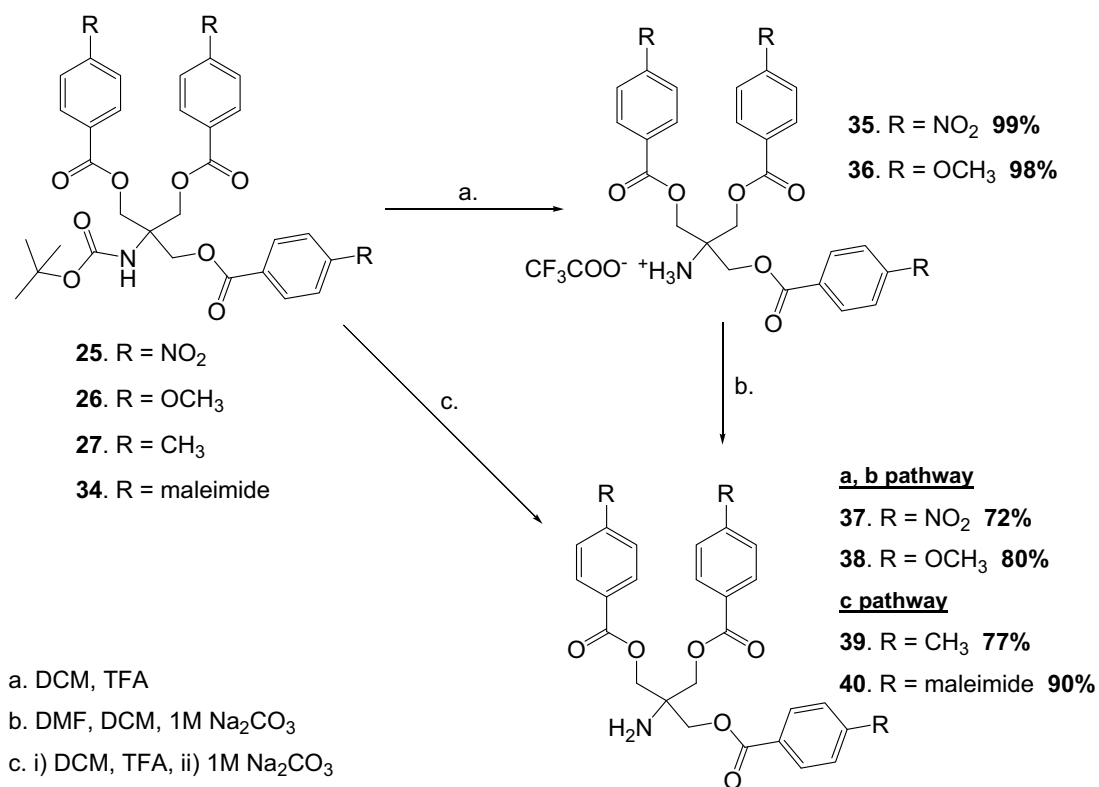


Scheme 1-12

1.2.2.3 Deprotection of dendrons

Deprotection of the *p*-nitrobenzoyl 3-mer **25** (Scheme 1-13) was performed by adding trifluoroacetic acid (TFA) to a DCM solution of **25** and refrigerating the

solution overnight (5°C). The mixture was then poured into 1M Na₂CO₃ and the resultant precipitate collected by filtration and dried. Analysis (¹H NMR) of the isolated product confirmed the formation of the TFA salt of the *p*-nitrobenzoyl 3-mer **35** in a 90% yield.



Scheme 1-13

The NH and BOC-CH₃ resonances (δ 7.5 and δ 1.3 ppm) present in the spectrum of **25** were absent in the spectrum of **34**. Furthermore, a broad NH₃⁺ resonance at δ 9.32ppm was observed. Single crystals suitable for X-ray crystallography, obtained by slow evaporation from a concentrated solution of the compound in DMF, confirmed the structure of **35** as a DMF solvate (Figure 1-9).

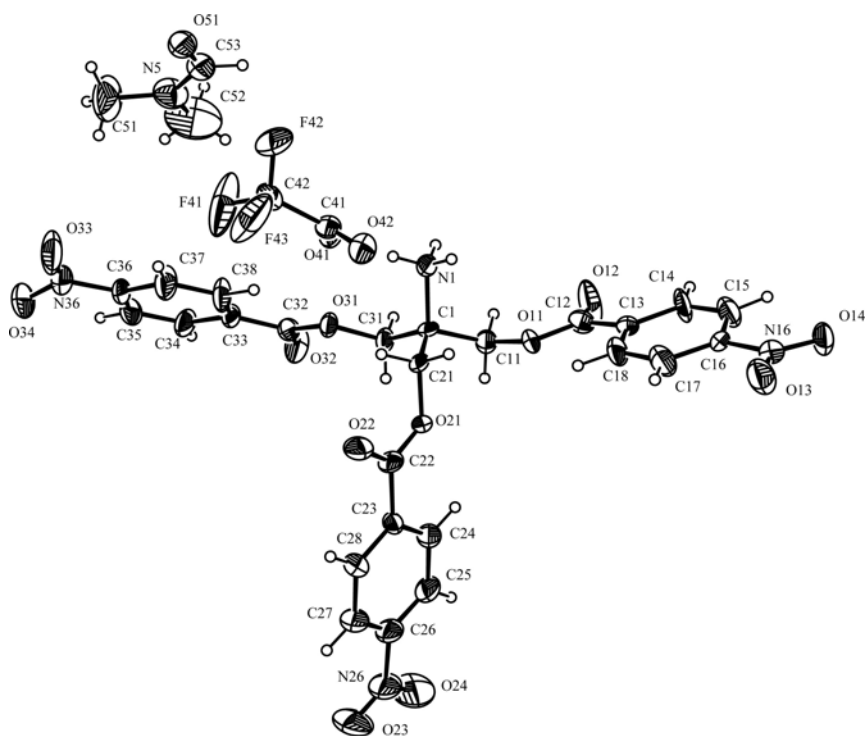


Figure 1-9. ORTEP diagram for the molecular structure of **35**.

An initial attempt was made to couple **35** with the tri-isocyanate core **15** in DCM at room temperature. However, analysis of the reaction by ^1H NMR showed incomplete conversion to the product. Presumably, the limited solubility of the ammonium salt **35**, in DCM was a limiting factor. Consequently the free base amine was generated by washing a DMF/DCM solution of **35** with 1M Na_2CO_3 . The free amine **37** was isolated in a 72% yield.

Deprotection of the *p*-anisoyl 3-mer **26** also resulted in the isolation of the TFA salt **36** in a 98% yield that was converted to the free base **38** *via* the same method, with a recovery of 80%. The *p*-toluoyl and *p*-maleimidobenzoyl 3-mers **27** and **34** were deprotected and immediately converted to the free base without isolation of the intermediate salt, as on pouring the DCM/TFA deprotection solution into aqueous sodium carbonate, no precipitate was observed to form. The amine products were

isolated in 77% (**39**) and 90% (**40**) yields respectively. Figure 1-10 shows the assigned ^1H NMR spectrum of **39**, with the broad NH_2 peak observed at 2.14 ppm.

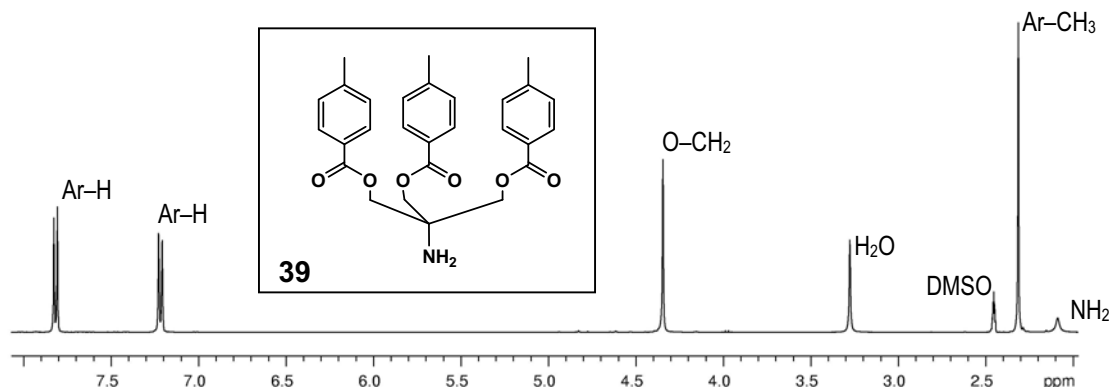


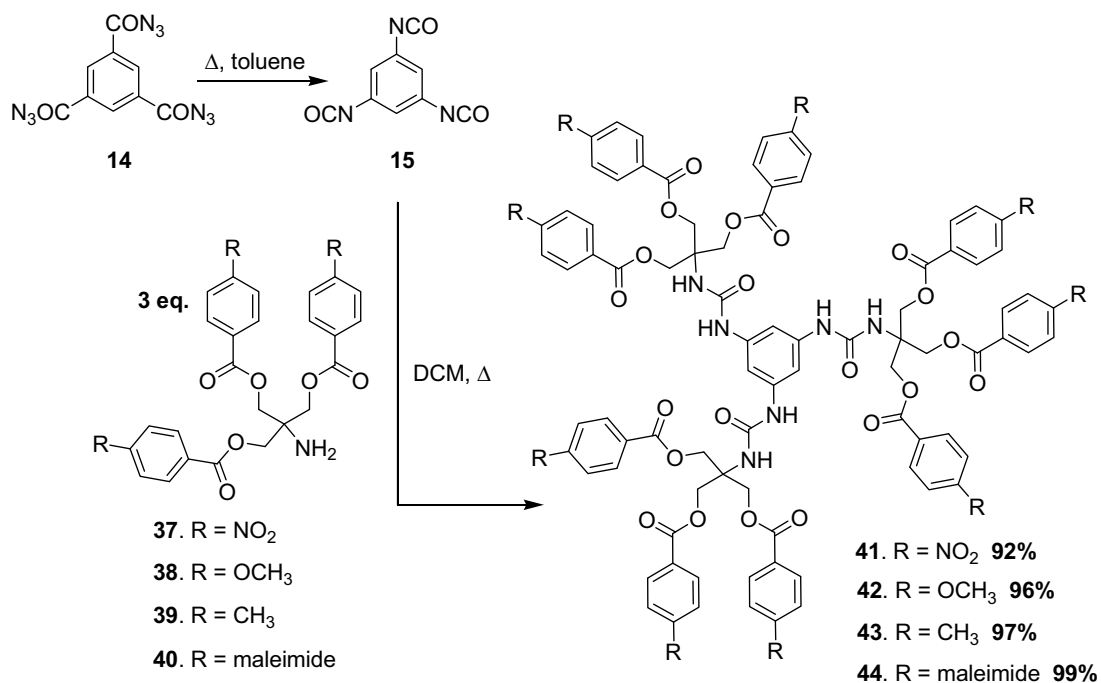
Figure 1-10. ^1H NMR spectrum (400 MHz, $\text{DMSO-}d_6$) of **39**.

Deprotection of the isonicotinoyl compound **29** was attempted a number of times using the DCM/TFA mixture, with refrigeration and at room temperature, however ^1H NMR analysis after the “deprotection” reaction showed that the BOC group remained mostly intact although significant cleavage of the ester linkages was observed. It is presumed that the pyridyl rings were preferentially promoting cleavage of the ester groups, indeed the literature states that a number of bases including pyridine have been shown to catalyse ester hydrolysis.⁸⁹ Due to these difficulties it was decided not to continue with this isonicotinoyl functionality at this stage, however future investigations may trial the oxidation of the isonicotinoyl rings with dimethyldioxirane to give the *N*-oxide before this deprotection step.

1.2.3 Coupling of the dendrons to the trifunctional core

The initial attempt at coupling the free amine of the *p*-nitrobenzoyl 3-mer **37** to the core **15** did not proceed cleanly. The isocyanate core **15** was formed by heating the

acyl azide precursor **14** in toluene for one hour, with subsequent removal of the toluene, addition of 3 equivalents of **37** in DCM and stirring at room temperature overnight. Analysis (^1H NMR) of the reaction products (collected by filtration) showed a mixture of partially and fully substituted dendritic molecules. Repeating the reaction under conditions of gentle reflux for 16 hours however, resulted in conversion to the fully substituted dendritic molecule, *p*-nitrobenzoyl 9-mer **41**, in excellent yield (92%) (Scheme 1-14).



Scheme 1-14

Evidence for the formation of **41** included a MS peak at 1929 amu corresponding to M+Na. The 2D gHMBC spectrum (Figure 1-11) shows cross peaks correlating the resonances of the NH protons of the urea linkage with the central C=O ^{13}C resonance, thus confirming the formation of the urea linkage in the product.

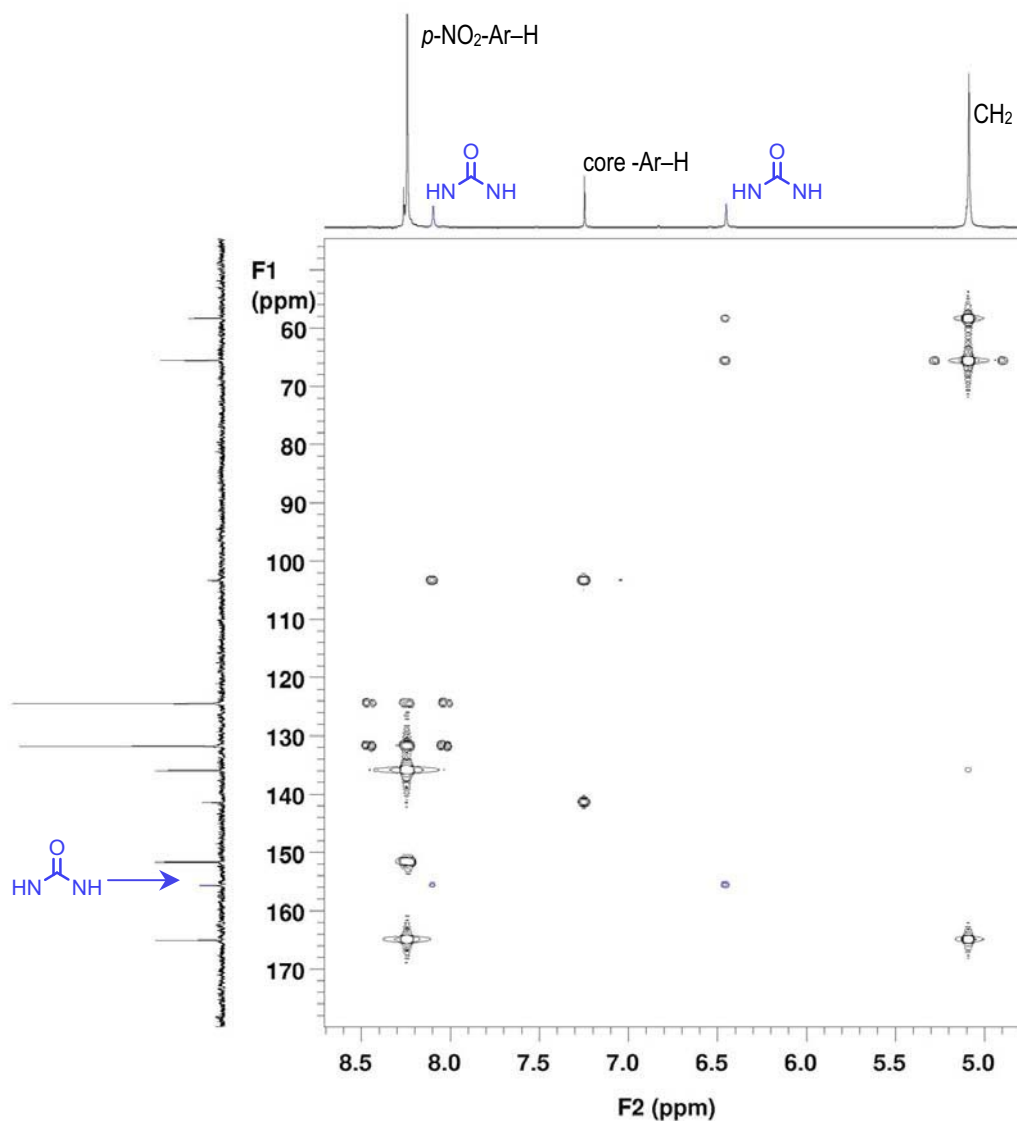


Figure 1-11. Expansion of the $^1\text{H}/^{13}\text{C}$ gHMBC spectrum of the *p*-nitrobenzoyl 9-mer, **41** (400 MHz, acetone- d_6). Basic ^1H and $^{13}\text{C}\{^1\text{H}\}$ spectra are provided as axial references with the cross-peaks correlating to the NH protons and the carbon of the central carbonyl of the urea linkage highlighted in blue.

This synthetic methodology used for the preparation of **41** was successfully applied to prepare analogues arising from our other functionalised dendrons (Scheme 1-14). The *p*-anisoyl 9-mer **42** was isolated in a yield of 96% as a white solid. ESMS in the positive mode showed peaks at 1778 amu and 1794 amu corresponding to the lithium

and sodium adducts respectively and the formation of the urea linkage was also confirmed by 2D NMR techniques. The *p*-toluoyl 9-mer **43** was isolated as a white solid in a 97% yield, with the successful formation evidenced by ESMS results (Figure 1-12) with peaks observed in the positive mode at [M+Li] 1633 amu and [M+Na] 1649 amu. 2D NMR techniques confirmed the formation of the urea linkage.

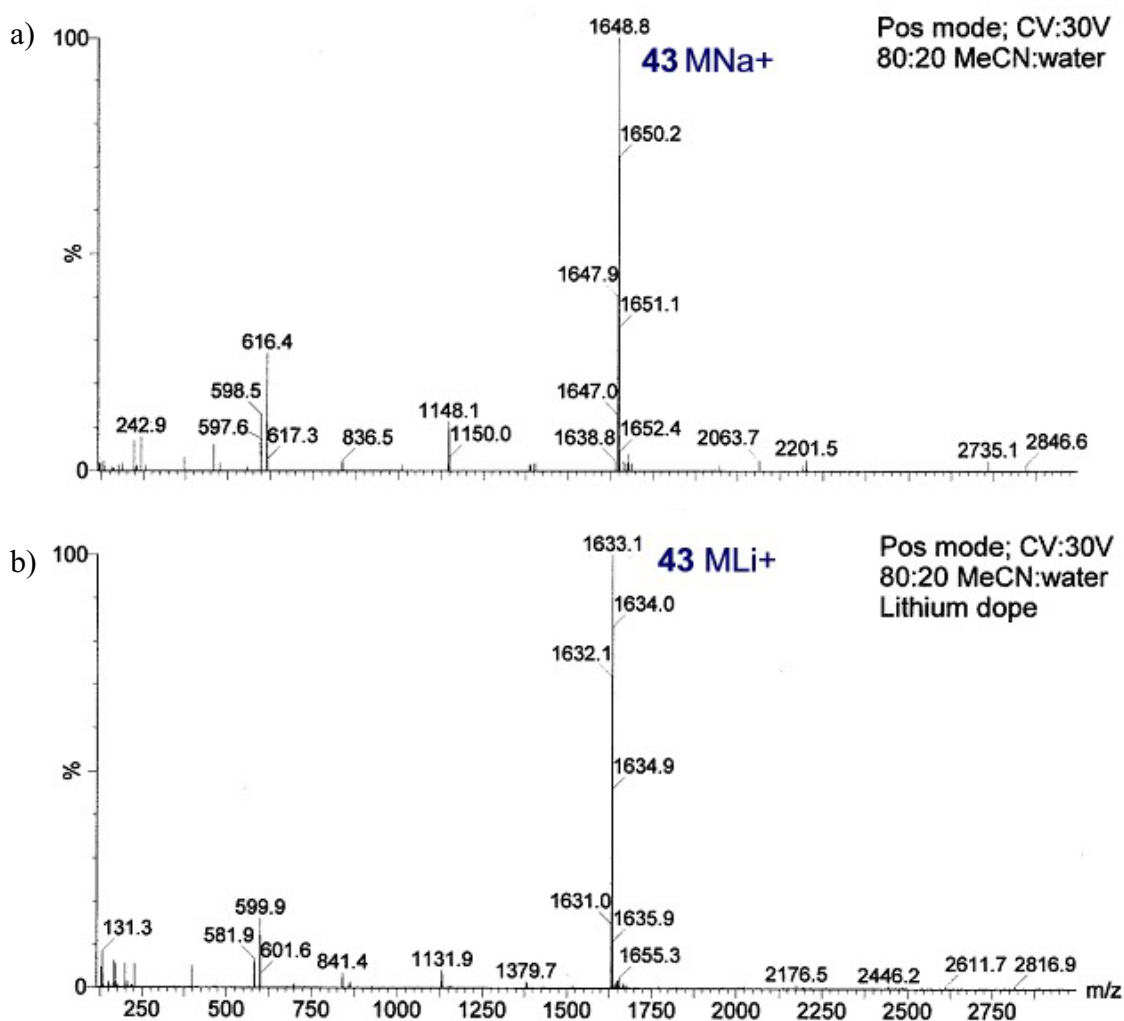


Figure 1-12. ESMS spectra of **43** in a) the positive mode, and b) lithium doped.

The *p*-maleimidobenzoyl 9-mer **44** was isolated in a 99% yield with microanalysis results revealing the incorporation of one water molecule ($\text{C}_{120}\text{H}_{81}\text{N}_{15}\text{O}_{39}\cdot\text{H}_2\text{O}$) despite thorough drying of the product. Further confirmation of the formation of **44**

was revealed by ESMS in the positive mode with a peak corresponding to the sodium adduct observed at 2378 amu.

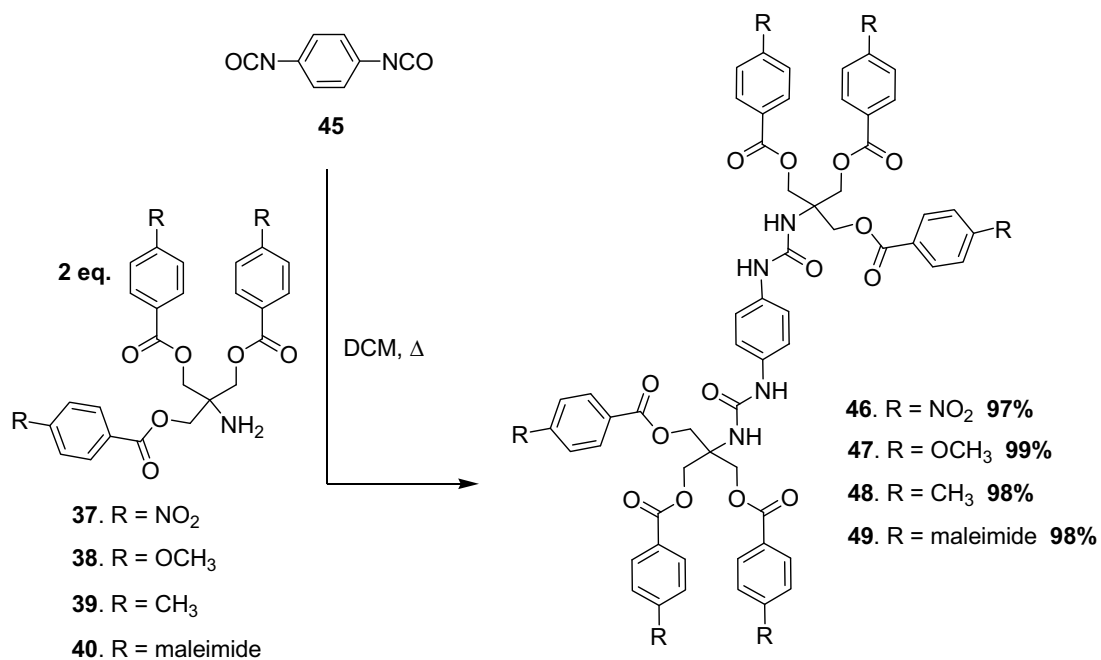
The overall success of our strategy for the formation of dendritic species bearing 9 peripheral functionalities can be seen on review of the yields obtained for each of the reaction steps. The branch point synthon **23** is readily obtained in 73% yield and unreacted starting material can be recovered and re-used. Formation of the 3-mer dendrons resulted in highly pure compounds in yields ranging from 50 – 92%. Deprotection of the amines also proceeded cleanly and afforded products in 72-90% yields. In all cases except for the isonicotinic acid derived species, the deprotected 3-mer dendrons could then be readily coupled to our core synthon under mild conditions to afford the corresponding 9-mer dendritic molecules in near quantitative yields and in very high purity.

1.2.4 Coupling of the dendrons to the bifunctional core

A second core synthon 1,4-phenylenediisocyanate **45** was also used for the preparation of dendritic-type species as it is commercially available and had structural similarity to **15**. Coupling of the 3-mers **37**, **38**, **39** and **40** to this core was again straightforward. Following the addition of two equivalents of the 3-mer to one equivalent of **45** in DCM, the solution was heated at reflux for 18 hours and the product isolated by filtration or removing the solvent *in vacuo* (Scheme 1-15).

The *p*-nitrobenzoyl 6-mer **46** was isolated in a 97% yield as a pale yellow solid, NMR analysis confirming the formation of the product. Isolation of the *p*-anisoyl 6-mer **47** as a white solid, was achieved in a 99% yield with evidence for its formation

observed by ESMS in the positive mode. Peaks were observed at 1213 amu [M+Li] and 1229 amu [M+Na]. Additionally, NMR analysis (Figure 1-13) gave spectral data consistent with the structure.



Scheme 1-15

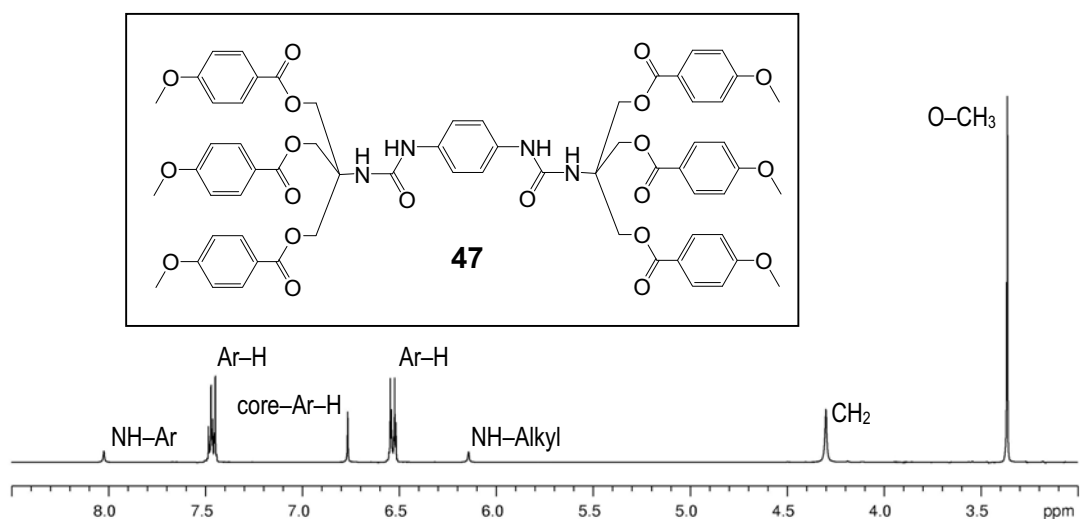


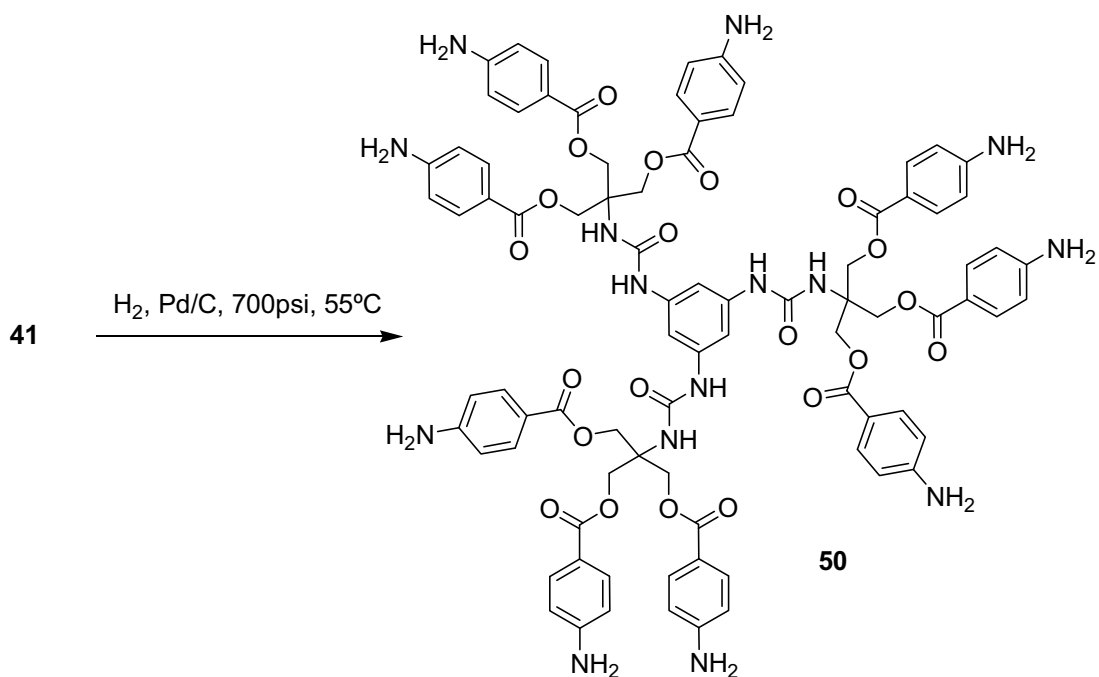
Figure 1-13. ¹H NMR spectrum (400 MHz, DMSO-*d*₆) of 47.

The *p*-toluoyl 6-mer **48** was isolated in a 98% yield. ESMS in the positive mode revealed peaks at 1117 amu [M+Li] and 1133 amu [M+Na]. The *p*-maleimidobenzoyl 6-mer **49** was isolated in a 98% yield, once again, NMR analysis afforded spectra consistent with expected values.

1.2.5 Functional Group Interconversions on Dendritic Molecules

1.2.5.1 Hydrogenation - Nitro to Amino

Catalytic hydrogenation reactions using a heterogeneous catalyst (*e.g.* Pt or Pd/C) result in the clean reduction of an aromatic nitro group to the corresponding amine function. Attempts to reduce the *p*-nitrobenzoyl functionalised 9-mer **41** and 6-mer **46**, at atmospheric and high pressure in ethanol solution were unsuccessful. The reactions however, proceed cleanly using DMF as the solvent, at elevated temperature and pressure. In a typical reaction **41** dissolved in DMF with a catalytic amount of 5% Pd/C present was placed in a sealed reaction vessel, under pressure of hydrogen gas (700psi) at a temperature of 55°C for 15 hours (Scheme 1-16). After cooling, work up simply involved filtration of the solution to remove the catalyst. Evaporation of the solvent under reduced pressure, afforded a brown oily residue that solidified upon addition of DCM. Filtration afforded the completely reduced *p*-aminobenzoyl 9-mer **50** in a 90% yield.



Scheme 1-16

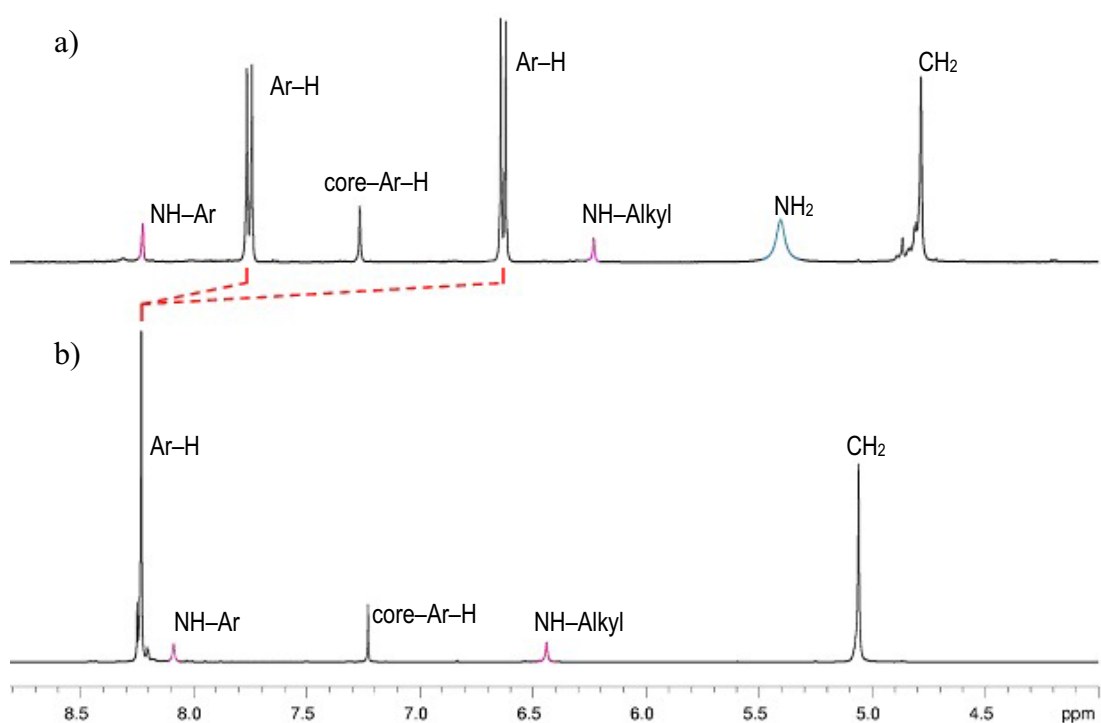
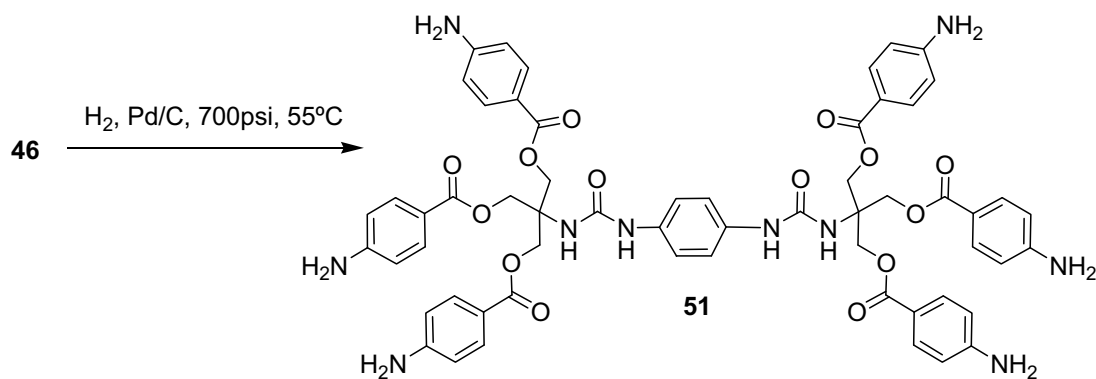


Figure 1-14. ^1H NMR spectra (400 MHz, acetone- d_6) comparing a) the hydrogenation product **50** [*p*-aminobenzoyl 9-mer] and b) the parent compound **41** [*p*-nitrobenzoyl 9-mer].

The IR spectrum provided evidence for the formation of **50**, NH stretching and bending bands were observed at 3365 cm^{-1} and 1603 cm^{-1} . The appearance of a broad NH_2 resonance in the proton NMR with a relative integral area of 18 protons and the migration of the Ar-H resonances were also consistent with the reduced product (Figure 1-14). The calculated mass for $[\text{M}+\text{H}]^+$ 1636.5804, matched the observed signal of 1636.5692.

Hydrogenation of the *p*-nitrobenzoyl 6-mer **46** was carried out in a similar fashion by suspending **46** with a catalytic amount of 5% Pd/C in DMF, under pressure of hydrogen gas (700psi) and at a temperature of 55°C for 18 hours (Scheme 1-17). After cooling, filtration to remove the catalyst and removal of the solvent *in vacuo*, the residue was solidified by the addition of DCM. Supporting evidence for the formation of **51** included a high resolution MS calculated for $[\text{M}+\text{Na}]^{1+}$ at 1139.3870, matching the observed mass of 1139.3829. The IR spectrum showed NH bands at 3366 cm^{-1} and 1602 cm^{-1} and the appearance of a broad NH resonance in the proton NMR at δ 5.99 ppm with a relative integral area of 12 protons also supported the structure of **51**.

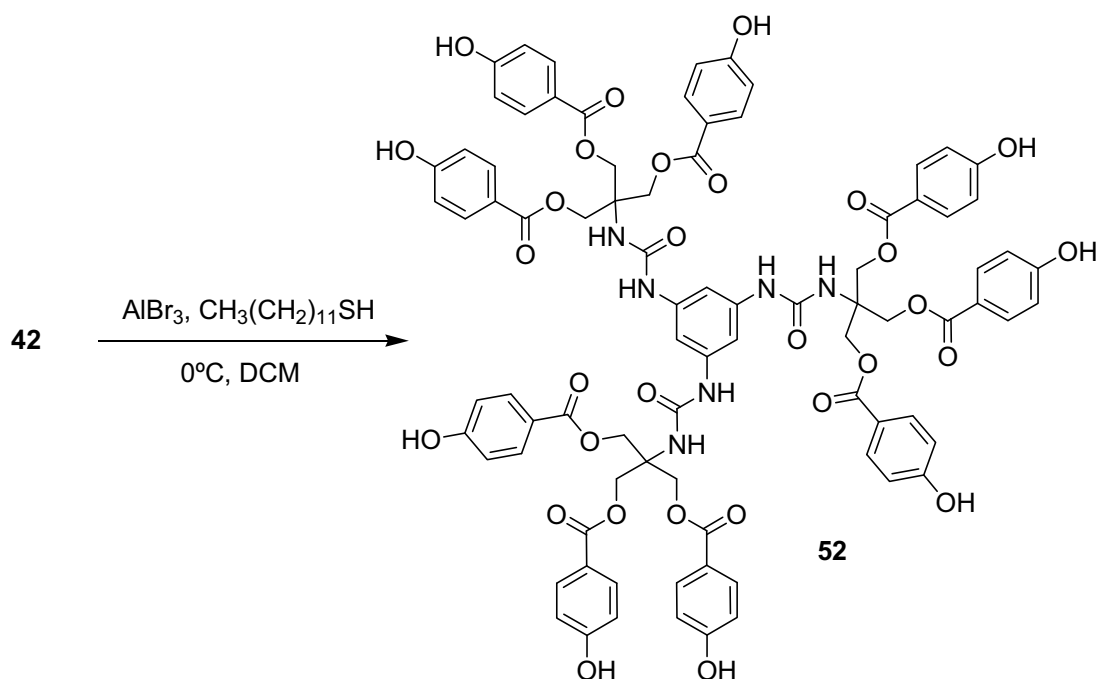


Scheme 1-17

1.2.5.2 Ether Cleavage

Polyphenolic compounds have numerous and varied applications in synthetic, medicinal, supramolecular and industrial chemistry (for a recent review refer to Handique *et. al.*⁹⁰). One route to such systems utilises the cleavage of the methyl ether groups of the *p*-anisoyl 9-mer to form the corresponding polyphenolic product. Aluminium halides in the presence of ethane thiol are known to effect the cleavage of methyl ethers even in the presence of ester groups.⁹¹ For our particular reaction the metal halide AlBr₃ was used, as it is more reactive than AlCl₃, and nine methyl ethers on the one molecule required simultaneous cleavage. Dodecane thiol was used in place of the commonly used ethane thiol as literature precedent⁹² has shown it gives comparable results without the associated stench, due to its reduced volatility. Thus addition of **42** as a solid to a cooled suspension of AlBr₃ and dodecane thiol in DCM (0°C) under an atmosphere of nitrogen. Gradual warming of the reaction to room temperature with stirring for 16 hours (Scheme 1-18) followed by pouring the reaction mixture into water with subsequent acidification to pH 1, afforded the crude product as a highly pure, white solid **52** which was collected by filtration in an 87% yield. The formation of **52** was supported by signals from the ESMS in the negative mode at 1643 amu [M⁻] and in the positive mode at 1643 amu [M+Na]. The mass to charge ratio (*m/z*) for the doubly charged species [M-2H]²⁻ was observed by HRMS at 821.2094 matching the calculated value of 821.2073. The IR spectra contained the expected broad band at 3383 cm⁻¹ indicative of the presence of -OH functions. Figure 1-15 shows the assigned ¹H NMR spectra of both the *p*-anisoyl 9-mer and its phenolic derivative, highlighting the anisoyl -OCH₃ resonance and the observed phenolic resonance at δ 10.35 ppm. Interestingly a significant increase in the melting point was observed from the parent compound **42** (114-5°C) to 168-9°C for **52**,

reflecting presumably the increased potential for intermolecular hydrogen bonding in the species bearing terminal phenol units.



Scheme 1-18

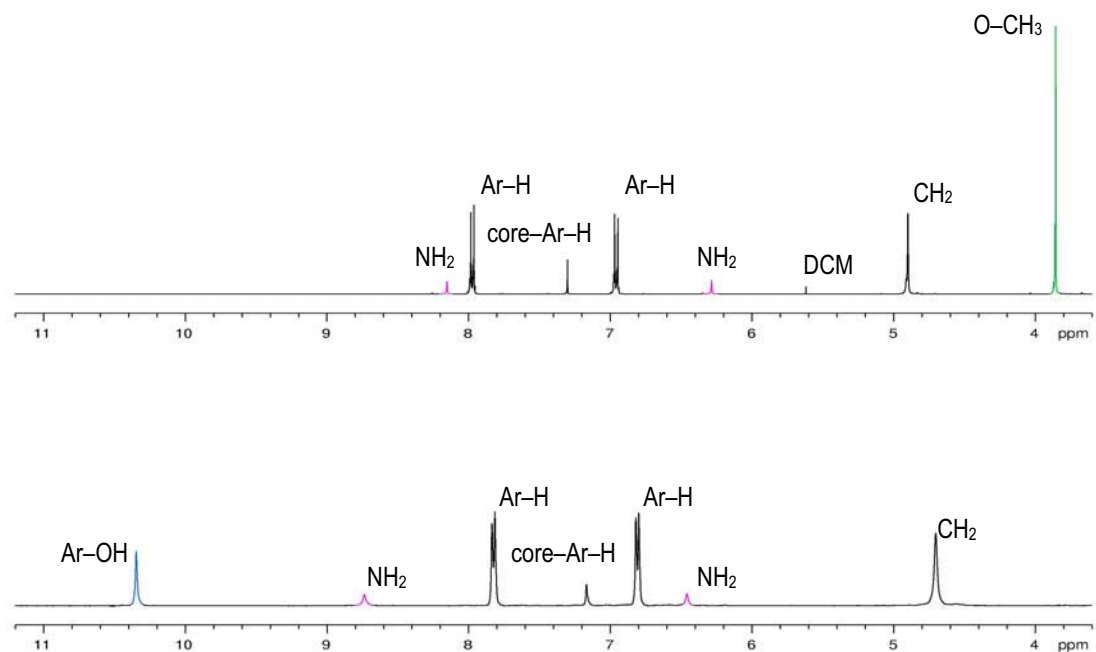


Figure 1-15. ^1H NMR spectra (400 MHz, $\text{DMSO}-d_6$) comparing a) the parent compound **42** [*p*-anisoyl 9-mer] (green highlights $-\text{OCH}_3$) and b) **52** after the ether cleavage reaction [*p*-phenoxy 9-mer] (blue highlights $-\text{OH}$).

Attempts were made to crystallise each of the aforementioned functionalised dendritic species (9-mers and 6-mers) trialling both diffusion and evaporation techniques with various solvent combinations unfortunately however, all attempts were unsuccessful.

1.2.6 Summary

The work presented within this chapter has demonstrated the facile, modular synthesis of a number of highly monodisperse branched molecules possessing a range of peripheral functionalities. The use of the quantitative reaction between the amines on the branched dendrons and the isocyanates present on the bi- and tri-functionalised core molecules as the linking reaction for the formation of the dendritic molecules lead to the high yields and straightforward isolation of highly pure dendritic species. Furthermore the ester and urea linkages of the dendritic frameworks are relatively robust and thus functional group transformations are achievable. At present, investigations are continuing into the application of these molecules as a basis for the assembly of more complex macromolecular structures for applications in biological and materials science.

1.3 References

- (1) Fréchet, J. M. J.; Tomalia, D. A. *Dendrimers and Other Dendritic Polymers*; John Wiley & Sons: Chichester, 2001.
- (2) Newkome, G. R.; Moorefield, C. N.; Vogtle, F. *Dendrimers and Dendrons: Concepts, Syntheses, Applications*; Wiley - VCH: Weinheim, 2001.
- (3) Fischer, M.; Vogtle, F. *Angew. Chem. Int. Ed. Engl.* **1999**, *38*, 884-905.
- (4) Buhler, E.; Wehner, W.; Vogtle, F. *Synthesis* **1978**, 155-158.
- (5) Bryant-Jr., L. H.; Bulte, J. W. M. *Focus on Biotechnology (Physics and Chemistry: Basis of Biotechnology)* **2001**, *7*, 47-69.
- (6) Ashton, P. R.; Boyd, S. E.; Brown, C. L.; Jayaraman, N.; Nepogodiev, S. A.; Stoddart, J. F. *Chem. Eur. J.* **1996**, *2*, 1115-1128.
- (7) Lindhorst, T. K.; Diekmann, S. *Rev. Mol. Biotech.* **2002**, *90*, 157-158.
- (8) Tomalia, D. A.; Fréchet, J. M. J. *J. Polym. Sci., Part A: Polym. Chem.* **2002**, *40*, 2719-2728.
- (9) Fréchet, J. M. J. *J. Polym. Sci., Part A: Polym. Chem.* **2003**, *41*, 3713-3725.
- (10) Stiriba, S.-E.; Frey, H.; Haag, R. *Angew. Chem. Int. Ed. Engl.* **2002**, *41*, 1329-1334.
- (11) Dagani, R. *Chem. Eng. News* **1996**, 1-8.
- (12) Ashton, P. R.; Anderson, D. W.; Brown, C. L.; Shipway, A. N.; Stoddart, J. F.; Tolley, M. S. *Chem. Eur. J.* **1998**, *4*, 781-795.
- (13) Hawker, C. J.; Fréchet, J. M. J. *J. Chem. Soc., Chem. Commun.* **1990**, 1010-1013.
- (14) Fréchet, J. M. J. *Science* **1994**, *263*, 1710-1715.
- (15) Cao, X.; Wang, F.; Guo, S. *Synth. Commun.* **2002**, *32*, 3149-3158.

- (16) Wooley, K. L.; Hawker, C. J.; Fréchet, J. M. J. *J. Am. Chem. Soc.* **1991**, *113*, 4252-4261.
- (17) Wooley, K. L.; Hawker, C. J.; Fréchet, J. M. J. *Angew. Chem. Int. Ed. Engl.* **1994**, *106*, 123-126.
- (18) Spindler, R. *J. Chem. Soc., Perkin Trans. 1* **1993**, 913-918.
- (19) Kawaguchi, T.; Walker, K. L.; Wilkins, C. L.; Moore, J. S. *J. Am. Chem. Soc.* **1995**, *117*, 2159-2165.
- (20) Matthews, O. A.; Shipway, A. N.; Stoddart, J. F. *Prog. Polym. Sci.* **1998**, *23*, 1-56.
- (21) Roovers, J.; Comanita, B. *Adv. Polym. Sci.* **1999**, *142*, 179-228.
- (22) Kim, Y.; Zimmerman, S. C. *Curr. Opin. Chem. Biol.* **1998**, *2*, 733-742.
- (23) Kojima, C.; Kono, K.; Maruyama, K.; Takagishi, T. *Bioconjugate Chem.* **2000**, *11*, 910-917.
- (24) Gillies, E. R.; Fréchet, J. M. J. *J. Am. Chem. Soc.* **2002**, *124*, 14137-14146.
- (25) Liu, M.; Fréchet, J. M. J. *Pharm. Sci. Technol. Today* **1999**, *2*, 393-401.
- (26) Ihre, H. R.; Jesus, O. L. P. D.; Jr., F. C. S.; Fréchet, J. M. J. *Bioconjugate Chem.* **2002**, *13*, 443-452.
- (27) Aulenta, F.; Hayes, W.; Rannard, S. *Eur. Polym. J.* **2003**, *39*, 1741-1771.
- (28) Stears, R. L.; Getts, R. C.; Gullans, S. R. *Physiol. Genomics* **2000**, *3*, 93-99.
- (29) Tokuhisa, H.; Zhao, M.; Baker, L. A.; Phan, V. T.; Dermody, D. L.; Garcia, M. E.; Peez, R. F.; Crooks, R. M.; Mayer, T. M. *J. Am. Chem. Soc.* **1998**, *120*, 4992-4501.
- (30) Muller, T.; Yablon, D. G.; Karchner, R.; Knapp, D.; Kleinman, M. H.; Fang, H.; Durning, C. J.; Tomalia, D. A.; Turro, N. J.; Flynn, G. W. *Langmuir* **2002**, *18*, 7452-7455.

- (31) Wang, J.; Jia, W.; Zhong, H.; Luo, Y.; Zhao, X.; Cao, W.; Li, M. *Chem. Mater.* **2002**, *14*, 2854-2858.
- (32) Zeng, F.; Zimmerman, S. C. *Chem. Rev.* **1997**, *97*, 1681-1712.
- (33) Seo, Y.-S.; Kim, K.-S.; Shin, K.; White, H.; Rafailovich, M.; Sokolov, J. *Langmuir* **2002**, *18*, 5927-5932.
- (34) Hedrick, J. L.; Magbitang, T.; Connor, E. F.; Glauser, T.; Volksen, W.; Hawker, C. J.; Lee, V. Y.; Miller, R. D. *Chem. Eur. J.* **2002**, *8*, 3309-3319.
- (35) Ghosh, S.; Banthia, A. K.; Maiya, B. G. *Org. Lett.* **2002**, *4*, 3603-3606.
- (36) Tully, D. C.; Fréchet, J. M. J. *Chem. Commun. (Cambridge)* **2001**, 1229-1239.
- (37) Wang, J.; Jiang, M. *J. Am. Chem. Soc.* **1998**, *120*, 8281-8282.
- (38) Chang, A.-C.; Gillespie, J. B.; Tabacco, M. B. *Anal. Chem.* **2001**, *73*, 467-470.
- (39) Emmrich, E.; Franzka, S.; Schmid, G. *Nano Lett.* **2002**, *2*, 1239-1242.
- (40) Xu, F.-t.; Curry, M.; Huang, F.; Ye, P.-p.; Rar, A.; Street, S. C.; Barnard, J. *A. Mat. Res. Soc. Symp. Proc.* **2002**, *710 (Polymer Interfaces and Thin Films)*, 253-258.
- (41) Tully, D. C.; Wilder, K.; Fréchet, J. M. J.; Trimble, A. R.; Quate, C. F. *Adv. Mater.* **1999**, *11*, 314-318.
- (42) Hong, M.-Y.; Yoon, H. C.; Kim, H.-S. *Langmuir* **2003**, *19*, 416-421.
- (43) McKendry, R.; Huck, W. T. S.; Weeks, B.; Fiorni, M.; Abell, C.; Rayment, T. *Nano Lett.* **2002**, *2*, 713-716.
- (44) Simanek, E. E.; Gonzalez, S. O. *J. Chem. Educ.* **2002**, *79*, 1222-1231.
- (45) Liu, Y.; Zhao, M.; Bergbreiter, D. E.; Crooks, R. M. *J. Am. Chem. Soc.* **1997**, *119*, 8720.

- (46) Kuzadel, S. A.; Monning, C. A.; Newkome, G. R.; Moorefield, C. N. *J. Chem. Soc., Chem. Commun.* **1994**, 2139.
- (47) Kolb, H. C.; Finn, M. G.; Sharpless, K. B. *Angew. Chem. Int. Ed. Engl.* **2001**, *40*, 2004-2021.
- (48) Demko, Z. P.; Sharpless, K. B. *Angew. Chem. Int. Ed. Engl.* **2002**, *41*, 2110-2113.
- (49) Demko, Z. P.; Sharpless, K. B. *Angew. Chem. Int. Ed. Engl.* **2002**, *41*, 2113-2116.
- (50) Wu, P.; Feldman, A. K.; Nugent, A. K.; Hawker, C. J.; Scheel, A.; Voit, B.; Pyun, J.; Fréchet, J. M. J.; Sharpless, K. B.; Fokin, V. V. *Angew. Chem. Int. Ed. Engl.* **2004**, *43*, 3928-3932.
- (51) Kolb, H. C.; Sharpless, K. B. *Drug Discovery Today* **2003**, *8*, 1128-1137.
- (52) Seo, T. S.; Li, Z.; Ruparel, H.; Ju, J. *J. Org. Chem.* **2003**, *68*, 609-612.
- (53) Collman, J. P.; Devaraj, N. K.; Chidsey, C. E. D. *Langmuir* **2004**, *20*, 1051-3.
- (54) Joralemon, M. J.; O'Reilly, R. K.; Matson, J. B.; Nugent, A. K.; Hawker, C. J.; Wooley, K. L. *Macromolecules* **2005**, *38*, 5436-5443.
- (55) Fokin, V.; Sharpless, K. B.; Wu, P.; Feldman, A. (2006) Click Chemistry Route to Triazole Dendrimers, US Patent WO2006005046 US.
- (56) Malkoch, M.; Schleicher, K.; Drockenmuller, E.; Hawker, C. J.; Russell, T. P.; Wu, P.; Fokin, V. V. *Macromolecules* **2005**, *38*, 3663-3678.
- (57) Lee, J. W.; Kim, J. H.; Kim, B.-K.; Shin, W. S.; Jin, S.-H. *Tetrahedron* **2005**, *62*, 894-900.
- (58) Lee, J. W.; Kim, B.-K. *Bull. Korean Chem. Soc.* **2005**, *26*, 658-660.
- (59) Lee, J. W.; Kim, B.-K.; Jin, S.-H. *Bull. Korean Chem. Soc.* **2005**, *26*, 833-836.

- (60) Smith, M. B.; March, J. *March's Advanced Organic Chemistry: Reactions, Mechanisms and Structure*; 5th ed. ed.; Wiley-Interscience: New York, 2001.
- (61) Kumar, A.; Meijer, E. W. *Chem. Commun. (Cambridge)* **1998**, 1629-1630.
- (62) Alonso, B.; Casado, C. M.; Caudrado, I.; Moran, M.; Kaifer, A. E. *Chem. Commun. (Cambridge)* **2002**, 1778-1779.
- (63) Stephan, H.; Spies, H.; Johannsen, B.; Klein, L.; Vogtle, F. *Chem. Commun. (Cambridge)* **1999**, 1875-1876.
- (64) Cooke, G.; Sindelar, V.; Rotello, V. M. *Chem. Commun. (Cambridge)* **2003**, 752-753.
- (65) Rosenfeldt, S.; Dingenouts, N.; Ballauff, M.; Werner, N.; Vogtle, F.; Lindner, P. *Macromolecules* **2002**, *35*, 8098-8105.
- (66) Banerjee, D.; Broeren, M. A. C.; VanGenderen, M. H. P.; Meijer, E. W.; Rinaldi, P. L. *Macromolecules* **2004**, *37*, 8313-8318.
- (67) Boas, U.; Karlsson, A. J.; deWaal, B. F. M.; Meijer, E. W. *J. Org. Chem.* **2001**, *66*, 2136-2145.
- (68) Precup-Blaga, F. S.; Schenning, A. P. H. J.; Meijer, E. W. *Macromolecules* **2003**, *36*, 565-572.
- (69) Newkome, G. R.; Weis, C. D.; Moorefield, C. N.; Baker, G. R.; Childs, B. J.; Epperson, J. *Angew. Chem. Int. Ed. Engl.* **1998**, *37*, 307-310.
- (70) Newkome, G. R.; Childs, B. J.; Rourk, M. J.; Baker, G. R.; Moorefield, C. N. *Biotechnology and Bioengineering (Combinatorial Chemistry)* **1998/1999**, *61*, 243-253.
- (71) Pittelkow, M.; Nielsen, C. B.; Broeren, M. A. C.; vanDongen, J. L. J.; vanGenderen, M. H. P.; Meijer, E. W.; Christensen, J. B. *Chem. Eur. J.* **2005**, *11*, 5126-5135.

- (72) Pittelkow, M.; Christensen, J. B.; Meijer, E. W. *J. Polym. Sci., Part A: Polym. Chem.* **2004**, *42*, 3792-3799.
- (73) deGroot, D.; DeWaal, B. F. M.; Reek, J. N. H.; Schenning, A. P. H. J.; Kamer, P. C. J.; Meijer, E. W.; vanLeeuwen, P. W. N. M. *J. Am. Chem. Soc.* **2001**, *123*, 8453-8458.
- (74) Precup-Blaga, F. S.; Garcia-Martinez, J. C.; Schenning, A. P. H. J.; Meijer, E. W. *J. Am. Chem. Soc.* **2003**, *125*, 12953-12960.
- (75) Broeren, M. A. C.; deWaal, B. F. M.; vanGenderen, M. H. P.; Sanders, H. M. H. F.; Fytas, G.; Meijer, E. W. *J. Am. Chem. Soc.* **2005**, *127*, 10334-10343.
- (76) Broeren, M. A. C.; Linhardt, J. G.; Malda, H.; DeWaal, B. F. M.; Bersteegen, R. M.; Meijer, J. T.; Lowik, D. W. P. M.; VanHest, J. C. M.; VanGenderen, M. H. P.; Meijer, E. W. *J. Polym. Sci., Part A: Polym. Chem.* **2005**, *43*, 6431-6437.
- (77) Boas, U.; Sontjens, S. H. M.; Jensen, K. J.; Christensen, J. B.; Meijer, E. W. *ChemBioChem* **2002**, *3*, 433-439.
- (78) Broeren, M. A. C.; deWaal, B. F. M.; vanDongen, J. L. J.; vanGenderen, M. H. P.; Meijer, E. W. *Org. Biomol. Chem.* **2005**, *3*, 281-285.
- (79) Ambade, A. V.; Kumar, A. *J. Polym. Sci., Part A: Polym. Chem.* **2001**, *39*, 1295-1304.
- (80) Abdelrehim, M.; Komber, H.; Langenwalter, J.; Voit, B.; Bruchmann, B. *J. Polym. Sci., Part A: Polym. Chem.* **2004**, *42*, 3062-3081.
- (81) Peerlings, H. W. I.; VanBentham, R. A. T. M.; Meijer, E. W. *J. Polym. Sci., Part A: Polym. Chem.* **2001**, *39*, 3112-3120.
- (82) Okaniwa, M.; Takeuchi, K.; Asai, M.; Ueda, M. *Macromolecules* **2002**, *35*, 6224-6231.

- (83) Okaniwa, M.; Takeuchi, K.; Asai, M.; Ueda, M. *Macromolecules* **2002**, *35*, 6232-6238.
- (84) Lebreton, S.; How, S.-E.; Buchholz, M.; Yingyongnarongkul, B.-E.; Bradley, M. *Tetrahedron* **2003**, *59*, 3945-3953.
- (85) vanGorp, J. J.; Vekemans, J. A. J. M.; Meijer, E. W. *J. Am. Chem. Soc.* **2002**, *124*, 14759-14769.
- (86) Kang, J.-H.; Chung, H.-E.; Kim, S. Y.; Kim, Y.; Lee, J.; Lewin, N. E.; Pearce, L. V.; Blumberg, P. M.; Marquez, V. E. *Bioorg. Med. Chem.* **2003**, *11*, 2529-2539.
- (87) Oishi, T.; Fujimoto, M. *J. Polym. Sci., Part A: Polym. Chem.* **1992**, *30*, 1821-1830.
- (88) Jonsson, E. S.; Lee, T. Y.; Viswanathan, K.; Hoyle, C. E.; Roper, T. M.; Guymon, C. A.; Nason, C.; Khudyakov, I. V. *Progress in Organic Coatings* **2005**, *52*, 63-72.
- (89) Bender, M. L.; Turnquest, B. W. *J. Am. Chem. Soc.* **1956**, *79*, 1656.
- (90) Handique, J. G.; Baruah, J. B. *Reactive & Functional Polymers* **2002**, *52*, 163-188.
- (91) Node, M.; Nishide, K.; Fuji, K.; Fujita, E. *J. Org. Chem.* **1980**, *45*, 4275-4277.
- (92) Node, M.; Kumar, K.; Nishide, K.; Ohsugi, S.-i.; Miyamoto, T. *Tetrahedron Lett.* **2001**, *42*, 9207-9210.

CHAPTER TWO

SELF ASSEMBLED MONOLAYERS ON GOLD

2.1 Introduction

The work outlined in this chapter are preliminary studies in substrate design and surface modification for future applications in the development of functioning devices, such as biosensors and microarrays, by the CRC for microTechnology. It describes the development of a methodology for the covalent attachment of fluorescent proteins to self-assembled monolayers on gold surfaces and preliminary studies towards the development of a new compound that could act as a novel heat activated SAM surface for the preparation of high density biomolecular arrays.

2.1.1 Functioning Devices

Biosensors are analytical devices that utilise biological reactions or the molecular recognition events of biomolecules. The devices produce a signal for the detection or measurement of the event to which it responds.¹ Molecular recognition covers a set of phenomena controlled by specific noncovalent interactions. Such phenomena are crucial in biological systems, and a great deal of modern chemical research is motivated by the prospect that molecular recognition by design could lead to new technologies.² A biosensor is usually composed of a sensing (biological recognition) element, tethered to a transducer or signalling element by a linker. The sensing element recognises the target and the recognition event is subsequently converted by the transducing element into a measurable macroscopic response.³ There are two types of biosensors, depending on the nature of the recognition event. Bioaffinity-based devices rely on the selective binding of the target analyte to a ligand (eg. an antibody or oligonucleotide) while biocatalytic devices use an immobilized enzyme to recognise the target substrate.⁴

The miniaturisation of conventional assays is also a general trend in biomedical research as they minimise reaction volumes, increase the sample concentration and reduce reagent consumption. Microarrays are formed *via* the immobilization or covalent attachment of molecules, such as partial DNA sequences, to a surface, at precise locations, in an ordered and highly defined arrangement.⁵ An important feature of these array systems is the site-specific and functional immobilisation of the biomolecules which requires the surface to be biocompatible, homogeneous and stable.^{6,7} Although current microarrays focus on nucleic acid hybridisation, emerging microarray technology is developing techniques for the parallel analysis of proteins, lipids, carbohydrates and small molecules.⁵

2.1.2 Substrate Choice – Why gold?

Research has centred on a number of substrates as platforms for the development of the aforementioned functioning devices. Typically, surfaces used for such applications are solid inorganic matter (such as glass, gold or silicon) and are not directly suitable for the site specific immobilisation of proteins and other biomolecules. However, some solid inorganic surfaces can be functionalised with organic molecules that interface between the solid substrate and the attached ligands. Gold is one of the easiest materials to use as a substrate, in experimental terms. Unlike other metals, gold does not readily oxidize or irreversibly contaminate upon exposure to the atmosphere. The most commonly employed method for the generation of gold surfaces has been the evaporative deposition of gold onto a relatively flat substrate, such as silicon wafers, glass microscope slides or mica, to produce a thin film. Since the level of adhesion between the deposited gold film and these substrates is weak, an intermediate film of chromium (titanium can also be used) is applied to

enhance adhesion. Gold films do not require handling in specialised facilities such as clean rooms. For example, high quality self-assembled monolayers can routinely be obtained from gold films that have been exposed to the variety of airborne contaminants found in a typical organic chemistry laboratory, as thiol and disulfide adsorbates readily displace weakly adsorbed materials during the assembly of the self-assembled monolayer. Silicon wafers and glass are also frequently used as they can be functionalised with silanes that form self-assembled monolayers on the surface. However, the silanisation process requires an inert atmosphere and as a consequence its preparation is experimentally less robust than organic functionalisation of gold.

2.1.3 Self-Assembled Monolayers

Self assembled monolayers (SAMs) are a class of organic thin films that are a versatile tool for the modification of surfaces.⁸ They are ordered molecular assemblies^{9, 10} that are formed spontaneously by the chemisorption of an adsorbate (SAM monomer), which has a specific head group to a solid surface.¹¹ Additional non-covalent, typically hydrophobic, interactions (e.g. van der Waals) between the adsorbate molecules produce a dense, uniformly packed, monolayer.¹² SAM systems are usually categorised in terms of the adsorbate/solid substrate used. A number of combinations have been developed including organosilanes on silicon oxide and glass,^{8, 13} carboxylic acids on metal oxide substrates^{14, 15} and sulphur containing compounds on gold^{12, 16, 17} to list a few. The feature common to each of these systems is the strong affinity between the head group of the adsorbate and the substrate surface.¹⁰ The emphasis of this chapter will be limited to alkane thiols and disulfides on gold, for a recent review, the reader is directed to Gooding.¹⁸

2.1.3.1 SAMs of Thiols on gold

An important advantage of using gold as a substrate is that a stable oxide is not formed on the surface under ambient laboratory conditions.¹⁹ A gold-sulfur bond is formed when the thiol groups (or disulfides and thioethers) are chemisorbed onto the gold surface.²⁰ These SAMs are typically prepared using a very simple solution based assembly methodology. A freshly cleaned gold surface is immersed in a dilute (~1 mM) solution of an appropriate thiol in an organic solvent, generally ethanol, in a sealed vial. The thiols are rapidly chemisorbed onto the surface resulting in approximately 90% of the final monolayer coverage being attained in the first few minutes.¹² On standing, the molecules undergo a slower ordering process and self-assemble to form a dense packed, uniform monolayer (Figure 2-1). The substrate is removed from the thiol solution, thoroughly rinsed, and dried with a stream of nitrogen. Several factors affect the formation and packing density of monolayers such as the roughness of the substrate, solvent effects, temperature, the nature of the adsorbate and its concentration in solution.¹² For most substrates, vigorous cleaning procedures are necessary prior to monolayer formation²¹ typically involving the use of oxidising agents to remove any organic contaminants adsorbed onto the gold surface. Other methods of SAM assembly in common use include microcontact printing^{22, 23} and vapour phase deposition²⁴ (of volatile alkanethiols).

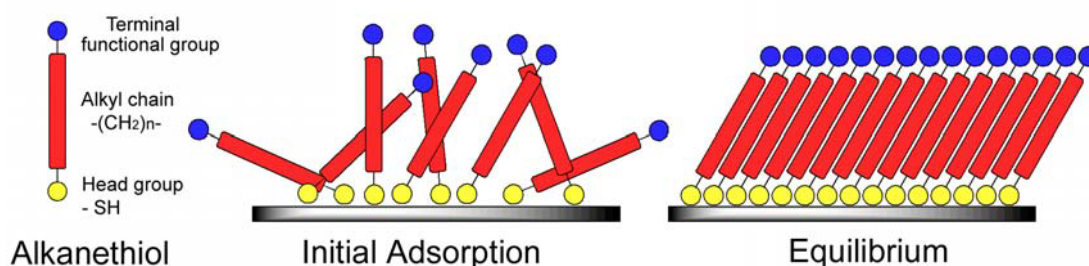


Figure 2-1. Formation of a Self-Assembled Monolayer.

2.1.3.2 Applications of SAMs

SAMs tolerate tremendous flexibility and versatility with respect to their terminal functionality (eg. hydrophilic, hydrophobic, chemically reactive or inert). Simple substituent variations, such as varying X through CH₃, OH, COOH, CONH₂ *etc.* for the thiol HS-R-X, and more sophisticated variations, such as the attachment of ligands, antibodies, oligonucleotides and proteins for biosensor applications,²⁵⁻²⁹ have been investigated by many groups worldwide. Several applications have been identified, for example, long chain alkane thiols produce a highly packed and ordered surface that can provide a membrane like micro-environment useful for immobilising biological molecules.^{27, 30, 31} Other applications of these materials include their use as bio-active³² or inactive surfaces^{33, 34} for gene chips⁸ and biosensors.^{27, 28} SAMs can also function as substrates for cellular adhesion,³⁵ switching devices,³⁶ ionic sensors,³⁷ *etc.*, for an overview see Gooding *et. al.*³⁸

2.1.4 Patterning Techniques for SAMs

Patterning of SAMs is widely used for the construction of multi-component functioning materials and a variety of techniques for the fabrication of these patterned SAMs are available. Photolithography and microcontact printing in particular have been used extensively for patterning of alkanethiol monolayers.³⁹ Other approaches include micromachining, electron and ion beam lithography and probe lithography i.e. AFM and STM.⁴⁰

2.1.4.1 UV Lithography

UV-patterning is a well established and convenient technique that involves UV irradiation of a SAM surface in air, through a mask (Figure 2-2). Thiols that are

adsorbed on the surface and exposed to the UV light oxidise to the corresponding sulfonate,^{41, 42} whereas the thiols masked from the UV light remain intact. When the surface is then placed in a second thiol solution, the oxidised molecules are desorbed from the surface and replaced by thiols from the solution to reform the monolayer. Thus, photolithography represents a clean way of producing multifunctional surfaces capable of having many spatially resolved components with typical resolution on the micrometre scale.

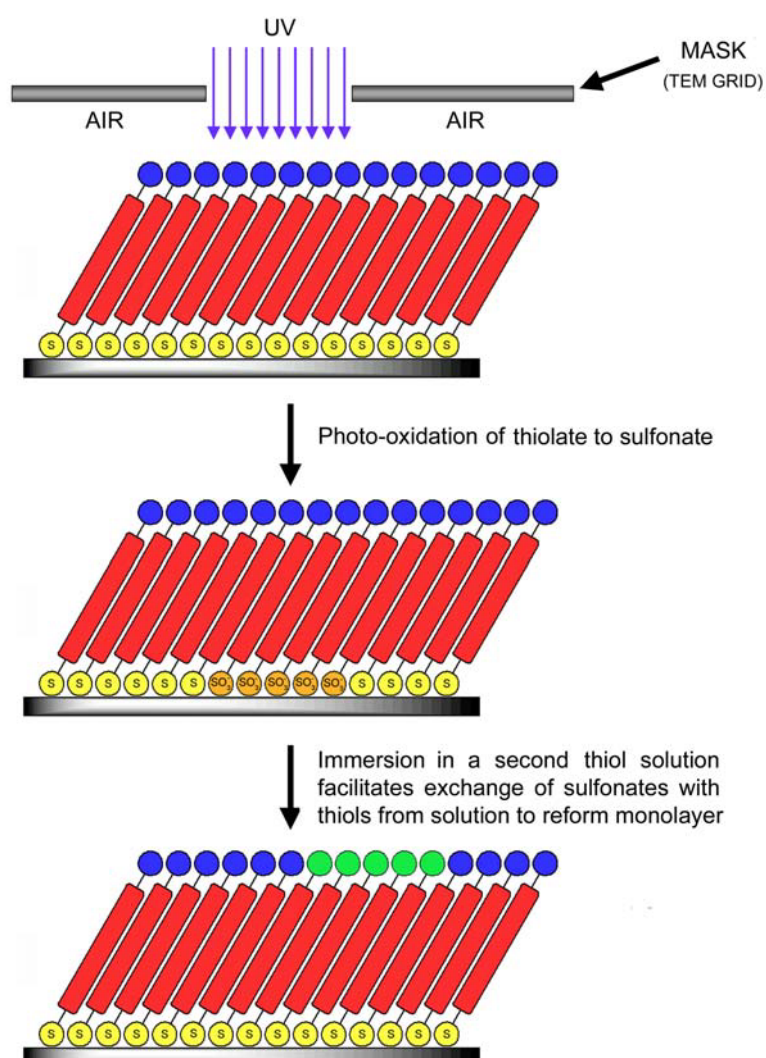


Figure 2-2. Schematic illustration of UV Lithography as a patterning technique for thiol-SAMs on gold.

2.1.4.2 Microcontact Printing

Microcontact printing (μCP)^{22, 43} is a technique where an elastomeric stamp, moulded from a master, is allowed to adsorb a thiol (neat or from ethanolic solution). When the 'inked' stamp is brought into contact with a clean gold substrate a monolayer is formed on the gold surface in the areas of contact. This facile approach to patterning not only enables uniform patterns over large areas to be produced, but also high resolutions, in the order of nanometres, to be achieved.^{23, 44} At present, the technique is suitable for producing two and possibly three component surfaces with applications in microfabrication.⁴⁵ The largest drawback of this technique is the tendency of the elastomeric stamps that are used to sag, restricting the dimensions of the structures which can be produced. However μCP remains an excellent technique for the fabrication of SAMs on gold.

2.1.4.3 Other Patterning Techniques

The proximal probe and beam lithography methods are both high resolution techniques that require either an SPM tip or an electron/ion beam to be sequentially scanned across a surface.⁴⁰ In spite of the advantages of having a higher resolution, the relatively slow speed of these serial techniques limits their usefulness. For a recent review the reader is directed to Smith *et. al.*³⁹

2.1.5 Chemical Reactions and Transformations on Surface of SAMs

The newly emerging area of click chemistry, as described in the previous chapter, involves the application of reproducible, mild and selective reaction conditions to the formation of products that require minimal purification due to high yields and the low occurrence of side reactions.⁴⁶ At this stage, only a few documented articles pertain to the attachment of molecules to a surface *via* a click-type reaction. Examples include the Cu(I) catalysed alkyne-azide coupling reaction, that has been used to form a triazole linkage between an azide and an acetylene, covalently attaching a molecule to a particular surface. The preparation of carbohydrate microarrays on a microtitre plate,⁴⁷ the surface derivatisation of a SAM on silicon⁴⁸ and the attachment of ferrocene molecules to a SAM on gold (Figure 2-3)⁴⁹ have been achieved.

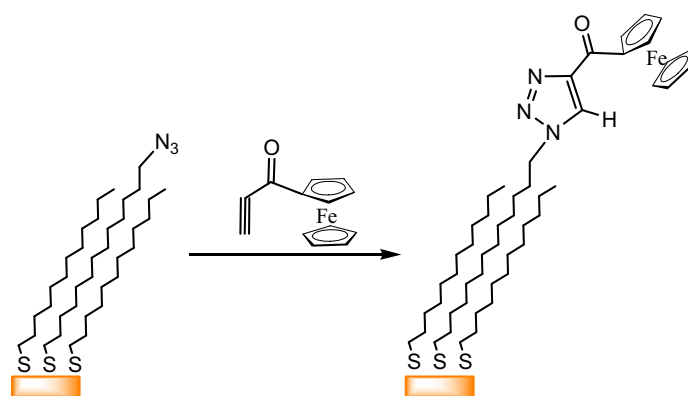


Figure 2-3. Attachment of ferrocene to a SAM surface on gold via ‘Click-type’ chemistry.⁴⁹

Chemical transformations on SAMs can be studied in detail and may provide new directions to tailor surface properties. ‘Switchable’ SAMs pertain to monolayers where the properties of the SAM are changed by an external stimulus, such as light. Examples of developments in ‘switchable’ SAMs have been recently reviewed⁵⁰ and include the use of a photo-isomerisable monolayer (*ie. trans-to-cis* isomerisation of

azobenzene moieties) to direct the motion of a liquid in contact with the SAM,⁵¹ and the switching of SAMs from a hydrophilic to a hydrophobic surface by altering the electrochemical potential.⁵² Protein/cell resistant surfaces such as SAMs terminated with short oligomers of ethylene glycol have been ‘switched’ to promote cellular adhesion by reacting with Br₂, that is electro-generated from bromine ions in aqueous solution by a microelectrode.⁵³

2.1.6 Attachment of Proteins to Surfaces

The successful immobilization of biomolecules onto solid surfaces has been crucial for the development of functioning devices such as biosensors, biomaterials, affinity chromatography systems, micro-array systems and prospective biochips.⁵⁴⁻⁵⁶ The ability to control the interaction of proteins with surfaces at the molecular level using SAMs, is vital to realise the potential to design and fabricate functional nanomaterials.^{31, 57} A number of different physical and chemical procedures have been developed to attach proteins, other biomolecules and unnatural chemical entities to SAM surfaces.^{9, 30} The most common methods rely on the noncovalent association of proteins with a surface. These techniques are experimentally simple, exploiting hydrophobic and electrostatic interactions, however, they are not well controlled. Methods in which the proteins are covalently bound to the surface are inherently more controlled, however and of course produce surfaces where the protein cannot dissociate from the surface and/or exchange with other proteins in solution.⁵⁸ Thus the terminal functionalisation of the alkyl chains of SAMs with reactive end groups is an excellent option to support the immobilisation of biomolecules *via* covalent chemical coupling.^{7, 59, 60} A variety of surface reactions have been utilised for the attachment of proteins to surfaces, the most successful based on the formation of amide and

disulfide bonds.^{58, 61} Examples include the covalent attachment of glucose oxidase (GOx) to a self-assembled monolayer on gold by utilising the chemical oxidation of GOx carbohydrate residues. The resulting aldehydic enzyme was coupled with the terminal amino group of the 11-aminoundecanethiol SAM forming the required covalent bond.²⁸ Furthermore, the covalent attachment of various proteins via their amine-containing residues to an N-hydroxysuccinimide (NHS) terminated SAM have also been reported.^{61, 62}

2.1.7 Techniques for the Characterisation and Analysis of Surfaces

A number of analytical tools have been developed for the analysis and characterisation of thin films on surfaces. These techniques allow the measurement of film thickness, the elemental composition on the surface and information on molecular packing, density, orientation, and hydrophobicity of the surface. Some of the techniques used for the analysis of thin films on surfaces are briefly introduced here, however, this is not intended as an exhaustive review. For further detailed information on these techniques and others not discussed here, the reader is referred to Ulman¹² and others.⁶³⁻⁶⁵

2.1.7.1 Contact Angle Measurements

Contact angle measurements have been used as a characterisation technique to evaluate the hydrophilicity or hydrophobicity of the surfaces of monolayer films.⁶⁶ These surface properties can be determined by observing the shape of droplets of water (or other liquids, such as hexadecane) of a fixed volume, when applied to the surface of the material. As the liquid droplet comes into contact with the surface, the angle formed between the film and the droplet, the contact angle, θ , can be measured

(Figure 2-4). For example, if the surface is hydrophobic, the contact angle of a water droplet on the surface will be large, however, for more hydrophilic surfaces the water droplet will form a smaller contact angle, as the hydrophilic surface will be more effectively wet by the water. The contact angle measurement can also provide information on the surface order of a monolayer film,⁶⁷ for example, the contact angle of an exposed surface of close-packed methyl (-CH₃) groups will differ from that of a disordered film exposing interior methylene (-CH₂-) groups to the surface. Contact angle measurements can also indicate the incorporation of functional groups as the contact angle will change with variations in film composition. Thus contact angle provides useful information on surface order and hydrophobicity of the SAM surface.

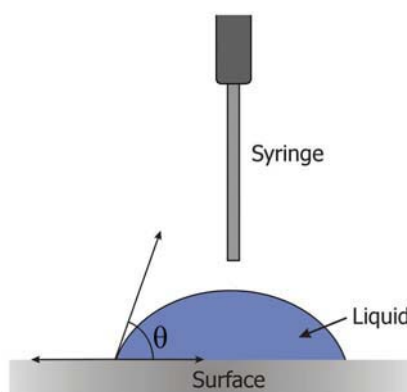


Figure 2-4. Diagram of a contact angle measurement.

2.1.7.2 IR Spectroscopy

The analysis of thin films on high refractive index substrates, such as silicon and gold, by infrared spectroscopy has always been problematic. Reflective substrates such as gold are frequently examined by external reflectance or ‘grazing angle’ spectroscopy.¹² In this technique, light is reflected from a smooth, mirror-like sample and a reflection/adsorption spectrum is recorded. Thin film coatings in the range of nanometers to micrometers, such as SAMs on metal substrates, can be examined using this technique, however data collection usually requires repetitive sampling, over a long period of time, to obtain well defined spectra.

Attenuated total reflectance (ATR) spectroscopy can be used for the analysis of solids, liquids, powders and thin films. The sample is placed in close contact with a more-dense or high refractive index crystal, typically a germanium or zinc selenide crystal. The IR beam is directed onto the bevelled edge of the ATR crystal and reflected internally through the crystal. The beam of radiation penetrates a short distance beyond the interface ($\sim 1\mu\text{m}$) producing an evanescent wave at the reflecting surface (Figure 2-5). From the interaction of the evanescent wave with the sample, a spectrum similar to a transmission spectra can be recorded. The absorbance bands for the monolayer are weak, however, generally in the order of the noise for the typical FTIR spectrometer and again long acquisition times are required. Furthermore, as the substrate is hard and inflexible, it is difficult to obtain the necessary ‘intimate contact’ between the crystal and the sample. Nevertheless, IR techniques may still provide valuable information, on the molecular orientation and the functional groups present, in the analysis of thin films.

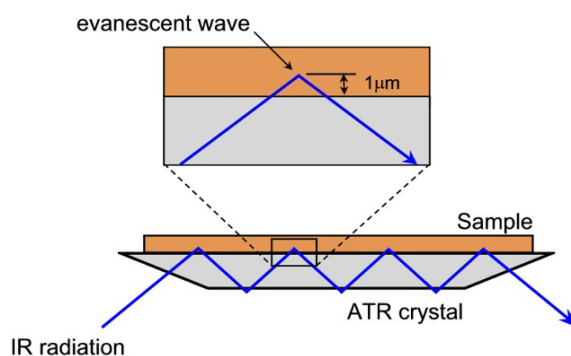


Figure 2-5. Schematic illustration of the principle of ATR spectroscopy.

2.1.7.3 X-ray Photoelectron Spectroscopy

X-ray photoelectron spectroscopy (XPS) is used to survey the chemical nature of SAM surfaces. Briefly, a surface is irradiated with soft x-rays, causing the ejection of electrons from the core shells of atoms within the SAM, in response to the irradiation. The low kinetic energy (up to 1500eV) of these emitted electrons limit the depth from

which they can emerge. Consequently, XPS is a very surface-sensitive technique with a sampling depth in only the nanometre range. The electrons are collected and analysed by the instrument to produce a spectrum of emission intensity versus electron binding energy. In general, the bands are characteristic of each element so that the spectra provides information on the elemental composition, and elemental oxidation states of the SAM surface. Thus, XPS is a widely used, highly useful technique in the analysis of SAMs.

2.1.7.4 Atomic Force Microscopy

Scanning probe microscopy techniques have been used to study surface structures in minute detail. The atomic force microscope⁶⁸ (AFM) can provide true atomic resolution on surfaces, it can be operated under a variety of environments (in air or liquids) and does not require the use of an ultra high vacuum or a conductive sample for image generation.^{64, 65} By measuring the distance dependent forces between the surface being analysed and a molecular sized tip, the topography of samples can be probed on an atomic scale. Located at the end of a flexible cantilever, the tip is placed very close to the sample

surface. Short range attractive and repulsive forces cause a vertical deflection of the cantilever from its equilibrium position (Figure 2-6). A laser beam is pointed at the end of the cantilever, where the beam is reflected

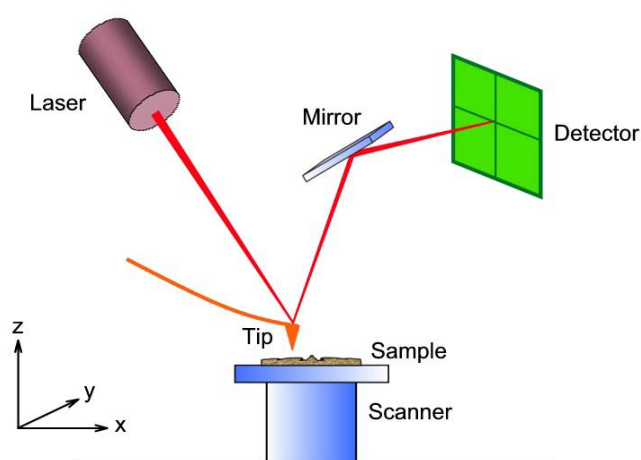


Figure 2-6. Diagram of AFM

and focused on to a four quadrant, position-sensitive detector. As the tip moves across the surface the deflection of the laser beam is detected, with the changes in signal monitored by a feed-back system and displayed upon a connected computer. A variety of operational modes can be used on the AFM including contact, non-contact, tapping, lateral force, chemical force and force distance.^{69, 70} In general AFM is most widely used, in the analysis of SAMs, as a way to map the surface topography.

2.1.7.5 Fluorescence Microscopy

Fluorescence microscopy provides a fast and highly sensitive means of visualising fluorescent material in microscope specimens. Fluorescence is a phenomenon whereby particular molecules or molecular fragments, termed fluorochromes or fluorophores (usually organic compounds containing conjugated double bonds), absorb light of a particular wavelength, exciting its electrons to higher energy levels. The fluorochrome then releases this energy *via* vibrational relaxation, emitting light at a lower energy and longer wavelength than the excitation light (Stokes Shift).⁷¹ A fluorescence microscope provides excitation energy to a sample. Optical filters within the microscope separate the brighter excitation light so that only the weaker, emitted fluorescent light is detected, allowing for the generation of high contrast images. The unique capabilities of fluorescence as a means of detection include its (i) sensitivity, as the emission from only a small number of fluorescent molecules is detectable, and (ii) specificity, as the excitation and emission spectra for particular fluorescent molecules are usually characteristic. This can be used to selectively analyse complex mixtures of molecular species in one sample.

Limitations of fluorescence detection include two photochemical phenomena, namely photobleaching and quenching. Photobleaching, or fading, is a photochemical reaction between the fluorophore, light and oxygen (a form of oxidation) that causes loss of fluorescence signal.⁷² Fluorescent molecules have a photochemical lifetime and will emit only a certain number of photons no matter how the excitation energy is delivered, therefore at low excitation energy levels, photobleaching is not prevented only the rate is reduced.⁷³ Quenching is also a significant effect in fluorescence microscopy that occurs when the excess energy of an excited fluorochrome is absorbed by a neighbouring molecule causing the depletion or loss of fluorescence. Despite these limitations, fluorescence microscopy is still a valuable technique for the analysis of fluorescent markers on surfaces.

2.1.8 Fluorescent Markers

Fluorescence detection is used extensively for a wide range of applications in the biosciences, such as DNA sequencing, antibody and DNA detection. The attachment of fluorescent tags to non-fluorescent molecules enables very sensitive detection of these otherwise visually undetectable molecules.

2.1.8.1 Fluorescein

Fluorescein is a molecule commonly used as a fluorophore in fluorescence microscopy with an absorption maximum at 494 nm and emission at 525 nm. Typically a fluorescein molecule will emit 30-40 thousand photons during its photochemical lifetime.⁷¹ A number of modified fluoresceins are commercially available, such as fluorescein isothiocyanate (FITC) and aminofluorescein, allowing for the straightforward attachment of this molecule to non-fluorescent systems.

2.1.8.2 Green Fluorescent Protein

Green fluorescent protein (GFP) is currently being explored as it has potential applications in devices such as molecular information storage systems and biophotonic-based sensing devices.^{55, 74, 75} The interest in this molecule stems from its unique molecular properties. GFP was first isolated from the jelly fish *Aequorea victoria*, it emits intense and stable fluorescence without any cofactors, shows considerable stability towards changes in environmental conditions,⁷⁶ eg. high salt concentrations, a wide pH range and temperatures up to 78°C. It is also less susceptible towards photo-bleaching than other fluorophores such as fluorescein.⁷⁷ The 27kDa protein possesses a tightly packed β -barrel tertiary structure with the chromophore contained within a coaxial alpha helix (Figure 2-7). The chromophore consists of a cyclic tripeptide derived from a Ser-Tyr-Gly sequence in the primary protein sequence. Importantly, the fluorophore only fluoresces when embedded within the complete GFP protein. A number of genetically modified fluorescent proteins are available including EGFP (enhanced green fluorescent protein) that is 35 times brighter than the wild type protein with an excitation maximum of 488 nm and emission at 507 nm.⁷¹

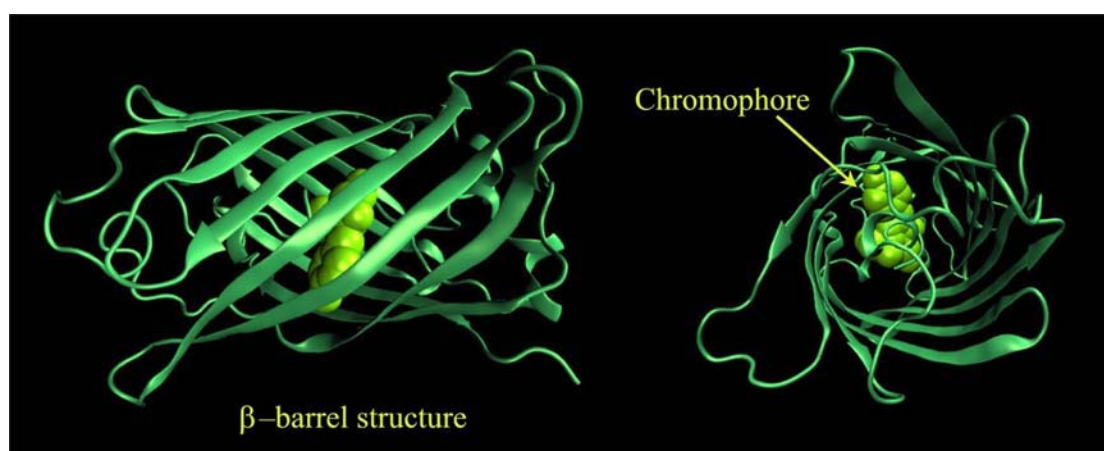


Figure 2-7. Cartoon representation of Green Fluorescent Protein, illustrating the β -barrel structure and the location of the chromophore within.

2.1.9 Background to Present Work

The aims of the work investigated in this chapter are twofold, 1) the preparation of N-hydroxysuccinimide terminated self assembled monolayer surfaces for the attachment of proteins (GFP) to a gold surface and 2) the preparation of a ‘heat activated’ SAM adsorbate monomer and formation of the corresponding SAM on gold and to conduct preliminary investigations into the thermally induced conversion of the acyl azide to the chemically reactive isocyanate on the surface.

Aim 1

Single molecules of GFP, immobilised in an aqueous polymer have previously been shown to exhibit on/off blinking and switching behaviour, that can be controlled by lasers.^{74, 78} This property could potentially be adapted for the development of biomolecular devices such as optical information storage devices and optical switches. Towards this end, we aimed to determine if the attachment of GFP to a SAM on gold would quench the fluorescence of the protein, as it has been reported that gold (and other metals) in the absence of a SAM can quench the fluorescence of GFP and other fluorophores.⁷⁹ If fluorescence could be maintained on covalent binding of the protein to the SAM surface, this could potentially be developed as a platform for the aforementioned applications.

Most of the literature relating to the attachment of GFP to a surface relies on the poly-histidine or arginine ‘tags’ that contain nitrogen atoms known to bind strongly, but reversibly, to cobalt and nickel. This property is used generally for the purification of these proteins. The poly-histidine tag has been found to bind directly to nano-clusters of gold pinned to a graphite surface.⁸⁰ Furthermore, a SAM terminated with

carboxylic acids was functionalised with nitrilotriacetic acid groups that complexes Ni(II), that subsequently binds the histidine tagged GFP to the surface.⁸¹ Monolayers of a chimera of cytochrome b562-GFP have been prepared on gold surfaces *via* the mutation of the cytochrome b562 to incorporate two exposed cysteine residues on the surface of the protein, as such these thiol groups were adsorbed onto the gold surface forming a monolayer with applications as a molecular photodiode.⁸² The covalent attachment of GFP via an *N*-hydroxysuccinimide terminated monolayer has, to the author's knowledge, only been reported on silicon.⁸³

Aim 2

This investigation centres on the development of a non-reversible 'switchable' SAM, that is the properties of the SAM are changed by an external stimulus such as, in our proposed case, the application of heat. We aim to prepare a 'pro-click' monolayer precursor possessing relatively unreactive chemical entities (acyl azide) that can be embedded within inert SAM films (Figure 2-8) and subsequently be selectively activated using localized heat to generate click compatible functional groups (isocyanate). Once activated these surfaces will have the potential to react with functional groups such as amines and alcohols *etc*, enabling tethering of macromolecular, dendritic or biomolecular entities to specific regions of the surface. Heat could then be focused on a different section of the surface and the procedure repeated.

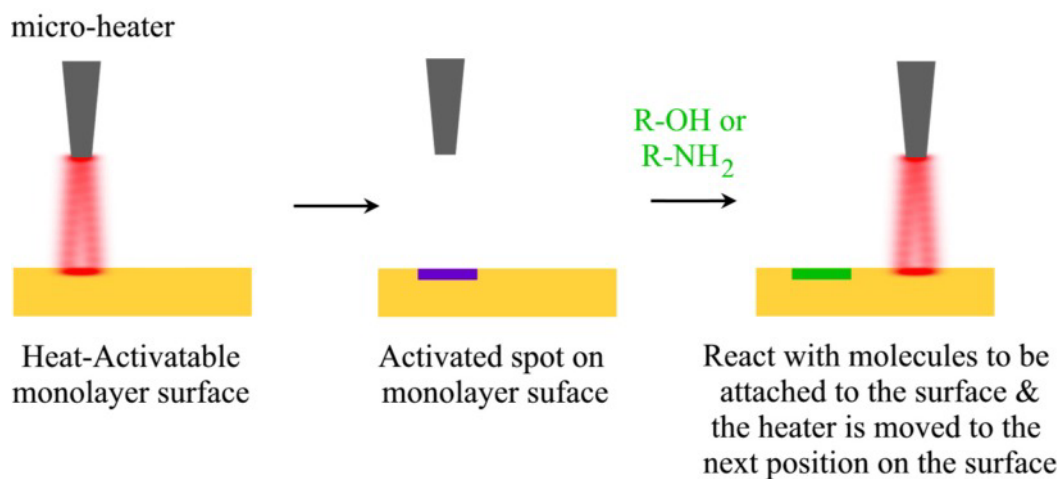


Figure 2-8. Potential for preparation of functionalised surfaces using heat activated monolayer.

Minimal literature is available on the reactivity of isocyanate terminated SAMs on gold, however there is literature precedent for the reaction of an hydroxyl terminated monolayer with 1,4-phenylene diisocyanate **45** to produce a carbamate linkage leaving one isocyanate group oriented towards the surface with the ability to react with alcohols and amines under mild conditions.⁸⁴

2.2 Results and Discussion

2.2.1 Preparation of Gold Surfaces

There are a number of well documented methods for the deposition of gold onto surfaces, for example evaporation, sputtering, chemical vapour deposition and electrodeposition.⁸⁵ Of these methods, two were available for use in this project, an evaporator and an argon ion sputterer. In the metal sputtering process (Figure 2-9), a vacuum chamber is evacuated and refilled with low pressure argon gas. A high voltage potential difference between the chamber and the target accelerates argon ions to strike the target, physically dislodging metal atoms that fall throughout the chamber, some depositing on the substrate to produce a high quality metal film.

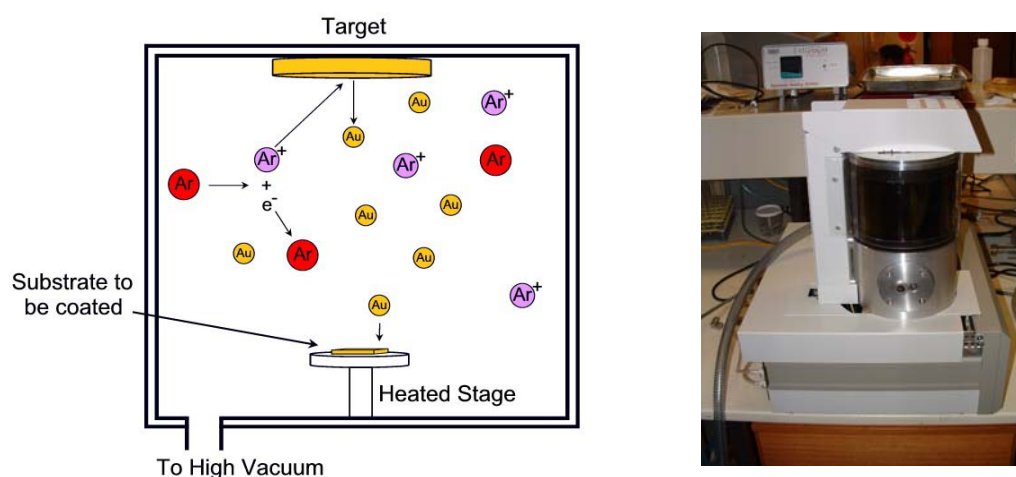


Figure 2-9. Schematic illustration of the sputtering process with photograph.

In an evaporator (Figure 2-10) the pressure inside the chamber is reduced to lower the sublimation point of the metal. The material to be deposited is then heated electrically in metal wires or containers. Metals such as tungsten(W) and molybdenum(Mo) are generally used to make the evaporation container as they maintain a low vapour pressure at the temperature required to evaporate gold. Alternatively some ceramics

may also be used. Once the metal vaporises, it condenses on all surfaces within the chamber including the substrate to form a thin metal coating.

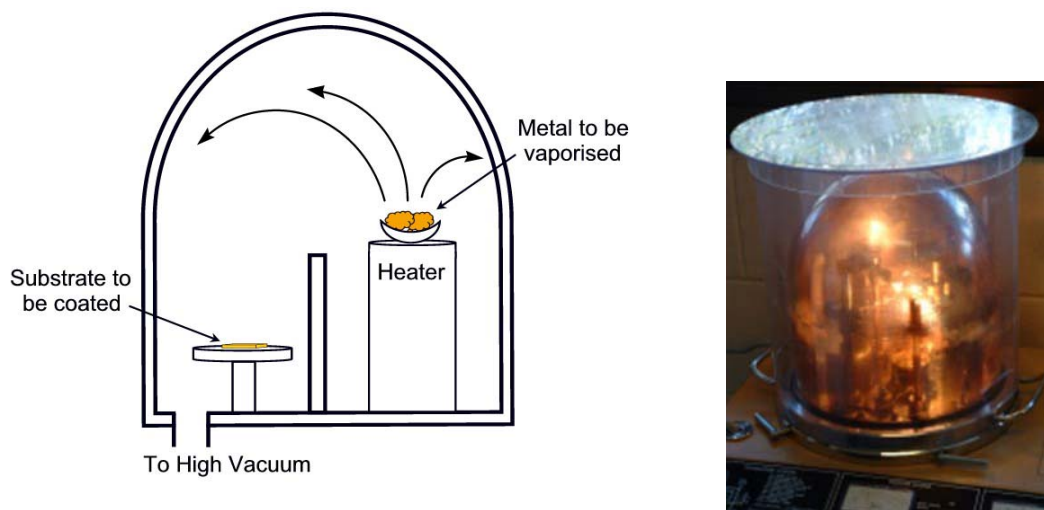


Figure 2-10. Schematic illustration of metal evaporation and photograph.

Both the evaporation and the sputtering methods were trialled, however, the argon ion sputterer was simpler to operate, produced consistent surfaces and was therefore used routinely for the preparation of our gold surfaces. Atomically flat silicon wafers, were purchased from Addison Engineering (100mm prime silicon wafers 1-20 Ω -cm, P/Boron doped), were diced into 1 cm squares. Immediately prior to the metal deposition, the silicon was cleaned by rinsing with high purity acetone to remove the protective coating and drying with a stream of nitrogen. Initially a layer of chromium was deposited as an adhesive layer⁸⁵ to prevent the gold from flaking off the substrate. A layer of gold (24 carat, 99.99% pure) was then deposited on the chromium surface. A detailed description of the operation procedure used for the sputterer is included in the experimental section of this thesis.

The sputterer stage could be heated to various temperatures and trials were carried out with the stage at 100°C, 200°C and 250°C. AFM analysis (Figure 2-11), using the

JEOL JSPM-4200, equipped with an 85×85 μm² tube scanner, of a sample from each batch of gold surfaces were carried out to assess their flatness, with typical RMS values of 7.1 nm, 5.1 nm and 5.2 nm respectively. As the difference in surface roughness between the surfaces prepared at the two higher temperatures was minimal and they were less rough than the surfaces prepared at the lowest temperature, 200°C was selected for use in the standard procedure.

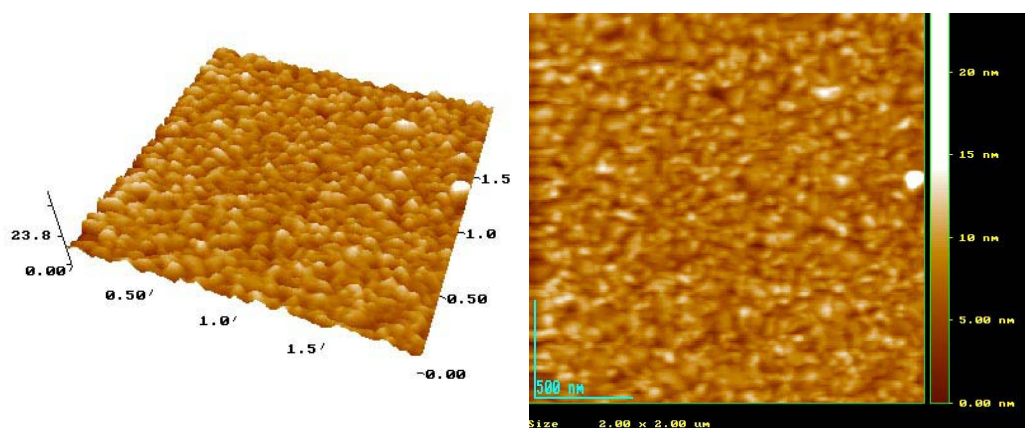


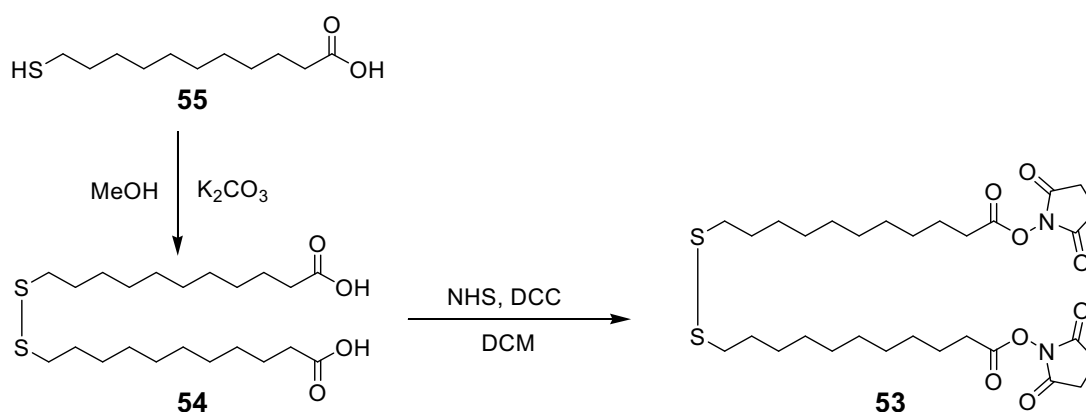
Figure 2-11. AFM image of gold surface sputtered at 200°C.

2.2.2 Chemical Synthesis of SAM monomers (adsorbates)

2.2.2.1 *N*-hydroxysuccinimide monomer

An amine reactive monomer (SAM adsorbate) was required to develop a method for covalently immobilising GFP onto surfaces. Dithiobisundecanoic acid di-*N*-hydroxysuccinate **53** was identified as a suitable target molecule, as the disulfide linkage chemisorbs to gold surface while the NHS groups remain reactive toward the primary amine groups of proteins or other molecules. Covalent attachment of other proteins onto gold surfaces has been achieved previously using this approach.^{61,62,86} Accordingly, 11,11'-dithiobisundecanoic acid **54**, was synthesised *via* a literature procedure,⁸⁷ from the corresponding thiol **55** (Scheme 2-1). In the method, **55** was

dissolved in methanol and stirred with potassium carbonate in an open vessel. Acidification of the reaction mixture, extraction with ethyl acetate and subsequent recrystallisation in hexane, afforded the disulfide product in a 72% yield. ESMS analysis of the product revealed peaks at 433 amu in the negative mode and 457 amu in the positive mode corresponding to the molecular ion and the sodium adduct respectively. ^1H and ^{13}C NMR spectra were consistent with the structure.



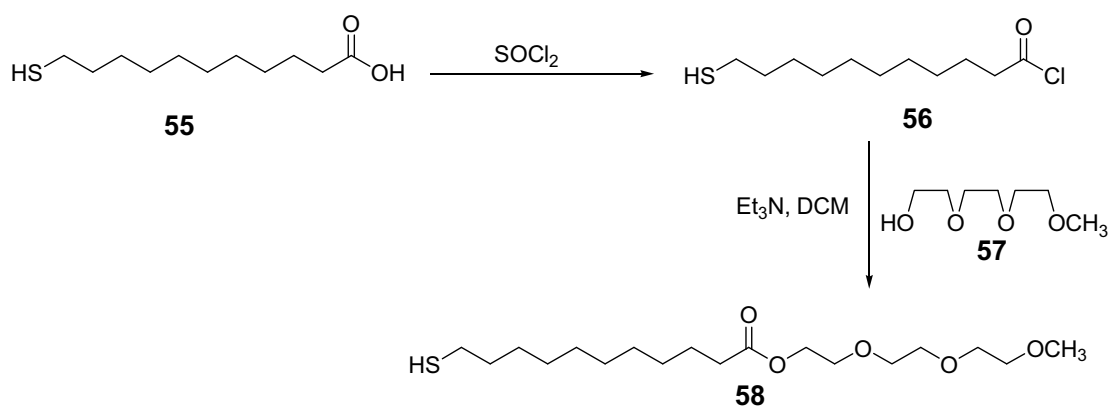
Scheme 2-1

The synthesis of the di-*N*-hydroxysuccinate analogue **53** involved the DCC coupling of **54** with NHS in DCM.²⁵ The crude material was purified by column chromatography (5:1 DCM/MeCN) with an isolated yield of 30%. The melting point and NMR spectra were consistent with literature reported values²⁵ and ESMS analysis revealed peaks corresponding to the lithium and sodium adducts at 635 amu and 651 amu respectively.

2.2.2.2 Tri(ethyleneglycol) monomer

Proteins adsorb onto many surfaces *via* noncovalent hydrophobic bonding or electrostatic interactions. It has been shown however, that polyethylene glycol type surfaces resist non-specific protein binding,^{88, 89} due to their hydrophilic nature, the presence of hydrogen bond acceptors and overall neutral electrical charge.⁹⁰ A novel

protein-resistant monomer possessing a tri(ethyleneglycol) end group was therefore synthesised (Scheme 2-2). 11-Mercaptoundecanoic acid **55**, was heated with thionyl chloride to form the corresponding acid chloride **56**. Excess thionyl chloride was removed and the crude material was dried under vacuum. Tri(ethyleneglycol) monomethyl ether **57**, was dissolved in DCM with triethylamine (2.4 eq.). The dried acid chloride **56**, was dissolved in DCM and the resultant solution added slowly to the tri(ethyleneglycol) solution under an atmosphere of nitrogen. Workup involved aqueous washes to remove triethylamine HCl salts. Removal of the solvent afforded a brown oil that was subsequently purified by column chromatography (60% Et₂O/hexane) affording the product **58** as a pale yellow oil in 72% yield. ESMS analysis gave peaks at 371 amu and 387 amu in the positive mode corresponding to the lithium and sodium adducts of **58** and ¹H and ¹³C NMR were consistent with the structure.

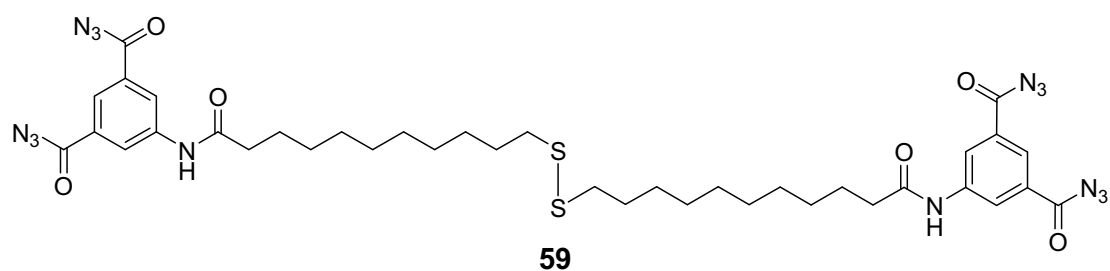


Scheme 2-2

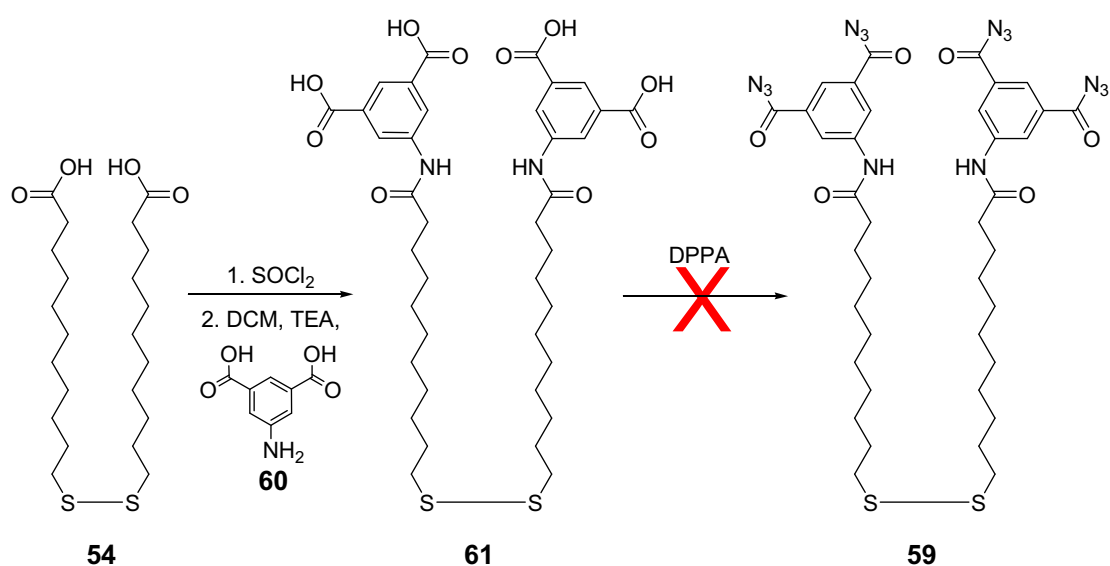
2.2.2.3 Acyl Azide monomer

An acyl azide functional group was selected as a feasible terminal group for the development of an irreversible ‘switchable’ SAM that could be activated by heat. Before the application of heat, this group is quite unreactive. However, on conversion to the corresponding isocyanate, a function is installed into the SAM that would be

exceptionally reactive towards amine groups. **59** was designed as a suitable target to investigate this hypothesis.



Initial attempts to synthesise the target molecule (Scheme 2-3) included the synthesis of di-isophthalic 11,11'-dithiobisundecanoic amide **61**. 11,11'-dithiobisundecanoic acid **54** was heated gently in SOCl_2 under an atmosphere of nitrogen for one hour. Excess thionyl chloride was removed in vacuo and the residue was dissolved in *N*-methylpyrrolidinone (NMP) and the solution added dropwise to a solution of 5-aminoisophthalic acid **60** and Et_3N in NMP cooled to 0°C . The reaction was stirred at room temperature for 18 hours and poured into water. The precipitate that formed was collected by filtration then recrystallised from chloroform/methanol affording the pure product **61** as an off white coloured solid.



Scheme 2-3

ESMS analysis gave peaks at 759 amu corresponding to the molecular ion in the negative mode and show a fragmentation peak at 379 amu corresponding to cleavage of the disulfide bond during ionisation (Figure 2-12). NMR and microanalysis results were consistent with the desired structure.

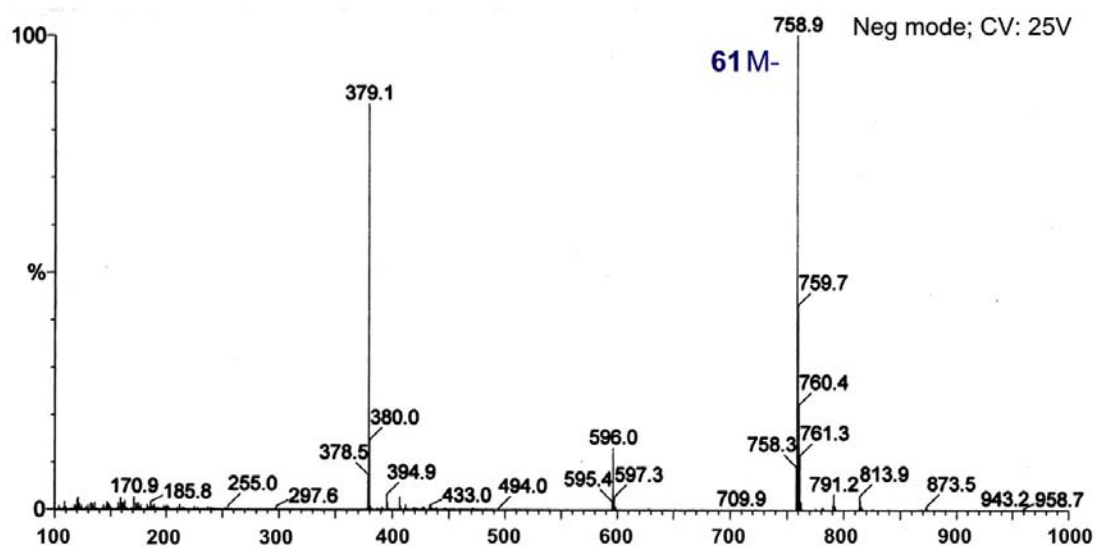


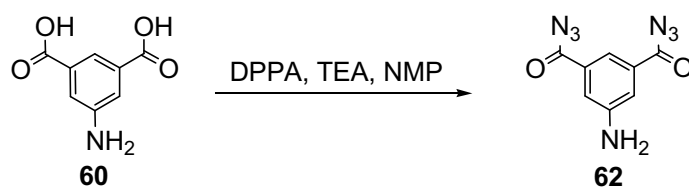
Figure 2-12. ESMS spectrum of **61**.

The di-isophthalic 11,11'-dithiobisundecanoic amide **61** was dissolved in THF under an atmosphere of nitrogen. On addition of Et_3N , a dense precipitate formed that adhered to the bottom of the flask, whereupon NMP was added to help solubilise the material. Diphenylphosphonylazide (DPPA) was subsequently added and the mixture stirred at room temperature overnight. The reaction mixture was then poured into water and the resultant precipitate collected by filtration and dried.

Analysis of this crude product by ^1H NMR showed the presence of starting material as no change was observed in the chemical shift of the proton resonances corresponding to the aromatic hydrogens or the NH (as would be expected if the acid groups were

converted to acyl azides) and the carboxylic acid proton resonance was still present at 13ppm. Furthermore, a large amount of DPPA (an expensive reagent) was required in the reaction. Consequently, an alternate synthetic path was sought. We elected to synthesise independently the acyl azide end group and attach this group to **54** *via* a coupling reaction. The approach was intended to circumvent the problems encountered with solubility and to reduce the total cost of the synthesis.

The requisite acyl azide end group, 5-amino-1,3-benzenedicarbonyl diazide **62**, was synthesised *via* a literature procedure.⁹¹ DPPA and Et₃N were added to a solution of 5-aminoisophthalic acid **60** in NMP and the mixture stirred at room temperature under an atmosphere of nitrogen (Scheme 2-4). The reaction mixture was poured into aqueous NaHCO₃ and the product collected by filtration and purified by recrystallisation affording **62** in a 96% yield.



Scheme 2-4

¹H and ¹³C NMR spectra were consistent with reported values and FTIR analysis showed the strong characteristic band of the CON₃ group at 2144 cm⁻¹ (Figure 2-13).

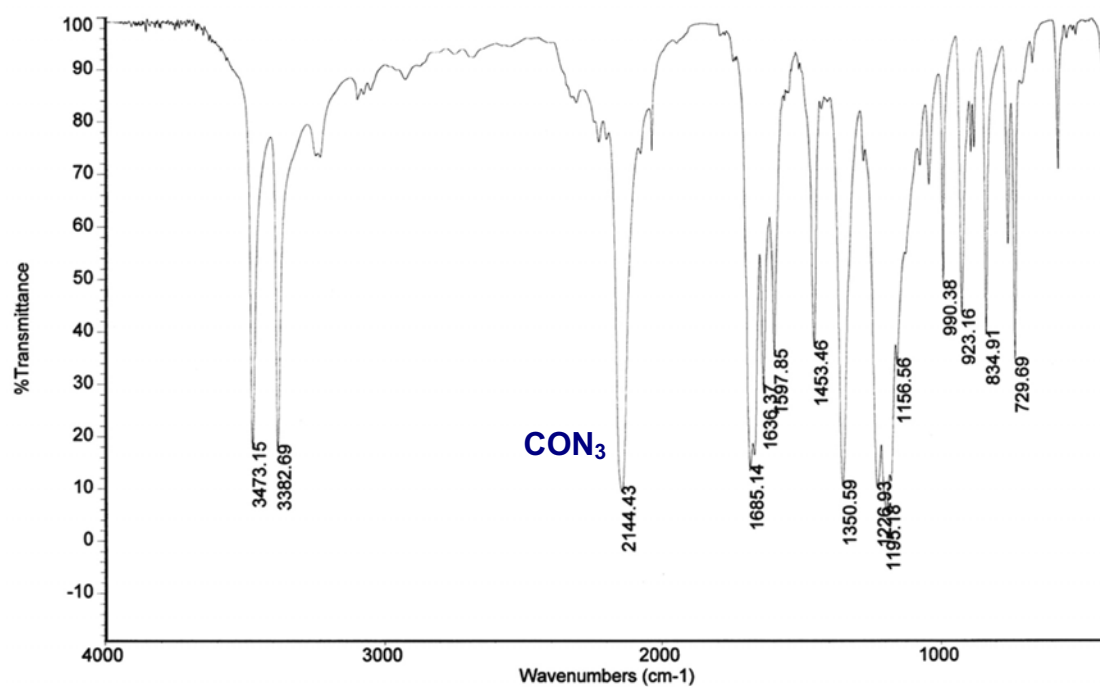
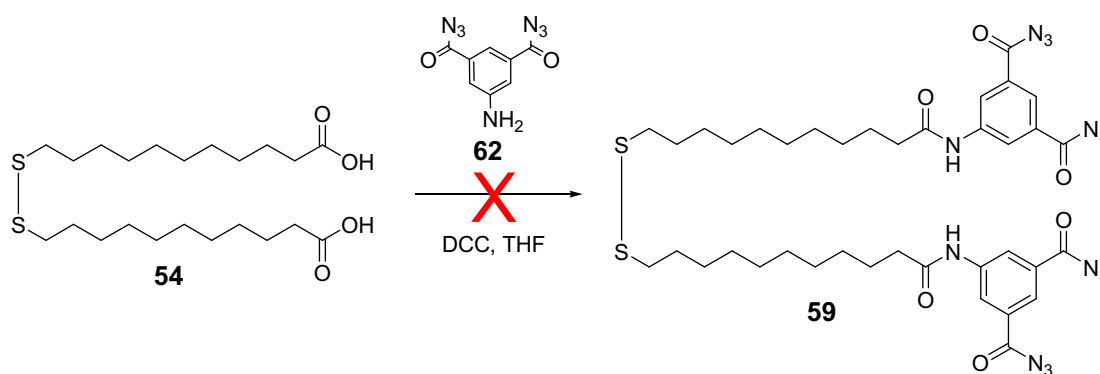


Figure 2-13. FTIR spectrum of **62**.

Initially, a DCC coupling of compounds **54** and **62** was attempted (Scheme 2-5). 11,11'-dithiobisundecanoic acid **54** was activated with DCC in a solution of THF and 2.5 equivalents of the acyl azide end group **62** were added. The reaction mixture was stirred for 18 hours and the precipitated DCU was removed by filtration. Evaporation of the solvent (under reduced pressure at 25°C) revealed a sticky oil that on analysis by ^1H NMR, showed a mixture of compounds including DCU, however the NH resonance of the amide was not observed suggesting an unsuccessful reaction.



Scheme 2-5

As the DCC coupling reaction was unsuccessful, we attempted a direct coupling of the acyl azide end group **62** to 11,11'-dithiobisundecanoic acid **54** via an acid chloride coupling. **54** was heated gently in SOCl_2 under an atmosphere of nitrogen for one hour. The excess thionyl chloride was removed *in vacuo*. The residue was dissolved in THF and added dropwise to a solution of 5-amino-1,3-benzenedicarbonyl diazide **62** and Et_3N in THF. The reaction was stirred at room temperature for 48 hours then the precipitated triethylamine hydrochloride was removed by filtration. The filtrate was evaporated (reduced pressure, 25°C) and the residue purified by column chromatography (4% $\text{EtOAc}/\text{CH}_2\text{Cl}_2$) to give **59**, in a 28% yield, as a yellow oil that solidified into thin plates on freezing.

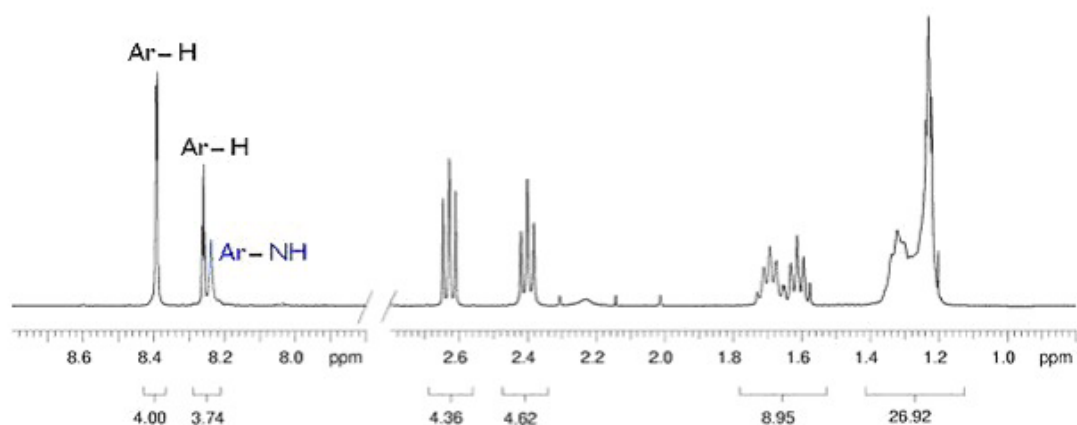
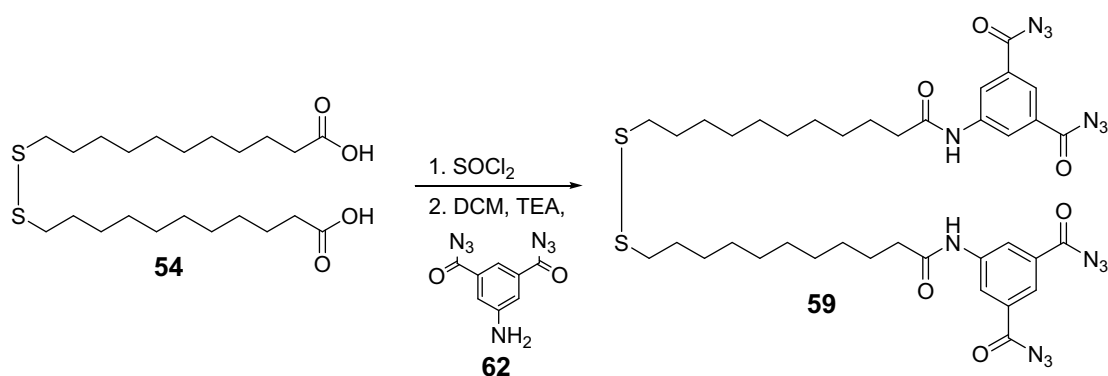


Figure 2-14. ^1H NMR spectrum (400MHz, 298K, CDCl_3) of the purified SAM adsorbate monomer, **59**. (proton resonance of the formed amide highlighted in blue)

The ^1H NMR spectrum of the acyl azide monomer (Figure 2-14) shows the *NH* resonance of the formed amide bond. Only the solvent signal (CDCl_3 , δ 7.27 ppm) was observed in the section removed from the spectrum for illustrative clarity.

2.2.3 Formation and Characterisation of Monolayers on Gold – GFP Studies

Our initial studies focussed on the preparation and analysis of one-component monolayers of dodecanethiol, the synthesised NHS terminated disulfide **53** and the protein resistant thiol **58** as precursors to the preparation of patterned surfaces of these monolayers. In each case, a cleaned gold surface was placed in a 1mM ethanolic solution of the required disulfide or thiol, allowed to stand in the solution, in a closed vial, at room temperature for 18-20 hours. After this time, the surfaces were removed from the solution, rinsed with ethanol and dried under a stream of nitrogen. Analysis of the surfaces were carried out immediately unless otherwise stated. Both grazing angle IR and ATR spectroscopy were trialled on the gold surfaces. Unfortunately, analysis of the surfaces using grazing angle IR did not reveal any signal and the spectra achieved using ATR were inconclusive despite the acquisition of ~1000 scans. Due to the poor quality of the data repeatedly obtained in these experiments we focussed on alternative characterisation methods for the analysis of the SAMS. Contact angles were measured for each of the monolayer surfaces and the results are reported in Table 2-1. These values were compared against the contact angle measured for a control surface (clean gold surface treated under the same conditions with pure ethanol, *ie* no thiol/disulfide present). Most of the prepared surfaces exhibit hydrophilic behaviour (low contact angle with water) with the exception of the dodecane thiol monolayer. This result for the dodecanethiol monolayer corresponds to

typical literature values¹² and indicates that the formed dodecanethiol monolayer is ordered.

Table 2-1. Water contact angles for self assembled monolayer surfaces on Au.

Standard deviations are given in parentheses.

SAM Surface	θ°
Dodecane thiol	111 (2.3)
53 (NHS)	74 (2.0)
58 (Protein resistant)	64 (3.0)
Bare Gold (EtOH)	61 (2.2)

Ideally, XPS analysis of the SAM surfaces would have been carried out immediately following their removal from the disulfide/thiol solution. However the practical limitation of off-site XPS analysis resulted in delays between preparation and analysis. The surfaces were unfortunately exposed to air in these intervals. Nevertheless, XPS survey spectra (Figure 2-15) were obtained for monolayers of samples **53** and **58** (synthesised in section 2.2.1.1 and 2.2.1.2). The spectra were referenced to the Au 4f doublet at a binding energy of 84 eV as common in the literature.⁹² The expected peaks arising from the ionisation of core electrons of C, N, O and S were observed in the spectra (Appendix B). The C 1s peak appeared at 285 eV for both surfaces, corresponding to the carbon atoms of the methylene groups, and a smaller peak was observed at ~289 eV on the **53** surface corresponding to the C=O groups⁹³ of the *N*-hydroxysuccinimide coated surface. There was a N 1s peak observed for the NHS surface at 400 eV. However, as expected, no nitrogen was found to be present in the monolayer of **58**. The O 1s peak was observed at ~531 eV for both compounds. The S 2p ionization was treated as a single peak centred at BE of

~163 eV, corresponding to the value reported for sulphur bound to gold as a thiolate,^{94,95} indicating successful formation of the monolayers.

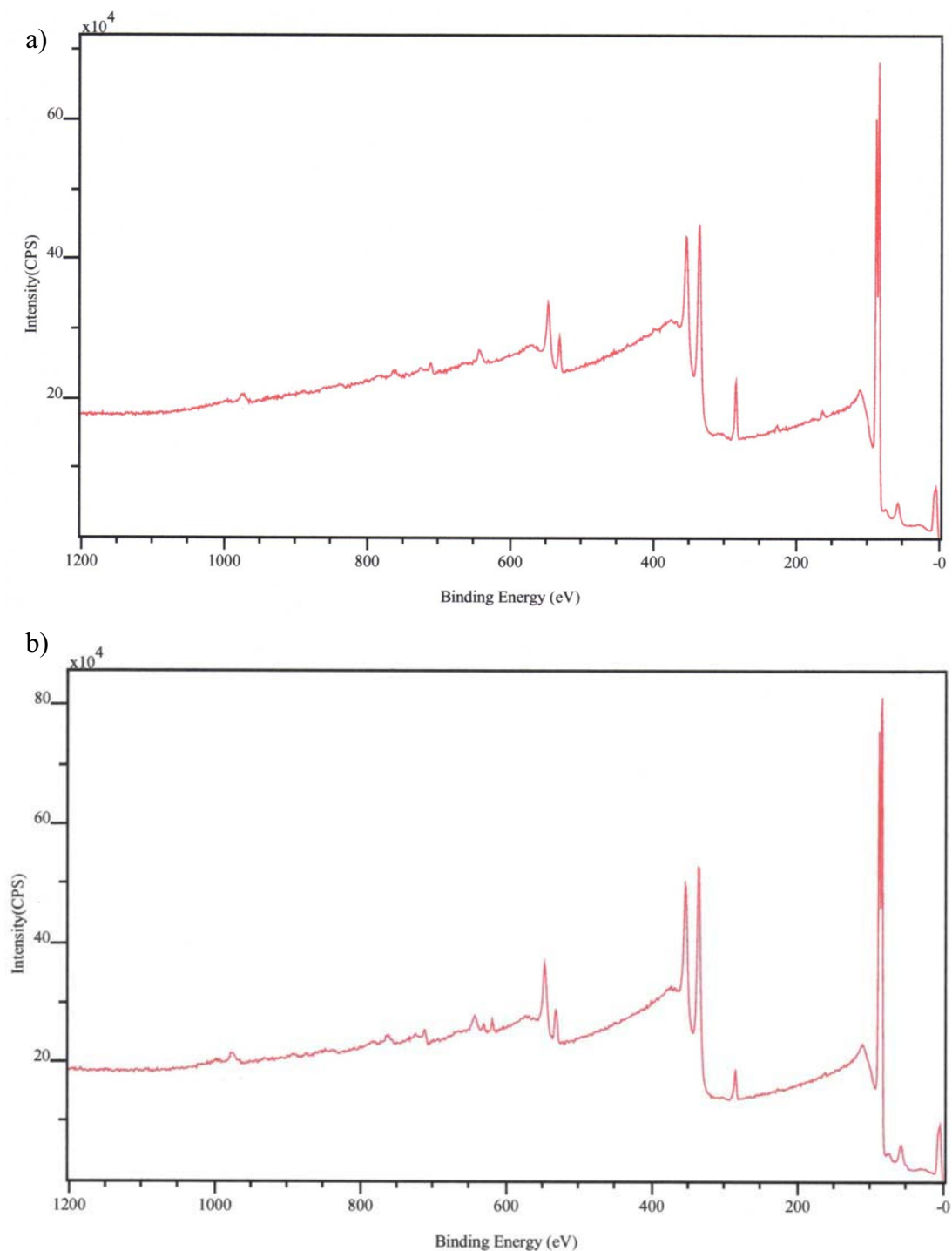


Figure 2-15. Survey scans of a) **53** and b) **59** monolayer surfaces.

Unfortunately, the XPS spectra also evidenced peaks indicative of contaminants. A peak at a BE of ~ 712 eV corresponding to Fe 2p and a peak at 619 eV corresponding to I 3d were observed, however the latter did not appear in the spectrum of **53**. At present the sources of these contaminants are unknown. A more detailed analysis of these results is beyond the scope of this work and will be an object of future studies.

In summary, we have demonstrated the successful formation of SAMs of dodecanethiol, **53** and **58** on gold surfaces through well documented solution based adsorption techniques. Contact angles and preliminary XPS data have been obtained for the materials.

2.2.4 SAM Patterning Trials

A UV patterning protocol was required in order to obtain a patterned surface for the attachment of GFP to a monolayer surface. Thus our test protocol was to form a dodecane thiol monolayer on a gold surface, expose this surface to UV irradiation through a mask, for varying lengths of time. The oxidised areas exposed to the UV light would then be filled with an *N*-hydroxysuccinimide terminated monolayer. The surface could then be treated with aminofluorescein. Successful patterning of the surface would thus be evidenced by fluorescence microscopy.

Initially, 1cm squares of silicon were used and a transmission electron microscope (TEM) grid used for the UV irradiation of monolayers under the UV lamp. In an attempt to simplify locating the irradiated regions on the 1cm² surfaces, circles of gold, the same size as a TEM grid, were sputtered onto the silica surface after a chromium adhesion layer was deposited, through a metal mask (Figure 2-16).

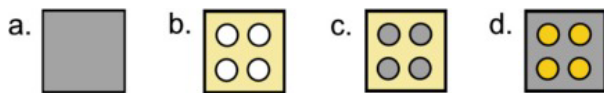


Figure 2-16. a) silicon wafer square; b) metal mask with holes the size of TEM grids; c) the mask is placed on top of the silicon wafer square and placed in the sputterer; d) on removal from the sputterer the silicon square has four gold circles sputtered onto the surface.

However, on cleaning of these gold surfaces in either piranha solution (30% H_2O_2 in H_2SO_4) or ammonia cleaning solution ($\text{H}_2\text{O} : \text{NH}_4\text{OH} : \text{H}_2\text{O}_2$ (5 : 1 : 1) at 75°C), the gold circles had a tendency to detach from the substrate. Much better adhesion was observed when the gold coated the entire surface.

Further attempts thus focussed on complete surfaces. Accordingly, gold was sputtered onto 0.5 cm^2 squares that were then cleaned in a freshly prepared piranha solution, rinsed thoroughly with milliQ water and dried under a stream of N_2 and placed in a sealed vial, containing a 1mM solution of dodecane thiol in ethanol (12 μl dodecanethiol in 50ml EtOH), for 18.5 hours. On removal from the solution, the surfaces were rinsed with ethanol, then water and dried with a stream of N_2 .

One of the dodecanethiol coated surfaces was taken as a control and 20 μL of a 20 mM solution of 5-aminofluorescein in DMF (7.3 mg in 1 ml) was placed on to the surface and the surface covered with a glass coverslip and placed in the refrigerator for 17 hours. The surface was then rinsed with DMF and then acetone and viewed under the fluorescence microscope. Virtually no fluorescence was observed.

Three dodecane thiol monolayer surfaces were exposed to the UV spot lamp, through a TEM grid (20 μm and 100 μm squares), for varying lengths of time, one for 10

minutes, the second for 20 minutes and the third for 30 minutes (timed in one minute bursts). The surfaces were then placed in a 1 mM solution of the *N*-hydroxysuccinimide disulfide (31.4 mg in 50 ml of ethanol) and allowed to stand for a further 18 hours, to replace the oxidised portions of the monolayer. The surfaces were removed from the solution, then rinsed with ethanol, then water and dried as above.

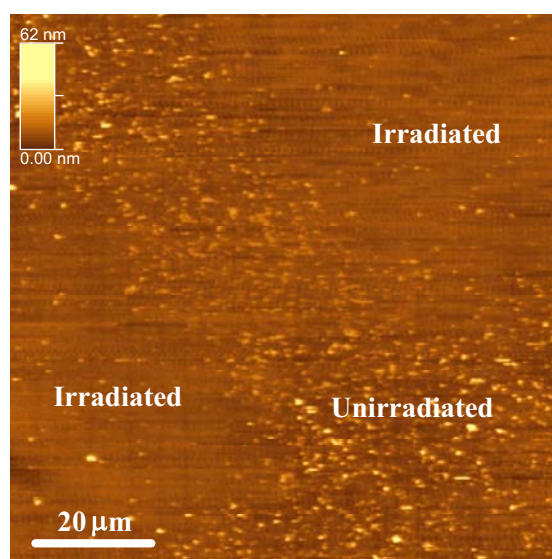


Figure 2-17. Topographical image (400 line resolution) of NHS/dodecanethiol SAM.

Previously, AFM imaging of alkane thiol monolayers adsorbed on gold under an alcohol solution of 2-methyl-2-propanol have achieved images with true molecular resolution.⁹⁶ We conducted our analyses of our surfaces using a TopoMetrix TMX 2000 Explorer, with a 130×130 μm² tripod liquid scanner, with a z-range of 9.7 μm. Images were obtained in the contact imaging mode of operation in neat 2-butanol. Figure 2-17 shows the AFM image obtained from an NHS/dodecane thiol patterned monolayer. Running diagonally through the centre of the image is an unirradiated section corresponding to the crossbar of a TEM grid used. The unirradiated sections

correspond to the dodecane thiol sections of the monolayer and the irradiated sections correspond to the *N*-hydroxysuccinimide monolayer filled squares.

Patterning was further examined using fluorescence labelling. A 20 mM solution of 5-aminofluorescein in DMF (7.3 mg in 1 ml) was prepared and a 20 μ L drop was placed on each of the NHS patterned surfaces, covered with a glass coverslip then placed in the refrigerator for 22 hours. The surfaces were rinsed with DMF then acetone and viewed under a fluorescence microscope. The sharpest image was observed from the dodecane thiol surface exposed to 30 minutes of irradiation followed by reaction with aminofluorescein (Figure 2-18). Suggesting that the oxidation of the thiols when exposed to UV irradiation, under our conditions, is a fairly slow process and that long exposure times are required in order to obtain well defined patterns on the surface.

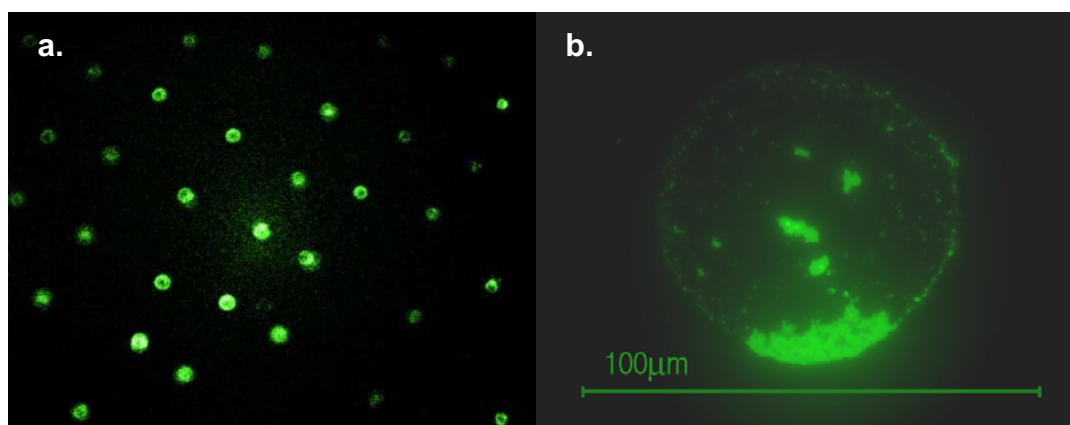


Figure 2-18. Fluorescence microscope images of (a) a 30 minute UV patterned [through a 20 μ m TEM grid] Dodecane/*N*-hydroxysuccinimide surface after reaction with aminofluorescein, and (b) magnified image of the same type of surface patterned through a 100 μ m TEM grid.

Analysis of these surfaces were also carried out using a TopoMetrix TMX 2000 Explorer, with a $130 \times 130 \mu\text{m}^2$ tripod liquid scanner, with a z-range of $9.7 \mu\text{m}$. Images were obtained, in the contact imaging mode of operation, in neat 2-butanol. In this experiment, clearer images were obtained from these surfaces than those analysed prior to functionalisation with aminofluorescein. These latter images (Figure 2-19) show distinct squares separated by crossbars, in both the topographical and lateral force modes. The unirradiated sections, corresponding to the dodecanethiol sections of the monolayer, and the irradiated sections, corresponding to the backfilled NHS monolayer after reaction with aminofluorescein are clearly in evidence.

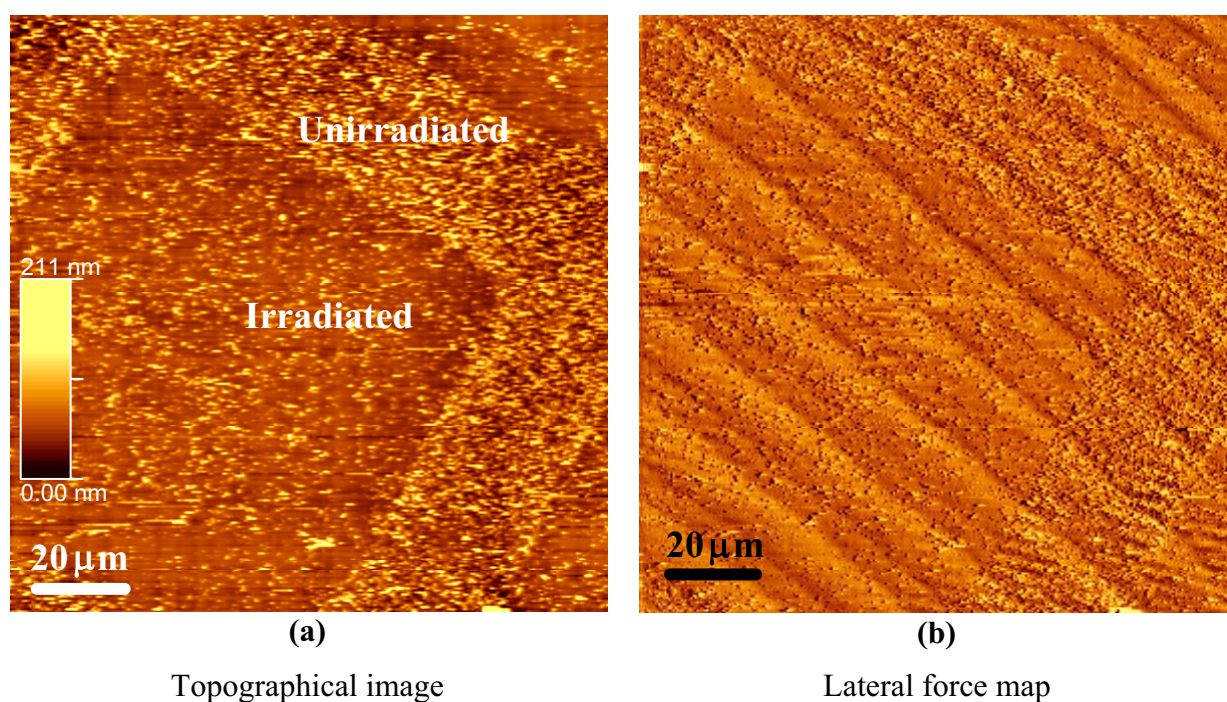


Figure 2-19. AFM images obtained from the dodecanethiol/NHS + aminofluorescein surfaces imaged under 2-butanol. a) Topographical image, b) lateral force.

A higher resolution image was also obtained from the same patterned surface (30 minutes exposure, aminofluorescein treated) and is included in Figure 2-20.

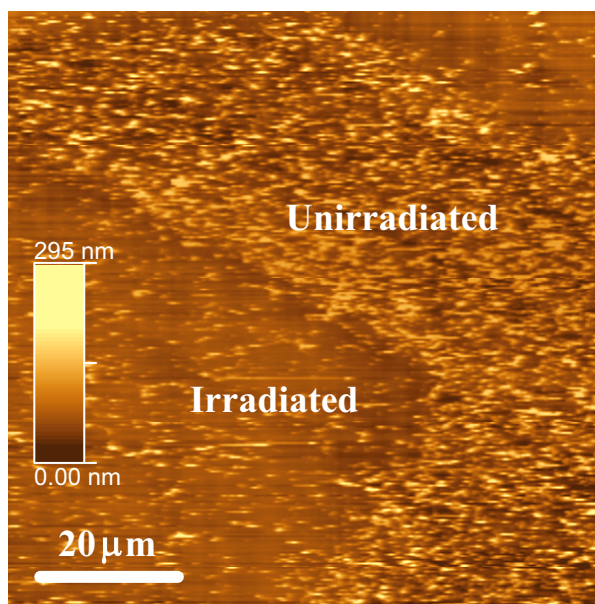


Figure 2-20. Higher resolution AFM image obtained from the dodecanethiol/NHS+aminofluorescein surfaces imaged under 2-butanol (300 line resolution).

We have thus developed a successful patterning protocol. Exposure of the monolayer surface to 30 x 1 minute bursts of UV irradiation in air, through a TEM mask placed on the SAM surface selectively alters the SAMs surface composition *via* oxidation of the exposed areas. These oxidised areas can be successfully backfilled with an amine reactive NHS terminated monolayer of **53**. Finally, we have also shown the successful reaction of the functionalised amine reactive NHS portion of a patterned monolayer with aminofluorescein and the successful visualisation of the patterned surface by fluorescence microscopy and AFM.

2.2.5 Attachment of GFP to SAM

With a suitable protocol for UV patterning of SAMs in hand, we turned our attention to trialling the attachment of proteins to gold surfaces, specifically green fluorescent protein (GFP). The successful functionalisation of a surface with proteins requires a

surface with a high specific affinity for the biomolecule, leading to a high amount immobilised at the surface in the required locations, while avoiding non-specific interactions that lead to poorly controlled adsorption. In addition, the immobilised entity must retain its native conformation to ensure proper function at the surface, such that once the protein is attached, no denaturing process due to the proximity of the surface should occur.⁹⁷

Thus, our aim was to prepare tri(ethyleneglycol) coated surfaces that would resist the non-specific adsorption of the protein. The resistant monolayer would be patterned *via* UV irradiation and the exposed areas refilled with an amine reactive NHS terminated monolayer. This could then be covalently coupled to the protein, as per figure 2-21. The EGFP used in this body of work was sourced from within the research group.⁹⁸

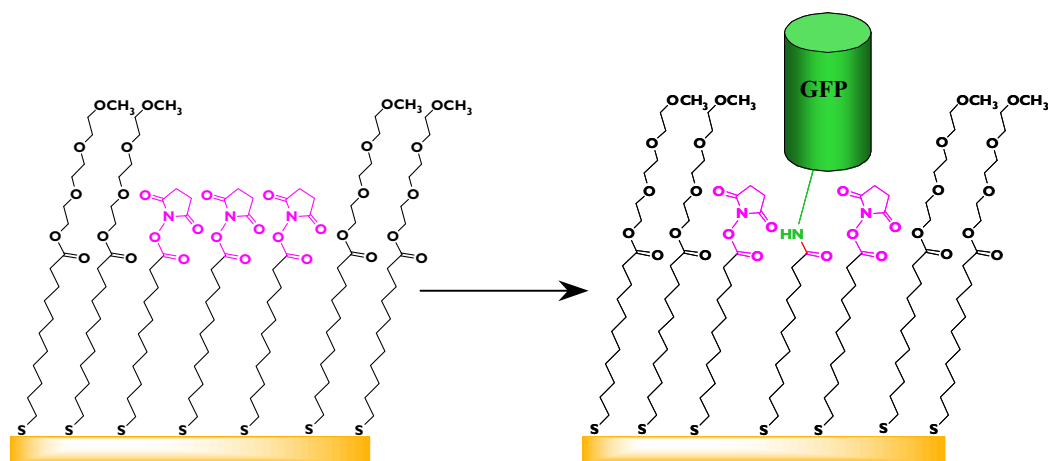


Figure 2-21. Diagram of the covalent attachment of GFP to the SAM.

Accordingly, as per our established protocol, gold surfaces (1cm^2) were cleaned in a freshly prepared piranha solution, rinsed thoroughly with water and dried under a stream of N_2 and placed in a sealed vial, containing a 1mM solution of the

tri(ethyleneglycol) terminated adsorbate monomer **58** in ethanol (6.3mg of **58** in 10ml EtOH), for 18.5 hours to form the protein-resistant monolayer surface. The surfaces were rinsed with ethanol on removal from the solution, then dried with a stream of N₂. One surface was again taken as a control and a 50 uL drop of a 2.7mg/ml solution of EGFP in 0.1M sodium phosphate buffer was spotted onto the surface and placed in the refrigerator overnight. The surface was rinsed with milliQ water and viewed under a fluorescence microscope. As before, essentially no fluorescence was observed on the surface of the control.

The remaining surfaces were exposed to the UV spot lamp, through a specially prepared film mask (1cm² with 9 x 9, 200 μm holes), for 30 minutes (timed in one minute bursts). It is noteworthy however, that the film was noticed to warp and turn opaque during the exposure to the UV light. The surfaces were then placed in a 1 mM solution of the *N*-hydroxysuccinimide disulfide (6.3 mg in 10 ml of ethanol) and allowed to stand for 18 hours. On removal from the solution, the surfaces were rinsed with ethanol, then water, and dried as above. A 50 uL drop of a 2.7mg/ml solution of EGFP in 0.1M sodium phosphate buffer was spotted onto each surface and the surface placed in the refrigerator overnight. The surfaces were rinsed with milliQ water and viewed under a fluorescence microscope. From the images obtained (Figure 2-22), it was observed that the UV irradiation through the film mask did cause some distortion to the patterning of the monolayer, as such, the fluorescent images show imperfect yet discrete patterning. A central bright green circle corresponding to the principle exposure region is observed with some additional, outlying attachment of the fluorescent protein surrounding this region.

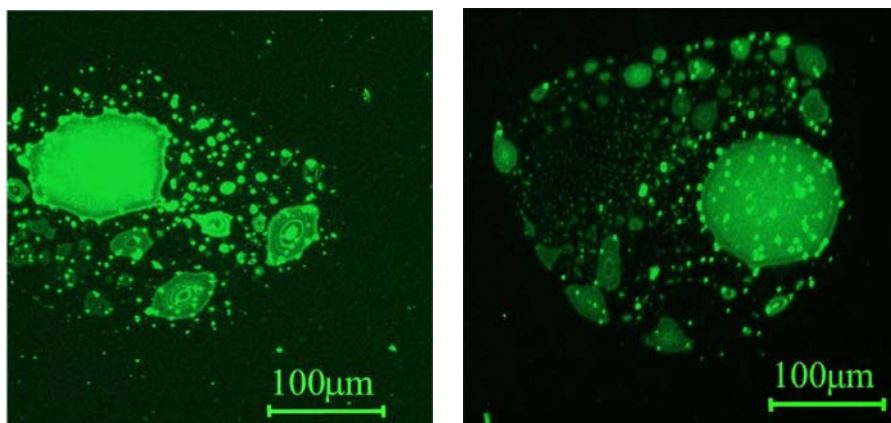


Figure 2-22. Fluorescence microscope images focusing in on the regions of GFP attached to the patterned surface.

AFM analysis of these surfaces in air, however, did not reveal any topographical images of the GFP molecules bound to the surface. Unfortunately, time did not permit the investigation of these surfaces by AFM in a liquid medium, however this will need to be investigated in future studies.

In summary, we have shown the formation of a tri(ethyleneglycol) terminated monolayer (**58**) that resisted the non-specific adsorption of GFP. We have also shown that patterning of the surface was successful despite the degradation of the film mask and most importantly, we have demonstrated that the fluorescence of the GFP was preserved on binding to the NHS monolayer on the gold surface. The surfaces were analysed using fluorescence microscopy and AFM.

2.2.6 Heat Activated SAM

Extending from the work completed in chapter one, a surface adsorbate monomer containing an acyl azide was prepared. The species is poised for activation, by heat, into an amine reactive isocyanate group (Figure 2-23). Literature precedent suggested that the monolayer surface could reasonably withstand the temperatures required to effect this conversion.⁹⁹ To the author's knowledge there has been no reported documentation of the transformation of acyl azides to isocyanates occurring on gold surfaces.

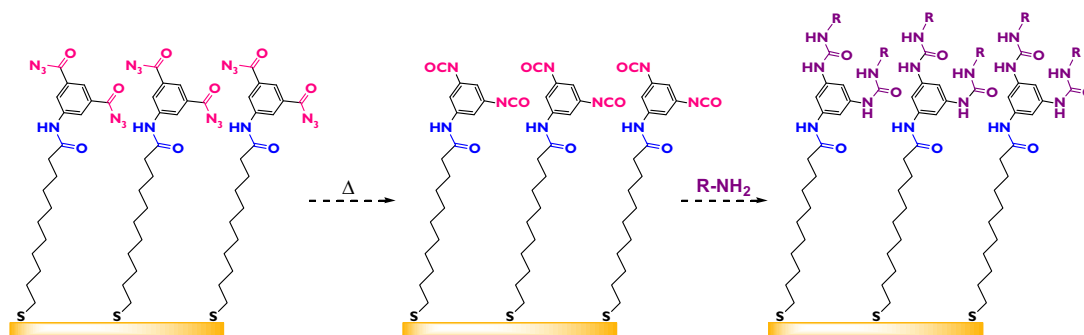


Figure 2-23. Schematic representation of heat activated SAM.

Gold surfaces were cleaned in a freshly prepared piranha solution, rinsed thoroughly with water and dried under a stream of N_2 and placed in a sealed vial, containing a 1mM solution of **59** (4.42mg in 5mL of THF) for 18 hours. On removal from solution, the surfaces were rinsed with THF and dried. Contact angles were measured for the monolayer surface and the results are reported in Table 2-2. The results can be compared with the contact angle measured for a control surface (clean gold surface treated under the same conditions with pure THF, i.e. no thiol/disulfide present). The increased contact angle of the acyl azide surface shows that it is more hydrophobic than the untreated surface, presumably due to the aromatic groups present at the surface.

Table 2-2. Water contact angles for self assembled monolayer surfaces on Au.

Standard deviations are given in parentheses.

SAM Surface	θ (H₂O)
Acyl Azide 59	77 (1.8)
59 (110°C, N ₂ , 1 hr)	69 (2.1)
59 (110°C, Toluene, 1 hr)	64 (1.5)
59 (<i>hν</i> , N ₂ , 1 hr)	75 (1.9)
Bare Gold (THF)	61 (2.5)

One surface was reserved as a control. A 10 μ L drop of a 20 mM solution of 5-aminofluorescein in DMF (7.6 mg in 1 ml) was placed on the surface and the surface covered with a glass coverslip then placed in the refrigerator for 15 hours. After rinsing the surface with DMF then acetone, no fluorescence was observed on the surface under the fluorescence microscope, as expected.

Preliminary investigations into converting the acyl azide to the isocyanate on the surface included heating the surface in refluxing dry toluene under an atmosphere of N₂ for one hour and heating the surface in a glass vessel under an atmosphere of N₂ heated in an oil bath at 110-120°C both for one hour. A further attempt was also made to effect the transformation from the acyl azide to the isocyanate by the application of UV light.^{100,101} Surfaces were placed in a quartz round bottomed flask under an atmosphere of N₂ in the presence of a UV light for one hour. In all cases, a 10 μ L drop of a 20 mM solution of 5-aminofluorescein in DMF (7.6 mg in 1 ml) was placed on the surface at the conclusion of the heating/irradiation step and the surface then covered with a glass coverslip and placed in the refrigerator for 22 hours. The surfaces were rinsed with DMF then acetone and viewed under a fluorescence microscope. Unfortunately, no fluorescence was observed on any of the surfaces examined.

Contact angles were also measured for the heat treated surfaces and are reported in Table 2-2. A decrease in contact angle was observed for each of the ‘activated’ surfaces, as the contact angle change was greatest for the heat in toluene for 1 hr, this surface was selected for XPS analysis.*

XPS analysis (Figure 2-24) was carried out on the acyl azide surface **59** and one that was heat treated (in refluxing toluene 1 hour). The spectra were referenced to the Au 4f doublet at a binding energy of 84 eV. The expected peaks were observed in the spectra arising from the ionisation of core electrons of C, N, O and S (Appendix B).

The C 1s peak was observed at 285 eV for both surfaces, corresponding to the carbon atoms of the methylene and phenyl groups, and a smaller peak was observed at ~289 eV on both surfaces, however it was smaller on the heat treated surface, corresponding to the C=O groups present. There was a N 1s peak observed for both surfaces at ~400 eV, the O 1s peak was observed at ~531 eV for both compounds however a much broader peak was observed for the **59** surface. Again the S 2p ionization was treated as a single peak centred at BE of ~163 eV, corresponding to the value reported for sulphur bound to gold as a thiolate, demonstrating successful formation of the monolayer of **59**, however the peak for the heated surface was very small, barely resolved from the baseline noise, perhaps this may be attributed to removal of some of the monolayer during the heating stage. Unfortunately, as observed in the XPS spectra for **53** and **58** a couple of peaks were assigned to contaminants, the peak at a BE of ~712 eV corresponding to Fe 2p and a peak at 619

* Due to limited funding not all surfaces were able to be analysed.

eV corresponding to I 3d were observed. A more detailed interpretation of these results is beyond the scope of this work and will be the object of future studies.

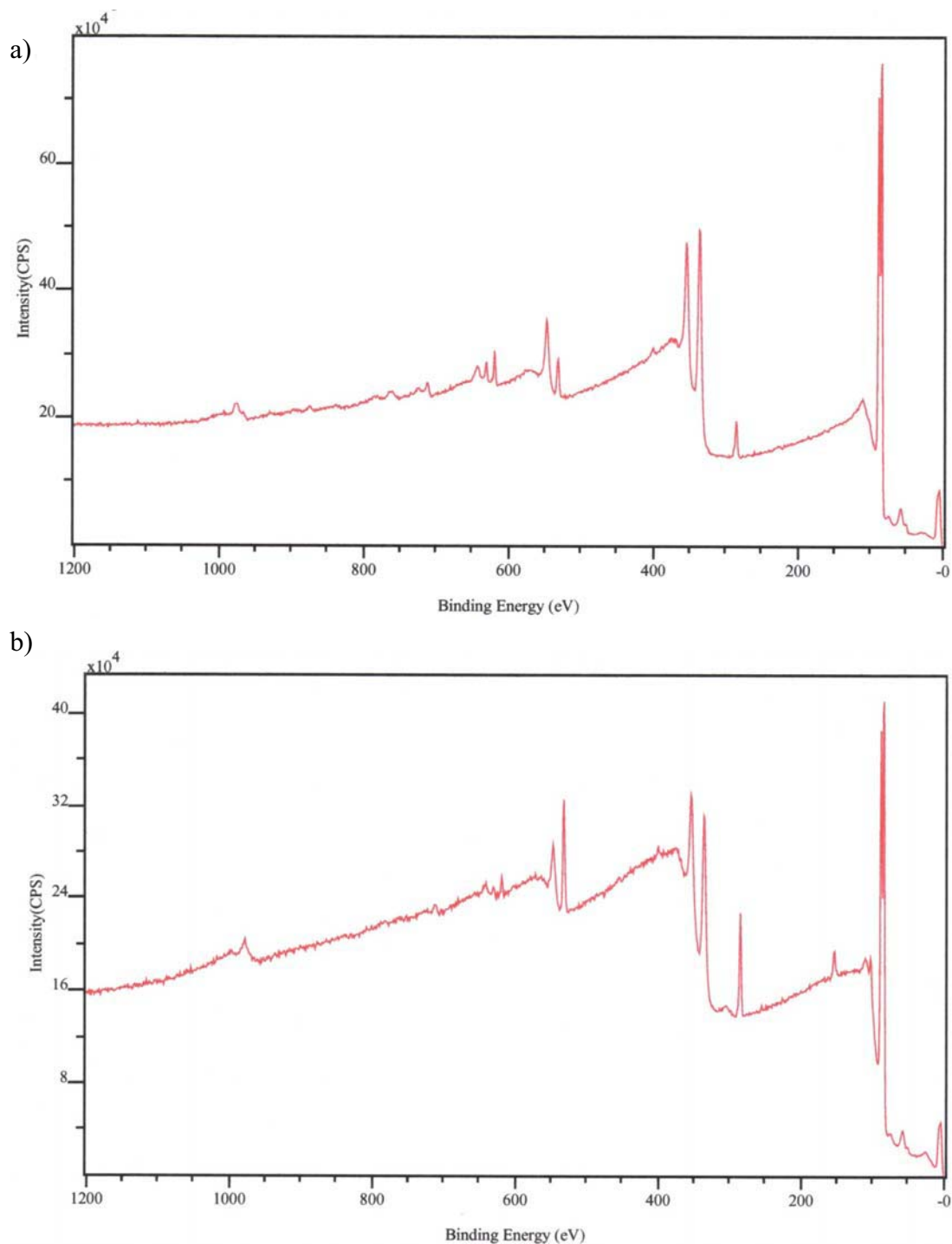


Figure 2-24. Survey scans of a) acyl azide **59** monolayer surface and b) after heating for one hour in a solution of toluene.

In summary, we have demonstrated the successful formation of a SAM of **59** on gold surfaces again using well documented solution based adsorption techniques. Our preliminary attempts to convert the acyl azide groups on the surface to an isocyanate via the application of heat were unsuccessful. XPS analysis of the surface heated in solution showed evidence that the monolayer may have been removed when heated in the toluene solution. Future work will further investigate the conditions required to effect the conversion of the acyl azide to the isocyanate.

2.2.7 Summary

The work presented within this chapter has demonstrated the fabrication of suitable gold surfaces for the preparation of SAMs on the surface. We have also successfully synthesised a number of compounds that were used for the preparation of self-assembled monolayers on gold. Investigations into a suitable protocol for the patterning of SAMs on gold *via* UV irradiation was developed and the attachment of green fluorescent protein to the monolayer surface with retention of the biomolecules' fluorescence was demonstrated. A SAM that has the potential to be activated by heat was successfully prepared however, preliminary investigations into the 'switching on' of this surface were not successful. Monolayers were characterised by the techniques available to us, however further detailed investigations into this area are continuing.

2.3 References

- (1) Wang, J. *Anal. Chem.* **1999**, *71*, 328R-332R.
- (2) Gellman, S. H. *Chem. Rev.* **1997**, *97*, 1231-1232.
- (3) Junhui, Z.; Hong, C.; Ruifu, Y. *Biotechnol. Adv.* **1997**, *15*, 43-58.
- (4) Wang, J. *Nucleic Acids Res.* **2000**, *28*, 3011-3016.
- (5) Schena, M.; Heller, R. A.; Theriault, T. P.; Konrad, K.; Lachenmeier, E.; Davis, R. W. *Trends Biotechnol.* **1998**, *16*, 301-306.
- (6) Busch, K.; Tampe, R. *Rev. Mol. Biotech.* **2001**, *82*, 3-24.
- (7) Vilan, A.; Cahen, D. *Trends Biotechnol.* **2002**, *20*, 22-29.
- (8) Ulman, A. *Chem. Rev.* **1996**, *96*, 1533-1554.
- (9) Riepl, M.; Enander, K.; Leidberg, B. *Langmuir* **2002**, *18*, 7016-7023.
- (10) Schreiber, F. *Prog. Surf. Sci.* **2000**, *65*, 151-256.
- (11) Sullivan, T. P.; Huck, W. T. S. *Eur. J. Org. Chem.* **2003**, 17-29.
- (12) Ulman, A. *An Introduction to Ultrathin Organic Films*; Academic Press: New York, 1991.
- (13) Li, J.; Wang, H.; Zhao, Y.; Cheng, L.; He, N.; L, Z. *Sensors* **2001**, *1*, 53-59.
- (14) Allara, D. L.; Nuzzo, R. G. *Langmuir* **1985**, *1*, 45-52.
- (15) Laibinis, P. E.; Whitesides, G. M. *J. Am. Chem. Soc.* **1992**, *114*, 1990-1995.
- (16) Houseman, B. T.; Gawalt, E. S.; Mrksich, M. *Langmuir* **2003**, *19*, 1522-1531.
- (17) Nuzzo, R. G.; Allara, D. L. *J. Am. Chem. Soc.* **1983**, *105*, 4481-4483.
- (18) Gooding, J. J. *Encyclopedia of Nanoscience and Nanotechnology* **2004**, *1*, 17-49.
- (19) Ulman, A. *Self-Assembled Monolayers of Thiols*; Academic Press: San Diego, 1998.

- (20) Walczak, M. M.; Popenoe, D. D.; Deinhammer, R. S.; Lamp, B. D.; Chung, C.; Porter, M. D. *Langmuir* **1991**, *7*, 2687-2693.
- (21) Zhu, M.; Schneider, M.; Papastavrou, G.; Akari, S.; Mohwald, H. *Langmuir* **2001**, *17*, 6471-6476.
- (22) Xia, Y.; Whitesides, G. M. *Angew. Chem. Int. Ed. Engl.* **1998**, *37*, 550-575.
- (23) Collard, D. M.; Sayre, C. N. *Synth. Met.* **1997**, *84*, 329-332.
- (24) Poirier, G. E.; Pylant, E. D. *Science* **1996**, *272*, 1145-1148.
- (25) Delamarche, E.; Sundarababu, G.; Biebuyck, H.; Michel, B.; Gerber, C.; Wolf, H.; Ringsdorf, H.; Xanthopoulos, N.; Mathieu, H. J. *Langmuir* **1996**, *12*, 1997-2006.
- (26) Chaki, N. K.; Vijayamohanan, K. *Biosens. Bioelectron.* **2002**, *17*, 1-12.
- (27) Wink, T.; vanZuilen, S. J.; Bult, A.; vanBennekom, W. P. *Analyst (Cambridge, U. K.)* **1997**, *122*, 43R-50R.
- (28) Nakano, K.; Doi, K.; Tamura, K.; Katsumi, Y.; Tazaki, M. *Chem. Commun. (Cambridge)* **2003**, 1544-1545.
- (29) Vijayamohanan, K.; Aslam, M. *Appl. Biochem. Biotechnol.* **2001**, *96*, 25-39.
- (30) Means, G. E.; Feeney, R. E. *Bioconjugate Chem.* **1990**, *1*, 2-12.
- (31) Liu, X.-h.; Wang, H.-k.; Herron, J. N.; Prestwich, G. D. *Bioconjugate Chem.* **2000**, *11*, 755-761.
- (32) Ostuni, E.; Yan, L.; Whitesides, G. M. *Colloids Surf., B: Biointerfaces* **1999**, *15*, 3-30.
- (33) Hodneland, C. D.; Lee, Y.-S.; Min, D.-H.; Mrksich, M. *Proc. Natl. Acad. Sci. U.S.A.* **2002**, *99*, 5048-5052.
- (34) Bieniarz, C.; Husain, M.; Barnes, G.; King, C. A.; Welch, C. J. *Bioconjugate Chem.* **1996**, *7*, 88-95.

- (35) Murphy, W. L.; Mercurius, K. O.; Koide, S.; Mrksich, M. *Langmuir* **2004**, *20*, 1026-1030.
- (36) Hamelmann, F.; Heinzmann, U.; Siemeling, U.; Bretthauer, F.; Bruggen, J. V. *D. Appl. Surf. Sci.* **2004**, *222*, 1-5.
- (37) Herranz, M. A.; Colonna, B.; Echegoyen, L. *Proc. Natl. Acad. Sci. U.S.A.* **2002**, *99*, 5040-5047.
- (38) Gooding, J. J.; Mearns, F.; Yang, W.; Liu, J. *Electroanalysis* **2002**, *15*, 81-96.
- (39) Smith, R. K.; Lewis, P. A.; Weiss, P. S. *Prog. Surf. Sci.* **2004**, *75*, 1-68.
- (40) Evans, S. D.; Williams, L. M. In *Functional Organic and Polymeric Materials*; Richardson, T. H., Ed.; John Wiley & Sons: Chichester, 2000, p 149-180.
- (41) Huang, J.; Hemminger, J. C. *J. Am. Chem. Soc.* **1993**, *115*, 3342-3343.
- (42) Tarlov, M. J.; Jr., D. R. F. B.; Gillen, G. *J. Am. Chem. Soc.* **1993**, *115*, 5305-5306.
- (43) Kumar, A.; Biebuyck, H. A.; Whitesides, G. M. *Langmuir* **1994**, *10*, 1498-1511.
- (44) Zhao, X.-M.; Xia, Y.; Whitesides, G. M. *J. Mater. Chem.* **1997**, *7*, 1069-1074.
- (45) Wilbur, J. L.; Kumar, A.; Biebuyck, H. A.; Kim, E.; Whitesides, G. M. *Nanotechnology* **1996**, *7*, 452-457.
- (46) Kolb, H. C.; Finn, M. G.; Sharpless, K. B. *Angew. Chem. Int. Ed. Engl.* **2001**, *40*, 2004-2021.
- (47) Fazio, F.; Bryan, M. C.; Blixt, O.; Paulson, J. C.; Wong, C.-H. *J. Am. Chem. Soc.* **2002**, *124*, 14397-14402.
- (48) Lummerstorfer, T.; Hoffmann, H. *J. Phys. Chem. B* **2004**, *108*, 3963-3966.

- (49) Collman, J. P.; Devaraj, N. K.; Chidsey, C. E. D. *Langmuir* **2004**, *20*, 1051-1053.
- (50) Liu, Y.; Mu, L.; Liu, B.; Kong, J. *Chem. Eur. J.* **2005**, *11*, 2622-2631.
- (51) Ichimura, K.; Oh, S.-K.; Nakagawa, M. *Science* **2000**, *288*, 1624-1626.
- (52) Lahann, J.; Mitragotri, S.; Tran, T.-N.; Kaido, H.; Sundaram, J.; Choi, I. S.; Hoffrer, S.; Somorjai, G. A.; Langer, R. *Science* **2003**, *299*, 371-374.
- (53) Zhao, C.; Witte, I.; Wittstock, G. *Angew. Chem. Int. Ed. Engl.* **2006**, *45*, 5469-5471.
- (54) Xiao, S.-J.; Brunner, S.; Wieland, M. *J. Phys. Chem. B* **2004**, *108*, 16058-16517.
- (55) Kukar, T.; Eckenrode, S.; Gu, Y.; Lian, W.; Megginson, M.; She, J.-X.; Wu, D. *Anal. Biochem.* **2002**, *306*, 50-54.
- (56) Blank, K.; Mai, T.; Gilbert, I.; Schiffmann, S.; Rankl, J.; Zivin, R.; Tackney, C.; Nicolaus, T.; Spinnler, K.; Oesterhelt, F.; Benoit, M.; Clausen-Schaumann, H.; Gaub, H. E. *Proc. Natl. Acad. Sci. U.S.A.* **2003**, *100*, 11356-11360.
- (57) Ostuini, E.; Yan, L.; Whitesides, G. M. *Colloids Surf., B: Biointerfaces* **1999**, *15*, 3-30.
- (58) Mrksich, M.; Whitesides, G. M. *Annu. Rev. Biophys. Biomol. Struct.* **1996**, *25*, 55-78.
- (59) Busch, K.; Tampe, R. *Rev. Mol. Biotech.* **2001**, *82*, 3-24.
- (60) Li, X.-M.; Huskens, J.; Reinhoudt, D. N. *J. Mater. Chem.* **2004**, *14*, 2954-2971.
- (61) Nakano, K.; Taira, H.; Maeda, M.; Takagi, M. *Anal. Sci.* **1993**, *9*, 133-136.
- (62) Wagner, P.; Hegner, M.; Kernen, P.; Zuagg, F.; Semenza, G. *Biophysical Journal* **1996**, *70*, 2052-2066.

- (63) Flink, S.; vanVeggel, F. C. J. M.; Reinhoudt, D. N. *Adv. Mater.* **2000**, *12*, 1315-1328.
- (64) Rivière, J. C.; Myhra, S. *Handbook of Surface and Interface Analysis: Methods for Problem Solving*; Marcel Dekker Inc: New York, 1998.
- (65) Hubbard, A. T. *The Handbook of Surface Imaging and Visualisation*; CRC Press: Boca Raton, 1995.
- (66) Whitesides, G. M.; Laibinis, P. E. *Langmuir* **1990**, *6*, 87-96.
- (67) Wang, H.; Chen, S.; Li, L.; Jiang, S. *Langmuir* **2005**, *21*, 2633-2636.
- (68) Binnig, G.; Quate, C. F.; Gerber, C. *Phys. Rev. Lett.* **1986**, *56*, 930-933.
- (69) Okabe, Y.; Furugori, M.; Tani, Y.; Akiba, U.; Fujihira, M. *Ultramicroscopy* **2000**, *82*, 203-212.
- (70) Morris, V. J.; Kirby, A. R.; Gunning, A. P. *Atomic Force Microscopy for Biologists*; Imperial College Press: London, 1999.
- (71) Herman, B. *Fluorescence Microscopy*; 2nd ed.; BIOS Scientific Publishers Ltd: Oxford, 1998.
- (72) Song, L.; Hennink, E. J.; Young, I. T.; Tanke, H. J. *Biophysical Journal* **1995**, *68*, 2588-2600.
- (73) Kraayenhof, R.; Visser, A. J. W. G.; Gerritsen, H. C. *Fluorescence Spectroscopy, Imaging and Probes*; Springer-Verlag: Berlin, 2002.
- (74) Dickson, R. M.; Cubitt, A. B.; Tsien, R. Y.; Moerner, W. E. *Nature* **1997**, *388*, 355-358.
- (75) Giuliano, K. A.; Taylor, D. L. *TIBTECH* **1998**, *16*, 135-140.
- (76) Chalfie, M.; Kain, S. *Green fluorescent protein: properties, applications and protocols*; Wiley-Liss: New York, 1998.
- (77) Zimmer, M. *Chem. Rev.* **2002**, *102*, 759-781.

- (78) Chirico, G.; Diaspro, A.; Cannone, F.; Collini, M.; Bologna, S.; Pellegrini, V.; Beltram, F. *Chem. Phys. Chem.* **2005**, *6*, 328-335.
- (79) Dubertret, B.; Calame, M.; Libchaber, A. (2002) *International Patent* WO 02/18951 A2.
- (80) Collins, J. A.; Zirouchaki, C.; Palmer, R. E.; Heath, J. K.; Jones, C. H. *Appl. Surf. Sci.* **2004**, *226*, 197-208.
- (81) Lee, J. K.; Kim, Y.-G.; Chi, Y. S.; Yun, W. S.; Choi, I. S. *J. Phys. Chem. B* **2004**, *108*, 7665-7673.
- (82) Lee, B.; Takeda, S.; Nakajima, K.; Noh, J.; Choi, J.; Hara, M.; Nagamune, T. *Biosens. Bioelectron.* **2004**, *19*, 1169-1174.
- (83) Volle, J.-N.; Chambon, G.; Sayah, A.; Reymond, C.; Fasel, N.; Gijis, M. A. *M. Biosens. Bioelectron.* **2003**, *19*, 457-464.
- (84) Persson, H. H. J.; Caseri, W. R.; Suter, U. W. *Langmuir* **2001**, *17*, 3643-3650.
- (85) Schmidbaur, H. *Gold: Progress in Chemistry, Biochemistry and Technology*; John Wiley & Sons: Chichester, 1999.
- (86) Zaugg, F. G.; Spencer, N. D.; Wagner, P.; Kernien, P.; Vinckier, A.; Groscurth, P.; Semenza, G. *J. Mater. Sci.: Materials in Medicine* **1999**, *10*, 255-263.
- (87) Koenig, N. H.; Sasin, G. S.; Swern, D. *J. Org. Chem.* **1958**, *23*, 1525-1530.
- (88) Prime, K. L.; Whitesides, G. M. *J. Am. Chem. Soc.* **1993**, *115*, 10714-10721.
- (89) Vanderah, D. J.; Valincius, G.; Meuse, C. W. *Langmuir* **2002**, *18*, 4674-4680.
- (90) Ostuni, E.; Chapman, R. G.; Holmlin, R. E.; Takayama, S.; Whitesides, G. M. *Langmuir* **2001**, *17*, 5605-5620.
- (91) Okaniwa, M.; Takeuchi, K.; Asai, M.; Ueda, M. *Macromolecules* **2002**, *35*, 6224-6231.

- (92) Pale-Grosdemange, C.; Simon, E. S.; Prime, K. L.; Whitesides, G. M. *J. Am. Chem. Soc.* **1991**, *113*, 12-20.
- (93) Bard, A. J. *Electroanalytical Chemistry*; Dekker: New York, 1976.
- (94) Castner, D. G.; Hinds, K.; Grainger, D. W. *Langmuir* **1996**, *12*, 5083-5086.
- (95) Hutchison, J. E.; Postlethwaite, T. A.; Murray, R. W. *Langmuir* **1993**, *9*, 3277-3283.
- (96) Butt, H. J.; Seifert, K.; Bamberg, E. *J. Phys. Chem.* **1993**, *97*, 7316-7320.
- (97) Schmid, E. L.; Keller, T. A.; Dienes, Z.; Vogel, H. *Anal. Chem.* **1997**, *69*, 1979-1985.
- (98) McRae, S. R.; Brown, C. L.; Bushell, G. R. *Protein Expression Purif.* **2005**, *41*, 121-127.
- (99) Delamarche, E.; Michel, B.; Kang, H.; Gerber, C. *Langmuir* **1994**, *10*, 4103-4108.
- (100) Zhu, Y.; Schuster, G. B. *J. Am. Chem. Soc.* **1990**, *112*, 8583-8585.
- (101) Woelfle, I.; Sauerwein, B.; Autrey, T.; Schuster, G. B. *Photochemistry and Photobiology* **1988**, *47*, 497-501.

CHAPTER THREE

SYNTHESIS OF HETEROBIFUNCTIONAL LINKERS

3.1 Introduction

Bioconjugation involves the coupling of a biomolecule with one or more synthetic or natural molecules. The resultant bioconjugate, exhibits properties of both principal components.¹ In general, the two components are connected *via* a third cross linking molecule or spacer. Consideration of the spacer element is important in the selection criteria for choosing a cross-linker as the length and type of cross-bridge can affect the properties of the bioconjugate, including its flexibility and hydrophilicity. Site specific bioconjugations are dependent on chemical reactions occurring between the reactive groups present on the cross-linking reagent and the functional groups present on the molecules to be coupled. The chemistry of bioconjugation reagents has been extensively reviewed.¹⁻³

Heterobifunctional conjugation reagents contain two different reactive groups that can covalently couple to specific functional groups located on each of the target molecules. This allows the regiospecific cross-linking of two molecular systems, hence affording better selectivity and control over the conjugation process. Connecting the two reactive ends is the asymmetrically substituted cross-bridge, linker or spacer. Some heterobifunctional cross-linker families differ solely in the length of their spacer. Cross-linking agents currently used in the preparation of bioconjugates exploit a wide variety of functionalities and reactivities, however the scope of this review will focus on heterobifunctional linking agents possessing irreversible thiol reactive and amine reactive ends.

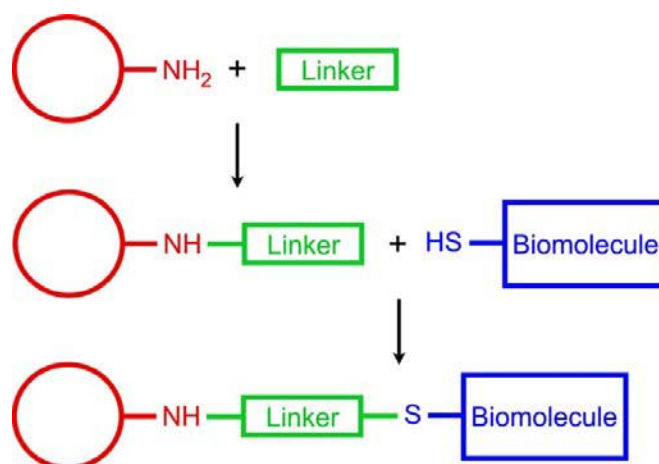


Figure 3-1. Cartoon representation of the bioconjugation process.

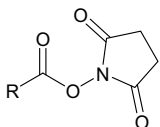
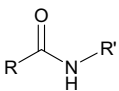
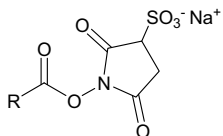
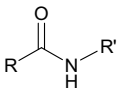
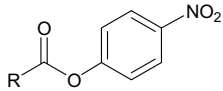
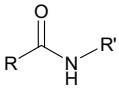
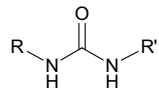
3.1.1 Amine Reactive Functionalities

An *N*-hydroxysuccinimide (NHS) ester is the most commonly used amine reactive functionality and the majority of commercially available amine reactive cross-linking or modification reagents utilise this group. NHS esters were first introduced as reactive ends of homobifunctional cross-linkers⁴ and react with nucleophiles such as primary and secondary amines, releasing *N*-hydroxysuccinimide as a leaving group, forming stable amide linkages.¹ The reaction of NHS esters with a thiol or a hydroxyl group does not lead to the formation of stable conjugates, as the resulting thioesters or ester linkages both hydrolyse in aqueous environments. Another group, the sulfo-NHS esters (Table 3-1) are a hydrophilic analogue of NHS esters that react with amines with the same specificity and reactivity, however, they are more water soluble and hydrolyse more slowly in water.

p-Nitrophenyl esters are not typically used as a reactive group in heterobifunctional cross-linking agents however, there are a few exceptions. This active ester is used in an analogous fashion to the NHS ester group, reacting with amines at slightly basic pH values (7-9), releasing *p*-nitrophenol as the leaving group, to form an amide bond.

Isocyanates can also react with amines forming chemically stable urea linkages and with alcohols to form urethanes. They are formed by the reaction of an aromatic amine with phosgene or created from acyl azides via the Curtius rearrangement.⁵ The reactivity of isocyanates is high, but they are not extensively used in linker chemistry as exposure to moisture causes rapid decomposition, releasing CO₂, resulting in the formation of a primary amine.¹ The structure and reaction product of each of these functional groups are summarised in the following table.

Table 3-1. Summary of Amine Reactive Groups

Amine Reactive Group	Structure	After reaction with NH ₂ -R
N-hydroxysuccinimide ester		
Sulfo-N-hydroxysuccinimide ester		
p-Nitrophenyl ester		
Isocyanate	$R-N=C=O$	

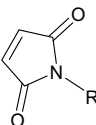
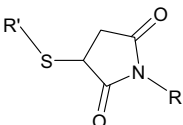
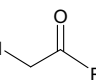
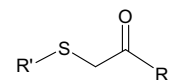
3.1.2 Irreversible Thiol Reactive Functionalities

The iodoacetyl group reacts with nucleophiles to form alkylated derivatives with subsequent loss of HI. Although this active halogen compound is used extensively to modify thiol groups in proteins and other molecules, the reaction can result in

mixtures of product due to the lack of selectivity in the reaction. Iodoacetyl derivatives can react with a number of functional groups within proteins including the SH of cysteine, both imidazolyl side chain nitrogens of histidine, the thioether of methionine, the primary amine group of lysine residues and N terminal amines.⁶ The relative reactivity of iodoacetates toward protein functionalities is thiol > imidazolyl > thioether > amine. The reaction may be directed specifically towards cysteine (SH) modification if the reaction is performed at a slightly alkaline pH and the concentration of the iodoacetate is maintained in a limiting quantity relative to the number of thiol groups present.¹

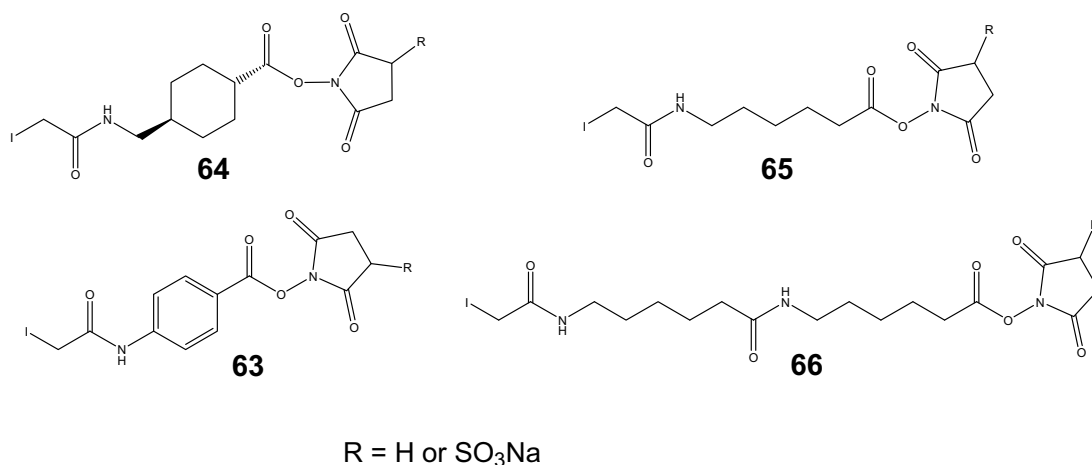
The double bond of the maleimide functional group can undergo a specific alkylation reaction with thiol groups to form stable thioether bonds.¹ Maleimide reactions are specific for thiols in the pH range of 6.5-7.5. However, at higher pH values some cross-reactivity with amine groups is observed.⁷ The maleimide group can also undergo hydrolysis to form an open maleamic acid that is unreactive toward thiols, the rate being proportional to pH however, it may also occur after a thiol has coupled to the maleimide. The higher specificity of maleimides over the iodoacetyl group towards thiols has made this functional group one of the most extensively used in linker chemistry.⁸ The structure and reaction product of these two thiol reactive functional groups are summarised in table 3-2.

Table 3-2. Summary of Thiol Reactive Functionalities

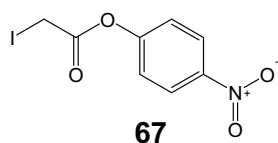
Thiol Reactive Group	Structure	After reaction with SH-R'
Maleimide		
Iodoacetyl		

3.1.3 Examples of Heterobifunctional Thiol/Amine Cross-Linkers:

There are four families of irreversible thiol reactive and amine reactive bifunctional linkers utilizing the reactive functional groups outlined above. The family of iodoacetate and NHS ester linkers have varied organic spacer elements between these two reactive functional groups including the aromatic derivative succinimidyl (4-iodoacetyl)aminobenzoate (**63**), the cycloalkyl derivative succinimidyl [(4-iodoacetyl)aminomethyl]cyclohexanecarboxylate (**64**), the alkyl chain derivative succinimidyl 6-[(iodoacetyl)amino]hexanoate (**65**) and its extended length analogue succinimidyl 6-[6-(((iodoacetyl)amino)hexanoyl)amino]hexanoate (**66**). Typical procedures for bioconjugations using these molecules involve initially reacting the NHS ester with the amine containing molecule then the iodoacetamide group subsequently reacts with the molecule containing the thiol. These linkers have been widely reported in the literature with some recent papers describing their use to (i) attach reduced antibody fragments containing thiols to amine functionalised porphyrins for diagnostic and therapeutic applications,⁹ (ii) to facilitate the attachment of nucleic acids to silicon and glass surfaces^{10,11} and (iii) to immobilize antibodies onto silver surfaces.¹²



There is only one reported member of the iodoacetyl and *p*-nitrophenyl ester family, *p*-nitrophenyl iodoacetate (**67**) however, there are no recent articles relating to the use of this molecule as a conjugation reagent for linking amine and thiol containing molecules.

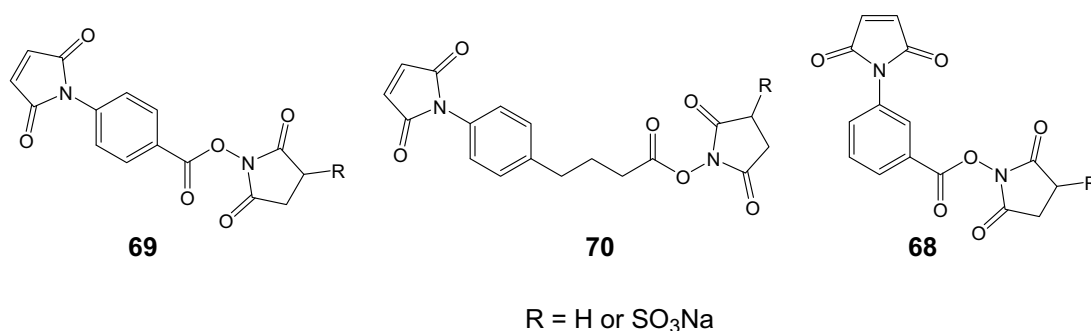


A number of earlier articles that outline its use to link subfragments of myosin adenosinetriphosphatase to investigate the amino acids involved in the active site of the protein¹³ and also to link several amine functionalised fluorophores to proteins containing a thiol.¹⁴

The maleimide and NHS ester family are by far the most popularly used heterobifunctional cross-linking agents.¹⁵ There are a number of groups within this family that include linkers containing aromatic, aliphatic chain and cyclohexyl spacer units. A two-step protocol is used for bioconjugation reactions using this family of linkers involving the reaction of the NHS ester end of the linker with the amine

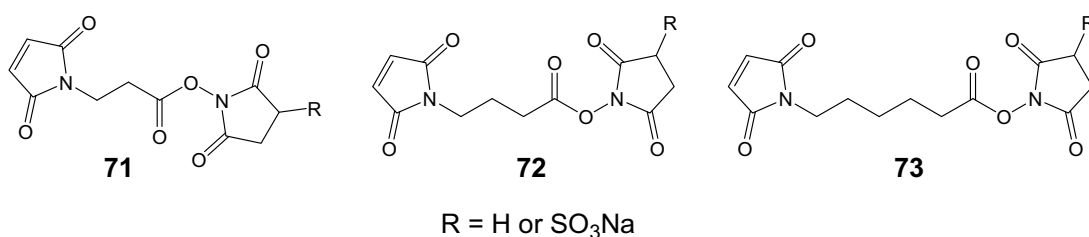
containing molecule to form an amide bond, followed by the subsequent conjugation to the thiol containing molecule *via* the maleimide group.

Succinimidyl (3-maleimido)benzoate (**68**), succinimidyl (4-maleimido)benzoate (**69**) and succinimidyl 4-[*p*-maleimidophenyl]butyrate (**70**) are members of the aromatic spacer group of this family of linkers, with **68** and **70** being reported extensively in the literature. **69** however, is reported in significantly fewer publications. Current literature examples of the use of these linker molecules include the attachment of fluorophore-labelled, thiolated DNA to an amine coated silica shell of unicellular algae, to be used as templates for nanoparticle assembly,¹⁶ and the linking of a TAT peptide to a silicon oxide surface for the development of platforms capable of supporting biochemical events.¹⁷ Studies have shown that the aromatic maleimides are relatively unstable in terms of hydrolysis.¹⁸ However, a number of alkyl and cycloalkyl derivatives have demonstrated improved stability.¹⁹

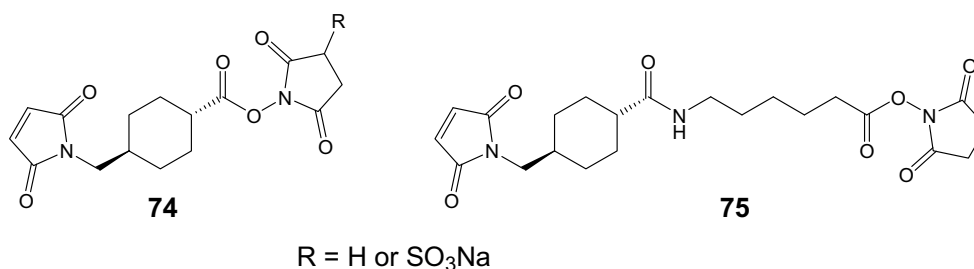


The aliphatic chain spacer group of the maleimide and NHS ester family of linkers are composed of a number of linkers of varying chain length. Most commonly the three carbon succinimidyl 3-maleimidopropanoate (SMP, **71**), the four carbon succinimidyl 4-maleimidobutyrate (**72**) and the six carbon succinimidyl 6-

maleimidohexanoate (**73**) linkers are used extensively in bioconjugation reactions. Specific examples include the use of these linkers to functionalise amine terminated self-assembled monolayers on gold with maleimide and NHS ester groups for attaching biomolecules on surfaces.²⁰ They have also been used to attach the adenovirus vector to thiol functionalised transport-peptides to facilitate their transfer into cells for the regulation of gene expression events.²¹

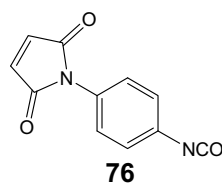


The cyclohexyl spaced linkers are frequently selected over the aromatic bridged linkers due to their increased stability towards maleimide hydrolysis. It is presumed that the cyclohexane ring stabilises the maleimide ring as a consequence of steric effects as well as its lack of aromatic character.¹ The two examples of this group shown above are succinimidyl 4-(N-maleimidomethyl)cyclohexanecarboxylic acid (SMCC, **74**) and its extended length analogue 4-(maleimidomethyl)-N-[6-[(succinimidyl)oxy]-6-oxohexyl]cyclohexanecarboxamide (**75**). Both linkers being extensively reported in the literature.



Literature examples of their use include a recent article using the sulfo-NHS derivative of **74** to link amine functionalised DNA to a thiol functionalised yellow fluorescent protein, producing fluorescent conjugates with applications in the self-assembly of photoactive supramolecular complexes such as artificial light harvesting systems.²²

The only reported maleimide and isocyanate linker is *p*-maleimidophenyl isocyanate¹⁵ (**76**). However, a patent exists encompassing all aromatic and cycloalkyl functionalised maleimide/isocyanate linkers.²³ This linker has been shown to react with hydroxyl groups present on vitamin B12, digoxigenin, digitoxigenin, estradiol, progesterone and serine containing peptides. Subsequently, these maleimide functionalised molecules were conjugated to thiolated alkaline phosphatase protein.



3.1.4 Background to Present Work

Heterobifunctional cross-linkers for conjugating amine and thiol containing molecules have been extensively investigated and many linkers are commercially available allowing the buyer to select linkers with characteristics that are specifically tailored to their purpose. Challenges in the advancement of linker chemistry involve the design of coupling reagents possessing several advantageous characteristics in terms of length, flexibility, hydrophilicity and their ability to introduce selective functionalities in site specific regions of biomolecules.

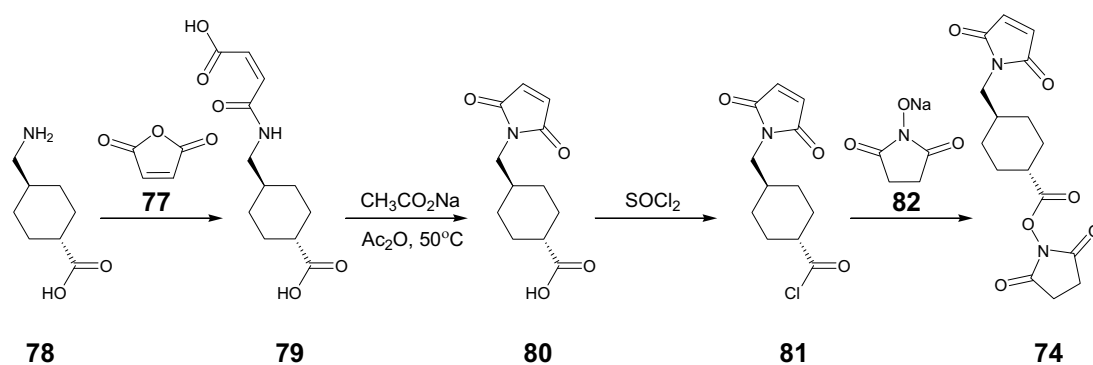
The aim of this body of work was to optimise the synthesis of a number of commercially available linkers, namely SMCC **74**, the extended length analogue **75** and SMP **71**. These materials are available commercially but their cost is prohibitive for their use in large amounts [**74** \$3095/g; **71** \$3255/g[†]]. Furthermore, extending the length of cross-linkers has been reported to improve the retention of the biological and/or chemical activity of the individual components after bioconjugation has occurred.⁸ Therefore a second aim was to investigate the extension of **74** to form a novel extended length heterobifunctional cross-linker compound similar to **75**. The third goal was to functionalise a crown ether with **74** with a view to producing a novel protein modification reagent for attachment to cysteine/thiol functionalised proteins. A more specific application of this work involved a collaboration with other members of the research group to form a bioconjugate of peptide nucleic acid (PNA) and green fluorescent protein using the linkers synthesised in this chapter. These linkers may eventually serve to provide a means of further functionalising our patterned SAM surfaces.

[†] Prices sourced from Sigma catalogue 2006-2007.

3.2 Results and Discussion

3.2.1 Synthesis of Known Maleimide/NHS ester Linkers

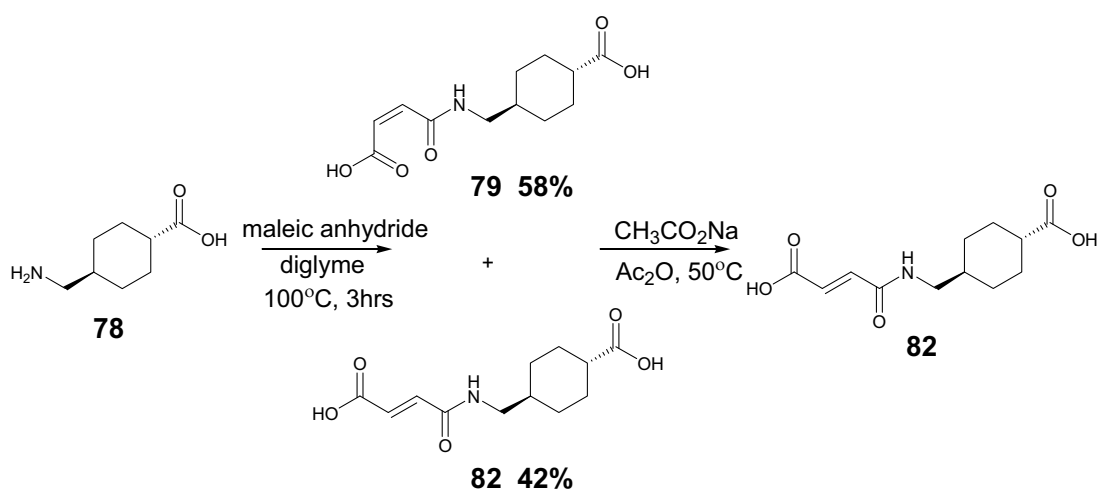
Traditional methods for the synthesis of SMCC **74**, involve a four step synthetic pathway (Scheme 3-1) *via* coupling of maleic anhydride **77** to tranexamic acid **78** to form the cisoidal maleamic acid **79**, followed by sodium acetate facilitated ring closure of the maleimide group to form **80**. Subsequent formation of the acid chloride **81** and coupling to the sodium salt of *N*-hydroxysuccinimide **82**, produces **74** with an overall yield of ~18%²⁴ for the four reaction steps.



Scheme 3-1

In order to develop a more efficient synthesis of **74** we elected to follow this path to produce **79**, then to use a one pot method to form the maleimide and the NHS ester via DCC coupling. The coupling of maleic anhydride **77** and tranexamic acid **78** in diglyme was carried out at an elevated temperature, to facilitate the solubility of the reactants as the tranexamic acid appeared to be insoluble in the solution. ^1H NMR analysis of the filtered product showed a mixture of products, determined to be the *trans* and *cis* isomers of *trans*-4-({[3-carboxyprop-2-enoyl]amino}-methyl)cyclohexanecarboxylic acid in a ratio of 1:1.4 (Scheme 3-2). An attempt was made to ring close the *cis* isomer from this product mixture directly, by heating the mixture, in acetic anhydride in the presence of sodium acetate, for two hours at 50°C .

Upon work up of the reaction, however, the isolated product was analysed by ^1H NMR and found to be the pure *trans* isomer of *trans*-4-({[3-carboxyprop-2-enoyl]amino}methyl)cyclohexane-carboxylic acid, a material that to our knowledge has not been reported in the literature. Unfortunately, repeated attempts to produce x-ray quality crystals of **82** were unsuccessful.



Scheme 3-2

Various solvents were trialled in attempts to increase the solubility of **78** in this initial reaction step, including DMF and acetic acid. These reactions were carried out at room temperature and both methods resulted in the exclusive formation of the requisite *cis* product. The acetic acid procedure was preferred however, due to the ease of product isolation (filtration), the higher yield (79% as opposed to 39% in DMF), and the cleaner product (^1H NMR). Expansions of the ^1H NMR spectra of **79** and **82** are provided in figure 3-2.

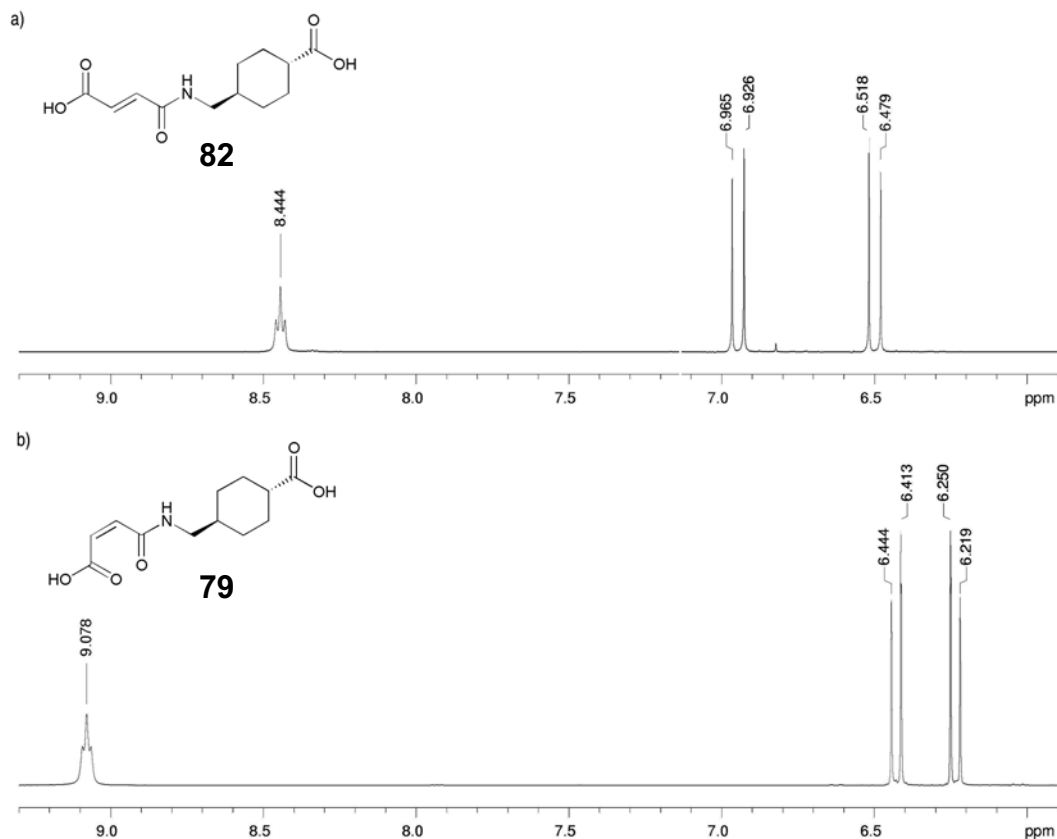
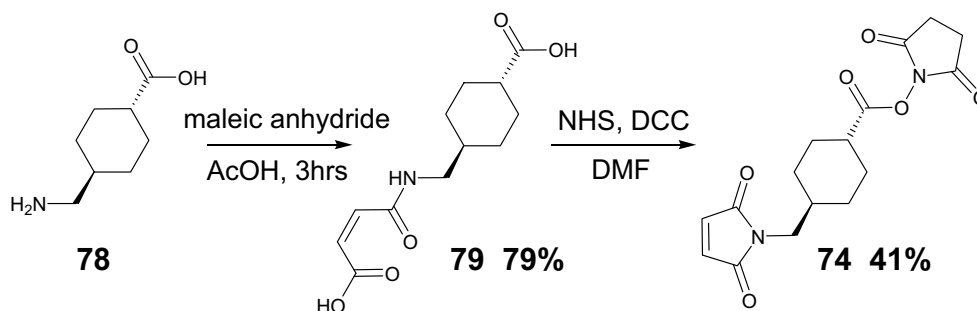


Figure 3-2. Expansion of ¹H NMR spectra (400MHz, DMSO-*d*₆) showing the NH and alkene proton resonances of a) the *trans* isomer **82** and b) the *cis* isomer **79** of *trans*-4-({[3-carboxyprop-2-enoyl]-amino}-methyl)-cyclohexanecarboxylic acid. Coupling constants calculated for the double bond were $^3J_{(\text{CH}=\text{CH})_{\text{trans}}} = 15.6\text{Hz}$ for **82** and $^3J_{(\text{CH}=\text{CH})_{\text{cis}}} = 12.4\text{Hz}$ for **79**.

The isolated *cis* product **79**, was then subjected to a one pot method to effect both the ring closure of the maleimide and NHS esterification of the acid (Scheme 3-3). Thus **79** was dissolved with NHS in cooled solution (0°C) of dry DMF under an atmosphere of N₂. DCC was added to this solution and the reaction stirred at room temperature. Precipitated DCU was removed by filtration and the filtrate was extracted, dried and the solvent removed by evaporation. The residue was

recrystallised from DCM/hexane to form SMCC **74** in a 41% yield (an overall yield of 32% for the two reaction steps).



This represented a 23% improvement in the overall yield reported for the four step synthetic method (~18%). Subsequently, however, a further improved one pot method for the synthesis of a number of maleimide/NHS ester linking reagents was found for the synthesis of **74**, which provided the species in a yield of 75%.²⁵ Thus, this procedure was adopted as the method of choice for the synthesis of **74**. The ¹H NMR of **74** with assignment is shown below in Figure 3-3.

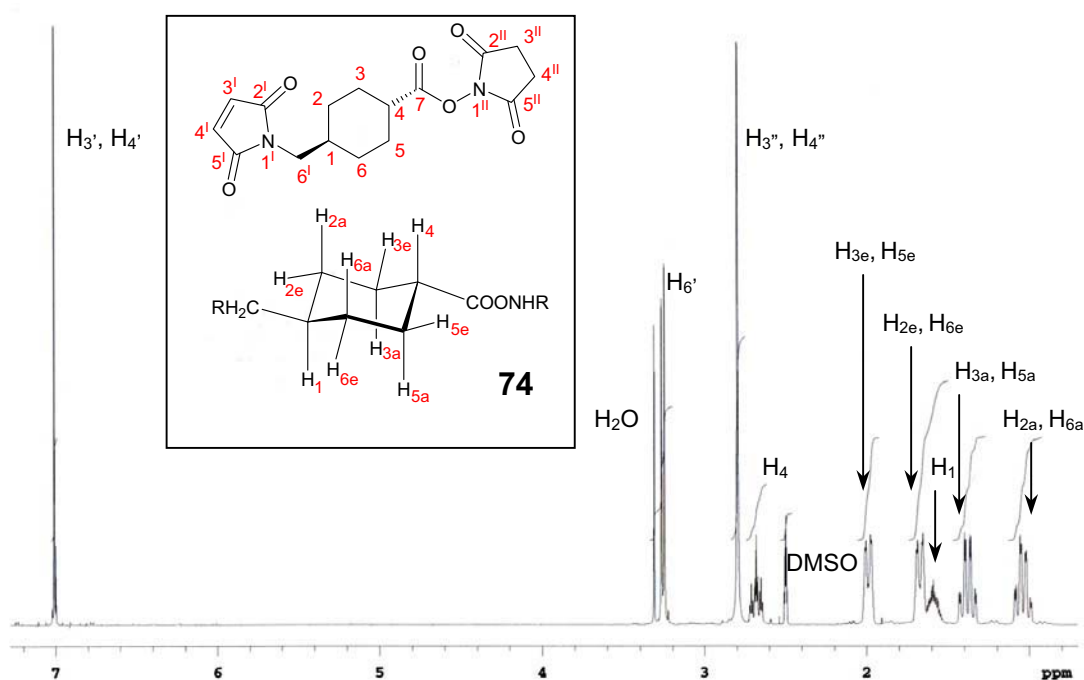


Figure 3-3. ¹H NMR (400 MHz, DMSO-d₆) of **74**

Crystals suitable for X-ray diffraction were obtained for **79** and **74** by recrystallisation from a mixture of acetone and methanol (Figure 3-4).

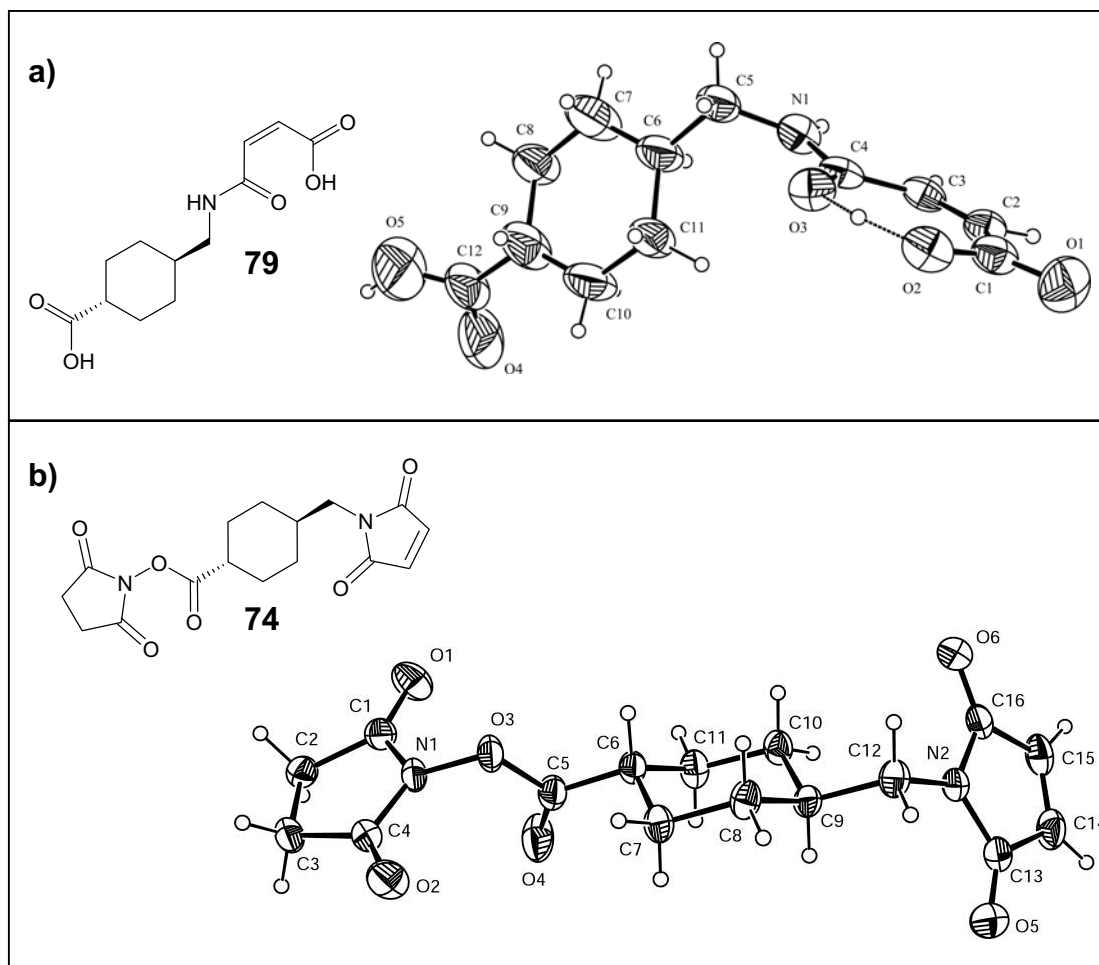
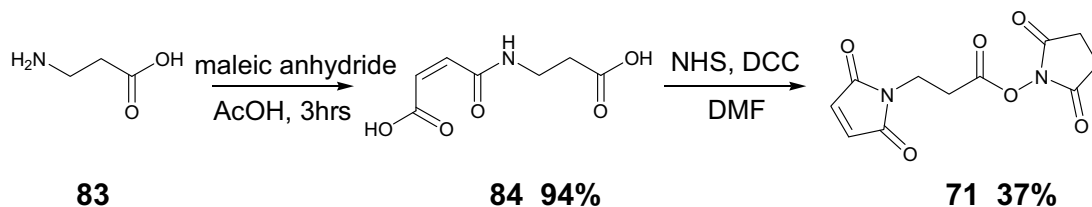


Figure 3-4. ORTEP diagram for the molecular structure of a) **79** and b) **74**.²⁶

A similar two step approach was employed for the synthesis of SMP **71**. This involved the reaction of maleic anhydride in acetic acid with β -alanine **83**. Isolation of the *cis* maleamic product **84** (94% yield) was followed by NHS esterification of the acid and cyclisation of the maleimide. A yield of 37% was obtained for **71**, an overall yield of 35% for the two reaction steps (Scheme 3-4). This compares with the literature reported yield of 33% for the synthesis of **71** via the one pot method

reported by Nielsen *et. al.*²⁵ Recrystallisation of **84** in acetone/methanol yielded crystals suitable for X-ray diffraction (Figure 3-5).



Scheme 3-4

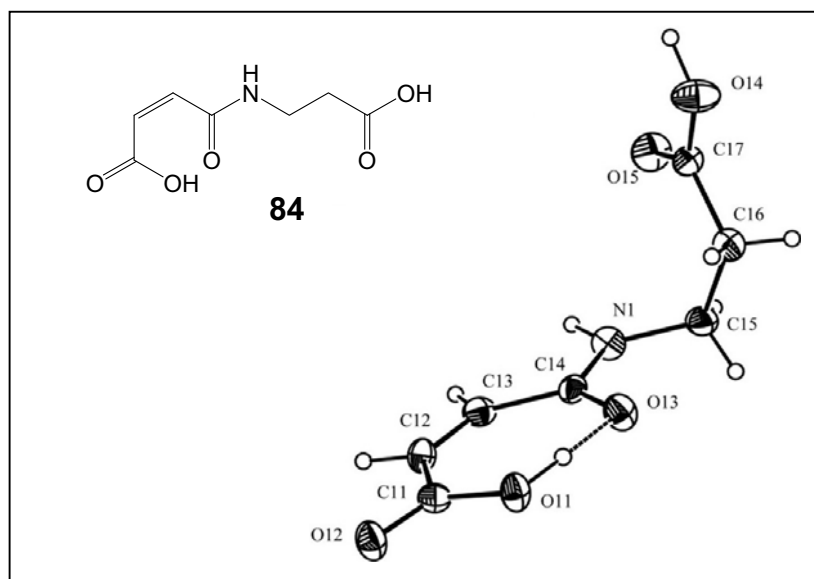
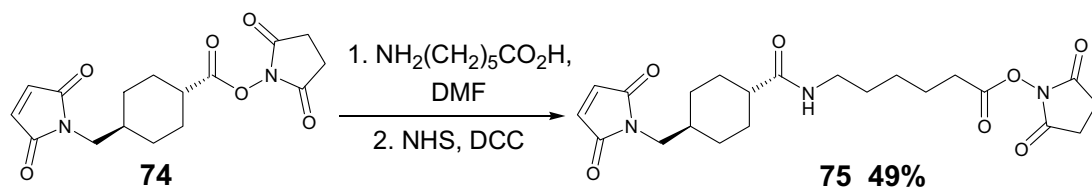


Figure 3-5. ORTEP diagram for the molecular structure of **84**.

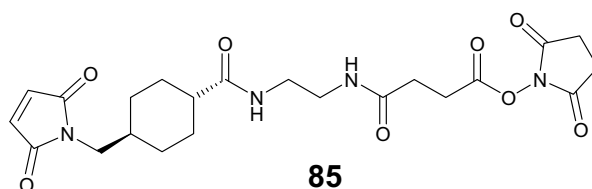
Extension of SMCC **74** with 6-aminocaproic acid to form the extended length heterobifunctional linker 4-[(2,5-dihydro-2,5-dioxo-1H-pyrrol-1-yl)methyl]-N-[6-[(2,5-dioxo-1-pyrrolidinyloxy]-6-oxohexyl]cyclohexanecarboxamide **75** (Scheme 3-5), was carried out according to a procedure adapted from the literature.⁸ **75** was isolated after column chromatography (5% MeOH/CHCl₃) in a 49% yield.



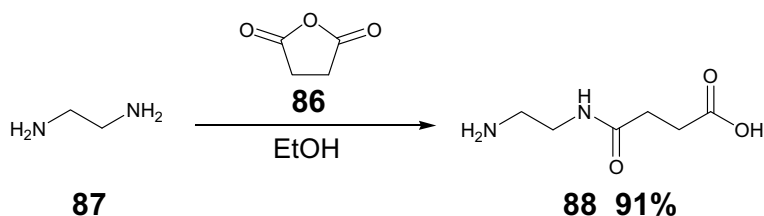
Scheme 3-5

3.2.2 Attempted Synthesis of Novel Maleimide/NHS linker

A novel extended length heterobifunctional linker was designed that had a similar length spacer unit to **75**, with an amide functional group present in the spacer **85**.

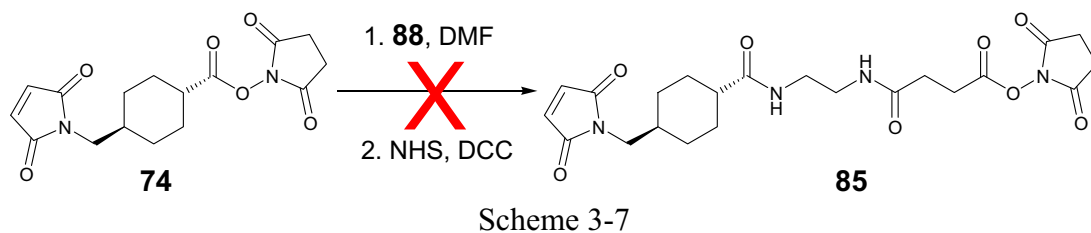


The initial concept was to synthesise the linker arm (Scheme 3-6) *via* a literature method²⁷ involving the reaction of one molar equivalent of succinic anhydride **86** with ethylene diamine **87** in ethanol. The amino acid product **88** precipitated from the reaction mixture and was isolated by filtration in a yield of 91%. The melting point, ¹H and ¹³C NMR data obtained for **88** were consistent with reported values.²⁷



Scheme 3-6

Subsequent coupling of **88** with **74** followed by NHS esterification should achieved the desired product (Scheme 3-7). However, this procedure proved unreliable as all attempts to couple **74** with **88** were unsuccessful. This is presumably attributable to the very poor solubility of the amino acid **88** even in polar organic solvents and organic/aqueous mixtures.



In our attempts to extend SMCC with the linker arm, in DMF, **74**, DCC and NHS were dissolved in DMF at room temperature, however, upon addition of the linker arm **88** to the reaction mixture a suspension formed. Work up of this reaction by filtration to remove the precipitated DCU also removed the insoluble amino acid **88** (^1H NMR). After removal of the solvent by evaporation, column chromatography (5% MeOH/ CHCl_3) of the residue isolated two compounds, 1) unreacted SMCC **74** and 2) a very small quantity of a clear crystalline solid that was determined by spectroscopic and x-ray crystallographic methods to be N,N'-ethylenedisuccinimide **89** (Figure 3-6).

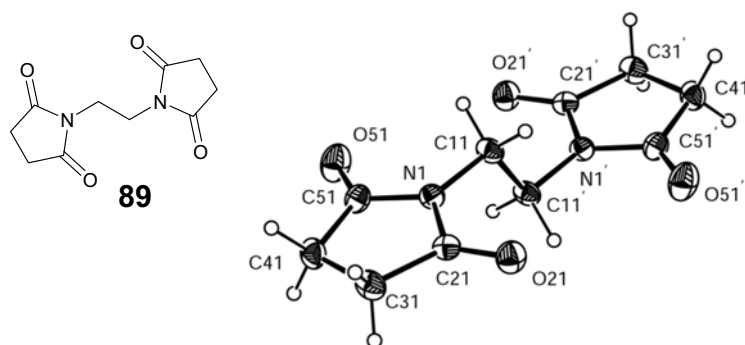
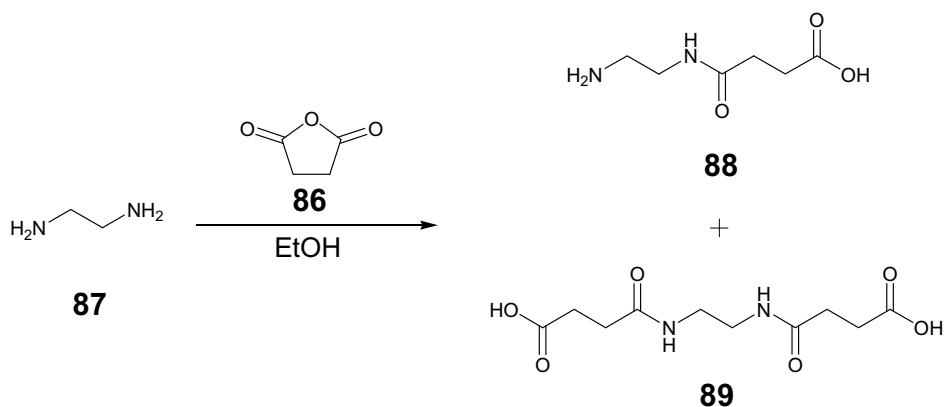


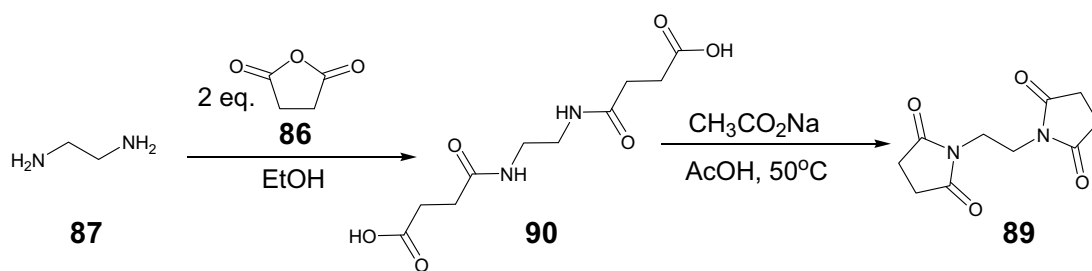
Figure 3-6. ORTEP diagram of the molecular structure of **89**.²⁸

This was an interesting result. When the mass spectrometry data was obtained for **88** it was observed that there were peaks corresponding to the lithium and sodium adducts of di-succinic acid substituted ethylenediamine **90**. Presumably this was a minimal by-product of the reaction between ethylene diamine **87** and succinic anhydride **86** (Scheme 3-8) as evidence of this compound did not appear in either the ^1H or ^{13}C NMR spectra of **88** (NMR analysis was carried out in D_2O , the sample was not filtered prior to analysis and no insoluble material was observed in solution).



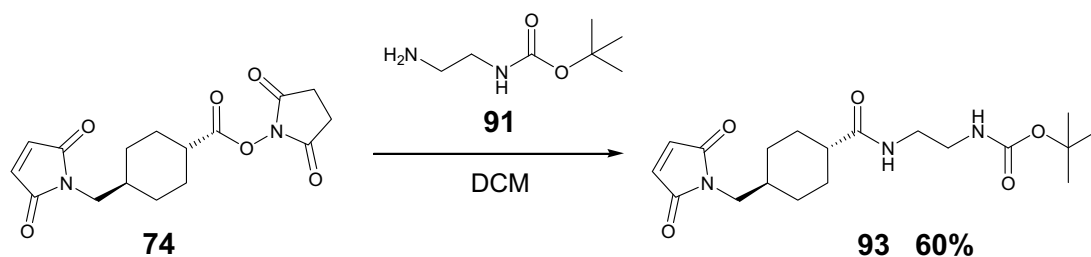
Scheme 3-8

It was postulated, and later observed, that **90** had a higher solubility in DMF than **88**. DCC and NHS facilitated the ring closure of this disuccinic acid substituted ethylenediamine **90** to form N,N'-ethylenedisuccinimide **89**. **90** was subsequently synthesised via a literature procedure²⁹ (Scheme 3-9) and the ring closure was achieved by heating in acetic anhydride in the presence of sodium acetate generating N,N'-ethylenedisuccinimide **89** in a yield of 58%. Spectroscopic data was identical to that obtained for the original isolated product.



Scheme 3-9

A new strategy was devised for the synthesis of the extended linker **85**. It was postulated that coupling of **74** with mono-BOC protected ethylenediamine **91**, followed by deprotection of the terminal amine, subsequent coupling with succinic anhydride **86**, followed by NHS esterification should afford the desired product. The reaction of **74** with mono BOC-ethylenediamine **91** (Scheme 3-10) was achieved by combining one molar equivalent of each in DCM under an atmosphere of N_2 . Isolation of the product by column chromatography (5% MeOH/DCM) afforded compound **93** in a 60% yield.



Scheme 3-10

Evidence for the formation of **93** was observed in the ESMS in the positive mode with peaks observed at $[\text{M}^+]$ 379 amu, $[\text{M}+\text{Li}]$ 386 amu and $[\text{M}+\text{Na}]$ 402 amu and microanalysis results were consistent with the calculated values. Assignment of the

aliphatic ^1H NMR resonances of **93** was facilitated by a 2D gCOSY experiment (Figure 3-7) showing correlations between the proton resonances.

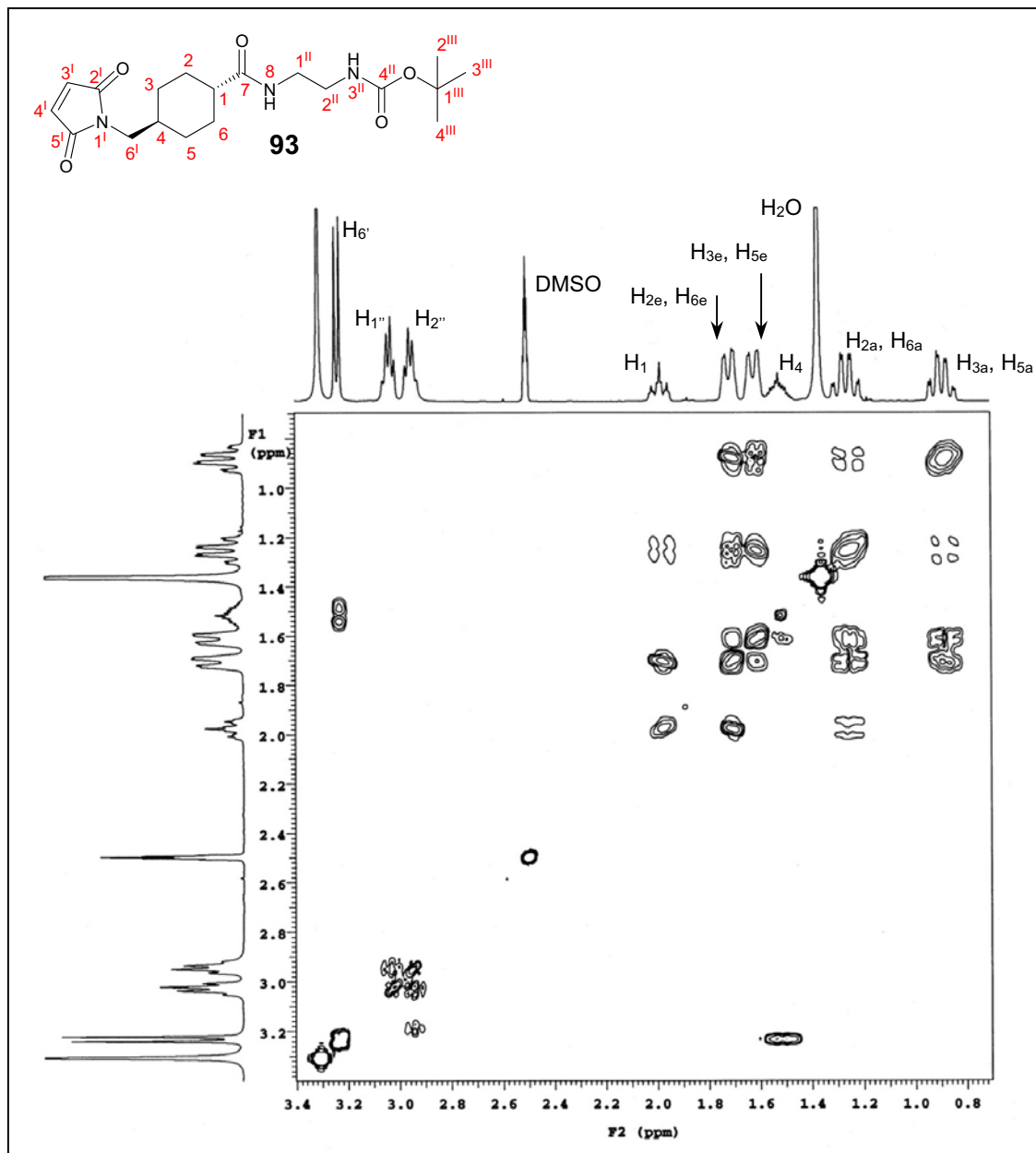
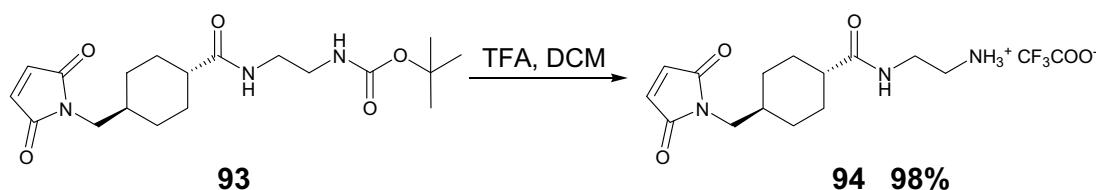


Figure 3-7. Expansion of the aliphatic region of the gCOSY spectrum (400MHz, $\text{DMSO-}d_6$) of **93**.

Deprotection of **93** with TFA in DCM (Scheme 3-11) was straightforward, affording **94** in an isolated yield of 98%. This compound was a low melting solid and quite

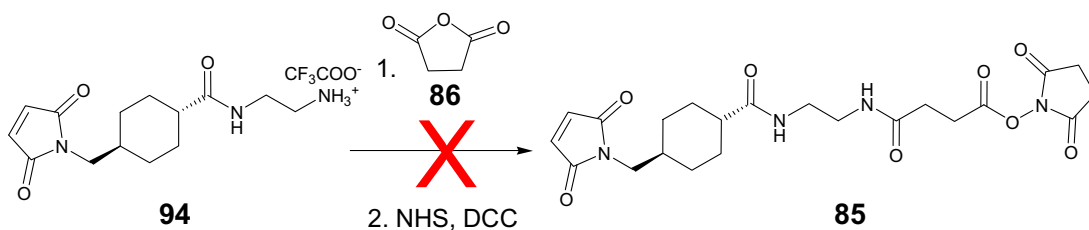
hygroscopic, as evidenced by the microanalysis results which are consistent with the presence of one molecule of H₂O for every two molecules of **94** *i.e.* C₁₆H₂₂F₃N₃O₅·½H₂O. ¹H and ¹³C NMR data were consistent with the loss of the BOC protecting group and subsequent formation of the TFA salt of the terminal amine.



Scheme 3-11

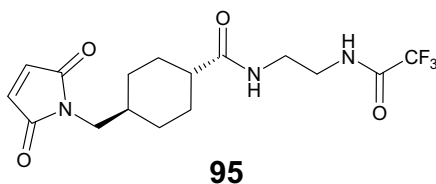
A number of attempts were made to prepare the free amine of **94** as it would be more reactive, in attempting to extend the linker arm, than the TFA salt. Organic solutions of **94** (DCM) was washed with various strengths of aqueous Na₂CO₃. However, in all cases, degradation of the maleimide group was observed by ¹H NMR. Thus all subsequent attempts to produce the extended linker, **85**, used the TFA salt **94**.

A one pot method was attempted for the coupling of **94** and succinic anhydride **86**, with NHS esterification of the resultant terminal acid (Scheme 3-12). The TFA salt **94** was dissolved in DMF under an atmosphere of N₂. One molar equivalent of **86** was added and, after stirring for one hour at room temperature, a slight excess of NHS and DCC were added to the reaction mixture. After stirring for a further 24 hours, the solvent was removed. The crude ¹H NMR showed a mixture of products.



Scheme 3-12

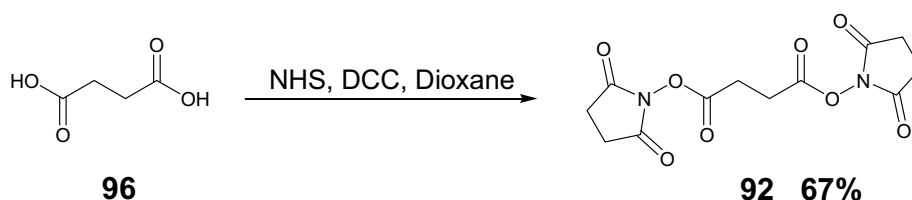
The residue was dissolved in a mixture of EtOAc/MeOH in preparation for purification of the product by column chromatography however a solid precipitated from the solution and was collected by filtration. Analysis of the ^1H and ^{13}C NMR spectra obtained for this material was not inconsistent with the formation of trans-4[(2,5-dioxo-2,5-dihydro-1H-pyrrol-1-yl)methyl]-N-{2-trifluoroacetyl}amino]ethyl}-cyclohexane carboxamide **95** with an isolated yield of 70%.



^1H NMR of this isolated material compared with **94** showed the conversion of the NH_3^+ resonance of **94** (7.79ppm, broad singlet, relative integral area of 3 hydrogens) into a second NH group in **95** (9.34ppm, broad triplet, relative integral area of 1 hydrogen). The ^{13}C NMR showed ^{19}F coupling to the carbons of the CF_3 and adjacent $\text{C}=\text{O}$, with the diagnostic downfield shift of this resonance 156.40 ppm for **95**. Previous reports have demonstrated the activation of trifluoroacetate (as a residual from BOC deprotection) towards trifluoroacetylation of amines in peptide coupling, particularly in the presence of DCC, see Merrifield³⁰ and references

contained within. As this was not the desired product, no further characterisation data was obtained for this compound.

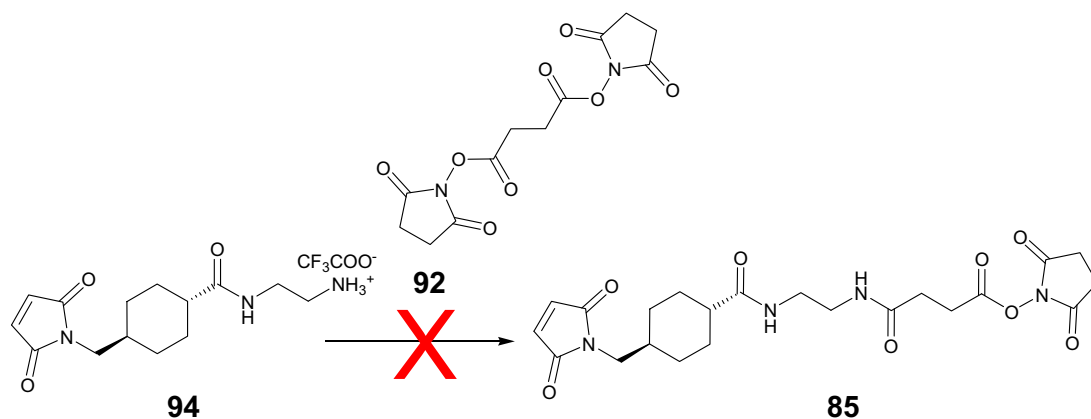
Another alternate route for the synthesis of **85** was devised whereby a homobifunctional linker, the disuccinimidyl ester of succinic acid would be synthesised and subsequently reacted with **74** to produce the desired product. The synthesis of the di-NHS ester of succinic acid (Scheme 3-13) was achieved via a literature procedure⁴ whereby succinic acid **96** was reacted with ~2.2 equivalents of NHS and DCC in 1,4-dioxane at 15°C under an atmosphere of N₂. The precipitated product and the formed DCU were collected by filtration, the product **92** extracted from this mixture by dissolving in acetonitrile and removing the DCU by filtration. Recrystallisation of the product (MeCN/EtOH) afforded **92** as a white solid in a yield of 67%. ESMS showed peaks corresponding to the sodium and lithium adducts of **92** at 319 amu and 335 amu respectively and NMR data was consistent with reported values.



Scheme 3-13

Coupling of the TFA salt of the partially extended SMCC **94** with the di-NHS ester **93** was attempted (Scheme 3-14) using a number of reaction conditions including cooling to 0°C in an ice bath on dropwise addition of **94** to a stirred solution of **92** in dry DMF, addition of **94** at room temperature, however after work up of each reaction, crude ¹H NMR analysis did not show the formation of the second amide

bond. The reason for the failure of these reaction attempts is at this stage unknown, but may perhaps be due to the hygroscopic nature of **94**.



Scheme 3-14

Unfortunately, due to a number of unsuccessful attempts at this final coupling step, the comparative number of reaction steps potentially required to prepare this extended linker and the fact that multiple stages of chromatography would be required renders this method a less feasible option in terms of manufacturing extended length heterobifunctional linkers than previously published examples⁸ therefore at this stage, the synthesis of **85** was abandoned.

3.2.3 Synthesis of Crown-Ether for Protein Modification

In an ongoing collaboration with a fellow group member, to investigate the bioconjugation of proteins with functional assemblies, a novel, maleimide functionalised crown ether, **98**, was synthesised. The coupling of **74** with 4'-aminobenzo-15-crown-5 **97** (Scheme 3-15) was achieved by stirring one molar equivalent of each compound in a solution of DCM in the dark under an atmosphere

of nitrogen. Isolation of the product by column chromatography (10% MeOH/EtOAc) afforded the maleimide crown-ether in a yield of 80%.

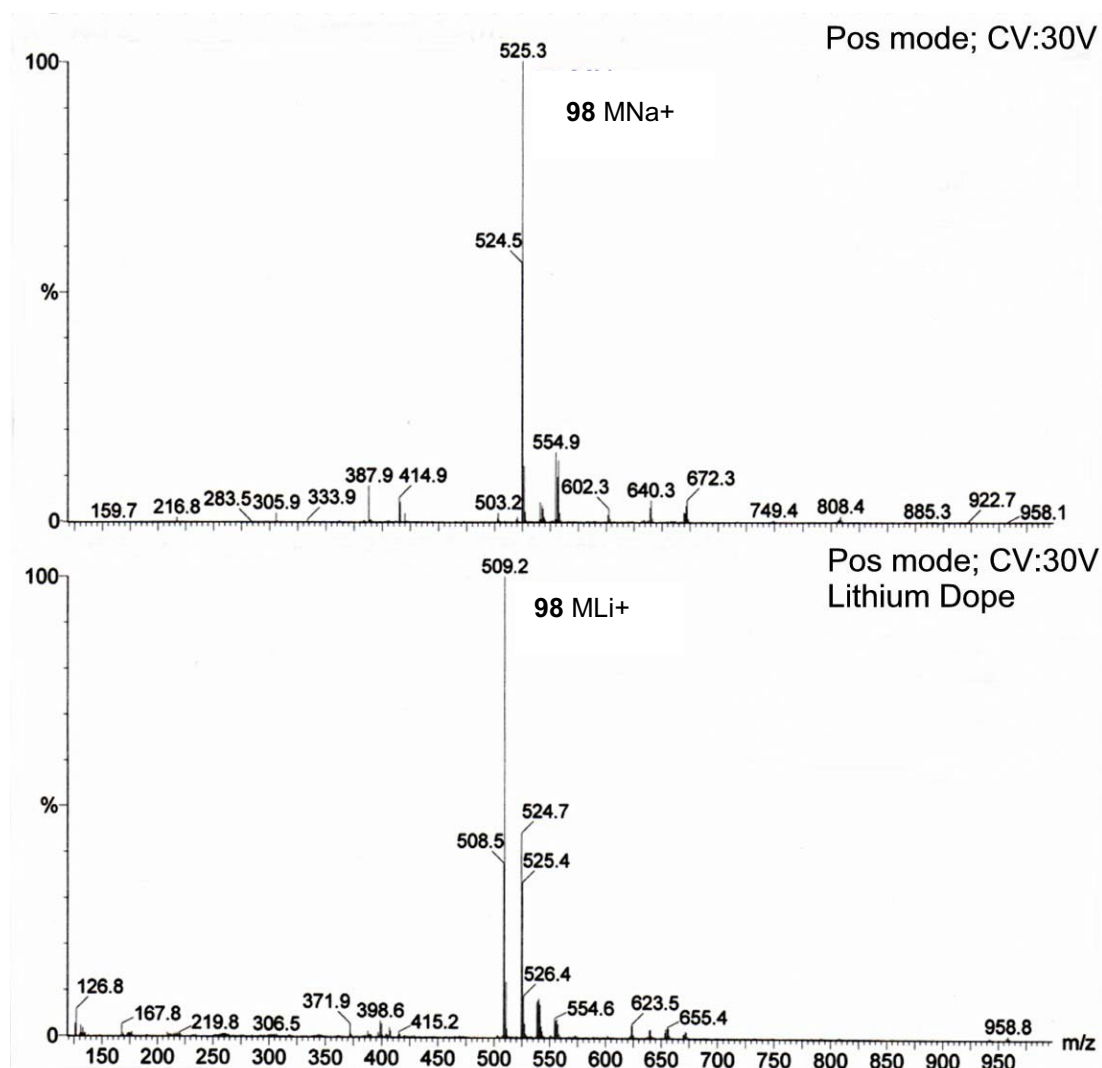
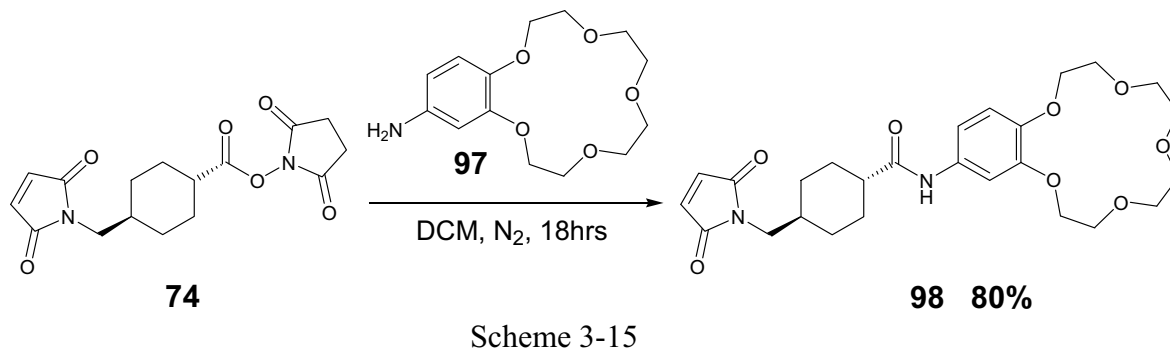


Figure 3-8. ESMS spectra of 98 in a) the positive mode and b) lithium doped.

Successful formation of **98** was evidenced by ESMS results (Figure 3-8) with peaks observed in the positive mode at [M+Li] 509 and [M+Na] 525 amu. 2D NMR techniques were used to assign both the ^1H and ^{13}C NMR spectra.

Work undertaken within the group, was directed towards the site-specific mutation of GFP's to bear nucleophilic thiol groups, on the surface of the protein. As such, **98** was designed as a test compound for bioconjugation studies to this mutant system. This compound could be used to ascertain whether the mutant proteins produced could be modified *via* reaction of the exposed thiol(s) with the maleimide group of **98**. The covalent attachment of **98** to a protein would produce a significant increase in the molecular weight of the protein such that, an increase of ~502 amu would be observed in the mass spectrum. This bioconjugate of GFP and the crown ether will be used in ion binding studies as a proof of principle for a GFP based ion sensitive detection system, however, these investigations are continuing³¹ and will be reported in future publications.

3.2.4 Further applications

Working towards the preparation of a bioconjugate of peptide nucleic acid (PNA) sequences and green fluorescent protein, a number of PNA sequences have been successfully functionalised with the linking reagents prepared in this manuscript.³² Work is continuing into the preparation of a suitably engineered GFP, to incorporate an exposed cysteine residue, to achieve this goal and will be reported in future publications. At the time of this projects inception, no such bioconjugate had been prepared however during the course of this work, a similar system was successfully

achieved by the attachment of an enhanced yellow fluorescent protein (EYFP) to a DNA sequence *via* a heterobifunctional linking molecule (Figure 3-9).²²

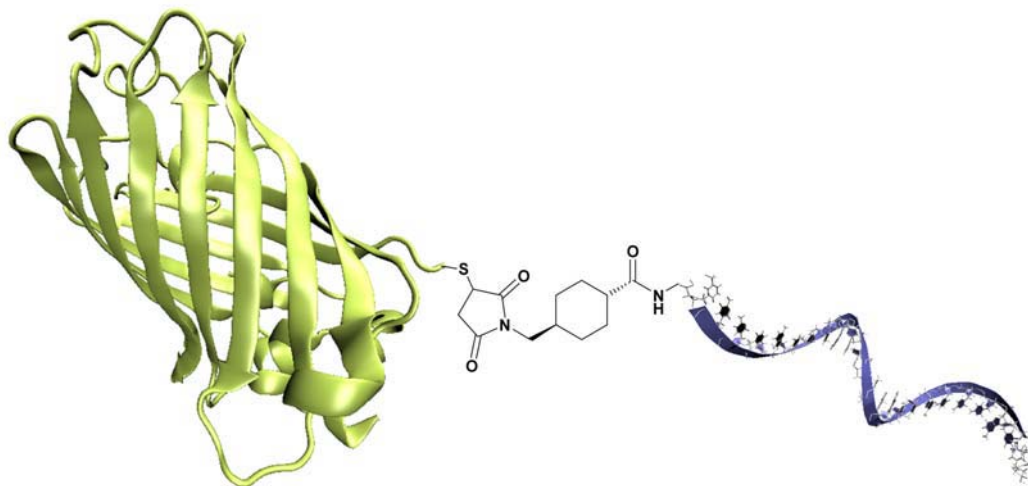


Figure 3-9. Representation of EYFP – DNA bioconjugate

The linkers synthesised in this body of work have also been used for the attachment of peptide nucleic acids to glass surfaces,³² however the results are not reported here as they are outside the scope of this body of work.

3.2.5 Summary

In summary, a number of heterobifunctional linkers were synthesised with yields similar to reported literature values for **71** and **75**. SMCC **74** was synthesised with a yield (32%) greater than the original reported literature value (18%) however a later article reported a one pot method for the synthesis of **74** with a greater yield than we were able to achieve (75%). Numerous attempts to synthesise an extended length heterobifunctional linker containing an amide function in the spacer were all unsuccessful. It was found that the synthesis of such a molecule was not a suitable alternative to **75**, due to the number of reaction steps and chromatography required

and most importantly our inability to achieve the successful synthesis of **85**. However, a novel protein modification reagent **98** was successfully synthesised for reaction with the free thiol groups present on the surface of proteins or particles.

3.3 References

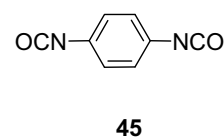
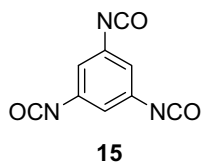
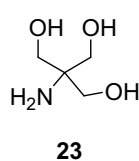
- (1) Hermanson, G. T. *Bioconjugate Techniques*; Academic Press: San Diego, 1996.
- (2) Means, G. E.; Feeney, R. E. *Bioconjugate Chem.* **1990**, *1*, 2-12.
- (3) Brinkley, M. *Bioconjugate Chem.* **1992**, *3*, 2-13.
- (4) Hill, M.; Bechet, J.-J.; d'Ablis, A. *FEBS Lett.* **1979**, *102*, 282-286.
- (5) Smith, M. B.; March, J. *March's Advanced Organic Chemistry: Reactions, Mechanisms and Structure*; 5th ed. ed.; Wiley-Interscience: New York, 2001.
- (6) Gurd, F. R. N. *Methods in Enzymology* **1967**, *11*, 532-541.
- (7) Brewer, C. F.; Riehm, J. P. *Anal. Biochem.* **1967**, *18*, 248-255.
- (8) Bieniarz, C.; Husain, M.; Barnes, G.; King, C. A.; Welch, C. J. *Bioconjugate Chem.* **1996**, *7*, 88-95.
- (9) Halime, Z.; Michaudet, L.; Lachkar, M.; Brossier, P.; Boitrel, B. *Bioconjugate Chem.* **2004**, *15*, 1193-1200.
- (10) Tang, K.; Fu, D.-J.; Julien, D.; Braun, A.; Cantor, C. R.; Koster, H. *Proc. Natl. Acad. Sci. U.S.A.* **1999**, *96*, 10016-10020.
- (11) Liang, Z.; Kumar, A. (2001) *European Patent* WO0142501.
- (12) Ramirez-Vick, J. E. (2000) *European Patent* WO0070345.
- (13) Hiratsuka, T. *Biochemistry* **1987**, *26*, 3168-3173.
- (14) Hudson, E. N.; Weber, G. *Biochemistry* **1973**, *12*, 4154-4161.
- (15) Annunziato, M. E.; Patel, U. S.; Ranade, M.; Palumbo, P. S. *Bioconjugate Chem.* **1993**, *4*, 212-218.
- (16) Rosi, N. L.; Thaxton, C. S.; Mirkin, C. A. *Angew. Chem. Int. Ed. Engl.* **2004**, *43*, 5500-5503.
- (17) Cho, Y.; Ivanisevic, A. *J. Phys. Chem. B* **2004**, *108*, 15223-15228.

- (18) Peeters, J. M.; Hazendonk, T. G.; Beuvery, E. C.; Tesser, G. I. *J. Immunol. Methods* **1989**, *120*, 133-143.
- (19) Ishikawa, E.; Yamada, Y.; Yoshitake, S.; Kawaguchi, H. *Enzyme Immunoassay*; Igaku Shoin: Tokyo, 1981.
- (20) Xiao, S.-J.; Brunner, S.; Wieland, M. *J. Phys. Chem. B* **2004**, *108*, 16058-16517.
- (21) Maeda, M.; Kida, S.; Hojo, K.; Eto, Y.; Gaob, J.-Q.; Kurachi, S.; Sekiguchi, F.; Mizuguchi, H.; Hayakawa, T.; Mayumi, T.; Nakagawa, S.; Kawasaki, K. *Bioorg. Med. Chem.* **2005**, *15*, 621-624.
- (22) Kukolka, F.; Niemeyer, C. M. *Org. Biomol. Chem.* **2004**, *2*, 2203-2206.
- (23) Palumbo, P. S. (1993) *European Patent* WO9322677.
- (24) Yoshitake, S.; Yamada, Y.; Ishikawa, E.; Masseyeff, R. *Eur. J. Biochem.* **1979**, *101*, 395-399.
- (25) Nielsen, O.; Buchardt, O. *Synthesis* **1991**, 819-821.
- (26) Brown, C. L.; Atkinson, S. J.; Healy, P. C. *Acta Cryst. E* **2005**, *E61*, o1203-o1204.
- (27) Grinberg, H.; Lamdan, S.; Gaozza, C. H. *J. Heterocycl. Chem.* **1975**, *12*, 763-766.
- (28) Brown, C. L.; Atkinson, S. J.; Healy, P. C. *Acta Cryst. E* **2005**, *E61*, o1072-o1073.
- (29) Asay, R. E. *J. Heterocycl. Chem.* **1977**, *14*, 85-90.
- (30) Kent, S. B. H.; Mitchell, A. R.; Engelhard, M.; Merrifield, R. B. *Proc. Natl. Acad. Sci. U.S.A.* **1979**, *76*, 2180-2184.
- (31) McRae, S. R.; Brown, C. L. *Private communication* **2005**.
- (32) Silvester, N.; Brown, C. L. *Private communication* **2005**.

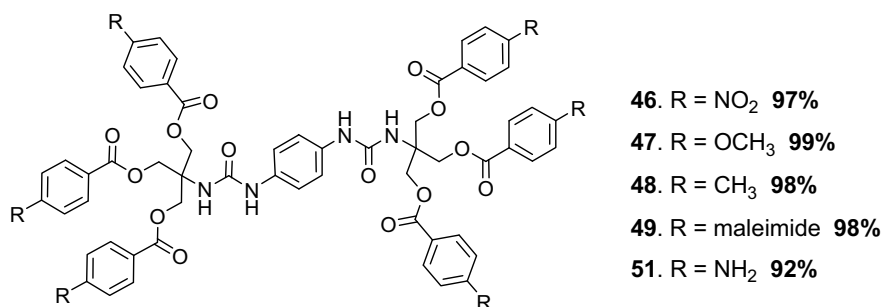
CHAPTER FOUR

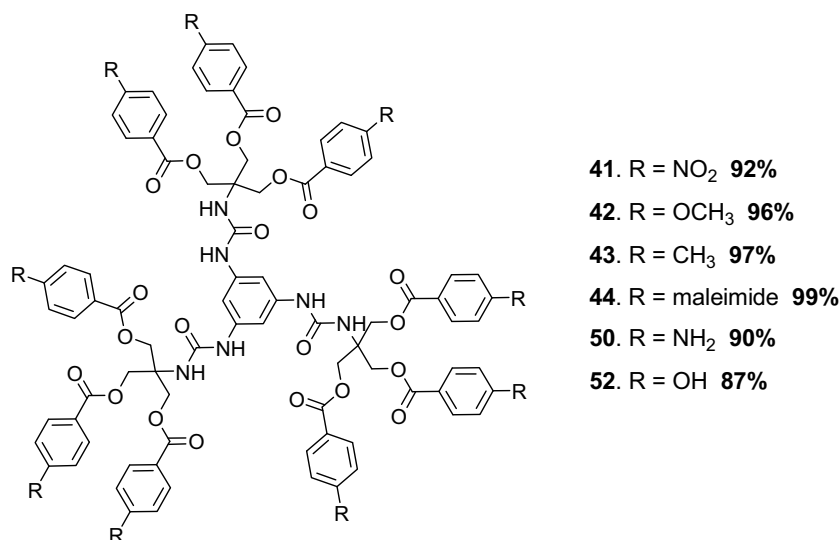
CONCLUDING COMMENTS

With rising interest in the synthesis of well-defined, functional materials, we have witnessed the use of an increasingly diverse range of building blocks and the development of synthetic procedures for the efficient assembly of these species. In an attempt to overcome the problems generally associated with the synthesis of large dendritic molecules, such as the requirement for high monomer loading and prolonged, repetitive, chromatographic separations that generate considerable waste, we developed a synthetic strategy utilizing the well-documented reaction between an isocyanate and an amine (Chapter 1). This proved to be a highly efficient, facile approach for the modular synthesis of a diverse range of peripherally functionalized dendritic structures. The peripheral functional groups were incorporated by preparing a number of branched subunits, based on tris(hydroxymethyl)aminomethane (TRIS), **23**, possessing three nitro, methoxy, methyl or maleimide terminal functionalities.

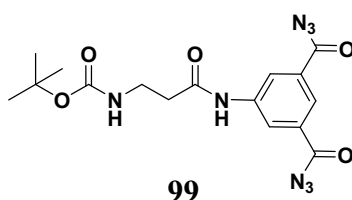


Deprotection and attachment of these branched units to the core molecules 1,4-phenylenediisocyanate **45** and 1,3,5-benzene triisocyanate **15** afforded the corresponding dendritic molecules possessing 6 (**46-49**) or 9 (**41-44**) peripheral functional groups.





In most cases the products precipitated from the reaction mixture and were isolated simply by filtration. Future optimisations could trial timed studies to determine the minimum reaction times required to achieve full functionalisation of the dendritic molecules. Functional group conversions on the dendritic molecules have been successfully carried out, including hydrogenation of the terminal nitro to the corresponding amine (**50** & **51**) and cleavage of the methoxy ether to give the corresponding phenol (**52**). It would be interesting in the future to further extend the synthetic strategy for the incorporation of other branching units within the dendritic framework, such as **99** to create larger dendritic structures. Heat activation of such a molecule would lead to the formation of two reactive isocyanate groups, that could lead the convergent synthesis of more highly substituted dendritic macromolecules.



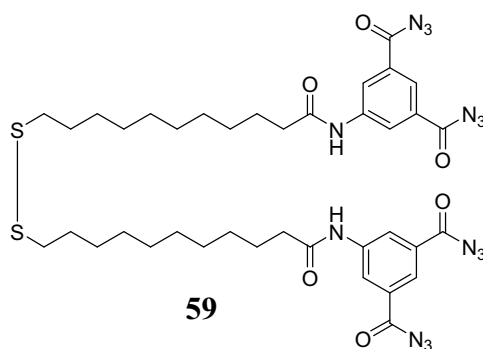
Future studies could also investigate other functional groups to be exposed to the surface of the dendrimers, such as acetylenes (for click chemistry attachment of azido species to the periphery).

Future investigations will centre on the potential applications of these molecules as a modular strategy provides ample opportunity for tailoring of the final molecules for specific applications. These systems may also serve as scaffolds for the assembly of more complex macromolecular structures for use in nanotechnology, biological and materials sciences as well as functional cores for the delivery of therapeutic agents and scaffolds for the attachment of biomolecules such as proteins. As such, the amine terminated dendritic molecules could be functionalised with heterobifunctional linking reagents (Chapter 3) to facilitate the attachment of biofunctional molecules via the thiol/maleimide reaction. These dendritic molecules could also be attached to SAM surfaces on gold (Chapter 2) for the development of surface arrays. Future studies could investigate the potential of the phenolic terminated 9-mer as a metal surface coating or metal ion binding agent. Further investigations could also be carried out in the area of core units, with potential for the preparation of tetra- or hexa-functionalised core molecules to build larger or more densely packed structures.

The large interest in the development of bio-sensing devices has driven research into the immobilisation of biomolecules onto solid surfaces. The ability to control the interaction and attachment of proteins with solid surfaces at the molecular level is paramount. As such the use of SAMs on gold for the achievement of these applications is increasing. In this body of work (Chapter 2), we have demonstrated the development of a UV patterning protocol, and shown the successful covalent attachment of GFP to a gold surface, by the reaction of the protein surface amine groups with an N-hydroxysuccinimide terminated monolayer, *via* fluorescence imaging. Future work will investigate AFM analysis of this surface, under liquid, to hopefully image the topography of these proteins on the surface, as the analyses

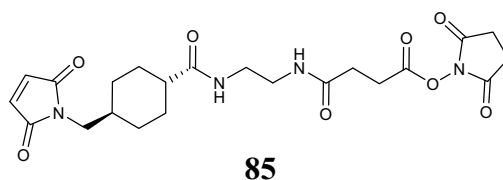
carried out in air did not. It would also be interesting to analyse these surfaces using XPS and surface IR techniques.

A 'heat activatable' surface monomer **59** was successfully synthesized and the formation of this monolayer on gold was successfully achieved (contact angle, XPS). Further analysis of this surface by AFM and other surface analysis techniques will be the object of future studies. Our preliminary investigations into the heat activation of this surface proved unsuccessful. Future investigations could perhaps look at a solution NMR study of **59** with and without the presence of an amine at elevated temperatures to determine the reactivity of **59** in solution. Following this, an NMR study of **59** adsorbed onto gold nano-particles could give some indication of the exact heating requirements needed to effect the conversion of the acyl azide to the isocyanate on the gold surface. Further to this, more in-depth XPS analysis of these heat treated surfaces would be required.

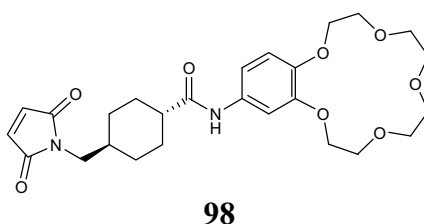


Once the heating requirements were optimized, it would be interesting to investigate the potential of **59** for the chemical attachment of bioactive molecules when embedded within a monolayer resistant to the non-specific binding of proteins.

The aim of Chapter 3 was to optimise the synthesis of some commercially available linkers. The synthesis of **74** *via* the two step method did improve the yield compared to the original literature procedure however a more recent publication of a one pot method reported a yield greater than we were able to achieve. Synthesis of **75** *via* the literature procedure obtained a similar yield to that reported. Another aim was to investigate the extension of **74** to form a novel extended length heterobifunctional cross-linker compound **85**. Exhaustive attempts and multiple synthetic strategies were applied however synthesis of **85** proved unsuccessful. Perhaps addition of TEA may facilitate the reaction of the TFA salt **94** with either succinic anhydride or the disuccinimidyl ester of succinic acid, that may be investigated at some stage.



The final goal within this section of work was to functionalise a crown-ether with **74** to produce a protein modification reagent **98** for its attachment to cysteine/thiol functionalised proteins, this was successfully synthesised with an 80% yield.



Future investigations in this area will centre on the finalisation of the collaborations within the group towards the attachment of PNA sequences to the Cys-modified GFP *via* the linking reagents, and subsequent attachment of these conjugates to gold monolayer surfaces.

CHAPTER FIVE

EXPERIMENTAL

5.1 General Procedures

Reagents and Solvents

All reagents were purified when necessary by literature methods.¹ In particular, anhydrous solvents were dried and distilled immediately before use; toluene and THF were predried over sodium then distilled from sodium/benzophenone, CH₂Cl₂ was dried and distilled from CaH₂, Et₃N and DMF were distilled from molecular sieves (4Å). Other anhydrous solvents used were obtained from commercial sources and used as received. Commercially available starting materials were used as obtained from the manufacturer. Air sensitive reactions were carried out under an inert atmosphere of nitrogen in flame dried glassware.

Purification

Analytical thin-layer chromatography (TLC) was carried out on Merck precoated aluminium TLC plates coated with silica gel 60 F₂₅₄ (0.2mm). Developed TLC plates were air dried, then visualised by means of ultra-violet light (λ 254nm) or in an iodine vapour tank. Chromatographic separations were carried out by column chromatography with Merck silica gel 60Å (230-400 Mesh) as the stationary phase. Gel permeation chromatography (GPC) was carried out using a Phenomenex Phenogel™ (500 Å) analytical column (300 x 7.8 mm) attached to a Waters 486 tunable absorbance detector set at 254nm and a Waters 600 controller, with a flow rate of the eluent (THF) at 1ml/minute. Millennium HPLC software was used for data acquisition and processing.

Characterisation

Melting points were measured using the capillary method on a Gallenkamp Variable Temperature Apparatus and are uncorrected. Mass Spectra were recorded on a Fisons VG-Platform II spectrometer, using electrospray in positive (ESMS+) and negative (ESMS-) modes as the ionisation technique. Mass Lynx Version I (IBM) software was used to acquire and process ESMS data. Lithium was added to ESMS scans as LiBr. High Resolution Mass Spectrometry were carried out by the FTMS Facility, Griffith University. Fourier transform infra-red (FTIR) spectra were recorded in the range 4000-400 cm^{-1} on a Thermo Nicolet-Nexus FTIR spectrometer. All spectra were recorded as KBr disc or as specified. Signals were recorded with the following abbreviations: s = strong, m = medium and w = weak. ^1H NMR (200MHz or 400MHz) and ^{13}C NMR (50MHz or 100MHz) spectra were obtained using a Varian Gemini 200 or a Varian Unity 400 spectrometer as indicated. All spectra were obtained by dissolving the sample in CDCl_3 , $\text{DMSO-}d_6$, $\text{Acetone-}d_6$, $\text{Toluene-}d_8$ or $\text{DMSO-}d_6$ / $\text{TFA-}d$ as indicated. Signals are recorded in terms of chemical shifts (δ ppm) relative to the referenced residual solvent peak: CDCl_3 7.27ppm (^1H) and 77.23ppm (^{13}C), $\text{DMSO-}d_6$ 2.50ppm (^1H) and 39.51ppm (^{13}C), $\text{Acetone-}d_6$ 2.05ppm (^1H) and 29.92ppm (^{13}C), $\text{Toluene-}d_8$ 2.09ppm (^1H) and 137.86ppm (^{13}C); multiplicity, coupling constants (in Hz), integration, and assignments are described in that order. The following abbreviations for multiplicity are used, s: singlet; d: doublet; t: triplet; dd: doublet of doublets; ddd: doublet of doublet of doublets; dddd: doublet of doublet of doublet of doublets; dt: doublet of triplets; ddt: doublet of doublet of triplets; q: quartet; m: multiplet. Ambiguous ^1H NMR and ^{13}C NMR assignments were further elucidated by the application of 2D gCOSY, gHSQC or

gHMBC experiments where appropriate. Elemental analyses were carried out by the Microanalytical Service, Department of Chemistry at the University of Queensland.

Nomenclature

The nomenclature and numbering used for novel compounds within the experimental is in accordance with the IUPAC convention for naming organic compounds.²

Published Compounds

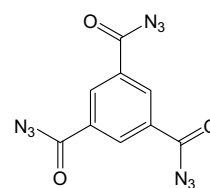
The characterisation data on compounds **24-27**, **34-44**, **50** and **52**,³ **75**,⁴ and **90**⁵ have been published elsewhere but are reported here for continuity of this body of work.

5.2 Chapter One

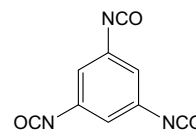
Modular Synthesis of Dendritic Molecules

Synthesis of 1,3,5-Benzenetricarbonyl triazide (14)

1,3,5-Benzenetricarbonyl chloride (10.010g, 37.7mmol) was dissolved in dry THF (50ml) and stirred at room temperature, under an atmosphere of N₂, with sodium azide (30.003g, 462mmol) for 48 hours. The reaction mixture was poured into water (350ml) and extracted with diethyl ether (5 x 150ml). The combined organics were washed with an aqueous 5% NaOH solution (200ml) and water (2 x 200ml), dried (MgSO₄), filtered and evaporated at room temperature to yield a white solid (8.169g, 28.6mmol, 76%, Lit.⁸ 71%). IR(KBr) 2150.62 (s, CON₃), 1699.87cm⁻¹ (s, C=O). ¹H NMR (400MHz, toluene-*d*₈) δ 8.61 (s, 3H, Ar-*H*). ¹³C NMR (100MHz, toluene-*d*₈) δ 169.99 (CON₃), 134.62 (ArC-H), 132.28 (ArCq).

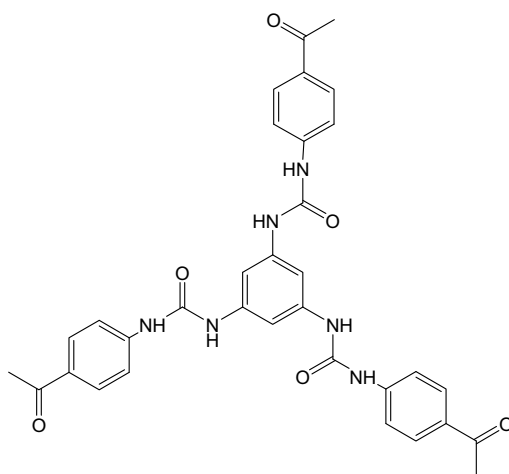


NMR test of conversion to the isocyanate **15** – 82mg of 1,3,5-benzenetricarbonyl triazide was dissolved in an ampoule of toluene-*d*₈ and ¹H and ¹³C NMR spectra were recorded as described above. The sample was then heated to reflux under N₂ for one hour and the ¹H and ¹³C NMR spectra were re-recorded showing complete conversion to 1,3,5-benzenetriisocyanate. ¹H NMR (400MHz, toluene-*d*₈) δ 5.73 (s, 3H, Ar-*H*). ¹³C NMR (100MHz, toluene-*d*₈) δ 135.09 (ArCq), 125.24 (N=C=O), 118.41 (ArC-H).



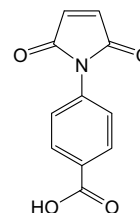
Synthesis of 1,3,5-tris-(((4-acetophenyl)amino)-carbonylamino)benzene (17)

1,3,5-Benzenetricarbonyl triazide (0.538g, 1.9mmol) was heated in dry toluene (20ml) at reflux for one hour under an atmosphere of nitrogen. The toluene was removed on a rotary evaporator, then 4-aminoacetophenone (0.772g, 5.7mmol) dissolved in CH₂Cl₂ (15ml) was added, under an atmosphere of N₂, and gently refluxed for 16 hours. The reaction mixture was then cooled to room temperature and the formed precipitate was filtered dried and evaporated. The resulting solid was sonicated in ethyl acetate, collected by filtration and dried (0.990g, 1.6mmol, 86%). mp 293-294°C. (ESMS-) 605 (M⁻, 70%). (ESMS+) 613 (MLi⁺, 100%), 629 (MNa⁺, 49%). IR(KBr) 3361 (m, NH), 1714 (s, C=O), 1655cm⁻¹ (s, C=O). ¹H NMR (400MHz, DMSO-*d*₆) δ 8.96 (br. s, 3H, NH), 8.93 (br. s, 3H, NH), 7.91 (m (AA'), 6H, Ar-H), 7.59 (m (XX'), 6H, Ar-H), 7.39 (s, 3H, core-Ar-H), 2.52 (s, 9H, CH₃). ¹³C NMR (100MHz, DMSO-*d*₆) δ 196.29 (RC=OCH₃), 152.01 (NHC=ONH), 144.29 (ArC-NHR), 140.10 (core-ArC-NHR), 130.46 (ArC-COCH₃), 129.68 (ArC-H), 117.12 (ArC-H), 102.15 (core-ArC-H), 26.34 (CH₃). Anal. calcd for C₃₃H₃₀N₆O₆: C, 65.34; H, 4.98; N, 13.85. Found: C, 63.35; H, 5.15; N, 13.65.



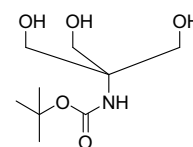
Synthesis of 4-Maleimidobenzoic acid (21)

N-(4-carboxyphenyl)maleamic acid (18.271g, 77.7mmol) and sodium acetate (6.373g, 77.7mmol) were stirred in acetic anhydride (60ml) between 55-60°C for two hours. The reaction mixture was then poured into water (800ml) and allowed to stand such that a solid formed. The yellow precipitate was collected by filtration and then sonicated in 800ml of water for three hours. The resulting white solid was collected by filtration and dried (13.884g, 63.9mmol, 82%). mp 233°C (Lit.⁷ 244°C). (ESMS-) 216 (M^- , 98%). ¹H NMR (400MHz, DMSO-*d*₆) δ 13.06 (br. s, 1H, CO₂H), 8.04 (m (AA'), 2H, Ar-H), 7.51 (m (XX'), 2H, Ar-H), 7.22 (s, 2H, RHC=CHR). ¹³C NMR (100MHz, DMSO-*d*₆) δ 169.55 (CONR), 166.70 (CO₂H), 135.50 (ArC-NR) 134.85 (RHC=CHR) 129.89 (ArC-H) 129.57 (ArC-CO₂H) 126.14 (ArC-H).



Synthesis of *N*-(*tert*-butyloxycarbonyl)-1,1,1-tris(hydroxymethyl)methyl-amine (24)

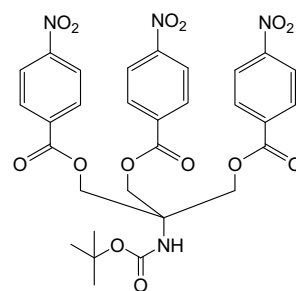
Tris(hydroxymethyl)aminomethane (11.7g, 97mmol) was added as a solid to a solution of di-*tert*-butyl dicarbonate (21.0g, 96mmol) in THF (200ml) under an atmosphere of N₂. The reaction mixture was stirred at room temperature for 4 days. The resulting precipitate was collected by filtration, washed thoroughly with cold THF and dried under high vacuum to yield a white powder (15.115g, 70mmol, 73%). mp 144-146°C (Lit.⁶ 147°C). (ESMS-) 220 (M^- , 20%); (ESMS+) 222 (M^+ , 15%), 228 (MLi^+ , 95%). ¹H NMR (400MHz, DMSO-*d*₆) δ 5.76 (br. s, 1H, NH), 4.49 (br. t, 3H, OH), 3.51 (d, 6H, CH₂), 1.37 (s, 9H, CH₃). ¹³C NMR (100MHz, DMSO-*d*₆) δ 155.03 (C=O), 77.83 (*C*_q-CH₃), 60.45 (CH₂), 60.24 (*C*_q-CH₂), 28.22 (CH₃).



Synthesis of *N*-(*tert*-butyloxycarbonyl)-1,1,1-tris(4-nitrobenzoyloxymethyl)methylamine (25)

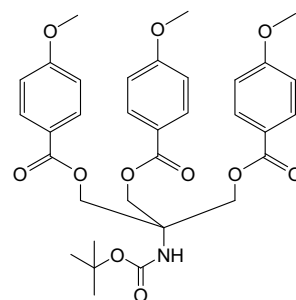
A solution of 4-nitrobenzoyl chloride (14.006g, 74.6mmol) dissolved in CH₂Cl₂ (30ml) was added dropwise, under an atmosphere of N₂, to a solution of *N*-(*tert*-butyloxycarbonyl)-1,1,1-tris(hydroxymethyl)methylamine (5.015g, 22.6mmol) and Et₃N (11ml, 79mmol) in dry CH₂Cl₂ (100ml). The reaction was gently refluxed for 20 hours, then cooled to room temperature and filtered to remove the precipitated triethylamine hydrochloride. The organic solution was washed with saturated aqueous NaHCO₃ (3 x 150ml) and saturated aqueous NaCl (5 x 150ml), dried (MgSO₄), filtered and evaporated under reduced pressure. The crude product was purified by column chromatography (4% ethyl acetate/CH₂Cl₂) to yield an ivory coloured solid (13.170g, 19.7mmol, 87%). mp 147.5-149°C. (ESMS⁺) 691 (MNa⁺, 65%), 675 (MLi⁺, 30%). IR(KBr) 3391 (m, NH), 1725 (s, C=O), 1526 (s, C-NO₂), 1349 (m, C-NO₂), 1276 cm⁻¹ (s, C-O-C). ¹H NMR (400MHz, DMSO-*d*₆) δ 8.29 (m (AA'), 6H, Ar-*H*), 8.18 (m (BB'), 6H, Ar-*H*), 7.51 (br. s, 1H, NH), 4.81 (s, 6H, CH₂), 1.34 (s, 9H, CH₃). ¹³C NMR (100MHz, DMSO-*d*₆) δ 163.84 (CO₂R), 154.74 (NH-C=O), 150.30 (ArC-NO₂), 134.68 (ArC-CO₂H), 130.74 (ArC-H), 123.76 (ArC-H), 78.79 (*Cq*-CH₃), 63.78 (CH₂), 56.57 (*Cq*-CH₂), 28.01 (C-CH₃).

Anal. calcd for C₃₀H₂₈N₄O₁₄: C, 53.89; H, 4.22; N, 8.38. Found: C, 54.12; H, 4.35; N, 8.23.



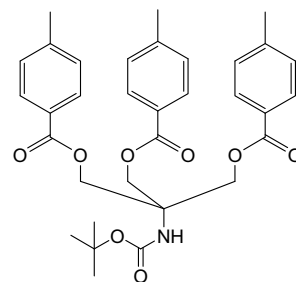
Synthesis of *N*-(*tert*-butyloxycarbonyl)-1,1,1-tris(4-methoxybenzyloxy)methylamine (26)

p-Anisoyl chloride (12.723g, 74.58mmol) was dissolved in CH₂Cl₂ (30ml) and added dropwise to a solution of *N*-(*tert*-butyloxycarbonyl)-1,1,1-tris(hydroxymethyl)methylamine (5.00g, 22.6mmol) and Et₃N (11ml, 79mmol) in CH₂Cl₂ (100ml) under an atmosphere of N₂. The reaction was left to stir at room temperature for 17 hours and then refluxed for 4 hours. The reaction was cooled to room temperature then filtered to remove the precipitated triethylamine hydrochloride. The organic filtrate was washed with saturated aqueous NaHCO₃ (3 x 150ml), saturated aqueous NaCl (5 x 150ml), dried (MgSO₄), filtered and evaporated under reduced pressure. The resulting crude product was purified by column chromatography (2% ethyl acetate/CH₂Cl₂) to yield a white solid (12.961g, 20.8mmol, 92%). Crystals suitable for X-ray diffraction were obtained by slow evaporation from a solution of DMF. mp 136°C. (ESMS+) 630 (MLi⁺, 100%), 647 (MNa⁺, 100%). IR(KBr) 3364 (m, NH), 2976 (w, ArC), 1718 (s, C=O), 1697 (s, C=O), 1606 (s, ArC-O-C), 1255cm⁻¹ (s, C-O-C). ¹H NMR (400MHz, DMSO-*d*₆) δ 7.91 (m (AA'), 6H, Ar-*H*), 7.34 (br. s, 1H, NH) 7.00 (m (XX'), 6H, Ar-*H*), 4.65 (s, 6H, CH₂), 3.82 (s, 9H, O-CH₃), 1.34 (s, 9H, C-CH₃). ¹³C NMR (100MHz, DMSO-*d*₆) δ 164.93 (CO₂R), 163.24 (ArC-OCH₃), 154.69 (NH-C=O), 131.37 (ArC-H), 121.53 (ArC-CO₂R), 113.93 (ArC-H), 78.47 (C_q-CH₃), 62.85 (CH₂), 56.77 (C_q-CH₂), 55.48 (O-CH₃), 28.04 (C-CH₃). Anal. calcd for C₃₃H₃₇NO₁₁: C, 63.55; H, 5.98; N, 2.25. Found: C, 63.64; H, 6.01; N, 2.21.



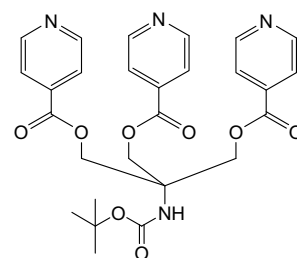
Synthesis of *N*-(*tert*-butyloxycarbonyl)-1,1,1-tris(4-methylbenzoyloxymethyl)methylamine (27)

p-Toluoyl chloride (11.69g, 10.0ml, 75.61mmol) was dissolved in dry CH₂Cl₂ (30ml) and added dropwise, under an atmosphere of N₂, to a solution of *N*-(*tert*-butyloxycarbonyl)-1,1,1-tris(hydroxymethyl)methylamine (5.035g, 22.7mmol) and Et₃N (11ml, 79mmol) in CH₂Cl₂ (100ml). The reaction was heated gently for 18 hours, then cooled to room temperature. The solution was filtered, washed with saturated aqueous NaHCO₃ (3 x 150ml) and saturated aqueous NaCl (5 x 150ml). The organic layer was dried (MgSO₄), filtered and evaporated under reduced pressure. The crude product was purified by column chromatography (gradient elution 50 – 65% CH₂Cl₂/hexane) to yield a white solid (11.999g, 20.8mmol, 92%). mp 129-131°C. (ESMS⁺) 582 (MLi⁺, 100%), 598 (MNa⁺, 100%). IR(KBr) 3378 (m, NH), 2977 (w, ArC), 1726 (s, C=O), 1704 (s, C=O), 1271 (s, C-O-C). ¹H NMR (400MHz, DMSO-*d*₆) δ 7.85 (m (AA'), 6H, Ar-*H*), 7.38 (br. s, 1H, NH), 7.28 (m (XX'), 6H, Ar-*H*), 4.67 (s, 6H, CH₂), 2.36 (s, 9H, Ar-CH₃), 1.33 (s, 9H, C-CH₃). ¹³C NMR (100MHz, DMSO-*d*₆) δ 165.25 (CO₂R), 154.69 (NH-C=O), 143.78 (ArC-CH₃), 129.29 (ArC-H), 129.20 (ArC-H), 126.61 (ArC-CO₂R), 78.49 (C_q-CH₃), 62.96 (CH₂), 56.73 (C_q-CH₂), 28.03 (C-CH₃), 21.13 (ArC-CH₃). Anal. calcd for C₃₃H₃₇NO₈: C, 68.85; H, 6.48; N, 2.43. Found: C, 69.12; H, 6.46; N, 2.42.



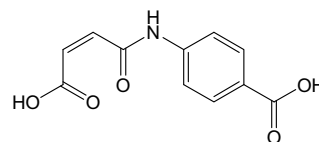
Synthesis of *N*-(*tert*-butyloxycarbonyl)-1,1,1-tris(isonicotinoyloxymethyl)methylamine (29)

Isonicotinic acid (9.186g, 74.6mmol) was gently refluxed in thionyl chloride (20ml) for 2 hours under an atmosphere of N₂. The solution was cooled to room temperature and the excess thionyl chloride was removed *in vacuo*. Residual thionyl chloride was further removed under high vacuum. The resulting solid was added gradually, under an atmosphere of N₂, to a stirred solution of *N*-(*tert*-butyloxycarbonyl)-1,1,1-tris(hydroxymethyl)methylamine (5.022g, 22.6mmol) and Et₃N (20ml, 144mmol) in CH₂Cl₂ (100ml). The reaction was heated gently for 18 hours then cooled to room temperature, filtered and washed with saturated aqueous NaHCO₃ (3 x 150ml) and saturated aqueous NaCl (5 x 150ml). The organic layer was dried (MgSO₄), filtered and evaporated under reduced pressure. The crude product was recrystallised in a mixture of CH₂Cl₂, diethyl ether and petroleum spirits, then dried under high vacuum to yield a glassy yellow solid (7.647g, 14.3mmol, 63%). mp 51°C. (ESMS+) 537 (M⁺, 100%), 543 MLi⁺, 20%). IR(KBr) 3379 (m, NH), 3246 (m, C-N), 2976 (w, ArC), 1733cm⁻¹ (s, C=O). ¹H NMR (400MHz, DMSO-*d*₆) δ 8.78 (m(AA'), 6H, Ar-*H*), 7.84 (m(XX'), 6H, Ar-*H*), 7.45 (br. s, 1H, NH), 4.78 (s, 6H, CH₂), 1.31 (s, 9H, CH₃). ¹³C NMR (100MHz, DMSO-*d*₆) δ164.19 (CO₂R), 154.71 (NH-C=O), 150.70 (ArC-H), 136.49 (ArC-CO₂R), 122.58 (ArC-H), 78.71 (*C*_q-CH₃), 63.60 (CH₂), 56.57 (*C*_q-CH₂), 27.99 (C-CH₃). Anal. calcd for C₂₇H₂₈N₄O₈: C, 60.44; H, 5.26; N, 10.44. Found: C, 60.37; H, 5.42; N, 10.18.



Synthesis of *N*-(4-carboxyphenyl)maleamic acid (32)

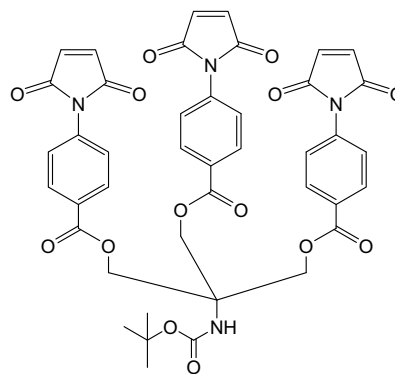
p-Aminobenzoic acid (14.010g, 102.2mmol) and maleic anhydride (10.023g, 102.2mmol) were dissolved in DMF (40ml) and stirred at room temperature under an atmosphere of N₂ for 16 hours. The reaction mixture was then poured into water (300ml) and the resulting precipitate was collected by filtration. The solid was then recrystallised from water to yield a yellow powder (23.776g, 101mmol, 99%). mp 222°C (Lit.⁷ 225-226°C). (ESMS-) 234 (M⁺, 100%). (ESMS+) 258 (MNa⁺, 100%). ¹H NMR (400MHz, DMSO-*d*₆) δ 12.82 (br. s, 2H, 2 x CO₂H), 10.60 (br. s, 1H, NH), 7.91 (m (AA'), 2H, Ar-H), 7.73 (m (XX'), 2H, Ar-H), 6.49 (d, 1H, ³J = 12Hz, C=CH), 6.32 (d, 1H, ³J = 12Hz, C=CH). ¹³C NMR (100MHz, DMSO-*d*₆) δ 166.96 (CO₂H), 166.92 (CO₂H), 163.70 (CONH), 142.76 (ArC-NH), 131.71 (HC=CH), 130.46 (ArC-H), 130.24 (HC=CH), 125.60 (ArC-CO₂H), 118.76 (ArC-H).



Synthesis of *N*-(*tert*-butyloxycarbonyl)-1,1,1-tris(4-maleimidobenzoyloxy)methyl)methylamine (34)

4-Maleimidobenzoic acid (12.021g, 55.35mmol) was gently refluxed in thionyl chloride (45ml) with *tert*-butyl catechol (0.010g) and stirred for 2 hours under an atmosphere of N₂. The solution was cooled to room temperature, the excess thionyl chloride removed *in vacuo* and the resulting solid dried under high vacuum. This solid was gradually added, under an atmosphere of N₂, to a solution of *N*-(*tert*-butyloxycarbonyl)-1,1,1-tris(hydroxymethyl)methylamine (3.711g, 16.77mmol) and Et₃N (20ml, 144mmol) in CH₂Cl₂ (200ml) with *tert*-butyl catechol (0.010g). The reaction was stirred at room temperature for 18 hours. The solution was filtered then

washed with saturated aqueous NaHCO₃ (3 x 150ml) and saturated aqueous NaCl (5 x 150ml). The organic layer was dried (MgSO₄), filtered and evaporated under reduced pressure. The crude product was purified by column chromatography (10% ethyl acetate/CH₂Cl₂) and dried under high vacuum (6.871g, 8.39mmol, 50%). mp 113-116°C. (ESMS+) 825 (MLi⁺, 100%), 841 (MNa⁺, 45%). IR(KBr) 3376 (w, NH), 3102 (w, C-N), 2977 (w, ArC), 1716 (s, C=O), 1267cm⁻¹ (s, C-O-C). ¹H NMR (400MHz, DMSO-*d*₆) δ 8.06 (m (AA'), 6H, Ar-*H*), 7.48 (m (XX'), 6H, Ar-*H*), 7.43 (br. s, 1H, NH), 7.22 (s, 6H, HC=CH), 4.76 (s, 6H, CH₂), 1.36 (s, 9H, CH₃). ¹³C NMR (100MHz, DMSO-*d*₆) δ 169.43 (C=ONC=O), 164.66 (CO₂R), 154.71 (NH-C=O), 135.95 (ArC-NR), 134.86 (RHC=CHR), 129.90 (ArC-H), 128.02 (ArC-CO₂R), 126.19 (ArC-H), 78.57 (C_q-CH₃), 63.31 (CH₂), 56.75 (C_q-CH₂), 28.05 (C-CH₃). Anal. calcd for C₄₂H₃₄N₄O₁₄: C, 61.61; H, 4.19; N, 6.84. Found: C, 61.76; H, 4.24; N, 6.87.



Synthesis of 1,1,1-tris(4-nitrobenzoyloxymethyl)methylamine trifluoroacetic acid salt (35)

N-(*tert*-butyloxycarbonyl)-1,1,1-tris(4-nitrobenzoyloxy-methyl)methylamine (3.540g, 5.3mmol) was dissolved in the minimum amount of CH₂Cl₂ then trifluoroacetic acid (3ml) was added and the solution was refrigerated for 18 hours. The organic solution was poured into 1M aqueous Na₂CO₃ and the resulting white precipitate was collected by filtration and dried (3.598g, 5.2mmol, 99%). Crystals suitable for X-ray diffraction were obtained by evaporation from a DMF solution. mp 158-159°C. (ESMS-) 113 (CF₃COO⁻, 95%). (ESMS+) 569 (M⁺, 100%). IR(KBr)

1742 (s, C=O), 1729 (s, C=O), 1267 cm^{-1} (s, C-O-C). ^1H NMR (400MHz, DMSO- d_6)

δ 9.32 (br. s, 3H, NH_3^+) 8.36 (m (AA'BB'), 12H, Ar-H),

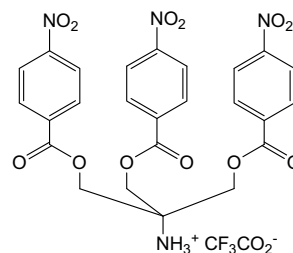
4.81 (s, 6H, CH_2). ^{13}C NMR (100MHz, DMSO- d_6) δ

163.79 (CO_2R), 150.55 (ArC- NO_2), 134.16 (ArC- CO_2R),

131.25 (ArC-H), 123.68 (ArC-H), 63.66 (CH_2), 56.38

(Cq). Anal. calcd for $\text{C}_{27}\text{H}_{21}\text{F}_3\text{N}_4\text{O}_{14}$: C, 47.52; H, 3.10;

N, 8.21. Found: C, 46.01; H, 2.95; N, 7.95.



Synthesis of 1,1,1-tris(4-methoxybenzoyloxymethyl)methylamine trifluoroacetic acid salt (36)

N-(*tert*-butyloxycarbonyl)-1,1,1-tris(4-methoxybenzoyloxymethyl)methylamine

(5.910g, 9.5mmol) was dissolved in CH_2Cl_2 (20ml) and trifluoroacetic acid (4ml)

was added. The solution was refrigerated overnight then poured into a 1M Na_2CO_3

solution. The resulting precipitate was collected by filtration and dried (5.918g,

9.3mmol, 98%). mp 150-151 $^\circ\text{C}$. (ESMS-) 113 (CF_3COO^- , 50%). (ESMS+) 524 (M^+ ,

100%). IR(KBr) 1731 (s, C=O), 1713 (s, C=O), 1259 cm^{-1} (s, C-O-C). ^1H NMR

(400MHz, DMSO- d_6) δ 9.06 (br. s, 3H, NH_3^+), 8.09 (m (AA'), 6H, Ar-H), 7.03 (m

(XX'), 6H, Ar-H), 4.65 (s, 6H, CH_2), 3.84 (s, 9H, O- CH_3). ^{13}C NMR (100MHz,

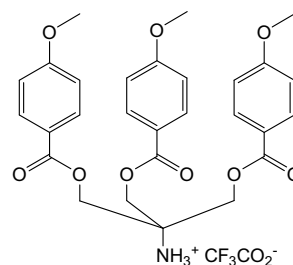
DMSO- d_6) δ 164.88 (CO_2R), 163.55 (ArC-O CH_3),

131.96 (ArC-H), 120.92 (ArC- CO_2R), 113.93 (ArC-H),

63.04 (CH_2), 56.49 (Cq), 55.56 (O- CH_3). Anal. calcd for

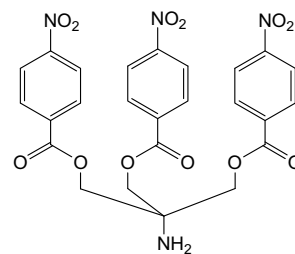
$\text{C}_{30}\text{H}_{30}\text{F}_3\text{NO}_{11}$: C, 56.52; H, 4.74; N, 2.20. Found: C,

54.06; H, 4.56; N, 2.15.



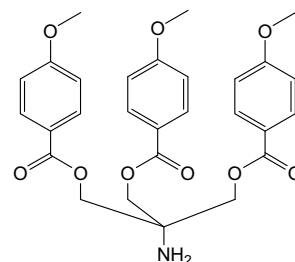
Synthesis of 1,1,1-tris(4-nitrobenzoyloxymethyl)methylamine (37)

The TFA salt of 1,1,1-tris(4-nitrobenzoyloxymethyl)methylamine (9.505g, 13.9mmol) was dissolved in DMF (100ml) then CH₂Cl₂ (200ml) was added. This organic solution was washed with 1M Na₂CO₃ (2 x 150ml) and water (2 x 150ml), then dried (MgSO₄), filtered and evaporated to yield the free amine (5.700g, 10.0mmol, 72%). mp 152-153°C. (ESMS+) 569 (M⁺, 100%). IR(KBr) 1725 (s, C=O), 1266cm⁻¹ (s, C-O-C). ¹H NMR (400MHz, DMSO-*d*₆) δ 8.22 (m (AA'BB'), 12H, Ar-*H*), 4.52 (s, 6H, CH₂), 2.34 (br. s, 2H, NH₂). ¹³C NMR (100MHz, DMSO-*d*₆) δ 164.04 (CO₂R), 150.22 (ArC-NO₂), 134.74 (ArC-CO₂R), 130.82 (ArC-H), 123.65 (ArC-H), 67.31 (CH₂), 54.25 (C_q). Anal. calcd for C₂₅H₂₀N₄O₁₂: C, 52.82; H, 3.55; N, 9.86. Found: C, 52.65; H, 3.49; N, 9.81.



Synthesis of 1,1,1-tris(4-methoxybenzoyloxymethyl)methylamine (38)

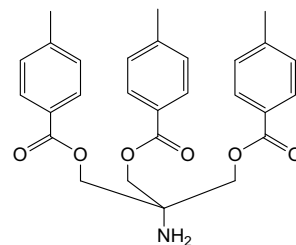
1,1,1-Tris(4-methoxybenzoyloxymethyl)methylamine trifluoroacetic acid salt (4.244g, 6.7mmol) was dissolved in DMF (50ml) and CH₂Cl₂ (250ml). The organic solution was washed with 1M Na₂CO₃ (2 x 150ml) and water (4 x 250ml) then dried (MgSO₄), filtered and evaporated to yield the product (2.803g, 5.4mmol, 80%). mp 93°C. (ESMS+) 524 (M⁺, 90%). IR(KBr) 3389 (m, NH), 2964 (m, ArC), 1705 (s, C=O), 1605 (s, C=O), 1256cm⁻¹ (s, C-O-C). ¹H NMR (400MHz, CDCl₃) δ 7.98 (m (AA'), 6H, Ar-*H*), 6.88 (m (XX'), 6H, Ar-*H*), 4.48 (s, 6H, CH₂), 3.83 (s, 9H, CH₃), 1.79 (br. s, 2H, NH₂). ¹³C NMR (100MHz, CDCl₃) δ 165.94 (CO₂R), 163.79 (ArC-OCH₃), 131.91 (ArC-H), 121.99 (ArC-CO₂R) 113.89 (ArC-H),



66.28 (CH₂), 55.58 (CH₃), 55.18 (C_q). Anal. calcd for C₂₈H₂₉NO₉: C, 64.24; H, 5.58; N, 2.68. Found: C, 64.12; H, 5.61; N, 2.65.

Synthesis of 1,1,1-tris(4-methylbenzoyloxymethyl)methylamine (39)

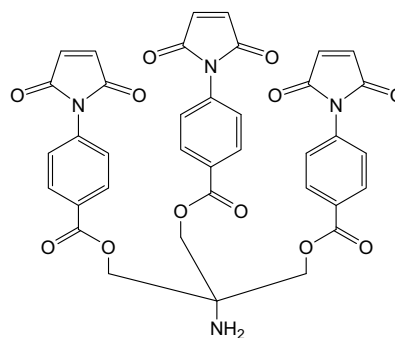
N-(*tert*-butyloxycarbonyl)-1,1,1-tris(4-methylbenzoyloxymethyl)methylamine (5.424g, 9.4mmol) was dissolved in CH₂Cl₂ (50ml) and trifluoroacetic acid (5ml) was added. The solution was refrigerated overnight. This organic solution was washed with 1M Na₂CO₃ (2 x 150ml) and water (2 x 150ml), then dried (MgSO₄), filtered and evaporated to yield the free amine (3.450g, 7.3mmol, 77%). mp 119°C. (ESMS⁺) 476 (M⁺, 100%), 483 (MLi⁺, 35%). IR(KBr) 3387 (m, NH), 2949 (w, ArC), 1727 (s, C=O), 1714 (s, C=O), 1261cm⁻¹ (s, C-O-C). ¹H NMR (400MHz, DMSO-*d*₆) δ 7.86 (m (AA'), 6H, Ar-*H*), 7.26 (m (XX'), 6H, Ar-*H*), 4.39 (s, 6H, CH₂), 2.36 (s, 9H, ArC-CH₃), 2.14 (br. s, 2H, NH₂). ¹³C NMR (100MHz, DMSO-*d*₆) δ 165.47 (CO₂R), 143.67 (ArC-CH₃), 129.33 (ArC-H), 129.18 (ArC-H), 126.66 (ArC-CO₂R), 66.58 (CH₂), 54.26 (C_q-CH₂), 21.14 (ArC-CH₃). Anal. calcd for C₂₈H₂₉NO₆: C, 70.72; H, 6.15; N, 2.95. Found: C, 70.76; H, 6.14; N, 2.98.



Synthesis of 1,1,1-tris(4-maleimidobenzoyloxymethyl)methylamine (40)

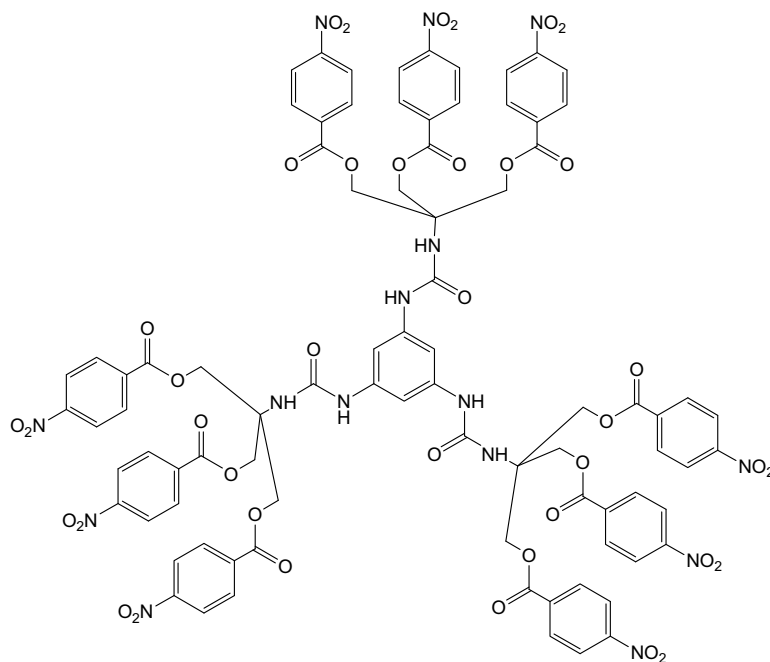
N-(*tert*-butyloxycarbonyl)-1,1,1-tris(4-maleimidobenzoyloxymethyl)methylamine (1.085g, 1.3mmol) was dissolved in CH₂Cl₂ (20ml) and trifluoroacetic acid (1ml) was added. The solution was refrigerated overnight. This organic solution was washed with 1M Na₂CO₃ (2 x 150ml) and water (2 x 150ml), dried (MgSO₄), filtered and evaporated to yield the free amine (0.838g, 1.2mmol, 90%). mp 111°C. (ESMS⁺) 719 (M⁺, 100%), 725 (MLi⁺, 30%). IR(KBr) 3475 (w, NH), 3102 (w,

ArC), 1716 (s, C=O), 1265 cm^{-1} (s, C-O-C). ^1H NMR (400MHz, Acetone- d_6) δ 8.13 (m (AA'), 6H, Ar-H), 7.49 (m (XX'), 6H, Ar-H), 7.06 (s, 6H, HC=CH), 4.63 (s, 6H, CH₂). ^{13}C NMR (100MHz, Acetone- d_6) δ 170.19 (C=ONC=O), 165.99 (CO₂R), 137.30 (ArC-NR), 135.61 (RHC=CHR), 131.02 (ArC-H), 129.59 (ArC-CO₂R), 126.80 (ArC-H), 68.10 (CH₂), 55.65 (C_q-CH₂). Anal. calcd for C₃₇H₂₆N₄O₁₂: C, 61.84; H, 3.65; N, 7.80. Found: C, 61.62; H, 3.74; N, 7.59.



Synthesis of 1,3,5-tris-((1,1,1-tris(4-nitrobenzoyloxymethyl)methylamino)carbonylamino)benzene (41)

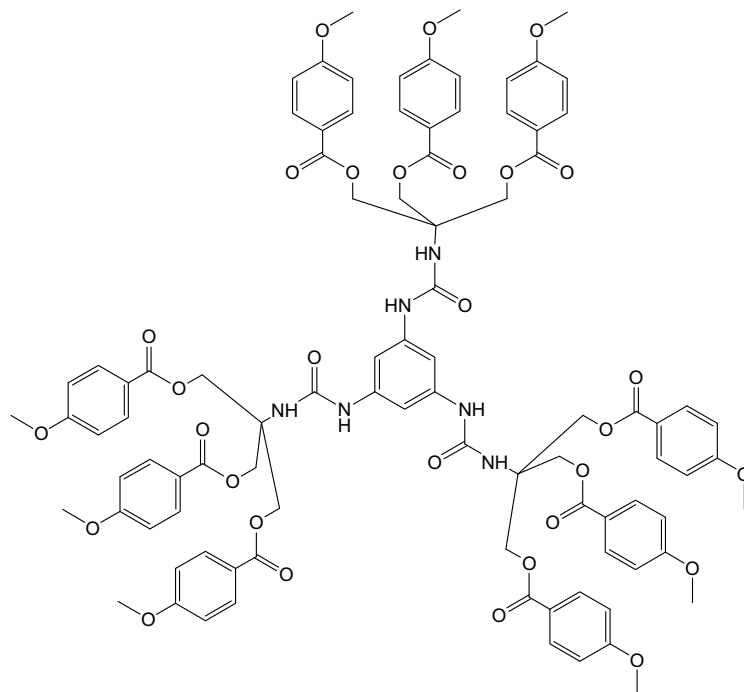
1,3,5-Benzenetricarbonyl triazide (0.088g, 0.3mmol) was dissolved in dry toluene (5ml) and refluxed for one hour under N₂. The reaction was allowed to cool, the toluene was removed on a rotary evaporator and 1,1,1-tris(4-nitrobenzoyloxymethyl)methylamine (0.526g, 0.9mmol) dissolved in CH₂Cl₂ (10ml) was added under an atmosphere of N₂. The reaction mixture was gently refluxed for 16 hours and cooled to room temperature. The resulting precipitate was filtered off to yield a yellow solid (0.527g, 0.27mmol, 92%). mp 143-145°C. (ESMS+) 1929 (MNa⁺). IR(KBr) 3397 (m, NH), 1733 cm^{-1} (s, C=O). ^1H NMR (400MHz, acetone- d_6) 8.23 (m (AA'BB'), 36H, *p*-NO₂-Ar-H), 8.08 (bs, 3H, NH), 7.22 (s, 3H, core-Ar-H), 6.43 (bs, 3H, NH), 5.07 (s, 18H, CH₂). ^{13}C NMR (100MHz, acetone- d_6) δ 165.03 (CO₂R), 155.67 (NHC=ONH), 151.70 (ArC-NO₂), 141.47 (ArC-NHR), 135.96 (ArC-CO₂R), 131.83 (*p*-NO₂-ArC-H), 124.51 (*p*-NO₂-ArC-H), 103.43 (core-ArC-H), 65.73 (CH₂), 58.50 (C_q). Anal. calcd for C₈₄H₆₃N₁₅O₃₉: C, 52.92; H, 3.33; N, 11.02. Found: C, 52.79; H, 3.41; N, 10.84.



Synthesis of 1,3,5-tris-((1,1,1-tris(4-methoxybenzoyloxymethyl)methylamino)carbonylamino)benzene (42)

1,3,5-Benzenetricarbonyl triazide (0.149g, 0.526mmol) was dissolved in dry toluene (7ml) and refluxed for one hour under an atmosphere of N_2 . The reaction was allowed to cool, the toluene removed on a rotary evaporator followed by the addition of 1,1,1-tris(4-methoxybenzoyloxymethyl)methylamine (0.823g, 1.56mmol) dissolved in CH_2Cl_2 (15ml) under an atmosphere of N_2 . The reaction mixture was gently refluxed for 16 hours and cooled to room temperature. The solvent was removed by rotary evaporation to yield a white solid (0.894g, 0.501mmol, 96%). mp 114-115°C. (ESMS⁺) 1778 (MLi^+ , 100%), 1794 (MNa^+ , 100%). IR(KBr) 3384 (m, NH), 2962 (w, ArC), 1717 (s, C=O), 1258 cm^{-1} (s, C-O-C). ¹H NMR (400MHz, Acetone-*d*₆) δ 8.15 (s, 3H, NH), 7.97 (m (AA'), 18H, *p*-CH₃O-Ar-H), 7.30 (s, 3H, core-Ar-H), 6.96 (m (XX'), 18H, *p*-CH₃O-Ar-H), 6.28 (s, 3H, NH), 4.90 (s, 18H, CH₂), 3.86 (s, 27H, CH₃). ¹³C NMR (100MHz, Acetone-*d*₆) δ 166.17 (CO₂R), 164.73 (ArC-OCH₃), 155.61 (NHC=ONH), 141.70 (ArC-NHR), 132.55 (*p*-CH₃O-ArC-H),

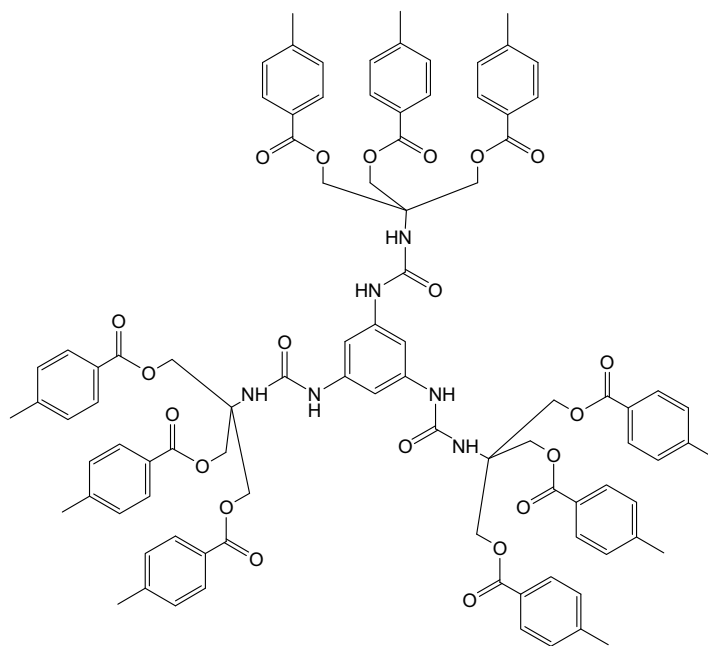
123.02 (ArC-CO₂R), 114.73 (*p*-CH₃O-ArC-H), 102.56 (core-ArC-H), 64.87 (CH₂), 58.57 (Cq), 56.01 (CH₃). Anal. calcd for C₉₃H₉₀N₆O₃₀: C, 63.05; H, 5.12; N, 4.74. Found: C, 63.09; H, 5.29; N, 4.74.



Synthesis of 1,3,5-tris-((1,1,1-tris(4-methylbenzoyloxymethyl)methylamino)carbonylamino)benzene (43)

1,3,5-Benzenetricarbonyl triazide (0.088g, 0.3mmol) was dissolved in dry toluene (5ml) and refluxed for one hour under an atmosphere of N₂. The reaction was allowed to cool and toluene was removed on a rotary evaporator. A solution of 1,1,1-tris(4-methylbenzoyloxymethyl)methylamine (0.428g, 0.9mmol) dissolved in CH₂Cl₂ (10ml) was added under an atmosphere of N₂. The reaction was gently refluxed for 16 hours and cooled to room temperature. The solvent was removed *in vacuo* to yield a white solid (0.473g, 0.29mmol, 97%). mp 111-112°C. (ESMS+) 1634 (MLi⁺, 100%), 1650 (MNa⁺, 100%). IR(KBr) 3392 (m, NH), 1718 (s, C=O), 1268cm⁻¹ (s, C-O-C). ¹H NMR (400MHz, DMSO-*d*₆) δ 8.14 (s, 3H, NH), 7.91 (m (AA'), 18H, *p*-CH₃-Ar-H), 7.28 (s, 3H, core-Ar-H), 7.25 (m (XX'), 18H, *p*-CH₃-Ar-

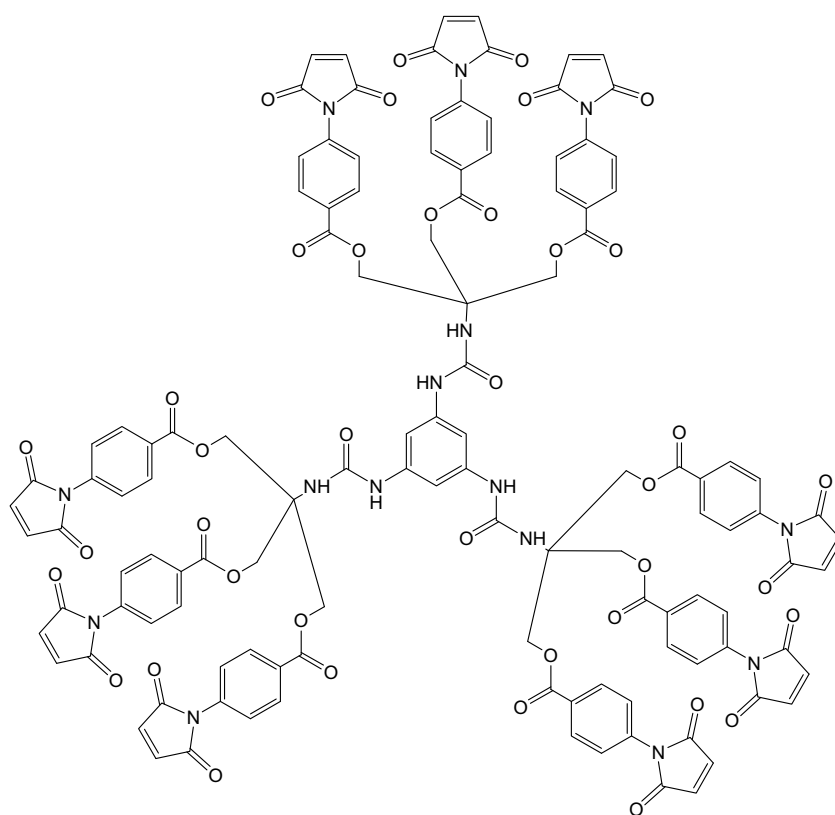
H), 6.30 (s, 3H, *NH*), 4.93 (s, 18H, *CH*₂), 2.37 (s, 27H, *CH*₃). ¹³C NMR (100MHz, DMSO-*d*₆) δ 166.49 (*CO*₂R), 155.58 (*NHC=ONH*), 144.90 (*ArC-CH*₃), 141.64 (*ArC-NHR*), 130.52 (*p-CH*₃-*ArC-H*), 130.10 (*p-CH*₃-*ArC-H*), 128.08 (*ArC-CO*₂R), 102.57 (*core-ArC-H*), 64.94 (*CH*₂), 58.53 (*Cq*), 21.66 (*CH*₃). Anal. calcd for C₉₃H₉₀N₆O₂₁: C, 68.62; H, 5.57; N, 5.16. Found: C, 68.63; H, 5.78; N, 5.02.



Synthesis of 1,3,5-tris-((1,1,1-tris(4-maleimidobenzoyloxymethyl)methylamino)carbonylamino)benzene (44)

1,3,5-Benzenetricarbonyl triazide (0.043g, 0.15mmol) was dissolved in dry toluene (3ml) and refluxed for one hour under an atmosphere of N₂. The reaction was cooled to room temperature and the toluene was removed on a rotary evaporator. A solution of 1,1,1-tris(4-maleimidobenzoyloxymethyl)methylamine (0.323g, 0.45mmol) dissolved in CH₂Cl₂ (10ml) was added under N₂. The reaction was gently refluxed for 18 hours, cooled to room temperature and the solvent was removed *in vacuo* to yield a yellow solid (0.352g, 0.149mmol, 99%). mp 200°C. (ESMS⁺) 2378 (MNa⁺, 100%). IR(KBr) 3387 (m, *NH*), 1716 (s, *C=O*), 1608 (m, *C=C*), 1267cm⁻¹ (s, *C-O-C*). ¹H NMR (400MHz, DMSO-*d*₆) δ 8.80 (br. s, 3H, *NH*), 8.04 (m (AA'), 18H, *Ar*-

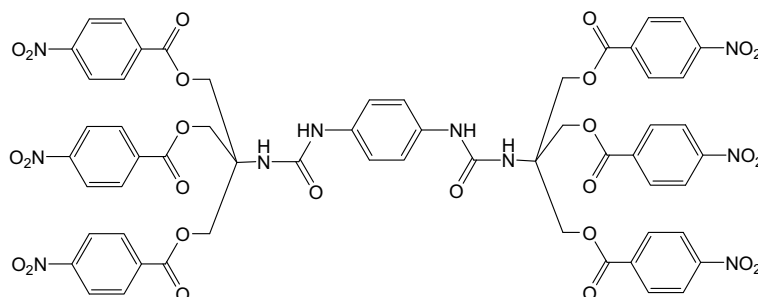
H), 7.44 (m (XX'), 18H, Ar-*H*), 7.22 (s, 3H, core-Ar-*H*), 7.19 (s, 18H, HC=CH), 6.53 (br. s, 3H, NH), 4.87 (s, 18H, CH₂). ¹³C NMR (100MHz, DMSO-*d*₆) δ 169.4 (C=ONC=O), 164.69 (CO₂R), 154.55 (NHC=ONH), 140.43 (core-ArC-NHR), 135.96 (ArC-NR₂), 134.83 (RHC=CHR), 129.93 (*p*-maleimide-ArC-H), 127.85 (ArC-CO₂R), 126.15 (*p*-maleimide-ArC-H), 100.57 (core-ArC-H), 64.20 (CH₂), 56.70 (*Cq*). Anal. calcd for C₁₂₀H₈₁N₁₅O₃₉: C, 61.15; H, 3.46; N, 8.91. Found: C, 60.43; H, 3.71; N, 8.71.



Synthesis of 1,4-di((1,1,1-tris(4-nitrobenzoyloxymethyl)methylamino)carbonylamino)benzene (46)

1,4-phenylene diisocyanate (0.048g, 0.3mmol) and 1,1,1-tris(4-nitrobenzoyloxymethyl)methylamine (0.341g, 0.6mmol) were dissolved in CH₂Cl₂ (10ml) under an atmosphere of N₂. The reaction mixture was gently refluxed for 18 hours and cooled to room temperature. The solvent was removed by rotary evaporation to yield a yellow solid. (0.377g, 0.29mmol, 97%). mp 249-250°C dec. IR(KBr) 3407 (m, NH),

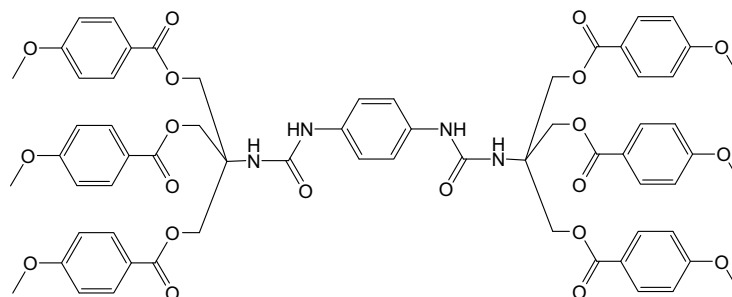
1725 (s, C=O), 1691 (s, C=O), 1527 (s, NO₂), 1400 (m, NO₂), 1267cm⁻¹ (s, C-O-C).
¹H NMR (400MHz, DMSO-*d*₆) δ 8.45 (s, 2H, NH), 8.27 (m(AA'), 12H, *p*-NO₂-ArH), 8.17 (m(BB'), 12H, *p*-NO₂-ArH), 7.21 (s, 4H, core-Ar-H), 6.73 (s, 2H, NH), 4.91 (s, 12H, CH₂). ¹³C NMR (100MHz, DMSO-*d*₆) δ 163.90 (CO₂R), 154.75 (NHC=ONH), 150.30 (ArC-NO₂), 134.56 (ArC-CO₂R), 133.94 (ArC-NHR) 130.78 (*p*-NO₂-ArC-H), 123.75 (*p*-NO₂-ArC-H), 118.76 (core-ArC-H), 64.58 (CH₂), 56.64 (C_q). Anal. calcd for C₅₈H₄₄N₁₀O₂₆: C, 53.71; H, 3.42; N, 10.80. Found: C, 53.64; H, 3.52; N, 10.76.



Synthesis of 1,4-di((1,1,1-tris(4-methoxybenzoyloxymethyl)methylamino)carbonylamino)benzene (47)

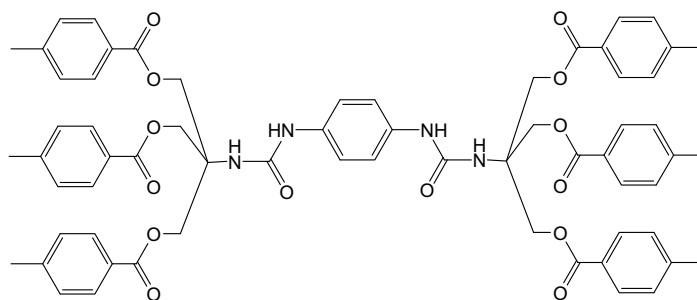
1,4-phenylene diisocyanate (0.048g, 0.3mmol) and 1,1,1-tris(4-methoxybenzoyloxymethyl)methylamine (0.314g, 0.6mmol) were dissolved in THF (10ml) under an atmosphere of N₂. The reaction mixture was gently refluxed for 18 hours and cooled to room temperature. The solvent was removed by rotary evaporation to yield a white solid. (0.360g, 0.29mmol, 99%). mp 197-200°C dec. (ESMS+) 1213 (MLi⁺, 100%), 1229 (MNa⁺, 100%). IR(KBr) 3388 (m, NH), 3367 (M, NH), 1711 (s, C=O), 1675 (s, C=O), 1605 (s, ArC-O-C), 1256cm⁻¹ (s, C-O-C). ¹H NMR (400MHz, DMSO-*d*₆) δ 8.48 (s, 2H, NH), 7.91 (m(AA'), 12H, *p*-CH₃O-ArH), 7.22 (s, 4H, core-Ar-H), 6.98 (m(BB'), 12H, *p*-CH₃O-ArH), 6.60 (s, 2H, NH), 4.75 (s, 12H, CH₂), 3.81 (s, 18H, CH₃). ¹³C NMR (100MHz, DMSO-*d*₆) δ 164.97 (CO₂R), 163.27 (ArC-OCH₃),

154.76 (NHC=ONH), 133.99 (ArC-NHR), 131.41 (*p*-CH₃O-ArC-H), 121.40 (ArC-CO₂R), 118.64 (core-ArC-H), 113.97 (*p*-CH₃O-ArC-H), 63.70 (CH₂), 56.79 (C_q), 55.49 (CH₃). Anal. calcd for C₆₄H₆₂N₄O₂₀: C, 63.68; H, 5.18; N, 4.64. Found: C, 63.88; H, 5.39; N, 4.65.



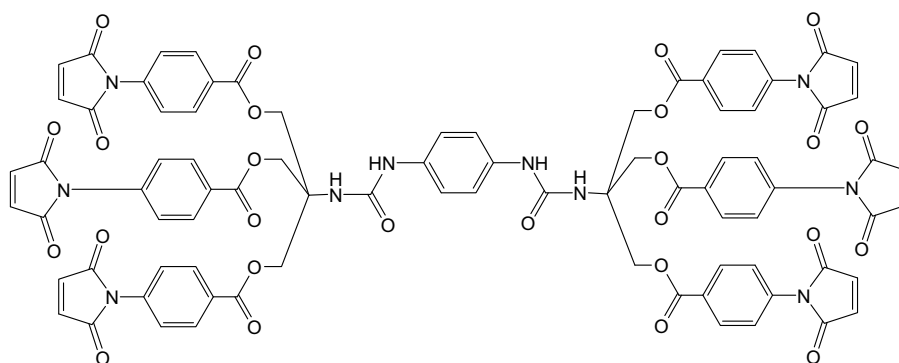
Synthesis of 1,4-di((1,1,1-tris(4-methylbenzoyloxymethyl)methylamino)carbon-ylamino)benzene (48)

1,4-phenylene diisocyanate (0.048g, 0.3mmol) and 1,1,1-tris(4-nitrobenzoyloxymethyl)methylamine (0.285g, 0.6mmol) were dissolved in CH₂Cl₂ (10ml) under an atmosphere of N₂. The reaction mixture was gently refluxed for 18 hours and cooled to room temperature. The solvent was removed by rotary evaporation to yield a yellow solid. (0.328g, 0.29mmol, 98%). mp 224°C dec. (ESMS⁺) 1117 (MLi⁺, 100%), 1133 (MNa⁺, 100%). IR(KBr) 3387 (m, NH), 1727 (s, C=O), 1715 (s, C=O), 1677 (s, NH), 1267cm⁻¹ (s, C-O-C). ¹H NMR (400MHz, DMSO-*d*₆) δ 8.46 (s, 2H, NH), 7.85 (m,(AA'), 12H, *p*-CH₃-ArH), 7.27 (m,(XX'), 12H, *p*-CH₃-ArH), 7.20 (s, 4H, core-Ar-H), 6.61 (s, 2H, NH), 4.77 (s, 12H, CH₂), 2.36 (s, 18H, CH₃). ¹³C NMR (100MHz, DMSO-*d*₆) δ 165.31 (CO₂R), 154.76 (NHC=ONH), 143.85 (ArC-CH₃), 133.97 (ArC-NHR), 129.32 (ArC-CO₂R), 129.23 (*p*-CH₃-ArC-H), 126.49 (*p*-CH₃-ArC-H), 118.64 (core-ArC-H), 63.79 (CH₂), 56.76 (C_q), 21.15 (CH₃). Anal. calcd for C₆₄H₆₂N₄O₁₄: C, 69.18; H, 5.62; N, 5.04. Found: C, 69.05; H, 5.70; N, 5.04.



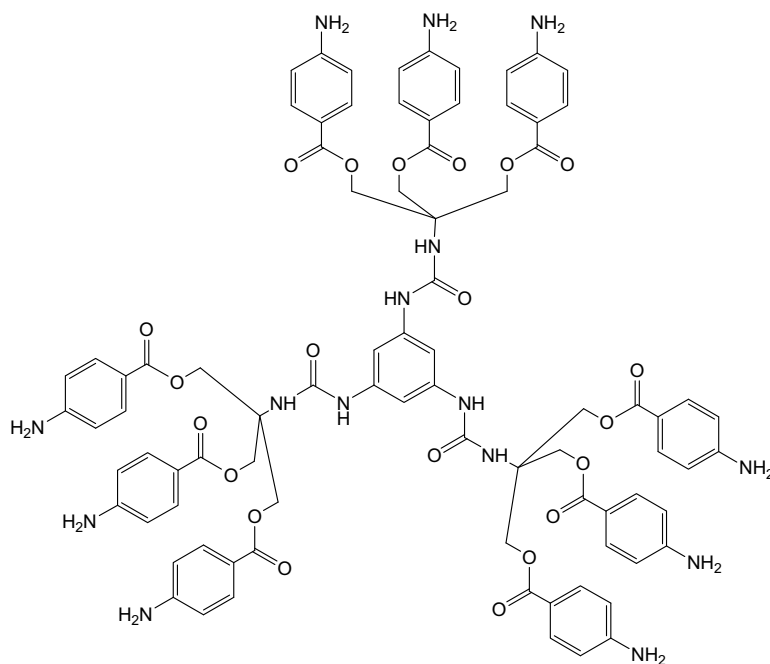
Synthesis of 1,4-di((1,1,1-tris(4-maleimidobenzoyloxymethyl)methylamino)carbonylamino)benzene (49)

1,4-phenylene diisocyanate (0.024g, 0.15mmol) and 1,1,1-tris(4-nitrobenzoyloxymethyl)methylamine (0.215g, 0.3mmol) were dissolved in THF (10ml) under an atmosphere of N₂. The reaction mixture was gently refluxed for 18 hours and cooled to room temperature. The solvent was removed by rotary evaporation to yield a yellow solid. (0.234g, 0.146mmol, 98%). mp 235°C. (ESMS) weak signal by MS. IR(KBr) 3392 (m, NH), 1716 (s, C=O), 1607 (m, NH), 1264cm⁻¹ (s, C-O-C). ¹H NMR (400MHz, DMSO-*d*₆) δ 8.50 (br. s, 2H, NH), 8.05 (m (AA'), 12H, Ar-H), 7.45 (m (XX'), 12H, Ar-H), 7.24 (s, 4H, core-Ar-H), 7.21 (s, 12H, HC=CH), 6.66 (br. s, 2H, NH), 4.87 (s, 12H, CH₂). ¹³C NMR (100MHz, DMSO-*d*₆) δ 169.43 (C=ONC=O), 164.72 (CO₂R), 154.80 (NHC=ONH), 135.97 (ArC-NR₂), 134.86 (RHC=CHR), 133.97 (ArC-NHR), 129.93 (*p*-maleimide-ArC-H), 127.90 (ArC-CO₂R), 126.18 (*p*-maleimide-ArC-H), 118.76 (core-ArC-H), 64.21 (CH₂), 56.75 (C_q). Anal. calcd for C₈₂H₅₆N₁₀O₂₆: C, 61.66; H, 3.53; N, 8.77. Found: C, 61.15; H, 3.70; N, 8.36.



Hydrogenation of 41 to produce 1,3,5-tris-((1,1,1-tris(4-aminobenzoyloxymethyl)methyl-amino)carbonylamino)benzene (50)

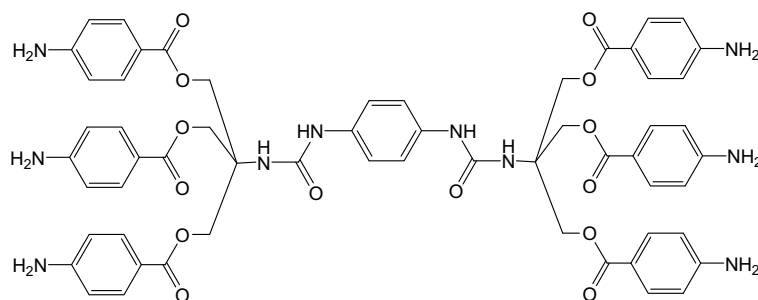
1,3,5-tris-((1,1,1-tris(4-nitrobenzoyloxymethyl)methylamino)carbonylamino)benzene (0.749g, 0.393mmol) was dissolved in dry DMF (6ml) and 0.075g of 5% Pd/C was added. The reaction mixture was pressurised with H₂ gas (700psi) and heated to 55°C for 48 hours. The solution was filtered and evaporated under reduced pressure to give a brown oil that was solidified by sonication in ethyl acetate, collected by filtration and dried under high vacuum to yield 1,3,5-tris-((1,1,1-tris(4-aminobenzoyloxymethyl)methylamino)carbonylamino)benzene (0.569g, 0.353mmol, 90%). mp 258-260°C. HRMS [M+H]¹⁺ Found 1636.5692. C₈₄H₈₁N₁₅O₂₁(+) requires 1636.5804. IR(KBr) 3365 (m, NH), 1699 (s, C=O), 1603 (s, NH), 1269cm⁻¹ (s, C-O-C). ¹H NMR (400MHz, DMSO-*d*₆) δ 8.72 (br. s, 3H, NH), 7.65 (m (AA'), 18H, Ar-H), 7.15 (s, 3H, core-Ar-H), 6.53 (m (XX'), 18H, Ar-H), 6.37 (br. s, 3H, NH), 5.98 (s, 18H, NH₂), 4.60 (s, 18H, CH₂). ¹³C NMR (100MHz, DMSO-*d*₆) δ 165.44 (CO₂R), 154.48 (NHC=ONH), 153.70 (ArC-NH₂), 140.51 (core-ArC-NHR), 131.29 (*p*NH₂-ArC-H), 115.18 (*p*NH₂-ArC-H), 112.62 (core-ArC-H), 62.89 (CH₂), 56.87 (Cq).



Hydrogenation of 46 to produce 1,4-di((1,1,1-tris(4-aminobenzoyloxymethyl)-methylamino)-carbonylamino)benzene (51)

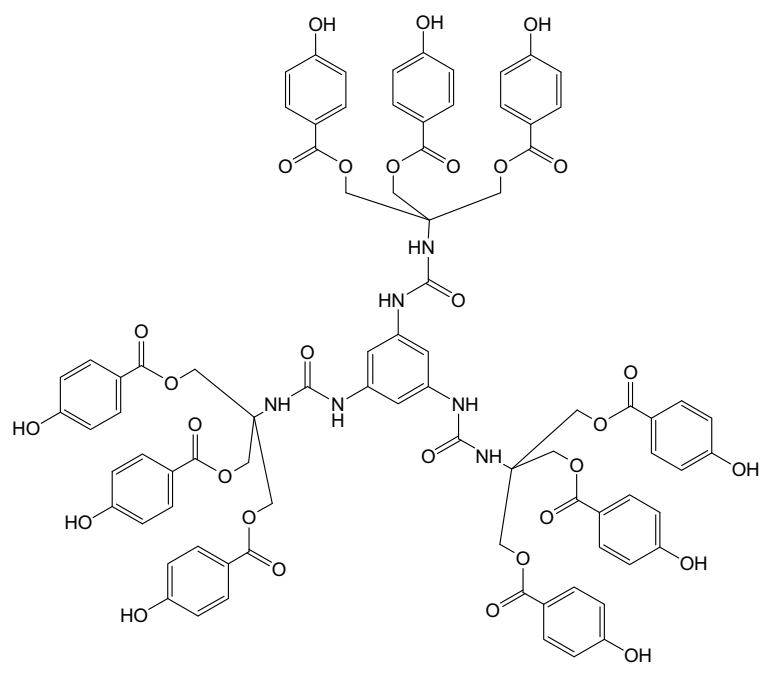
1,4-di((1,1,1-tris(4-nitrobenzoyloxymethyl)methylamino)carbonylamino)benzene (0.050g, 0.039mmol) was suspended in dry DMF (2ml) and 5% Pd/C (0.010g) was added. The reaction was pressurised with H₂ gas (700psi) and heated to 55°C for 24 hours. The solution was filtered and evaporated under reduced pressure. Trituration of the residue with DCM solidified the product that was collected by filtration and dried under high vacuum to yield 1,4-di((1,1,1-tris(4-aminobenzoyloxymethyl)-methylamino)carbonylamino)benzene (0.039g, 0.36mmol, 92%). mp 145°C. HRMS [M+Na]¹⁺ Found 1139.3829. C₅₈H₅₆N₁₀O₁₄(+Na) requires 1139.3870. IR(KBr) 3366 (m, NH), 1700 (s, C=O), 1624 (s, C=O), 1602 (s, NH), 1269cm⁻¹ (s, C-O-C). ¹H NMR (400MHz, DMSO-*d*₆) δ 8.49 (s, 2H, NH), 7.66 (m(AA'), 12H, *p*-NH₂-ArH), 7.20 (s, 4H, core-Ar-H), 6.54 (m(XX'), 12H, *p*-NH₂-ArH), 6.47 (s, 2H, NH), 5.99 (s, 12H, NH₂), 4.61 (s, 12H, CH₂). ¹³C NMR (100MHz, DMSO-*d*₆) δ 165.49 (CO₂R), 154.77 (NHC=ONH), 153.73 (ArC-NH₂), 134.00 (ArC-NHR), 131.31 (*p*-NH₂-ArC-

H), 118.50 (core-ArC-H), 115.25 (ArC-CO₂R), 112.61 (*p*-NH₂-ArC-H), 62.96 (CH₂), 56.95 (Cq).



Ether cleavage of 42 to produce 1,3,5-tris-((1,1,1-tris(4-hydroxybenzoyloxy-methyl)methyl-amino)carbonylamino)benzene (52)

A solution of aluminium bromide (1.011g, 3.8mmol) and dodecanethiol (2ml,) in dry DCM (7ml) was cooled in an ice bath under an atmosphere of N₂. 1,3,5-tris-((1,1,1-tris(4-methoxybenzoyloxymethyl)methylamino)carbonylamino)benzene (0.250g, 0.141mmol) was added as a solid and the reaction warmed to room temperature and stirred for 16 hours. The reaction mixture was poured into water (250ml) and acidified with 1M HCl. The aqueous solution was extracted with DCM (200ml) that was set aside then the aqueous layer was filtered to collect the precipitated white solid (0.202g, 0.123mmol, 87%). mp 168-169°C. HRMS [M-2H]²⁻ Found 821.2094. C₈₄H₇₀N₆O₃₀(-2) requires 821.2073. (ESMS-) 1643 (M⁻, 80%). (ESMS+) 1667 (MNa⁺, 100%). IR(KBr) 3383 (br, OH), 1698 (s, C=O), 1608 (s, NH), 1270cm⁻¹ (s, C-O-C). ¹H NMR (400MHz, DMSO-*d*₆) δ 10.35 (s, 9H, OH), 8.74 (s, 3H, NH), 7.82 (m (AA'), 18H, *p*-OH-Ar-H), 7.17 (s, 3H, core-Ar-H), 6.80 (m (XX'), 18H, *p*-OH-Ar-H), 6.46 (s, 3H, NH), 4.70 (s, 18H, CH₂). ¹³C NMR (100MHz, DMSO-*d*₆) δ 165.15 (CO₂R), 162.20 (ArC-OH), 154.51 (NHC=ONH), 140.50 (core-ArC-NHR), 131.66 (*p*-OH-ArC-H), 119.80 (ArC-CO₂R), 115.35 (*p*-OH-ArC-H), 100.15 (core-ArC-H), 63.51 (CH₂), 56.76 (Cq).



5.3 Chapter Two

Self-Assembled Monolayers on Gold

5.3.1 Preparation of Gold Surfaces

Silicon wafers were purchased from Addison Engineering (100mm prime silicon wafers) and 24 carat gold (99.99%) was used for surface deposition. Silicon surfaces were cut into 1 cm and 0.5 cm squares and rinsed with acetone to remove the protective film prior to metal deposition. Gold substrates were prepared by sputtering a chromium adhesion layer (~5 nm) followed by gold (~45 nm) onto the silicon substrate at 200°C in an Emitech K575X Peltier Cooled Dual Head DC sputterer with substrate heating system.

Sputterer Operation Instructions:

Turn the power on for the sputterer and check that there is sufficient argon in the gas cylinder and that the valve is open. Place cleaned samples on the stage and close the lid. Set the stage temperature on the heating system control panel. Press 'Enter' on the front panel and cycle through the options to 'Twin Head Cycle'. Set the currents for Target B: Chrome foil (Oxidising) at 20mA and for Target A: Gold foil (Noble) at 60mA with a deposition time of 1 minute. (Note: higher currents give a faster rate of deposition) When the parameters are set, return to the main menu and press start to begin the sputtering process. When prompted, select the oxidising cycle (to deposit the chromium layer). When this cycle is complete and the instrument prompts to select a cycle, select the noble cycle. Finally when this cycle is complete and the instrument displays 'preparing for next coating', press the stop button. The turbo pump will spin down and air will gradually be allowed into the system. Wait

until the system returns to the start menu before opening the lid of the chamber and removing the samples.

Cleaning of Gold Substrates

Before use, the gold surfaces were cleaned by immersing in freshly prepared piranha solution (30% H₂O₂ in H₂SO₄) (Caution! Piranha Solution is a very strong oxidant and can spontaneously detonate upon contact with organic material) or a solution of H₂O : NH₄OH : H₂O₂ (5 : 1 : 1) at 75°C. The surface was then washed under running milliQ water for one minute, immersed in a milliQ water bath for 5 minutes and dried under a stream of nitrogen gas immediately prior to use.

SAM Formation on Gold Substrates

Monolayers were prepared by immersing the cleaned gold surfaces in a 1mM solution of an appropriate thiol or disulfide in a sealed vial and left undisturbed for 18-20 hours. The surfaces were then removed from the solution and rinsed with ethanol or THF and dried in a stream of nitrogen gas.

UV Patterning of SAMs

UV ablation of the SAM surface through a Tunnelling Electron Microscope (TEM) grid (100 μm squares) was performed using a LESCO Super Spot MK III UV lamp, in air, at a height of 1.5cm from the substrate surface and subjected to 30 x 1 minute exposures.

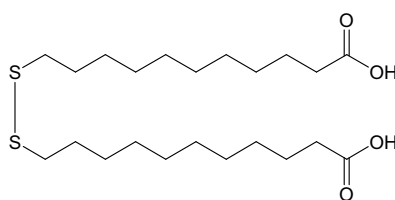
Characterisation of Surfaces

AFM images were acquired using a TopoMetrix TMX 2000 Explorer equipped with a $130 \times 130 \mu\text{m}^2$ tripod air and liquid scanners, with a z-range of $9.7 \mu\text{m}$; and a JEOL JSPM-4200, with 25×25 and $85 \times 85 \mu\text{m}^2$ tube scanners, with a z-range of ca. $3 \mu\text{m}$. The probe consists of a V-shaped cantilever integrated with a pyramidal Si_3N_4 tip on the end. Probes were obtained from Veeco (Digital Instruments). The nominal normal spring constant, k_N , was 0.06 nNm^{-1} . Images were obtained in the contact imaging mode of operation and recorded in topographic and frictional modes. Topometrix software was used for image processing. Contact angles were determined at ambient laboratory temperatures $\sim 25\text{-}30^\circ\text{C}$ using a CCD camera by applying ultra-pure water droplets ($4 \mu\text{l}$) via a Hamilton microsyringe to a freshly prepared monolayer surface. The reported values are the average of six readings on different locations of each surface. XPS measurements were conducted at the Brisbane Surface Analysis Facility at the University of Queensland. IR on surfaces were trialled on a Thermo Nicolet-Nexus FTIR spectrometer using grazing angle and ATR modes. The reflection of the incident beam were carried out at an angle of incidence at 81° and 60° respectively. Typically, 1000 scans at a resolution of 4.0 cm^{-1} were collected. Fluorescence microscopy photographs were acquired on an Olympus BX50 incident light fluorescence microscope fitted with a SPOT camera.

5.3.2 Synthesis of SAM Monomers

Synthesis of 11,11'-dithiobisundecanoic acid (54)

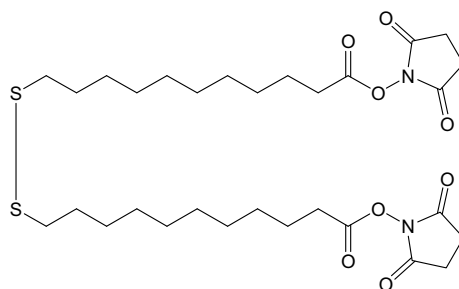
11-mercaptoundecanoic acid (2.001g, 9.0mmol) was dissolved in methanol (250ml) and stirred, in a round bottomed flask exposed to air, with K_2CO_3 (5.010g) for 18 hours. Iced water (250ml) was added followed by the slow addition of concentrated HCl (20ml). The mixture was extracted with ethyl acetate (3 x 200ml), washed with saturated aqueous NaCl (2 x 150ml), dried ($MgSO_4$) and evaporated to give a yellow oil that on cooling formed a white solid. Recrystallisation from hexane gave 11,11'-Dithiobisundecanoic acid (1.425g, 3.3mmol, 72%). mp $79^\circ C$ (Lit.⁹ $92^\circ C$). (ESMS-) 433 (M-, 100%). (ESMS+) 457 (MNa+, 100%). 1H NMR (400MHz, $CDCl_3$) δ 2.70 (t, $^3J = 7.4Hz$, 4H, 2 x S- CH_2), 2.36 (t, $^3J = 7.4Hz$, 4H, 2 x C= OCH_2), 1.72-1.26 (m, 32H, 16 x CH_2). ^{13}C NMR (100MHz, $CDCl_3$) δ 179.96 (2 x CO_2H), 39.55 (2 x S- CH_2), 34.20 (2 x CO_2H-CH_2), 29.50 (2 x CH_2), 29.44 (2 x CH_2), 29.51 (2 x CH_2), 29.34 (2 x CH_2), 29.33 (2 x CH_2), 29.13 (2 x CH_2), 28.64 (2 x CH_2), 24.87 (2 x CH_2).



Synthesis of 1,1'-[dithiobis[(1-oxo-11,1-undecanediyloxy)]bis-2,5-pyrrolidinedione or dithiobis(succinimide undecanoate) (53)

11,11'-dithiobisundecanoic acid (1.842g, 4.2mmol) was dissolved in CH_2Cl_2 (38ml) and DMF (5ml). *N*-hydroxysuccinimide (2.238g, 19.4mmol) was added as a solid and the reaction mixture was stirred under an atmosphere of N_2 at $0^\circ C$. DCC (1.501g, 7.3mmol) dissolved in CH_2Cl_2 (10ml) was added and the reaction stirred at room

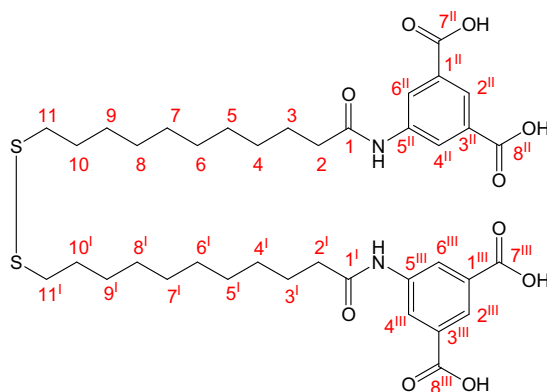
temperature overnight. The precipitated DCU was removed by filtration and the solvent was removed *in vacuo*. The crude product was purified by column chromatography (5:1 CH₂Cl₂/CH₃CN) to yield a white solid (0.755g, 1.2mmol, 30%). mp 107-107.5°C (Lit.¹⁰ 107°C). (ESMS+) 635 (MLi⁺, 70%), 651 (MNa⁺, 100%). ¹H NMR (400MHz, CDCl₃) δ 2.84 (s, 8H, NHS-CH₂), 2.68 (t, 4H, CH₂-S), 2.60 (t, 4H, CH₂-CO₂R), 1.67 (m, 8H, 4 x CH₂), 1.29 (m, 24H, 12 x CH₂). ¹³C NMR (100MHz, CDCl₃) δ 169.43 (NHS-C=O), 168.92 (CO₂R), 39.39 (CH₂-S), 31.15 (CH₂CO₂R), 29.58 (CH₂), 29.47 (CH₂), 29.42 (CH₂), 29.39 (CH₂), 29.25 (CH₂), 28.96 (CH₂), 28.71 (CH₂), 25.81 (NHS-CH₂) 24.77 (CH₂).



Synthesis of 5,5'-[(11,11'-dithiobisundecanoyl)diamino]disiophthalic acid (61)

11,11'-dithiobisundecanoic acid (0.399g, 0.9mmol) was heated gently in SOCl₂ (2ml) under an atmosphere of nitrogen for one hour. The excess thionyl chloride was removed *in vacuo*. The residue was dissolved in NMP (5ml) and added dropwise to a solution of 5-aminoisophthalic acid (0.338g, 1.8mmol) and Et₃N (0.25ml, 1.8mmol) in NMP (5ml) cooled to 0°C. The reaction was stirred at room temperature for 18 hours and poured into water (500ml). The precipitate that formed was collected by filtration then recrystallised from CH₃OH/CHCl₃ to give an ivory solid (0.175g, 0.2mmol, 26%). mp 231-232°C. (ESMS-) 759 (M⁻, 100%). IR(KBr) 3350 (w, N-H), 3172 (w, Aryl C-H), 2925 (m, Alkyl C-H), 1734 (s, C=O), 1700 (s, C=O), 1272 cm⁻¹ (m, C-S). ¹H NMR (400MHz, DMSO-d₆) δ 13.19 (br. s, 4H, 4 x CO₂H), 10.22 (br. s,

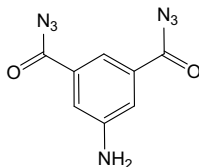
2H, 2 x NH), 8.43 (d, ${}^4J(H_2^{II}-H_4^{II}) (H_2^{III}-H_4^{III})$ and $(H_2^{II}-H_6^{II}) (H_2^{III}-H_6^{III}) = 1.2\text{Hz}$, 4H, H_4^{II} , H_4^{III} , H_6^{II} and H_6^{III}), 8.13 (t, ${}^4J(H_2^{II}-H_4^{II}) (H_2^{III}-H_4^{III})$ and $(H_2^{II}-H_6^{II}) (H_2^{III}-H_6^{III}) = 1.2\text{Hz}$, 2H, H_2^{II} and H_2^{III}), 2.66 (t, ${}^3J = 7.2\text{Hz}$ 4H, 2 x S-CH₂), 2.31 (t, ${}^3J = 7.6\text{Hz}$, 4H, 2 x C=OCH₂), 1.60-1.20 (m, 32H, 16 x CH₂). ¹³C NMR (100MHz, DMSO-*d*₆) δ 171.76 (C₁ and C₁^I), 166.51 (C₇^{II}, C₇^{III}, C₈^{II} and C₈^{III}), 139.88 (C₅^{II} and C₅^{III}), 131.69 (C₁^{II}, C₁^{III}, C₃^{II} and C₃^{III}), 124.31 (C₂^{II} and C₂^{III}), 123.39 (C₄^{II}, C₄^{III}, C₆^{II} and C₆^{III}), 37.86 (C₁₁ and C₁₁^I), 36.40 (C₂ and C₂^I), 28.84 (2 x CH₂), 28.81 (2 x CH₂), 28.73 (2 x CH₂), 28.58 (2 x CH₂), 28.52 (2 x CH₂), 28.49 (2 x CH₂), 27.69 (2 x CH₂), 24.95 (2 x CH₂). Anal. calcd for C₃₈H₅₂N₂O₁₀S₂: C, 59.98; H, 6.89; N, 3.68. Found: C, 59.92; H, 7.03; N, 3.39.



Synthesis of 5-amino-1,3-benzenedicarbonyl diazide (**62**)

Diphenylphosphonyl azide (DPPA) (2.2ml, 2.8g) and TEA (1g) were added to a solution of 5-aminoisophthalic acid (0.999g, 5.5mmol) in NMP (25 ml) under an atmosphere of N₂. The solution was stirred at room temperature for 12 h and poured into a 5% aqueous NaHCO₃ solution. The crude product was purified by dissolving in NMP and re-precipitating with a 5% aqueous NaHCO₃ solution to give **62** as a light yellow powder. The compound was dried in vacuo (1.279g, 99%) and stored in the freezer. IR(KBr) 3473 (m, NH₂), 3382 (m, NH₂), 2144 (s, CON₃), 1685 cm⁻¹ (s,

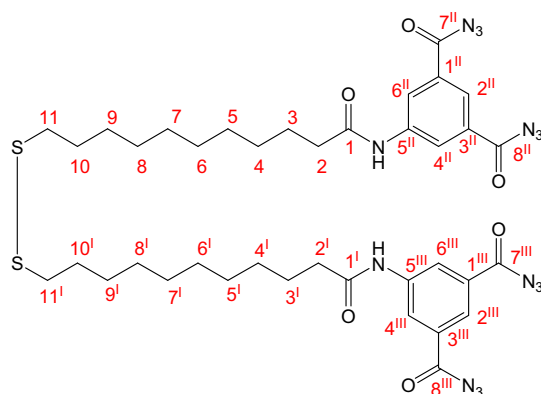
C=O). ^1H NMR (400MHz, CDCl_3) δ 7.62 (t, $^4\text{J}=1.6$ Hz, ArC-H), 7.45 (d, $^4\text{J}=1.6$ Hz, 2 x ArC-H), 5.95 (NH_2). ^{13}C NMR (100MHz, CDCl_3) δ 171.57 (C=O), 150.10 (ArC-NH₂), 131.41 (ArC-CON₃), 118.64 (2 x ArC-H), 116.06 (ArC-H).



Synthesis of acyl azide surface monomer (5,5'-[(11,11'-dithiobisundecanoyl)diamino]disiophthalic-acyl azide) (59)

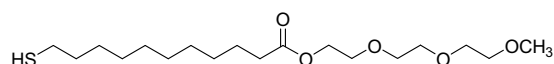
11,11'-dithiobisundecanoic acid (0.499g, 1.15mmol) was heated gently in SOCl_2 (2ml) under an atmosphere of nitrogen for one hour. The excess thionyl chloride was removed *in vacuo*. The residue was dissolved in THF (5ml) and added dropwise to a solution of 5-amino-1,3-benzenedicarbonyl diazide (0.542g, 2.34mmol) and Et_3N (0.5ml, 3.6mmol) in THF (10ml). The reaction was stirred at room temperature for 48 hours then the precipitated triethylamine hydrochloride was removed by filtration. The filtrate was evaporated and the residue purified by column chromatography (4% ethyl acetate/ CH_2Cl_2) to give a yellow oil (0.280g, 0.33mmol, 28%). IR(KBr) 3390 (m, N-H), 3175 (w, Aryl C-H), 2917 (m, Alkyl C-H), 2144 (s, CON₃), 1684 (s, C=O), 1653 (s, C=O), 1193 cm^{-1} (m, C-S). ^1H NMR (400MHz, CDCl_3) δ 8.43 (d, $^4\text{J}(\text{H}_2^{\text{II}}-\text{H}_4^{\text{II}})$ ($\text{H}_2^{\text{III}}-\text{H}_4^{\text{III}}$) and $(\text{H}_2^{\text{II}}-\text{H}_6^{\text{II}})$ ($\text{H}_2^{\text{III}}-\text{H}_6^{\text{III}}$) = 1.6Hz, 4H, H_4^{II} , H_4^{III} , H_6^{II} and H_6^{III}), 8.30 (t, $^4\text{J}(\text{H}_2^{\text{II}}-\text{H}_4^{\text{II}})$ ($\text{H}_2^{\text{III}}-\text{H}_4^{\text{III}}$) and $(\text{H}_2^{\text{II}}-\text{H}_6^{\text{II}})$ ($\text{H}_2^{\text{III}}-\text{H}_6^{\text{III}}$) = 1.6Hz, 2H, H_2^{II} and H_2^{III}), 8.28 (br. s, 2H, NH), 2.67 (t, $^3\text{J} = 7.2\text{Hz}$, 4H, 2 x $\text{CH}_2\text{-S}$), 2.44 (t, $^3\text{J} = 7.6\text{Hz}$, 4H, 2 x $\text{CH}_2\text{-CO}_2\text{R}$), 1.74 (m, 4H, 2 x CH_2), 1.65 (m, 4H, 2 x CH_2), 1.42-1.34 (m, 24H, 12 x CH_2). ^{13}C NMR (100MHz, CDCl_3) δ 172.33 (C_1 and C_1^{I}), 171.45 (C_7^{II} , C_7^{III} , C_8^{II} and C_8^{III}), 139.45 (C_5^{II} and C_5^{III}), 132.20 (C_1^{II} , C_1^{III} , C_3^{II} and C_3^{III}), 125.64 (C_2^{II} , C_2^{III} , C_4^{II} , C_4^{III} , C_6^{II} and C_6^{III}), 39.46 (C_{11} and C_{11}^{I}), 37.78 (C_2 and C_2^{I}), 29.61 (2

x CH₂), 29.58 (2 x CH₂), 29.55 (2 x CH₂), 29.43 (2 x CH₂), 29.35 (4 x CH₂), 28.60 (2 x CH₂), 25.58 (2 x CH₂).



Synthesis of protein resistant ester (58)

11-mercaptoundecanoic acid (0.501g, 2.3mmol) was heated gently with SOCl₂ (1mL) under a calcium chloride drying tube for one hour. The excess SOCl₂ was removed and the crude acid chloride was dried under high vacuum. Triethylene glycol monomethyl ether (0.38mL, 2.4mmol) was dissolved in DCM (2mL) with the addition of Et₃N (0.7mL). To this the acid chloride dissolved in DCM (22mL) was added slowly under an atmosphere of nitrogen. After stirring the reaction was washed, dried, filtered and evaporated to yield the crude product that was purified by column chromatography (60% ether/hexane) to yield a pale yellow oil. (0.619g, 1.7mmol, 72%). (ESMS⁺) 387 (MNa⁺, 100%), 371 (MLi⁺, 100%). ¹H NMR (400MHz, DMSO-d₆) δ 4.22 (t, 2H, CH₂), 3.65 (t, 2H, CH₂), 3.64 (s, 8H, 4 x CH₂), 3.39 (s, 2H, O-CH₃), 2.69 (t, 2H, CH₂), 2.32 (t, 2H, CH₂), 1.99 (m, 2H, CH₂), 1.68 (m, 3H, -SH and CH₂), 1.27 (m, 12H, 6 x CH₂). ¹³C NMR (100MHz, DMSO-d₆) δ 174.03 (CO₂R), 72.14 (O-CH₂), 70.82 (O-CH₂), 70.77 (2 x O-CH₂), 69.41 (O-CH₂), 63.57 (O-CH₂), 59.25 (O-CH₃), 39.35 (CH₂), 34.40 (CH₂), 29.64 (CH₂), 29.58 (CH₂), 29.44 (2 x CH₂), 29.41 (CH₂), 29.32 (CH₂), 28.71 (CH₂), 25.09 (CH₂).



5.4 Chapter Three

Synthesis of Linkers for Bioconjugation

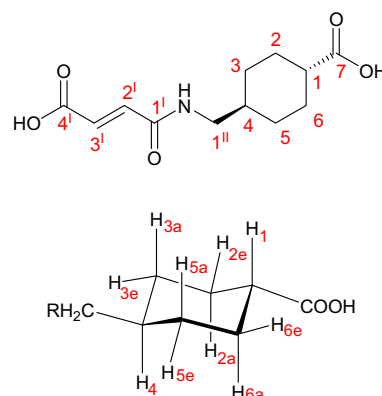
Formation of cis/trans isomers of 4-({[(2E)-3-carboxyprop-2-enoyl]amino}-methyl)cyclohexanecarboxylic acid

trans-4-(Aminomethyl)cyclohexanecarboxylic acid (3.920g, 0.025mol) and maleic anhydride (2.501g, 0.025mol) were stirred in dyglyme (30ml) for one hour at room temperature then heated to 100°C for 2 hours with stirring. The reaction mixture was cooled and filtered. Analysis of the solid product by ¹H NMR (200MHz, DMSO-*d*₆) showed a 1:1.4 ratio of the *trans* and *cis* isomers of 4-({[3-carboxyprop-2-enoyl]amino}methyl)cyclohexanecarboxylic acid by comparison of the integrations of the alkene protons.

Attempted preparation of *trans*-4-[(2,5-dioxo-2,5-dihydro-1H-pyrrol-1-yl)methyl]cyclohexanecarboxylic acid

The crude product mixture from the above reaction (1.670g) was mixed with sodium acetate (0.156g) in acetic anhydride (5ml) and warmed to 50°C for two hours under N₂. The reaction mixture was poured into water (350ml) then heated between 65-70°C with stirring for a further 2 hours. Activated charcoal was added and the mixture was filtered while hot. The filtrate was concentrated to half the volume and a pale orange solid precipitated. The solid was collected by filtration and subsequent analysis found to material to be *trans*-4-({[(2E)-3-carboxyprop-2-enoyl]amino}-methyl)cyclohexanecarboxylic acid **82**. (1.440g) mp 251°C. (ESMS-) 254 (M⁻, 100%). (ESMS+) 256 (M⁺, 100%), 278 (MNa⁺, 20%), 262 (MLi⁺, 30%). IR(KBr) 989 cm⁻¹ (s, *trans* C=C). ¹H NMR (400MHz, DMSO-*d*₆) δ 12.40 (br. s, 2H, 2 x

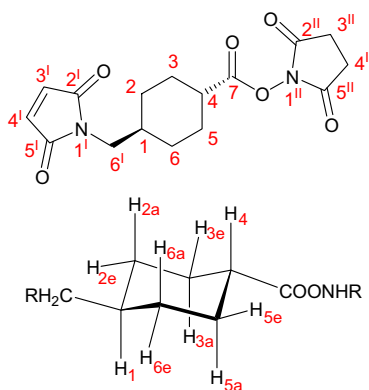
CO₂H), 8.44 (br. t, 1H, NH), 6.95 (d, 1H, ³J(H₂^I-H₃^I) = 15.6Hz, H₃^I), 6.50 (d, 1H, ³J(H₃^I-H₂^I) = 15.6Hz, H₂^I), 3.01 (dd, 2H, ³J(H₁^{II}-H₄) = 6Hz, H₁^{II}), 2.11 (tt, 1H, ³J(H₁-H_{2a}) and (H₁-H_{6a}) = 12Hz, ³J(H₁-H_{2e}) and (H₁-H_{6e}) = 3.2Hz, H₁), 1.88 (m, 2H, H_{2e} and H_{6e}), 1.72 (m, 2H, H_{3e} and H_{5e}), 1.38 (m, 1H, H₄), 1.25 (dddd, 2H, ²J(H_{2a}-H_{2e}) and (H_{6a}-H_{6e}) = 16Hz, ³J(H_{2a}-H_{3a}) and (H_{6a}-H_{5a}) = 13Hz, ³J(H_{2a}-H₁) and (H_{6a}-H₁) = 12Hz, ³J(H_{2a}-H_{3e}) and (H_{6a}-H_{5e}) = 3.2Hz, H_{2a} and H_{6a}), 0.92 (dddd, 2H, ²J(H_{3a}-H_{3e}) and (H_{5a}-H_{5e}) = 16Hz, ³J(H_{3a}-H_{2a}) and (H_{5a}-H_{6a}) = 13Hz, ³J(H_{3a}-H₄) and (H_{5a}-H₄) = 12Hz, ³J(H_{3a}-H_{2e}) and (H_{5a}-H_{6e}) = 3.4Hz, H_{3a} and H_{5a}). ¹³C NMR (100MHz, DMSO-*d*₆) δ 176.71 (C₇), 166.53 (C₄^I), 163.09 (C₁^I), 137.16 (C₂^I), 129.42 (C₃^I), 44.91 (C₁^{II}), 42.43 (C₁), 36.89 (C₄), 29.41 (C₃ and C₅), 28.24 (C₂ and C₆).



Synthesis of *trans*-4-({[(*Z*)-3-carboxyprop-2-enyl]amino}methyl)cyclohexanecarboxylic acid (79)

A solution of maleic anhydride (5.328g, 54.3mmol) in glacial acetic acid (25ml) was added slowly to a stirred solution of *trans*-4-(aminomethyl)cyclohexanecarboxylic acid (8.020g, 51mmol) in acetic acid (55ml) at room temperature. After stirring for three hours, the resulting white precipitate was collected by filtration. The product was washed with cold methanol then dried to yield a white powder (10.327g, 40.5mmol, 79%). Crystallisation from acetone/methanol yielded crystals with a mp of 190-192°C (Lit.¹¹ 188-190°C). (ESMS-) 254 (M⁻, 100%). (ESMS+) 256 (M⁺, 100%), 278 (MNa⁺, 82%), 262 (MLi⁺, 100%). IR(KBr) 849 cm⁻¹ (s, cis C=C). ¹H NMR (400MHz, DMSO-*d*₆) δ 12.5 (br. s, 2H, 2 x CO₂H), 9.09 (br. t, 1H, NH), 6.43

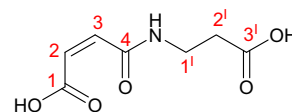
yl)methyl]-1*H*-pyrrole-2,5-dione (4.03g, 12mmol, 41%). This was crystallised from acetone/methanol. mp 171-174°C (Lit.¹¹ 164-180°C). (ESMS+) 357 (MNa⁺, 50%), 341 (MLi⁺, 30%). ¹H NMR (400MHz, DMSO-*d*₆) δ 7.01 (s, 2H, H₃^I and H₄^I), 3.26 (d, 2H, ³J(H₆^I-H₁) = 6.8Hz, H₆^I), 2.80 (s, 4H, H₃^{II} and H₄^{II}), 2.68 (tt, ³J(H₄-H_{3a}) and (H₄-H_{5a}) = 12Hz, ³J(H₄-H_{3e}) and (H₄-H_{5e}) = 3.6Hz, 1H, H₄), 1.99 (m, 2H, H_{3e} and H_{5e}), 1.67 (m, 2H, H_{2e} and H_{6e}), 1.59 (m, 1H, H₁), 1.38 (dddd, ²J(H_{3a}-H_{3e}) and (H_{5a}-H_{5e}) = 16.5Hz, ³J(H_{3a}-H₄) and (H_{5a}-H₄) = 13Hz, ³J(H_{3a}-H_{2a}) and (H_{5a}-H_{6a}) = 13Hz, ³J(H_{3a}-H_{2e}) and (H_{5a}-H_{6e}) = 3.6Hz, 2H, H_{3a} and H_{5a}), 1.04 (dddd, ²J(H_{2a}-H_{2e}) and H_{6a}-H_{6e}) = 16.5Hz, ³J(H_{2a}-H₁) and (H_{6a}-H₁) = 12Hz, ³J(H_{2a}-H_{3a}) and (H_{6a}-H_{5a}) = 13Hz, ³J(H_{2a}-H_{3e}) and (H_{6a}-H_{5e}) = 3.5Hz, 2H, H_{2a} and H_{6a}). ¹³C NMR (100MHz, DMSO-*d*₆) δ 171.24 (C₂^I and C₅^I), 170.85 (C₇), 170.19 (C₂^{II} and C₅^{II}), 134.37 (C₃^I and C₄^I), 42.73 (C₆^I), 39.39 (C₄), 35.65 (C₁), 28.55 (C₂ and C₆), 27.78 (C₃ and C₅), 25.41 (C₃^{II} and C₄^{II}).



Synthesis of (2*Z*)-4-[(2-carboxyethyl)amino]-4-oxobut-2-enoic acid (84)

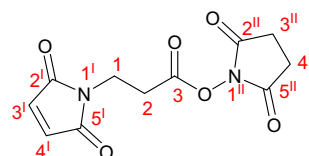
A solution of maleic anhydride (4.907g, 50mmol) in glacial acetic acid (20ml) was added slowly to a stirred solution of 3-aminopropionic acid (4.463g, 50mmol) in acetic acid (55ml) at room temperature. After stirring for three hours, the resulting white precipitate was collected by filtration. The product was washed with cold methanol then dried to yield a white powder (8.796g, 47mmol, 94%). Crystallisation from acetone/methanol yielded crystals with a mp of 158°C (Lit.¹² 159-160°C). (ESMS-) 186 (M⁻, 100%). (ESMS+) 188 (M⁺, 25%), 210 (MNa⁺, 100%), 194 (MLi⁺, 100%). ¹H NMR (400MHz, DMSO-*d*₆) δ 13.49 (br. s, 2H, 2 x CO₂H), 9.09 (t, 1H,

$^3J(\text{NH}-\text{H}_1^{\text{I}}) = 5.6\text{Hz}$, NH 6.39 (d, 1H, $^3J(\text{H}_2-\text{H}_3) = 12.6\text{Hz}$, H_2), 6.23 (d, 1H, $^3J(\text{H}_3-\text{H}_2) = 12.6\text{Hz}$, H_3), 3.36 (dt, 2H, $^3J(\text{H}_1^{\text{I}}-\text{NH}) = 5.6\text{Hz}$, $^3J(\text{H}_1^{\text{I}}-\text{H}_2^{\text{I}}) = 6.8\text{Hz}$, H_1^{I}), 2.47 (t, 2H, $^3J(\text{H}_2^{\text{I}}-\text{H}_1^{\text{I}}) = 6.8\text{Hz}$, H_2^{I}). ^{13}C NMR (100MHz, DMSO- d_6) δ 172.65 (CO_2H , C_3^{I}), 165.62, 165.43 (C_1 and C_4), 132.74 (C_2), 131.47 (C_3), 35.34 (C_1^{I}), 33.03 (C_2^{I}).



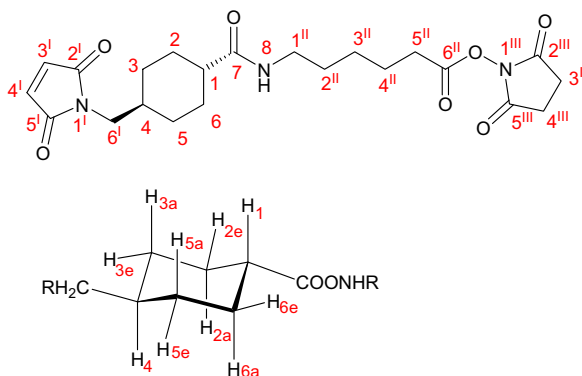
Synthesis of 1-{3-[(2,5-dioxopyrrolidin-1-yl)oxy]-3-oxopropyl}-1H-pyrrole-2,5-dione (71)

N-(2-carboxyethyl)maleamic acid (4.671g, 25mmol) and *N*-hydroxysuccinimide (3.456g, 30mmol) were dissolved in dry DMF (50ml) and cooled to 0°C. DCC (10.766g, 52mmol) was added to the stirred solution, stirred for a further hour at 0°C then warmed to room temperature. After 3 days the precipitated DCU was removed by filtration, water (200ml) was added to the filtrate and the solution was extracted with CHCl_3 (4 x 200ml). The combined organics were dried (MgSO_4), filtered and evaporated under reduced pressure to yield an off-white solid. This solid was redissolved in CH_2Cl_2 and precipitated by addition of hexane. The resulting white solid was collected by filtration (2.462g, 9.25mmol, 37%). Crystallisation from acetone/methanol afforded crystals with a mp of 165-6°C (Lit.¹³ 164-5°C). (ESMS+) 273 (MLi^+ , 100%), 289 (MNa^+ , 20%). ^1H NMR (400MHz, $\text{CDCl}_3/\text{DMSO}-d_6$) δ 6.69 (s, 2H, H_3^{I} and H_4^{I}), 3.87 (t, 2H, $^3J(\text{H}_1-\text{H}_2) = 7.0\text{Hz}$, H_1), 2.96 (t, 2H, $^3J(\text{H}_2-\text{H}_1) = 7.0\text{Hz}$, H_2), 2.77 (br. s, 4H, H_3^{II} and H_4^{II}). ^{13}C NMR (100.593MHz, $\text{CDCl}_3/\text{DMSO}-d_6$) δ 170.16 (C_2^{I} and C_5^{I}), 168.90 (C_2^{II} and C_5^{II}), 166.08 (C_3), 134.38 (C_3^{I} and C_5^{I}), 33.00 (C_1), 29.75 (C_2), 25.60 (C_3^{II} and C_4^{II}).



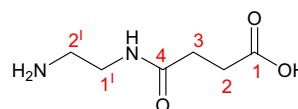
Synthesis of 4-[(2,5-dihydro-2,5-dioxo-1H-pyrrol-1-yl)methyl]-N-[6-[(2,5-dioxo-1-pyrrolidinyl)oxy]-6-oxohexyl]cyclohexanecarboxamide (75)

A 1ml dry DMF solution of 6-aminohexanoic acid (0.837g, 6.4mmol) was added to a stirred dry solution of 1-[(*trans*-4-[(2,5-dioxopyrrolidin-1-yl)oxy]carbonyl]-cyclohexyl)-methyl]-1*H*-pyrrole-2,5-dione (1.11g, 3.33mmol) in DMF (1ml) and stirred under an atmosphere of N₂ for 12 hours. A 1M solution of DCC in CH₂Cl₂ (3.33ml) was added *via* syringe followed by the addition of a dry solution of *N*-hydroxysuccinimide (0.383g, 3.33mmol) in DMF (1ml). The reaction mixture was stirred under N₂ for a further 48 hours. The precipitated DCU was removed by filtration and the solvent removed by evaporation to give a sticky solid. This was purified by column chromatography (5% methanol/CHCl₃) to give a white solid. (0.730g, 1.63mmol, 49%). mp 160°C (Lit.¹⁴ 147-149°C). (ESMS+) 448 (M⁺, 85%), 454 (MLi⁺, 100%), 470 (MNa⁺, 98%). ¹H NMR (400MHz, CDCl₃) δ 6.69 (s, 2H, H₃^I and H₄^I), 5.70 (br. t, ³J(NH-H₁^{II}) = 5.6Hz, 1H, NH), 3.35 (d, ³J(H₆^I-H₄^I) = 6.8Hz, 2H, H₆^I), 3.23 (dt, ³J(NH-H₁^{II}) = 5.6Hz, ³J(H₁^{II}-H₂^{II}) = 6.4Hz, 2H, H₁^{II}), 2.85 (s, 4H, H₃^{III} and H₄^{III}), 2.60 (t, ³J(H₅^{II}-H₄^{II}) = 7.2Hz, 2H, H₅^{II}), 2.01 (tt, ³J(H₁-H_{2a}) and (H₁-H_{6a}) = 12Hz, ³J(H₁-H_{2e}) and (H₁-H_{6e}) = 3.6Hz, 1H, H₁), 1.9-0.9 (m, 15H, H₂, H₃, H₄, H₅, H₆, H₂^{II}, H₃^{II}, H₄^{II}). ¹³C NMR (100.593MHz, CDCl₃) δ 175.84 (C₇), 171.21 (C₂^I and C₅^I), 169.42 (C₂^{III} and C₅^{III}), 168.68 (C₆^{II}), 134.17 (C₃^I and C₄^I), 45.40 (C₁), 43.87 (C₆^I), 38.96 (C₁^{II}), 36.52 (C₄), 31.03 (C₅^{II}), 30.07 (C₂ and C₆), 29.01 (C₃ and C₅), 25.79 (C₃^{III} and C₄^{III}), 29.03, 25.87, 24.37(C₂^{II}, C₃^{II} and C₄^{II}).



Synthesis of 4-[(2-aminoethyl)amino]-4-oxobutanoic acid (88)

1,2-Ethylene diamine (5.409g, 6ml, 90mmol) was dissolved in ethanol (15ml) and added dropwise to a stirred solution of succinic anhydride (9.030g, 90mmol) in ethanol (40ml). The reaction mixture was stirred for a further 45 minutes, allowed to cool then the formed precipitate was collected by filtration, triturated with CHCl_3 five times then dried under vacuum to yield a white solid (13.146g, 82mmol, 91%). mp 160-162°C (Lit.¹⁵ 159-162°C). (ESMS+) 161 (M^+ , 10%), 167 (MLi^+ , 40%), 183 (MNa^+ , 30%). ^1H NMR (400MHz, $\text{D}_2\text{O}/\text{DSS}$) δ 3.21, 3.15 (2 x s, 4H, H_1^I and H_2^I), 2.31 (s, 4H, H_2 and H_3). ^{13}C NMR (100MHz, $\text{D}_2\text{O}/\text{DSS}$) δ 183.45, 178.76 (C_1 and C_4), 41.33, 39.25 (C_1^I and C_2^I), 35.36, 34.88 (C_2 and C_3).

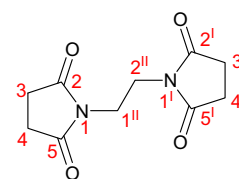


Attempt to extend SMCC with 4-[(2-aminoethyl)amino]-4-oxobutanoic acid

To a solution of 1-[(trans-4-[(2,5-dioxopyrrolidin-1-yl)oxy]carbonyl)cyclohexyl-methyl]-1H-pyrrole-2,5-dione (0.668g, 2mmol) in DMF (0.4ml) was added a suspension of 4-[(2-aminoethyl)amino]-4-oxobutanoic acid (0.320g, 2mmol) in DMF (0.4ml) and the reaction stirred for 12 hours at room temperature under an atmosphere of N_2 . Then a solution of DCC (0.433g, 2.1mmol) in DMF (0.2ml) was added followed by the solid addition of N-hydroxysuccinimide (0.230g, 2mmol). The reaction was allowed to stir for a further 18 hours. The precipitated DCU was removed by filtration and the filtrate was evaporated to give a white solid. Purification by column chromatography (5% methanol/ CHCl_3) isolated:

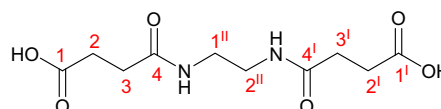
i. Rf (0.73) isolated unreacted 1-[(trans-4-[(2,5-dioxopyrrolidin-1-yl)oxy]carbonyl}cyclohexyl)-methyl]-1H-pyrrole-2,5-dione (0.495g). Spectroscopic data was identical to that obtained previously.

ii. Rf (0.65) a clear crystalline solid, 1,1'-ethane-1,2-diylpyrrolidine-2,5-dione **89** (0.027g). mp 252-253°C. (Lit.¹⁶ 249-250°C). (ESMS+) 225 (M⁺, 80%), 231 (MLi⁺, 100%). 247 (MNa⁺, 100%). ¹H NMR (400MHz, CDCl₃) δ 3.73 (s, 4H, H₁^{II} and H₂^{II}), 2.66 (s, 8H, H₃, H₃^I, H₄ and H₄^I). ¹³C NMR (100MHz, CDCl₃) δ 177.89 (C₂, C₂^I, C₅ and C₅^I), 37.30 (C₁^{II} and C₂^{II}), 28.34 (C₃, C₃^I, C₄, C₄^I).



Synthesis of 4,4'-(ethane-1,2-diylidimino)bis(4-oxobutanoic acid) (**90**)

1,2-Ethylenediamine (2.7g, 45mmol, 3ml) was added to a solution of succinic anhydride (9.063g, 90mmol) in ethanol (40ml). The solution was stirred at room temperature for 12 hours, the formed precipitate collected by filtration and dried (11.414g, 44mmol, 97%). mp 158-159°C. (Lit.¹⁷ 159-161°C). (ESMS-) 259 (M⁻, 100%). (ESMS+) 267 (MLi⁺, 100%), 283 (MNa⁺, 100%). ¹H NMR (400MHz, DMSO-*d*₆) δ 12.05 (br. s, 2H, 2 x CO₂H), 7.83 (br. s, 2H, 2 x NH), 3.06 (m, 4H, H₁^{II} and H₂^{II}), 2.41-2.29 (m, 8H, H₂, H₂^I, H₃ and H₃^I). ¹³C NMR (100MHz, DMSO-*d*₆) δ 173.85 (C₁ and C₁^I), 171.11 (C₄ and C₄^I), 38.327 (C₁^{II} and C₂^{II}), 30.05, 29.15 (C₂, C₂^I, C₃ and C₃^I).



Synthesis of 1,1'-ethane-1,2-diylpyrrolidine-2,5-dione (89)

A solution of 4,4'-(ethane-1,2-diyl-diimino)bis(4-oxobutanoic acid) (1.532g, 5.9mmol) with sodium acetate (0.100g) in acetic anhydride (10ml) was heated to 50°C for two hours. The solvent was removed *in vacuo* and the product was extracted from the residue with ethyl acetate (0.768g, 3.4mmol, 58%). The isolated product was analysed and the physical and spectroscopic data collected was identical to that obtained previously.

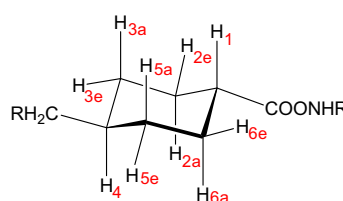
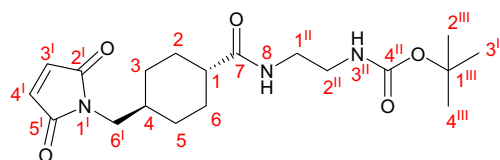
Synthesis of N-[tert-butyl[2-aminoethyl]carbamate]-4-(2,5-dioxo-2,5-dihydro-1H-pyrrol-1-yl)methyl]cyclohexanecarboxamide (93)

2-(*N*-tert-Butoxycarbonylamino)ethylamine (1.116g, 7mmol) was added to a solution of 1-[(*trans*-4-[(2,5-dioxopyrrolidin-1-yl)oxy]carbonyl]cyclohexyl)-methyl]-1H-pyrrole-2,5-dione (2.423g, 7.25mmol) in dry CH₂Cl₂ (20ml). The reaction was stirred in the dark under an atmosphere of N₂ for 48 hours. The solvent was removed *in vacuo* and the resulting yellow residue was purified by column chromatography (5% methanol/CH₂Cl₂) to yield a white solid (1.666g, 4.4mmol, 60%). mp 187°C. (ESMS⁺) 380 (M⁺, 50%), 386 (MLi⁺, 100%), 402 (MNa⁺, 40%). IR(KBr) 3354 (m, C=ONH), 2934 (m, alkyl CH), 1734 (s, C=O), 1684 cm⁻¹ (s, C=O). ¹H NMR (400MHz, DMSO-*d*₆/CDCl₃) δ 7.62 (br. t, ³J(NH₈-H₁^{II}) = 5.6Hz, 1H, NH₈), 6.97 (s, 2H, H₃^I and H₄^I), 6.70 (br. t, ³J(NH₃^{II}-H₂^{II}) = 5.6Hz, 1H, NH₃^{II}), 3.23 (d, ³J(H₆^I-H₄) = 7.2Hz, 2H, H₆^I), 3.03 (dt, ³J(H₁^{II}-NH₈) = 5.6Hz, ³J(H₁^{II}-H₂^{II}) = 6.4Hz, 2H, H₁^{II}), 2.94 (dt, ³J(H₂^{II}-NH₃^{II}) = 5.6Hz, ³J(H₂^{II}-H₁^{II}) = 6.4Hz, 2H, H₂^{II}), 1.98 (tt, ³J(H₁-H_{2a}) and (H₁-H_{6a}) = 12.8Hz, ³J(H₁-H_{2e}) and (H₁-H_{6e}) = 3.2Hz, 1H, H₁), 1.71 (m, 2H, H_{2e} and H_{6e}), 1.61 (m, 2H, H_{3e} and H_{5e}), 1.52 (m, 1H, H₄), 1.37 (s, 9H, H₂^{II}, H₃^{II} and H₄^{II}), 1.26 (dddd, ²J(H_{2a}-H_{2e}) and (H_{6a}-H_{6e}) = 16.4Hz, ³J(H_{2a}-H_{3a}) and (H_{6a}-H_{5a}) = 13Hz,

$^3J(H_{2a}-H_1)$ and $(H_{6a}-H_1) = 12.8\text{Hz}$, $^3J(H_{2a}-H_{3e})$ and $(H_{6a}-H_{5e}) = 3.2\text{Hz}$, 2H, H_{2a} and H_{6a} , 0.88 (dddd, $^2J(H_{3a}-H_{3e})$ and $(H_{5a}-H_{5e}) = 16.4\text{Hz}$, $^3J(H_{3a}-H_{2a})$ and $(H_{5a}-H_{6a}) = 13\text{Hz}$, $^3J(H_{3a}-H_4)$ and $(H_{5a}-H_4) = 12.8\text{Hz}$, $^3J(H_{3a}-H_{2e})$ and $(H_{5a}-H_{6e}) = 3.2\text{Hz}$, 2H, H_{3a} and H_{5a}). ^{13}C NMR (100.593MHz, DMSO- d_6 /CDCl $_3$) δ 174.99 (C_7), 171.09 (C_2^I and C_5^I), 155.58 (C_3^{II} and C_4^{II}), 134.25 (C_3^I

and C_4^I), 77.51 (C_1^{III}), 43.79 (C_1), 43.01 (C_6^I), 39.63 (C_2^{II}), 38.59 (C_1^{II}), 36.09 (C_4), 29.38 (C_3 and C_5), 28.42 (C_2 and C_6), 28.16 (C_2^{III} , C_3^{III} and C_4^{III}). Anal. calcd for $C_{19}H_{29}N_3O_5$: C, 60.14; H, 7.70; N, 11.07.

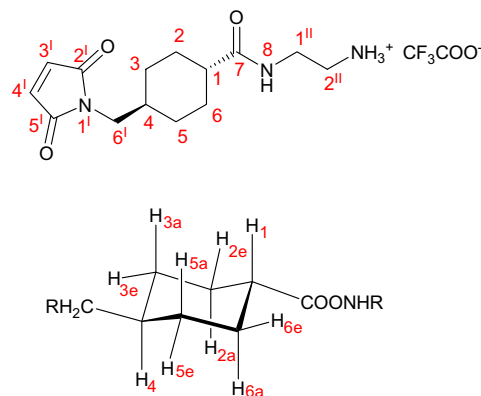
Found: C, 60.14; H, 7.84; N, 11.16.



Synthesis of N-(2-aminoethyl)-4-[(2,5-dioxo-2,5-dihydro-1H-pyrrol-1-yl)methyl]cyclohexanecarboxamide trifluoroacetic acid salt (94)

N-[tert-butyl[2-aminoethyl]carbamate]-4-(2,5-dioxo-2,5-dihydro-1H-pyrrol-1-yl)methyl]cyclohexanecarboxamide (0.171g, 0.45mmol) was dissolved in CH $_2$ Cl $_2$ (50ml) and trifluoroacetic acid (1ml) was added. The solution was refrigerated overnight and the solvent was removed in vacuo affording a clear oil. This was solidified by trituration with hexane and methanol to yield a white solid (0.174g, 0.44mmol, 98%). mp 59-62°C. (ESMS-) 113 (CF $_3$ CO $_2^-$, 100%). (ESMS+) 280 (M $^+$, 97%). IR(KBr) 2932 (m, alkyl CH), 1698 cm $^{-1}$ (s, C=O). ^1H NMR (400MHz, DMSO- d_6) δ 7.89 (br. t, 1H, NH), 7.79 (br. s, 3H, NH $_3^+$), 7.00 (s, 2H, H_3^I and H_4^I), 3.24 (m, 4H, H_1^{II} and H_6^I), 2.83 (m, 2H, H_2^{II}), 2.01 (tt, , $^3J(H_1-H_{2a})$ and $(H_1-H_{6a}) = 12\text{Hz}$, $^3J(H_1-H_{2e})$ and $(H_1-H_{6e}) = 3.6\text{Hz}$, 1H, H_1), 1.75 (m, 2H, H_{2e} and H_{6e}), 1.62 (m, 2H, H_{3e} and H_{5e}), 1.52 (m, 1H, H_4), 1.25 (dddd, $^2J(H_{2a}-H_{2e})$ and $(H_{6a}-H_{6e}) = 16.4\text{Hz}$, $^3J(H_{2a}-H_{3a})$ and

$(H_{6a}-H_{5a}) = 13.2\text{Hz}$, ${}^3J(H_{2a}-H_1)$ and $(H_{6a}-H_1) = 12.4\text{Hz}$, ${}^3J(H_{2a}-H_{3e})$ and $(H_{6a}-H_{5e}) = 3.2\text{Hz}$, 2H, H_{2a} and H_{6a} , 0.89 (dddd, ${}^2J(H_{3a}-H_{3e})$ and $(H_{5a}-H_{5e}) = 16\text{Hz}$, ${}^3J(H_{3a}-H_{2a})$ and $(H_{5a}-H_{6a}) = 13.2\text{Hz}$, ${}^3J(H_{3a}-H_4)$ and $(H_{5a}-H_4) = 12.4\text{Hz}$, ${}^3J(H_{3a}-H_{2e})$ and $(H_{5a}-H_{6e}) = 3.2\text{Hz}$, 2H, H_{3a} and H_{5a} . ${}^{13}\text{C}$ NMR (100MHz, DMSO- d_6) δ 175.79 (C_7), 171.29 (C_2^I and C_5^I), 158.48 (q, CF_3COO^-), 134.39 (C_3^I and C_4^I), 115.53 (q, CF_3), 43.78 (C_1), 43.06, (C_6^I), 38.71 (C_2^{II}), 36.40 (C_4), 36.17 (C_1^{II}), 29.39 (C_3 and C_5), 28.41 (C_2 and C_6). Anal. calcd for $\text{C}_{16}\text{H}_{22}\text{F}_3\text{N}_3\text{O}_5$: C, 48.85; H, 5.64; N, 10.68. Found: C, 47.84; H, 5.63; N, 10.17.



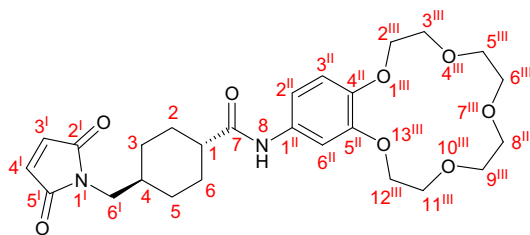
Isolation of *trans*-4-[(2,5-dioxo-2,5-dihydro-1H-pyrrol-1-yl)methyl]-N-{2-[(trifluoroacetyl)amino]ethyl}cyclohexane carboxamide (95)

N-(2-aminoethyl)-4-[(2,5-dioxo-2,5-dihydro-1H-pyrrol-1-yl)methyl]cyclohexanecarboxamide trifluoroacetic acid salt (0.692g, 1.76mmol) was dissolved in DMF (1ml) and succinic anhydride (0.177g, 1.76mmol) was added and left to stir for one hour under an atmosphere of N_2 . 1M DCC in DCM (1.8 mL) was added along with NHS (0.204g, 1.8mmol) and the reaction left to stir for a further 24 hours. The reaction mixture was filtered and the solvent was removed in vacuo affording a clear oil. This was dissolved in EtOAc/MeOH in preparation for purification by column chromatography however a white solid precipitated from solution (0.462g, 1.23mmol, 70%). ${}^1\text{H}$ NMR (400MHz, DMSO- d_6) δ 9.34 (br. t, 1H, NH_{11}), 7.81 (br. t, 1H, NH_8), 7.01 (s, 2H, H_3^I and H_4^I), 3.20 (m, 6H, H_9 , H_{10} and H_6^I), 1.98 (tt, , ${}^3J(H_1-$

Synthesis of 4-[(2,5-dihydro-2,5-dioxo-1H-pyrrol-1-yl)methyl]-N-2,3,5,6,8,9,11,12-octahydro-1,4,7,10,13-benzopentaoxacyclopentadecine]cyclohexanecarboxamide (SMCC-CROWN) (98)

4'-aminobenzo-15-crown-5 (0.400g, 1.4mmol) dissolved in CH₂Cl₂ (5ml) was added dropwise to a solution of 1-[(trans-4-[(2,5-dioxopyrrolidin-1-yl)oxy]carbonyl}cyclohexyl)-methyl]-1H-pyrrole-2,5-dione (0.468g, 1.4mmol) in CH₂Cl₂ (5ml). The reaction mixture was stirred at room temperature in the dark under an atmosphere of N₂ for 18 hours. The solvent was removed in vacuo and the crude product was purified by column chromatography (10% methanol/ethyl acetate) yielding a yellow brown solid (0.567g, 1.1mmol, 80%). mp 85-91°C. (ESMS+) 509 (MLi⁺, 100%), 525 (MNa⁺, 100%). IR(KBr) 3448 (m, N-H), 2962 (m, alkyl C-H), 1718 (s, C=O), 1701 cm⁻¹ (s, C=O). ¹H NMR (400MHz, CDCl₃) δ 7.56 (br. s, 1H, NH), 7.35 (d, ⁴J(H₆^{II}-H₂^{II}) = 2Hz, 1H, H₆^{II}), 6.88 (dd, ³J(H₃^{II}-H₂^{II}) = 8.8Hz, ⁴J(H₂^{II}-H₆^{II}) = 2Hz, 1H, H₂^{II}), 6.75 (d, ³J(H₂^{II}-H₃^{II}) = 8.8Hz, 1H, H₃^{II}), 6.71 (s, 2H, H₃^I and H₄^I), 4.08, 3.87, 3.74 (3 x m, 16H, H₂^{III}, H₃^{III}, H₅^{III}, H₆^{III}, H₈^{III}, H₉^{III}, H₁₁^{III} and H₁₂^{III}), 3.39 (d, ³J(H₄-H₆^I) = 6.8Hz, 2H, H₆^I), 2.18 (tt, ³J(H₁-H_{2a}) and (H₁-H_{6a}) = 12.4Hz, ³J(H₁-H_{2e}) and (H₁-H_{6e}) = 3.2Hz, 1H, H₁), 1.98 (m, 2H, H_{2e} and H_{6e}), 1.77 (m, 2H, H_{3e} and H_{5e}), 1.72 (m, 1H, H₄), 1.52 (dddd, ²J(H_{2a}-H_{2e}) and (H_{6a}-H_{6e}) = 16Hz, ³J(H_{2a}-H_{3a}) and (H_{6a}-H_{5a}) = 13.2Hz, ³J(H_{2a}-H₁) and (H_{6a}-H₁) = 12.4Hz, ³J(H_{2a}-H_{3e}) and (H_{6a}-H_{5e}) = 2.8Hz, 2H, H_{2a} and H_{6a}), 1.03 (dddd, ²J(H_{3a}-H_{3e}) and (H_{5a}-H_{5e}) = 16Hz, ³J(H_{3a}-H_{2a}) and (H_{5a}-H_{6a}) = 13.2Hz, ³J(H_{3a}-H₄) and (H_{5a}-H₄) = 12.4Hz, ³J(H_{3a}-H_{2e}) and (H_{5a}-H_{6e}) = 2.8Hz, 2H, H_{3a} and H_{5a}). ¹³C NMR (100MHz, CDCl₃) δ 174.32 (C₇), 171.26 (C₂^I and C₅^I), 149.17 (C₅^{II}), 145.49 (C₁^{II}), 132.52 (C₄^{II}), 134.21 (C₃^I and C₄^I), 114.67 (C₃^{II}), 112.52 (C₂^{II}), 107.06 (C₆^{II}), 70.87, 70.76, 70.40, 70.25, 69.64, 69.47 and 69.43

(C₂^{III}, C₃^{III}, C₅^{III}, C₆^{III}, C₈^{III}, C₉^{III}, C₁₁^{III}, C₁₂^{III}), 46.20 (C₁), 43.84 (C₆^I), 36.52 (C₄),
29.96 (C₃ and C₅), 29.00 (C₂ and C₆).



5.4 References

- (1) Perrin, D. D.; Armarego, W. L. F. *Purification of Laboratory Chemicals*; 3rd ed.; Permagon Press: Oxford, 1988.
- (2) Panico, R.; Powell, W. H.; Richer, J.-C.; Eds.; *A Guide to IUPAC Nomenclature of Organic Compounds (Recommendations 1993)*; Blackwell Scientific Publications: Oxford, 1993.
- (3) Atkinson, S. J.; Ellis, V.-J.; Boyd, S. E.; Brown, C. L. *New J. Chem* **2007**, *31*, 155-162.
- (4) Brown, C. L.; Atkinson, S. J.; Healy, P. C. *Acta Cryst. E* **2005**, *E61*, o1203-o1204.
- (5) Brown, C. L.; Atkinson, S. J.; Healy, P. C. *Acta Cryst. E* **2005**, *E61*, o1072-o1073.
- (6) Kang, J.-H.; Chung, H.-E.; Kim, S. Y.; Kim, Y.; Lee, J.; Lewin, N. E.; Pearce, L. V.; Blumberg, P. M.; Marquez, V. E. *Bioorg. Med. Chem.* **2003**, *11*, 2529-2539.
- (7) Oishi, T.; Fujimoto, M. *J. Polym. Sci., Part A: Polym. Chem.* **1992**, *30*, 1821-1830.
- (8) Ambade, A. V.; Kumar, A. *J. Polym. Sci., Part A: Polym. Chem.* **2001**, *39*, 1295-1304.
- (9) Koenig, N. H.; Sasin, G. S.; Swern, D. *J. Org. Chem.* **1958**, *23*, 1525-1530.
- (10) Delamarche, E.; Sundarababu, G.; Biebuyck, H.; Michel, B.; Gerber, C.; Wolf, H.; Ringsdorf, H.; Xanthopoulos, N.; Mathieu, H. J. *Langmuir* **1996**, *12*, 1997-2006.
- (11) Yoshitake, S.; Yamada, Y.; Ishikawa, E.; Masseyeff, R. *Eur. J. Biochem.* **1979**, *101*, 395-399.

- (12) Rich, D. H.; Gesellchen, P. D.; Tong, A.; Cheung, A.; Buckner, C. K. *J. Med. Chem.* **1975**, *18*, 1004-1010.
- (13) Nielsen, O.; Buchardt, O. *Synthesis* **1991**, 819-821.
- (14) Bieniarz, C.; Husain, M.; Barnes, G.; King, C. A.; Welch, C. J. *Bioconjugate Chem.* **1996**, *7*, 88-95.
- (15) Grinberg, H.; Lamdan, S.; Gaozza, C. H. *J. Heterocycl. Chem.* **1975**, *12*, 763-766.
- (16) Kato, K.; Yoshida, M. *Kogyo Gijutsu Shikensho Hokoku* **1968**, *329*, 45-56.
- (17) Asay, R. E. *J. Heterocycl. Chem.* **1977**, *14*, 85-90.
- (18) Hill, M.; Bechet, J.-J.; d'Ablis, A. *FEBS Lett.* **1979**, *102*, 282-286.

APPENDIX A

CRYSTAL STRUCTURES

Data collection, structure solution and refinement

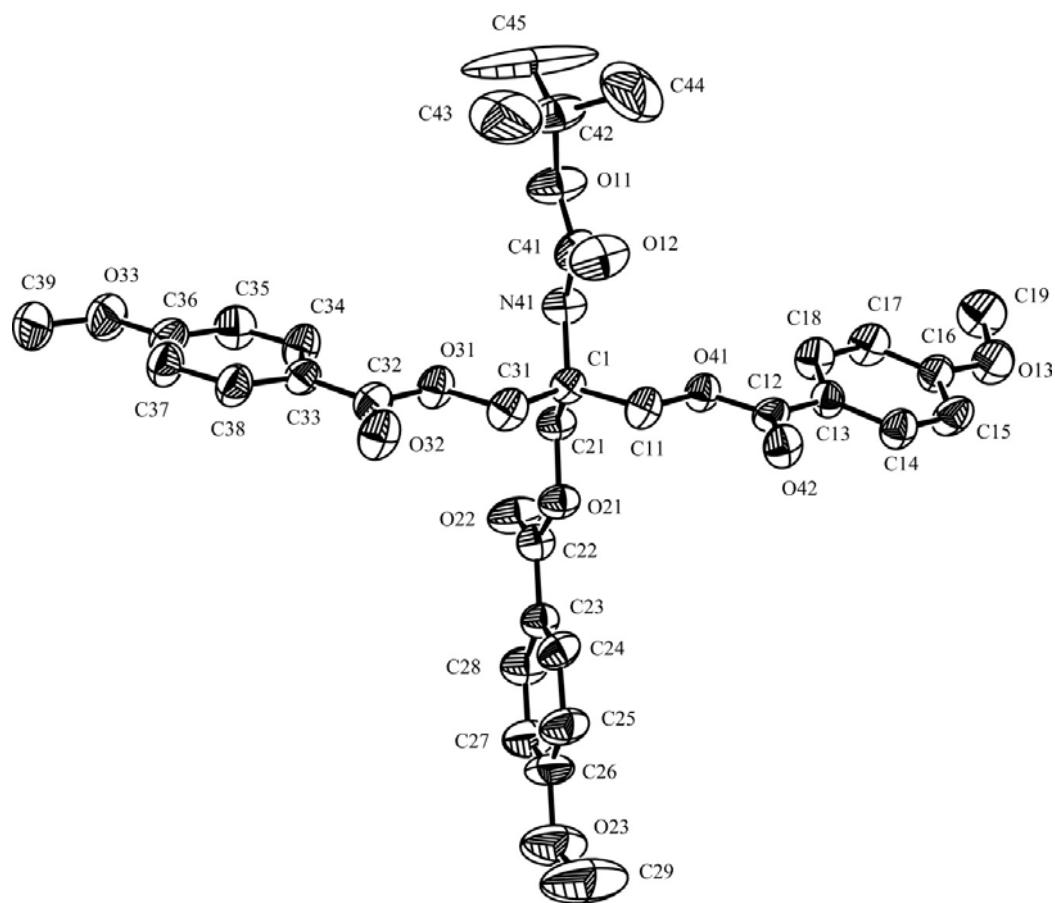
Data sets for compounds **26**, **35**, **74**, **79**, **84** and **89** were measured using a Rigaku AFC-7R four circle diffractometer (ω - 2θ scan mode, monochromated Mo-K α radiation $\lambda = 0.71069 \text{ \AA}$) at 295 K, yielding N independent reflections, N_o with $I > 2\sigma(I)$ being considered 'observed'. Computation used the teXsan crystallographic software package for Windows version 1.06 of the molecular structure corporation¹, ORTEP-3² and PLATON.³

¹ teXsan for Windows, Single Crystal Structure Analysis Software, **2001**, Version 1.06, The Woodlands, Molecular Structure Corporation.

² Farrugia, L. J. *J. Appl. Cryst.* **1997**, *30*, 565.

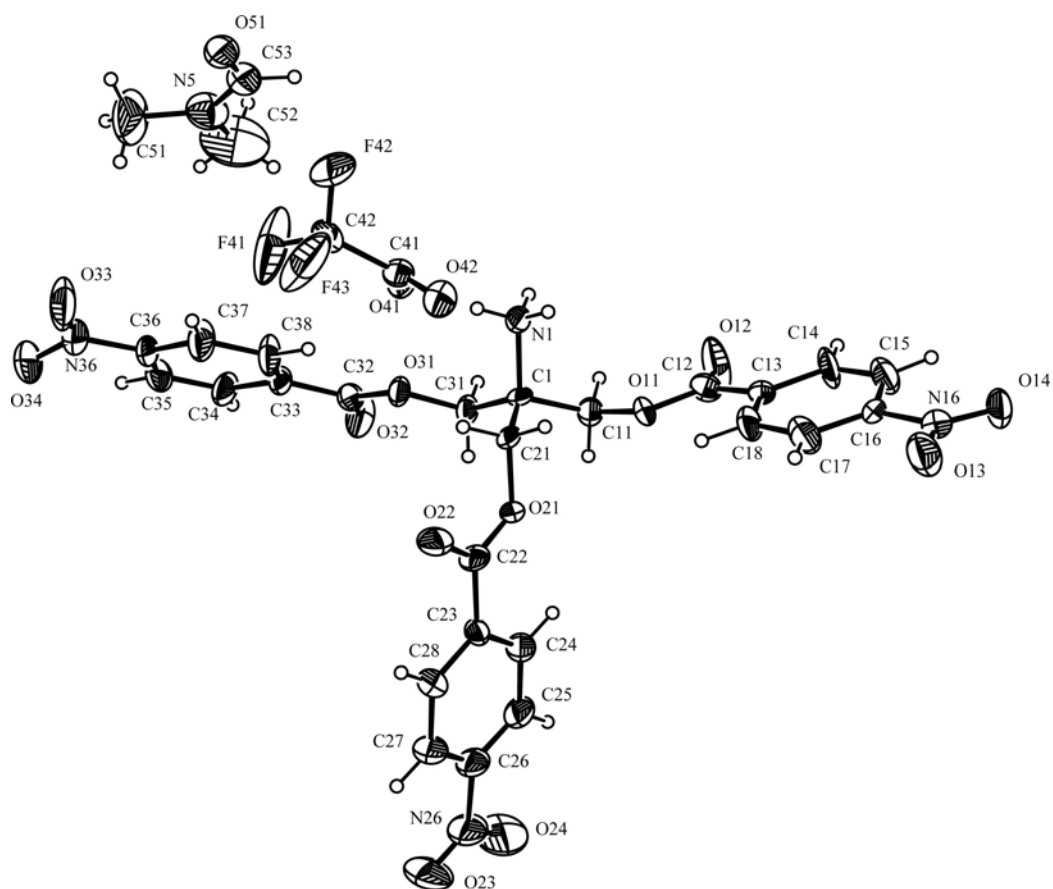
³ Spek AL, PLATON for Windows, Version 121201. Utrecht, University of Utrecht.

N-(tert-butyloxycarbonyl)-1,1,1-tris(4-methoxybenzoyloxy-methyl)methylamine **26**



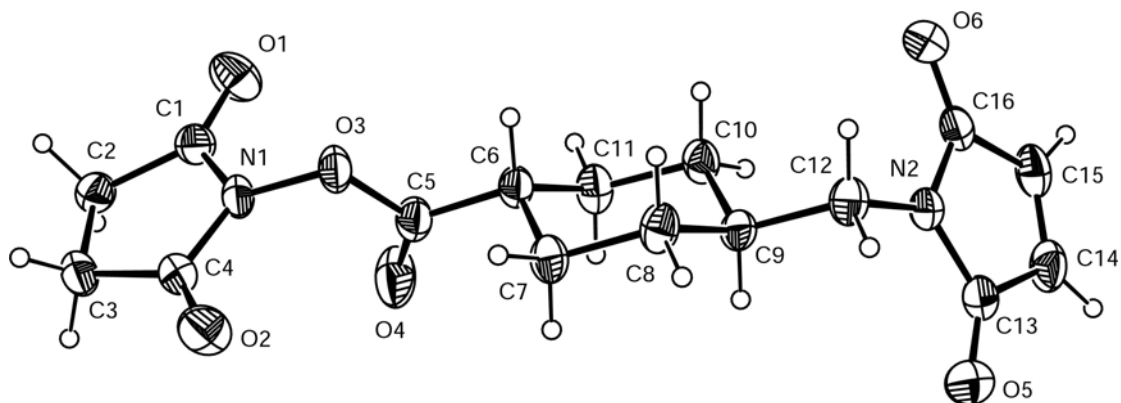
Prismatic, colourless crystals of **26** were formed by the slow diffusion of diethyl ether into a solution of **26** in dichloromethane, mp 136°C. $C_{33}H_{37}NO_{11}$ $M = 623.6$, tetragonal, space group, I 41/a, $a = 33.07(5)$, $b = 33.07(5)$, $c = 12.33(2)$ Å. $V = 13484(36)$ Å³, $Z = 16$, $D_x = 1.23$ g cm⁻³, $\theta = 5.0$ - 6.3° , $\mu = 0.09$ mm⁻¹, Crystal size: 0.30 x 0.20 x 0.15 mm, $N = 5963$, $N_o = 1249$, $R = 0.069$, $R_w = 0.163$.

1,1,1-tris(4-nitrobenzoyloxymethyl)methylamine trifluoroacetic acid salt **35**



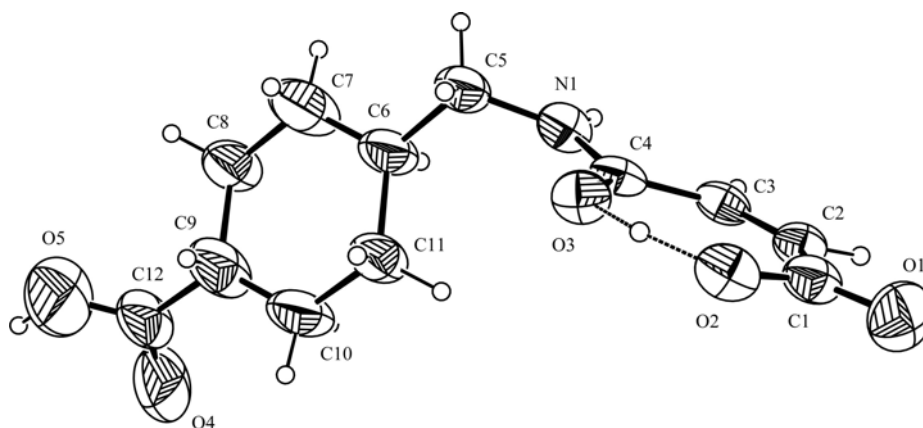
Colourless plates of **35** were formed by slow evaporation of a saturated solution of **35** in dimethylformamide, mp 158-159°C. $C_{30}H_{28}F_3N_5O_{15}$ $M = 755.6$, triclinic, space group, $P-1$, $a = 15.125(2)$, $b = 18.431(3)$, $c = 6.292(8)$ Å. $V = 1730.2(4)$ Å³, $Z = 2$, $D_x = 1.450$ g cm⁻³, $\theta = 10.0$ - 12.1° , $\mu = 0.13$ mm⁻¹, Crystal size: 0.25 x 0.20 x 0.05 mm, $N = 4531$, $N_o = 2062$, $R = 0.142$, $R_w = 0.386$.

1-[(*trans*-4-{[(2,5-dioxopyrrolidin-1-yl)oxy]carbonyl}cyclohexyl)-methyl]-1*H*-pyrrole-2,5-dione (SMCC) **74**



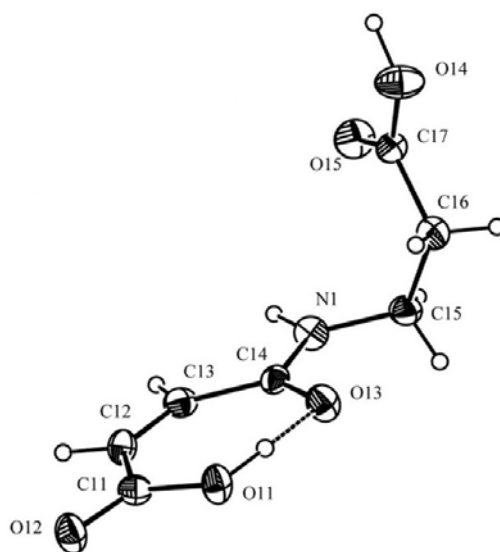
Prismatic, colourless crystals of **74** were formed by recrystallisation of **74** in a mixture of acetone and methanol, mp 171-174°C. $C_{16}H_{18}N_2O_6$ $M = 334.3$, orthorhombic, space group, $Pbca$, $a = 20.203(5)$, $b = 17.021(6)$, $c = 9.643(3)$ Å. $V = 3316.0(18)$ Å³, $Z = 8$, $D_x = 1.339$ g cm⁻³, $\theta = 12.7$ -17.3°, $\mu = 0.10$ mm⁻¹, Crystal size: 0.50 x 0.50 x 0.30 mm, $N = 3816$, $N_o = 1926$, $R = 0.043$, $R_w = 0.132$.

trans-4-({[(2*Z*)-3-carboxyprop-2-enoyl]amino}methyl)cyclohexanecarboxylic acid **79**



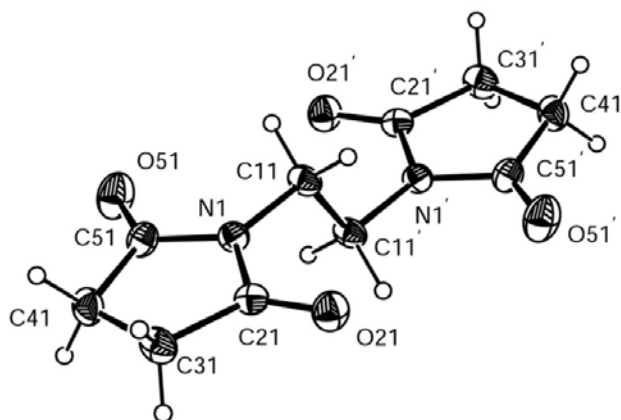
Prismatic, colourless crystals of **79** were formed by recrystallisation of **79** in a mixture of acetone and methanol, mp 190-192°C. C₁₂H₁₇NO₅ $M = 255.3$, monoclinic, space group, $P 21/a$, $a = 7.228(2)$, $b = 31.110(15)$, $c = 5.746(3)$ Å. $V = 1287.4(10)$ Å³, $Z = 4$, $D_x = 1.317$ g cm⁻³, $\theta = 10.4$ -13.0°, $\mu = 0.10$ mm⁻¹, Crystal size: 0.50 x 0.25 x 0.15 mm, $N = 2276$, $N_o = 1012$, $R = 0.092$, $R_w = 0.280$.

(2Z)-4-[(2-carboxyethyl)amino]-4-oxobut-2-enoic acid **84**



Colourless needles of **84** were formed by recrystallisation of **84** in a mixture of acetone and methanol, mp 158°C. C₇H₉NO₅ *M* = 187.2, orthorhombic, space group, *P* 2₁ 2₁ 2₁, *a* = 17.428(9), *b* = 18.728(8), *c* = 10.177(5) Å. *V* = 3322.0(3) Å³, *Z* = 16, *D*_x = 1.497 g cm⁻³, *θ* = 8.6-12.1°, *μ* = 0.13 mm⁻¹, Crystal size: 0.40 x 0.10 x 0.10 mm, *N* = 3286, *N*_o = 1486, *R* = 0.062, *R*_w = 0.143.

N,N'-ethylenedisuccinimide **89**



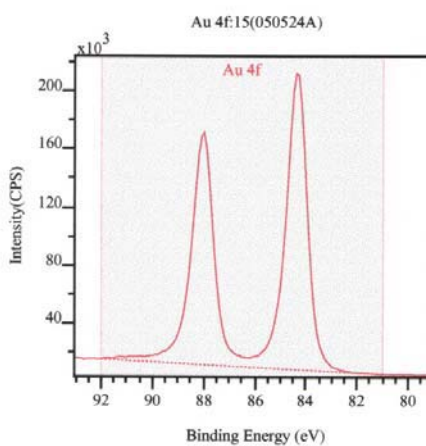
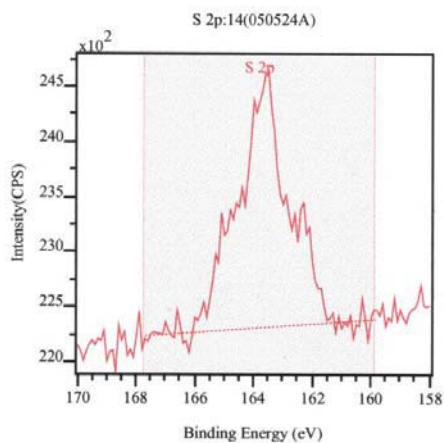
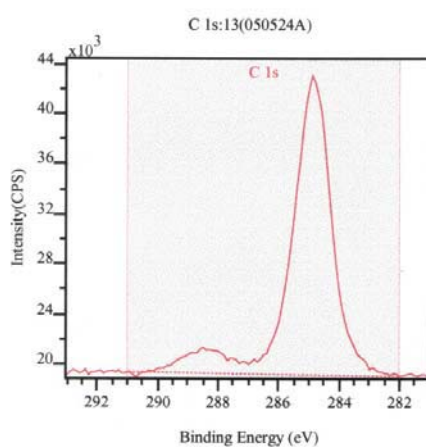
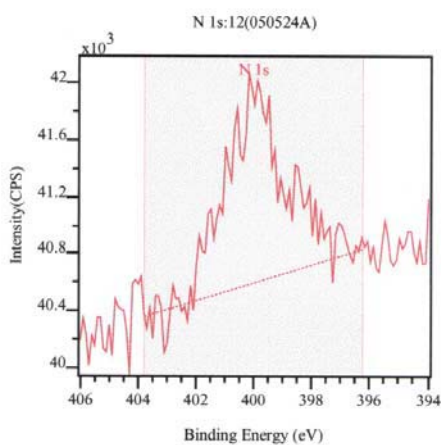
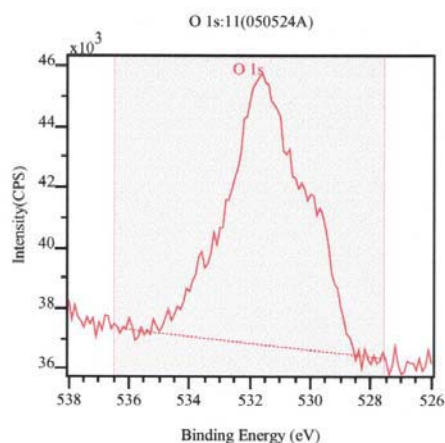
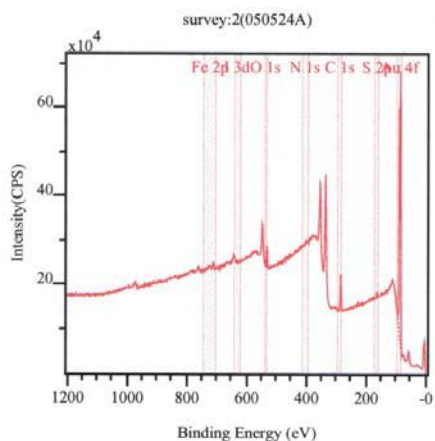
Prismatic, colourless crystals of **89** were formed by slow evaporation from a solution of methanol/chloroform, mp 252-253°C. $C_{10}H_{12}N_2O_4$ $M = 224.2$, monoclinic, space group, $P 21/c$, $a = 12.565(13)$, $b = 8.361(10)$, $c = 9.929(15)$ Å. $V = 1043.0(2)$ Å³, $Z = 4$, $D_x = 1.428$ g cm⁻³, $\theta = 8.3$ -10.6°, $\mu = 0.11$ mm⁻¹, Crystal size: 0.50 x 0.40 x 0.30 mm, $N = 2396$, $N_o = 1825$, $R = 0.048$, $R_w = 0.124$.

APPENDIX B

XPS DATA AND SPECTRA

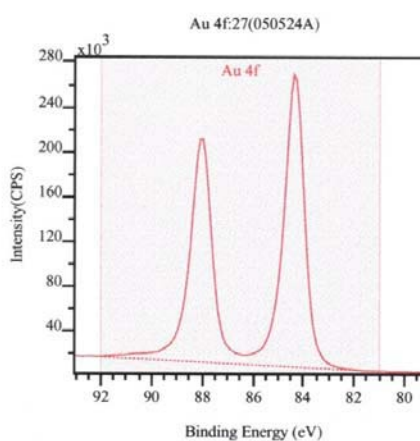
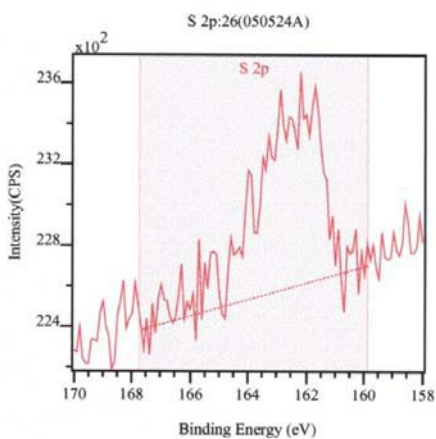
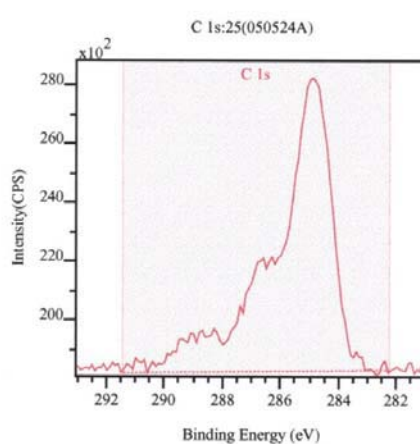
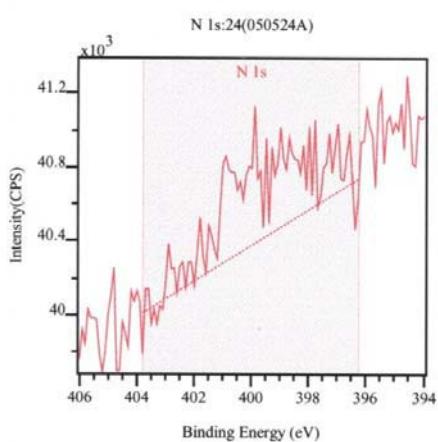
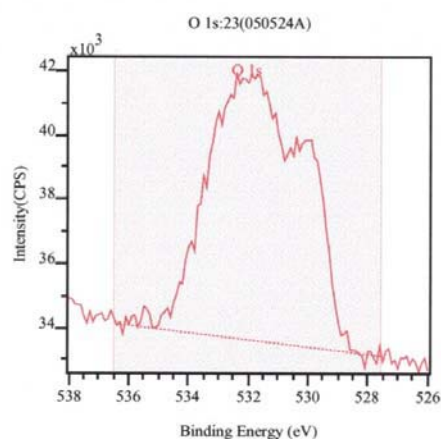
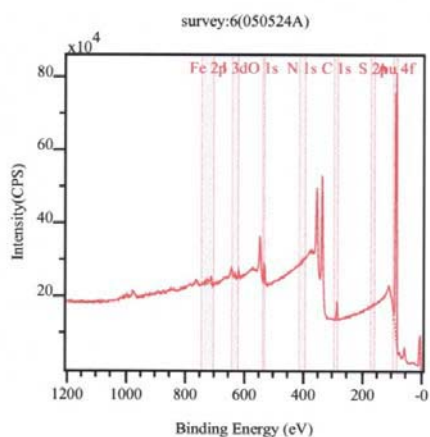
XPS Data and Spectra for *N*-hydroxysuccinimide (**53**) monolayer

Peak	Position BE (eV)	FWHM (eV)	Raw Area (CPS)	RSF	Atomic Mass	Atomic Conc %	Mass Conc %
Au 4f	84.000	2.854	3090510.2	6.250	196.967	25.72	81.80
C 1s	284.000	3.067	286030.0	0.278	12.011	53.47	10.37
O 1s	531.000	3.661	191400.0	0.780	15.999	12.94	3.34
S 2p	163.000	3.397	37124.1	0.668	32.065	2.89	1.50
N 1s	400.000	4.454	20150.0	0.477	14.007	2.20	0.50
Fe 2p	711.000	4.548	146160.2	2.957	55.846	2.77	2.49
I 3d	619.000	0.779	0.0	10.343	126.904	0.00	0.00



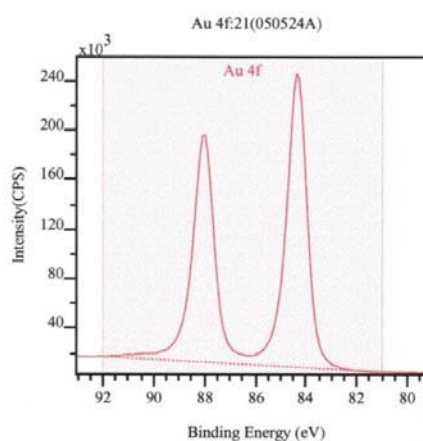
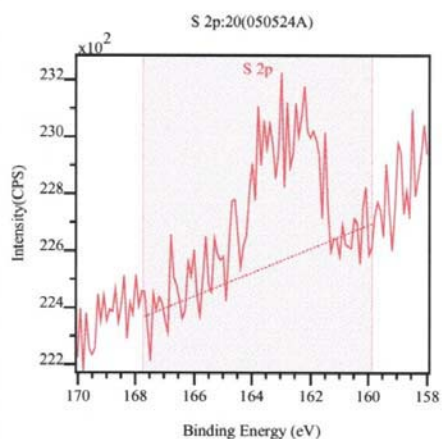
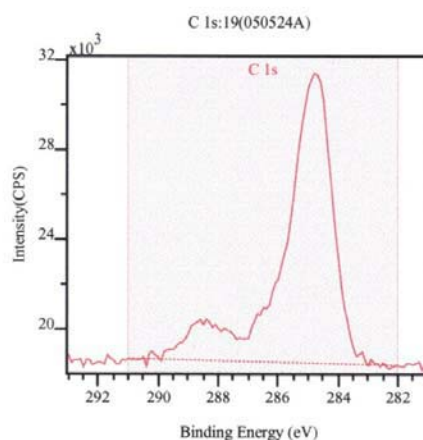
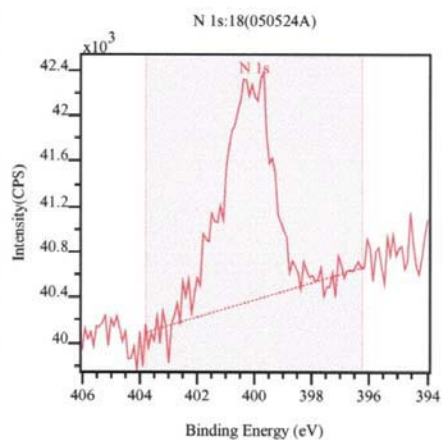
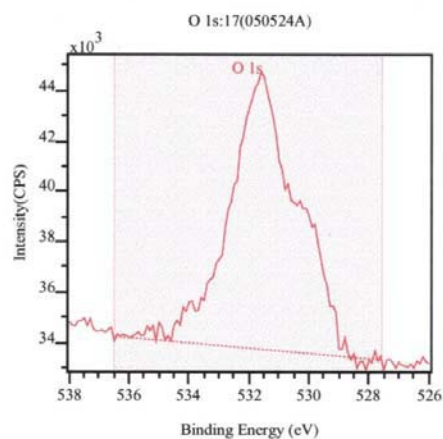
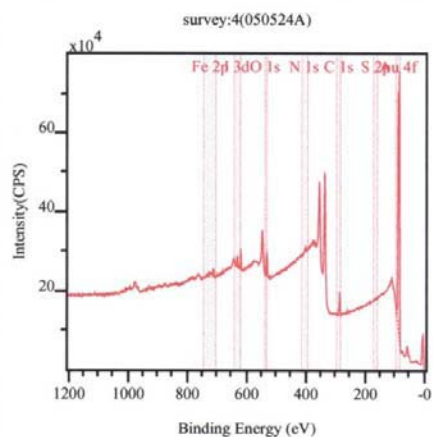
XPS Data and Spectra for Protein Resistant (58) monolayer

Peak	Position BE (eV)	FWHM (eV)	Raw Area (CPS)	RSF	Atomic Mass	Atomic Conc %	Mass Conc %
Au 4f	84.000	2.874	3941770.0	6.250	196.967	36.65	86.98
C 1s	285.000	3.223	193940.0	0.278	12.011	40.50	5.86
O 1s	532.000	4.369	214910.0	0.780	15.999	16.24	3.13
S 2p	162.000	3.476	15846.1	0.668	32.065	1.38	0.53
N 1s	401.000	1.201	5830.0	0.477	14.007	0.71	0.12
Fe 2p	712.000	4.245	195950.3	2.957	55.846	4.14	2.79
I 3d	619.000	2.836	65560.0	10.343	126.904	0.38	0.58



XPS Data and Spectra for Acyl Azide (**59**) monolayer

Peak	Position BE (eV)	FWHM (eV)	Raw Area (CPS)	RSF	Atomic Mass	Atomic Conc %	Mass Conc %
Au 4f	84.000	2.846	3619940.0	6.250	196.967	31.89	83.81
C 1s	285.000	3.197	220405.0	0.278	12.011	43.61	6.99
O 1s	531.000	3.653	200880.0	0.780	15.999	14.38	3.07
S 2p	163.000	2.720	9041.9	0.668	32.065	0.75	0.32
N 1s	400.000	3.771	35896.1	0.477	14.007	4.15	0.77
Fe 2p	712.000	4.873	201564.8	2.957	55.846	4.04	3.01
I 3d	619.000	2.590	217600.0	10.343	126.904	1.20	2.03



XPS Data and Spectra for Heated Acyl Azide monolayer

Peak	Position BE (eV)	FWHM (eV)	Raw Area (CPS)	RSF	Atomic Mass	Atomic Conc %	Mass Conc %
Au 4f	84.000	2.839	1846060.0	6.250	196.967	17.26	74.38
C 1s	285.000	2.775	258395.0	0.278	12.011	54.27	14.26
O 1s	532.000	3.015	311010.0	0.780	15.999	23.63	8.27
S 2p	155.000	0.000	0.0	0.668	32.065	0.00	0.00
N 1s	400.000	2.363	25807.0	0.477	14.007	3.16	0.97
Fe 2p	712.000	5.739	75870.3	2.957	55.846	1.61	1.97
I 3d	619.000	2.350	9120.0	10.343	126.904	0.05	0.15

